Microbial iron cycling

in pelagic aggregates (iron snow) and

sediments of an acidic mine lake

Dissertation

zur Erlangung des akademischen Grades
doctor rerum naturalium (Dr. rer. nat.)

vorgelegt dem
Rat der Biologisch-Pharmazeutischen Fakultät
der Friedrich-Schiller-Universität Jena

von Master of Science
Shipeng Lu

geboren am 26.08.1980 in Nanjing, China

Jena, im Aug. 2012

Gutachter:

1. Prof. Dr. Kirsten Küsel (Friedrich-Schiller-Universität Jena)

2. Prof. Dr. Joel Kostka (Georgia Institute of Technology, USA)

3. Prof. Dr. Gabriele Diekert (Friedrich-Schiller-Universität Jena)

Tag der öffentlichen Disputation: 12th December 2012

Contents

Summary

The acidic lignite mine lake 77 is located in the Lusatian district of Brandenburg, Germany. Previous research suggests that the less acidic groundwater inflow from north shoreline of Lake 77 changes the sediment pore water chemistry and triggers a further pH increase. Additionally, differences in color of biogenic Fe(III)-rich aggregates from north and central water bodies were observed. The objective of this dissertation was to investigate and compare the Fe-cycling microbial communities in Fe(III)-rich aggregates and sediments at different pH conditions.

The water body of the Lake 77 is separated by a bank rising from the bottom of the lake, forming two basins that differ in stratification patterns and pelagic boundary conditions. From 2009 to 2012, the central basin exhibited a dimictic water regime while the northern basin was meromictic with stratification persisting over the last 4 years. Biogenic iron-rich particles (iron snow) formed at steeply opposing gradients of oxygen and Fe(II) within the redoxcline of both basins and were highly colonized by microbial cells (~10^{10} cells [g dry weight]$^{-1}$). The iron snow was different from other aggregates from other lakes. It had a smaller diameter of up to 380 µm and a higher sedimentation velocity (~2 m h^{-1}). The organic carbon content was below 11%, compared to other lake snow containing 20-40% of organic carbon, and the iron content more than 35%, primarily in the form of schwertmannite (>91% mineral content).

Microbial Fe-cycling appeared to be the dominant metabolism in the iron snow, because RNA-based cloning and qPCR assigned up to 61% of active bacteria as Fe-cycling microorganisms (FeM) including the Fe oxidizers *Acidimicrobium* and *Ferrovum*, and Fe reducers *Acidiphilium*, *Albidiferax* (*Rhodoferax*) and *Geobacter*. Metaproteomics revealed 70 unique proteins from iron snow collected from the central basin and 283 unique proteins from

43 genera from the northern basin. Those proteins were likely involved in primary production, motility and metabolism of FeM. Based on these results, we proposed a three-stage developmental model of iron snow in these waters. In brief, acidophilic autotrophic Fe-oxidizing microorganisms, such as *Ferrovum, Acidimicrobium, Acidithiobacillus*, and *Thiobacillus*, initialized the first step of iron snow formation by coupling Fe(II) oxidation with CO_2 fixation, serving as primary producers. At the second stage heterotrophic microbes, including Fe-reducing microorganisms (FeRM) *Acidiphilium*, *Albidiferax (Rhodoferax)* and *Geobacter*, started to colonize the iron snow. Due to its high specific surface area, iron snow provided reactive Fe(III) as an electron acceptor for anaerobic microbial respiration during and after sedimentation in the deeper anoxic water layers (third stage).

Similar microbial communities were found in iron snow and sediment surface at same locations by DGGE. However, the differences between central and northern basin were more pronounced. The microbial communities in north shore line sediments were investigated using cultivation-independent and -dependent approaches. 117 isolates were obtained that grouped into 38 different strains, including 27 putative new species. Among the isolated strains, 22 strains were able to oxidize Fe(II), 34 were able to reduce schwertmannite and 21 could do both. Most of the acidophilic FeRM preferred microoxic conditions for Fe(III) reduction.

The results strongly suggested that iron snow acted as carriers bringing iron, organic carbon and living microorganisms from the water column to the lake sediment. In addition, pH might be the major driving force shaping the microbial communities responsible for Fe-cycling in the iron snow and sediments.

Zusammenfassung

Der saure Braunkohlerestsee 77 befindet sich in der Lausitz in Brandenburg in Deutschland. Bisherige Forschung hat gezeigt, dass der weniger saure Grundwasserzustrom von der nördlichen Uferlinie des Sees die Porenwasserchemie des Sedimentes verändert und einen weiteren pH-Anstieg auslöst. Desweiteren wurden Unterschiede in der Farbe biogener Fe(III)-reicher Aggregate aus dem nördlichen und zentralen Wasserkörper beobachtet. Das Ziel dieser Dissertation ist es, die am Fe-Kreislauf beteiligten mikrobiellen Gemeinschaften der Fe(III)-reichen Aggregate und der Sedimente unter verschiedenen pH Bedingungen zu untersuchen und zu vergleichen.

Der Wasserkörper des Sees 77 ist durch eine Bank geteilt, die vom Grunde des Sees aufsteigt, wodurch zwei Becken entstehen, die sich in ihrem Stratifikationsmuster und den Bedingungen der pelagischen Phasengrenze unterscheiden. Das Zentralbecken zeigt ein dimiktisches Wasserregime, wohingegen das Nordbecken meromiktisch mit einer über Jahre gleichbleibenden Stratifikation ist. Biogene eisenreiche Partikel (*iron snow*) bilden sich an stark gegenläufigen Gradienten von Sauerstoff und Fe(II) innerhalb der Redoxkline beider Becken und sind stark mit Mikroorganismen besiedelt (~10^{10} Zellen [g Trockengewicht]$^{-1}$). Der *iron snow* unterschied sich von anderen natürlich gebildeten Partikeln. Er hatte einen Durchmesser von bis zu 380 µm und eine hohe Sedimentationsgeschwindigkeit (~2 m h^{-1}). Der organische Kohlenstoffgehalt des *iron snow* war niedriger als 11% und der Eisengehalt mehr als 35%, primär in der Form von Schwertmannit (>91% Mineralgehalt).

Der mikrobielle Eisenkreislauf erschien als der dominierende Stoffwechsel im *iron snow*, da RNA-basiertes Klonieren und qPCR bis zu 61% der aktiven Bakterien als Eisen-verwertende Mikroorganismen (FeM) auswiesen. Metaproteom-Analysen zeigten 70 einzigartige Proteine im *iron snow* des Zentralbeckens und 283 einzigartige Proteine aus 43 Gattungen aus dem Nordbecken auf. Diese Proteine sind wahrscheinlich in die

Primärproduktion, Bewegung und den Stoffwechsel der FeM involviert. Auf diesen Ergebnissen basierend schlagen wir ein dreistufiges Entwicklungsmodell für *iron snow* im See 77 vor. In Kürze dargestellt, initialisieren acidophile autotrophe Fe(II)-oxidierende Mikroorganismen, wie beispielsweise *Ferrovum, Acidimicrobium, Acidithiobacillus* und *Thiobacillus*, den ersten Schritt der *iron snow*-Bildung, indem sie Fe(II)-Oxidation mit CO_2-Fixierung koppeln und so als Primärproduzenten dienen. Im zweiten Stadium beginnen heterotrophe Mikroben, wie die Fe-reduzierenden Mikroorganismen (FeRM) *Acidiphilium*, *Albidiferax (Rhodoferax)* und *Geobacter*, den *iron snow* zu kolonisieren. Aufgrund seiner hohen spezifischen Oberfläche bietet der *iron snow* reaktives Fe(III) als Elektronenakzeptor für die anaerobe mikrobielle Atmung während und nach der Sedimentation in den tieferen anoxischen Wasserschichten (drittes Stadium).

Mittels DGGE wurden ähnliche mikrobielle Gemeinschaften im *iron snow* und an der Sedimentoberfläche des jeweils gleichen Beckens gefunden. Hingegen waren die Unterschiede zwischen dem Zentralbecken und dem Nordbecken deutlicher. Die mikrobiellen Gemeinschaften des Sedimentes wurden mit kultivierungsabhängigen und -unabhängigen Methoden untersucht. Es wurden 117 Isolate erhalten, die in 38 unterschiedliche Stämme gruppiert wurden. 27 dieser Stämme sind vermeintlich neue Arten. Unter den isolierten Stämmen waren 22 in der Lage Fe(II) zu oxidieren, 34 konnten Schwertmannit reduzieren, und 21 konnten beides. Die meisten der acidophilen FeRM bevorzugten mikrooxische Bedingungen für die Fe(III) Reduktion.

Die Ergebnisse weisen stark darauf hin, dass *iron snow* als Träger fungiert, indem er Eisen, organischen Kohlenstoff und lebende Mikroorganismen von der Wassersäule zum Seesediment transportiert. Außerdem könnte der pH die Hauptantriebskraft der Zusammensetzung der mikrobiellen Gemeinschaften sein, welche für den Eisenkreislauf in *iron snow* und Sediment verantwortlich sind.

研究摘要

大型露天煤矿被废弃后，由于人工注水或天然地下水流入，煤层硫化物(主要为黄铁矿 pyrite)氧化后释放出酸根离子而形成酸性尾矿湖。煤矿酸性水的典型特征为低 pH 值，高浓度 Fe^{2+}和 SO_4^{2-}，因而具有很强的溶解性和侵蚀性，能够携带大量的重金属及有害化学物质进入环境。德国东部勃兰登堡州卢萨蒂亚地区为前东德大型露天褐煤矿区，二十世纪六十年代该矿区废弃后形成了一系列的尾矿湖。过去 15 年来研究人员对这些尾矿湖开展了大量广泛而深入的环境科学研究。其中，77 号酸性尾矿湖的湖水 pH 值约为 3，湖表总面积为 0.24km^2，体积约 1m^3，湖水最深处为 9m。前期水文学研究表明，77 号湖北部尾矿渣沥滤形成的富含 Fe^{2+}和 SO_4^{2-}的微酸性（～pH4.5）地下水由湖底渗入，改变了该湖底泥层的水化学特性，提高了 pH 值，从而形成了一个由湖底至湖面逐渐酸化的 pH 梯度。Fe^{2+}在此含氧酸性湖水中通过多种耐酸微生物介导的氧化反应，形成富含三价铁氧化物的絮凝物，主要成分为铁的含水硫酸盐矿物斯沃特曼矿(schwertmannite）。本文研究和比较了湖水絮凝物和湖底泥中在不同 pH 值条件下参与铁循环（或铁呼吸）的微生物群落。

水文研究发现，湖中心底部突出的高约 4m 的堆积将 77 号湖水分隔成两部分，形成两个相对独立并具不同湖水分层类型和边界条件的盆地。中心盆地具有二次循环湖特性，而北盆地则为常年不完全对流湖。微生物介导生成的富铁絮凝物形成于水体溶解氧和 Fe^{2+}反向浓度梯度骤减的氧化/还原跃层。该絮凝物富含大量微生物（每克干重约含~10^{10} 细胞），颗粒直径最大为 380μm，沉降速率为约每小时 2m，有机碳含量小于 11%，而铁含量大于 35%，其中超过 91%的矿物为斯沃特曼矿。这些特征明显区别于其他淡水湖及海洋中形成的天然絮凝物。因此，我们首次把此酸性尾矿湖富铁絮凝物称为 iron snow。

微生物介导的铁循环几乎是 iron snow 形成中的主导代谢过程。16S rRNA 基因克隆文库以及定量 PCR（qPCR）检测到多达 61%的活性细菌为铁循环细菌。宏蛋白质组学分析从中心盆地 iron snow 中共检出 70 种蛋白，而从北盆地中共检出来源于 43 个细菌属的 283 种蛋白。这些蛋白参与铁循环细菌初级生产（光合自养），能动性和新陈代谢。基于以上研究结果，我们提出了一个尾矿湖水体中 iron snow 发育的三阶段模型。第一阶段是嗜酸光合自养型铁氧化细菌偶联 Fe^{2+}氧化和 CO_2 固定进行初级生产，启动 iron snow 的形成。这些细菌包括 *Ferrovum,* 酸微菌属（*Acidimicrobium*）,酸硫杆

状菌属（*Acidithiobacillus*）以及热酸硫杆状菌属（*Thiobacillus*）。在第二阶段，异养型细菌开始附着于初期形成的 iron snow。这些包括各种铁还原细菌，嗜酸杆菌属（*Acidiphilium*），红育菌属（*Rhodoferax*, 现更名为 *Albidiferax*）以及地杆菌属（*Geobacter*）。在第三阶段，随着 iron snow 向湖水无氧深层沉降，它为厌氧微生物，尤其是铁还原细菌呼吸提供了较大比表面积的反应场所和电子受体 Fe^{3+}。

变性梯度凝胶电泳（DGGE）分析表明 iron snow 中的微生物群落与湖底泥表面的微生物群落相似。中心盆地较北盆地中的微生物群落差异更明显。通过分子生物学方法，系统地研究了北盆地沿岸湖底泥的微生物群落，进而与中心盆地底泥微生物群落进行了分析对比。通过使用双层培养技术，共分离纯化出 38 种，共 117 株细菌，其中 27 株为新菌种。在这些被分离的细菌中，有 22 株菌可以氧化 Fe^{2+}，34 株可以还原斯沃特曼矿，21 株可以同时具有还原和氧化铁的能力。大部分的嗜酸铁还原菌喜好微氧条件。

综上所述，iron snow 在尾矿湖中由微生物介导生成，并作为铁，有机碳和微生物的载体将它们从水体中带入湖底沉积物。在此过程中，湖水 pH 值为 iron snow 与湖底泥中的铁循环微生物群落成型的主要驱动因素。

1 Introduction

1.1 Acid Mine Drainage

Acid mine drainage (AMD) is the term used to describe effluent from active and abandoned mine sites that is characterized by low pH, high concentrations of Fe(II) and sulfate, and high Fe(III) solubility (Hoffert, 1947; Lundgren and Silver, 1980). The geochemistry of AMD can differ greatly, for example in terms of salinity, dissolved oxygen concentrations, metal(loid) (e.g. arsenic) concentrations, and sediment loads, as well as other parameters (Blowes *et al.*, 2003). The impacts of complex pollutant dynamics on the environment vary within and between ecosystems, however, in general AMD is regarded as one of the most serious environmental problems of water pollution in parts of the world with active or historic mining activities.

AMD is caused primarily by the enhanced oxidative dissolution of sulfide minerals, mainly pyrite (FeS_2), when mining of metals and coals causes ore bodies and seams to be disrupted and exposed to the atmosphere (Moses *et al.*, 1987; Nordstrom, 1982). In an initiator reaction, pyrite is oxidized chemically by oxygen:

$$FeS_2 + 3.5\ O_2 + H_2O \rightarrow Fe^{2+} + 2\ SO_4^{2-} + 2\ H^+ \qquad (1)$$

This slow oxidation generates protons and leads to the development of acidic conditions under which the ferrous iron (Fe^{2+}) is relatively stable in the presence of oxygen (Singh *et al.*, 1997). In the following step, acidophilic lithoautotrophic bacteria rapidly catalyze the oxidation of Fe^{2+} to ferric iron (Fe^{3+}), which is soluble under acidic conditions below approximately pH 2.5 (Kappler and Straub, 2005):

$$2Fe^{2+} + 0.5\ O_2 + 2\ H^+ \rightarrow 2\ Fe^{3+} + 2\ H_2O \qquad (2)$$

This is the rate-determining step of pyrite oxidation in AMD mediated by microorganisms (Colmer and Hinkle, 1947; Singer and Stumm, 1970; Temple and Colmer, 1951). Then,

formed Fe^{3+} reacts spontaneously with more pyrite to oxidize the pyrite to Fe^{2+}, sulfate and protons (Pronk and Johnson, 1992; Singh *et al.*, 1997):

$$FeS_2 + 14\ Fe^{3+} + 8\ H_2O \rightarrow 15\ Fe^{2+} + 2\ SO_4^{2-} + 16\ H^+ \quad (3)$$

A Fe redox cycle is set in motion, and the Fe^{2+} formed in equation (3) is re-oxidized *de novo* microbiologically. Thus, pyrite is oxidized with a progressive, rapidly increasing rate. Reservoirs of Fe^{3+} exist as pools of dissolved Fe^{3+} and as various ferric sulfate and oxide minerals, which essentially stores Fe^{3+} until transport and/or dissolution allows this oxidant to come into contact with pyrite surfaces. Thus, the overall reaction for pyrite dissolution is given by:

$$FeS_2 + 3.5\ O_2 + H_2O \rightarrow Fe^{2+} + 2\ SO_4^{2-} + 2\ H^+ \quad (4)$$

Leaching of pyrite oxidation products into surrounded streams causes severe environmental problems due to increased acidity and high concentrations of dissolved metal(loid)s including iron, aluminum, copper, cadmium, manganese, arsenic, cobalt, chromium, etc. (Lundgren and Silver, 1980; Schippers *et al.*, 1996; Singh *et al.*, 1997). Abandoned mines are one of the main sources of freshwater pollution (Davis *et al.*, 2000; Druschel *et al.*, 2004; Younger, 2002). Acidity may be the most important variable governing ecotoxicity in AMD-impacted environments. Exposure to AMD kills not only most plant life (Hill *et al.*, 2000; Nixdorf *et al.*, 2001a) but also affects vertebrate (particularly shrimp and fish) and invertebrate organisms (hydras, flatworms, etc.) (Gerhardt *et al.*, 2004), along with microbial species that are indigenous to non-polluted waters (Johnson, 1995).

1.2 Acidic Microbial Fe-cycling

Biologically mediated Fe-cycling is performed by a number of prokaryotes that are capable of either Fe(II) oxidation and/or dissimilatory Fe(III) reduction, including respiratory growth with Fe(III) as the sole electron acceptor (Baker and Banfield, 2003; Kappler and Straub, 2005; Lovley, 2006). Highly concentrated Fe(II) can function as electron donor for Fe-

oxidizing microorganisms (FeOM) under both oxic and anoxic conditions forming Fe(III)-(oxy)hydroxides (Baker and Banfield, 2003; Weber *et al.*, 2006). Under extremely acidic conditions Fe(II) oxidation is solely mediated by microorganisms (Figure 1.1) as

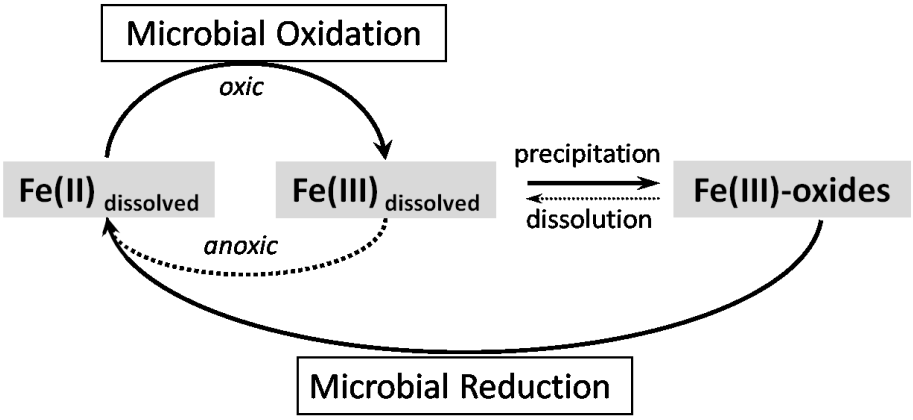

Figure 1.1. Microbial Fe-cycling at low pH conditions.

chemical Fe(II) oxidation is completely inhibited below pH < 4 (Meruane and Vargas, 2003) where microbes do not need to compete with chemical oxidation. The amorphous Fe(III)-(oxy)hydroxide products are attractive terminal electron acceptors for Fe-reducing microorganisms (FeRM) due to the high redox potential of the redox pair Fe^{3+} /Fe^{2+} at low pH (+770 mV at pH 1) close to the one of O_2/H_2O (Kappler and Straub, 2005) and the high solubility of Fe(III) under extremely acidic conditions. Therefore, prokaryotes involved in microbial Fe oxidation and reduction under acidic and pH-neutral conditions appear to be dissimilar.

A broad range of acidophilic Fe-cycling microorganisms (FeM) including FeOM and FeRM have been detected and/or isolated. *Acidithiobacillus*, *Thiobacillus*, *Leptospirillum, Ferrovum*, *Acidimicrobium, Ferrimicrobium, Ferrithrix, Alicyclobacillus, Sulfobacillus* and *Ferroplasma* are known FeOM, while *Acidiphilium*, *Acidocella, Acidisphaera, Acidobacterium, Serratia* and *Acidicaldus* are reported as FeRM (Johnson, 2009; Johnson and Hallberg, 2009). The characteristics of acidophilic FeM are quite unique compared to the neutrophilic ones. Many acidophilic FeRM prefer microoxic conditions to reduce Fe(III) (Johnson and McGinness, 1991) and some can co-respire oxygen and Fe(III) (Küsel *et al.*,

2002). A considerable fraction of acidophiles also have the capacity to both reduce and oxidize Fe, such as some species of *Acidithiobacillus, Acidimicrobium, Alicyclobacillus, Ferrimicrobium, Ferrithrix* and *Sulfobacillus* (Coupland and Johnson, 2008; Johnson, 2009).

For detecting and identifying microbial life in such acidic environments, a number of cultivation-dependent and -independent approaches are used, including solid media for isolation and nucleic acid based molecular tools. With novel techniques, such as quantitative PCR and the 'omics' approaches, sophisticated acidic microbial communities have been revealed. For example, significant progress has been made recently using metaproteomic analyses for the AMD site at Iron Mountain, California (Belnap *et al.*, 2010; Lo *et al.*, 2007; Ram *et al.*, 2005). Using this technique the complete protein suites were identified, followed by protein identification to link organisms and community structures. *Leptospirillum* was detected as the dominant FeOM and its *in situ* metabolic functions have been investigated. However, to date, this mass-spectrometry-based metaproteomic method has been applied to Iron Mountain AMD site merely.

1.3 Acidic Lignite Mine Lakes

During extensive surface lignite mining activities, many open pit mines are excavated below the zone of saturation of ground water. Surface water is diverted around open pits and dewatering pumps are used to control groundwater inflow and direct rainfall. Lignite mine lakes form when the pumps are shut off and post-mining drainage accumulates in the pit. Due to microbial Fe^{2+} oxidation in surface oxygenic water (Cornell and Schwertmann, 2003; Davison, 1993; Jönsson *et al.*, 2006; Murad and Rojik, 2005), these acidic lakes characteristically contain high amounts of acidity and sulfate (Geller *et al.*, 1998; Klapper and Schultze, 1995; Nixdorf *et al.*, 2001b), dissolved Fe(III) and poorly crystalline Fe(III)-(oxy)hydroxides or high Fe/S ratio oxyhydroxysulfates such as amorphous $Fe(OH)_3$, goethite

[α-FeOOH], schwertmannite [$Fe_8O_8(OH)_x(SO_4)_y$ with $1 \leq y \leq 1.75$, and $2y = 8 - x$] and jarosite [$KFe_3(OH)_6(SO_4)_2$].

In Lusatian district of Brandenburg and eastern Saxony, Germany, an interconnected chain of strip mining lakes was formed after flooding the mining area (Schultze and Geller, 1996) (Figure 1.2). Flooding started in 1965 to 1968 and was completed some years later. Many of the lakes that form the middle part of this chain were intensively studied for many years (Blodau *et al.*, 1998; Blöthe *et al.*, 2008; Friese *et al.*, 1998; Küsel, 2003; Nixdorf and Kapfer, 1998; Peine *et al.*, 2000; Porsch *et al.*, 2009; Wendt-Potthoff *et al.*, 2010). The surface areas of those lakes range from approximately 0.07 to 1 km^2 and the maximum depth of the lakes can reach 11 m. Temperatures in the lakes range from 2 to 26^oC, depending on the water depth and seasons and concentrations of sulfate range from 8 to 15 mM. Concentrations of nitrate, phosphate, and ammonium are negligible in the lake water (Karakas *et al.*, 2003; Peine, 1998). The acidic lakes receive their inflow mostly by a ditch connecting the lakes (Figure 1.2) and only secondarily from adjacent aquifer (Blodau, 2006). The acidity balances change considerably and systematically along the flow path. Lakes located down gradient of mine dumps receive most of their water (>50%) from the acidic, Fe(II)-rich underground AMD inflow. The pH of these lakes is approximately 3 and large amounts of iron precipitates are deposited onto the lake bottom. Within a few kilometers distance downstream, the acidic groundwater inflow diminishes and water residence time decreases. Lake 116, for instance, which is located only four lakes downstream from Lake 77 (Figure 1.2), receives 2.5% of the total water input from the surrounding dump aquifers and <1% from the remaining aquifer and thus has a water pH > 6 (Blodau, 2006; Weber, 2000). Most of these acidic mine lakes exhibit a dimictic water regime with an anoxic hypolimnion during summer stratification and a complete mixture of the water column during winter (Blodau *et al.*, 1998; Peine, 1998). However, few of the other lakes tend to be meromictic,

which means that the deepest part of the water body is excluded from seasonal overturn and thus from contact to the atmosphere (Boehrer and Schultze, 2006; Karakas *et al.*, 2003).

Lake 77 is the first lake that receives most of the AMD headwater in the chain of the

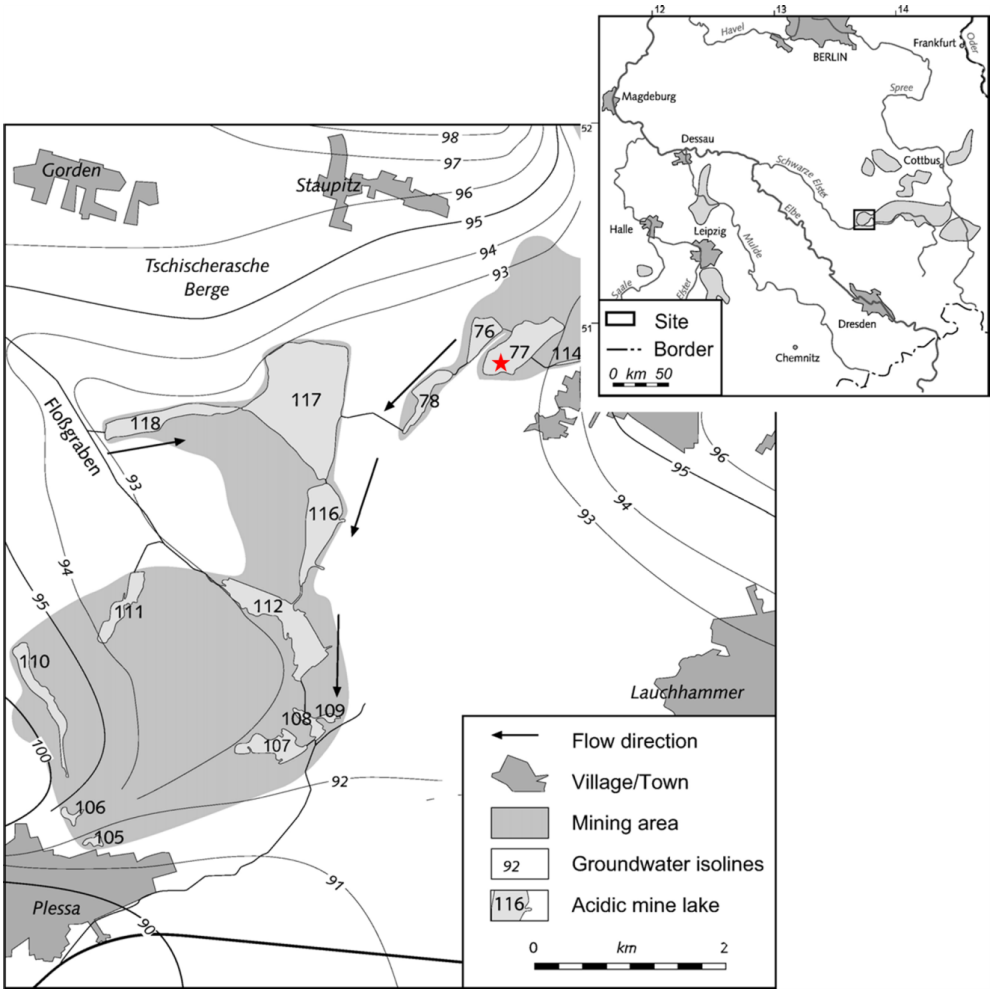

Figure 1.2. Map of the location of the interconnected chain of strip lignite mine lakes and surrounding areas in Lusatian, Brandenburg, Germany (Blodau, 2006).

interconnected mine lakes in Lusatian area (Figures 1.2 and 1.3). It was created after lignite mining activity had ceased in this area in the 1960s and studies on hydrology, microbiology and geochemistry data have accumulated since the early 1990s. (Blodau, 2006; Blöthe *et al.*, 2008; Küsel, 2003; Peine *et al.*, 2000). The lake has a surface area of ~ 0.24 km^2, a volume of ~ 1 km^3, and a maximum depth of about 9 m. The general pattern of water exchange is characterized by the Fe(II)- and sulfate-rich groundwater inflow from the dump area at the north end of the lake and the outflow of lake water to the aquifer in the south (Blodau, 2006).

The depth profiles of oxygen concentration in Lake 77 water demonstrate that the chemocline can shift from a depth of 6 m in January upwards to about 4 m in May (Peine, 1998). Due to water mixing from autumn, the concentration of oxygen reaches near

Figure 1.3. Panoramic photograph of acidic lignite mine Lake 77 in Lusatian area, Germany (photo courtesy of Marco Reiche).

saturation at the water-sediment interface during the period from winter to spring. However, in some years, the lake water keeps stratified, and the maximum oxygen concentrations close to the water-sediment interface reach only 2 to 7% during winter (Peine, 1998).

Fe(III)-rich aggregates form and precipitate in the oxic pelagic zone (Figure 1.4A, B) with high sedimentation rates of 570 g m^{-2} a^{-1} (Peine *et al.*, 2000), yielding a brownish orange and fluffy top sediment zone (zone I in Figure 1.4C). This zone has a pH close to lake water (~3) and is enriched with reactive iron, mainly schwertmannite whose formation requires oxic, acidic (pH 2.5–4), and sulfate-rich (> 10 mM) conditions (Bigham *et al.*, 1994; Blöthe *et al.*, 2008). Zone II is a yellowish-brownish sediment zone and zone III has dark stripes which are usually enriched in goethite (Blöthe *et al.*, 2008; Peine *et al.*, 2000). The remaining part of the sediment cores (zone IV) is brownish to black, has a higher density than upper zones, and goethite is the dominant Fe solid phase. The amount of reactive iron decreases with increasing sediment depth (Blöthe *et al.*, 2008; Peine *et al.*, 2000). In general, sediment cores from different sampling sites in this lake have similar appearances; however, differences were noticed in terms of color and density. Sediment cores from central part of

the lake always had a thicker yellowish-brown top layer with fewer dark stripes while those from northern area were less fluffy and darker colored.

Acidophilic microbial communities and microbial Fe-cycling and in Lake 77 sediment

Figure 1.4. Fe(III) forms a crust on a fallen tree at the shoreline of lignite mine Lake 77 (A, photo courtesy of Marco Reiche). The red-orange coloration of the lake shore is due to high levels of Fe(III) in the water; Fe(III) oxyhydrooxide particles formed in the lake water body (B); sediment core obtained from the central of Lake 77 showing four layers defined by the sediment color and density.

from the central part of the lake were studied previously (Blöthe *et al.*, 2008; Küsel and Dorsch, 2000; Küsel *et al.*, 1999; Küsel *et al.*, 2002; Peine *et al.*, 2000; Wenderoth and Abraham, 2005). The facultative anaerobe *Acidiphilium cryptum* JF-5 was isolated from sediments incubations showing anaerobic glucose-utilizing Fe(III)- reduction (Küsel *et al.*, 1999). The non-fermentative *A. cryptum* JF-5 can utilize several sugars, alcohols, H_2, and most organic acids of the tricarboxylic acid cycle under anoxic Fe(III)-reducing conditions. It was the first isolate shown to oxidize glucose completely to CO_2 with 83-102% of the glucose-derived reducing equivalents recovered in Fe(II). Cells of JF-5 grown under Fe(III)-reducing conditions form intracellular vesicles and protrusions and it can be speculated that an enlargement of the cytoplasmic membrane might facilitate contact of the cells with the electron accepter Fe(III). (Küsel *et al.*, 1999). Comparisons of soluble Fe(III) reduction

revealed that reduction rate of JF-5 is about 3 to 4 times higher than that obtained from *A. cryptum*^{T} (Küsel, 2003). Due to the absence of sulfide, Fe(II) formed in the upper 6 cm of the sediment diffuses to oxic zones in the water layer where it might be reoxidized by *Acidithiobacillus* species. Thus, acidic conditions are stabilized by the cycling of iron which inhibits fermentative and sulfate-reducing activities (Peine *et al.*, 2000). With increasing sediment depth, the amount of reactive iron decrease, the pH increases above 5, and fermentative and as yet unknown FeRM apprea to be involved in the dissimilatory reduction of Fe(III) (Küsel, 2003). Recently, research combining several molecular methods and isolation demonstrated that the bacterial phylum *Acidobacteria* is likely a major player in acidic Fe-cycling activities (Blöthe *et al.*, 2008). *Acidisphaera* and *Geobacter* are obtained by group-specific PCR, and phylogenetic analysis of clone libraries obtained from Fe(III)-reducing enrichment cultures grown at pH 5.5 reveals that betaproteobacterium *Thiomonas* is the majority of clones. The results show that the upper acidic sediment is inhabited by acidophiles or moderate acidophiles which can also reduce Fe(III) under slightly acidic conditions. The majority of Fe(III) reducers inhabiting the slightly acidic sediment have only minor capacities to be active under acidic conditions (Blöthe et al., 2008). However, it is still unclear that who are the key players of Fe-cycling in less acidic sediments of this lake.

1.4 Project Background and Research Aims

As mentioned above, previous work on geochemistry and microbiology of Lake 77 mostly focused on samples obtained from the central part of the lake. However, inflowing groundwater near the north shore line of the lake has higher pH (~ 4.5), higher ferrous iron (6-20 mM) and sulfate (5-60 mM) concentrations (Blodau, 2005). The inflow has changed the sediment pore water chemistry and triggered a further pH increase to around 5.5. Collectively, it could be speculated that due to the differences in geochemical conditions (especially the pH values) in the sediment from the north to the central section, microbial

communities in the north shore sediment might be dissimilar and dominated by less acid-tolerant microorganisms, including FeM.

The grant KU 1367/8-1 (Deutsche Forschungsgemeinschaft, DFG) was set to investigate the groundwater chemistry, biogeochemical characteristics and microbiology of the north shore sediment of Lake 77. This was a joint project between three research groups from the Friedrich Schiller University Jena and the University of Bayreuth. Dr. Marco Reiche (Friedrich Schiller University Jena) was responsible for investigating Fe(III) reduction in the pH-elevated sediment. The others from the University of Bayreuth were focused on groundwater inflow and pore water chemistry. I joined the research team to investigate the interaction of Fe-oxidizing and Fe-reducing microorganisms, and to elucidate the complex microbial functions in pelagic aggregates and sediments. This was supported by the Graduate School of Excellence "Jena School for Microbial Communication (JSMC)" (DFG).

Based on the previous research, the first hypothesis of this thesis was as follows:

I. Microbial communities in less acidic sediment cores from north shore of Lake 77 are different from those in central sediment cores. Less acid-tolerant FeM might be able to oxidize and reduce Fe.

To test this hypothesis, my goals were to 1) examine the indigenous microbial communities in north shore sediments using molecular tools and compare them to previous research; and 2) study the ecophysiology of acidic Fe-cycling bacterial isolates using cultivation-dependent methods.

Large amounts of rust-colored Fe(III)-rich aggregates form in Lake 77 within the water body, likely due to microbial Fe(II)-oxidation (Figure 1.4B). These aggregates precipitate as the fresh input to the sediment. Dr. Marco Reiche found color differences in the water and Fe(III)-rich aggregates between the north (higher water pH) and central parts (lower pH) of the lake. Therefore, the Lake 77 is a perfect spot for the research on the biogenic formation of these Fe(III)-rich aggregates at different pH conditions. I hypothesized that:

II. Different microbial communities dominate the Fe(III)-rich aggregates from different locations in Lake 77.

III. Due to water pH differences in the north and central parts of the lake, different FeOM communities are responsible for the microbial Fe(II) oxidation. As a result, dissimilar Fe(III) minerals are formed.

IV. The Fe-(III)-rich aggregates function as microbial hotspots for the microbial iron cycling.

To address these hypotheses, I investigated the bio-geo significance of the Fe(III)-rich particles from different locations and water depths of Lake 77, with a focus on Fe-cycling microbial communities.

1.5 Thesis Structure

The research in **chapter two**, "Ecophysiology of Fe-cycling bacteria in acidic sediments," aims to elucidate the diversity of microorganisms involved in iron cycling and to resolve their *in situ* functional links in sediments of the acidic lignite mine Lake 77. Using cultivation-independent and -dependent approaches, a variety of acidophilic microorganisms are highlighted that are responsible for iron cycling in acidic environments.

Chapter three is titled "Pelagic boundary conditions affect the biological formation of iron-rich particles (iron snow) and their microbial communities." The iron-rich particles formed at steeply opposing gradients of oxygen and Fe(II) within the redoxcline of the acidic lake. Since these particles have a high iron content and low organic carbon and are fundamentally different from organic-rich ''snows'' from lakes, rivers, and oceans a new term, "iron snow," is proposed. The bio-genesis and microbial communities of iron snow were also studied.

In **chapter four**, "Elucidating microbial communities and their metabolic functions in iron-rich aggregates (iron snow) of an acidic lake," iron snow samples from different

locations and water depths were studied for their biological formation and transformation processes using DNA-, RNA- and protein-level methods. A three-stage developmental model of iron snow is proposed, emphasizing the initiation step by chemoautotrophic Fe(II) oxidizing microorganisms.

The mineralogy of iron snow was investigated in **chapter five**, "Quantification of the inorganic phase of iron snow aggregates provides valuable information concerning aggregate formation" using quantitative Raman spectroscopy performed by Valerian Ciobotă, combined with molecular methods. The inorganic phase of iron snow samples from different basins and water depth were all composed primarily of schwertmannite, with slight differences in terms of other minerals. Surprisingly, the differences in microbial communities did not lead to strikingly qualitative dissimilarities in the mineral composition.

In "General Discussion" the complete Fe-cycling processes, from the iron snow to the sediment, and a number of important Fe-cycling microorganisms are summarized in detail. In addition, other metabolism activities within the iron snow, indicated by proteins related to motility, gas vesicles, CO_2-fixing *et al.*, were also discussed.

2 Ecophysiology of Fe-cycling bacteria in acidic sediments

Shipeng Lu, Stefan Gischkat, Marco Reiche, Denise M. Akob, Kevin B. Hallberg and Kirsten Küsel

Manuscript published in *Applied and Environmental Microbiology* (Dec. 2010) Vol. 76, pp. 8174-8183

Abstract

Using a combination of cultivation-dependent and -independent methods, this study aimed to elucidate the diversity of microorganisms involved in iron cycling and to resolve their *in situ* functional links in sediments of an acidic lignite mine lake. Using six different media with a pH ranging from 2.5 to 4.3, 117 isolates were obtained that grouped into 38 different strains including 27 putative new species with respect to the closest characterized strains. Among the isolated strains, 22 strains were able to oxidize Fe(II), 34 were able to reduce Fe(III) in schwertmannite, the dominant iron oxide in this lake, and 21 could do both. All isolates falling into the *Gammaproteobacteria* (an unknown *Dyella*-like-genus and *Acidithiobacillus*-related strains) were obtained from the top acidic sediment zones (pH 2.8). *Firmicutes* strains (related to *Bacillus* and *Alicyclobacillus*) were only isolated from deep, moderately acidic sediment zones (pH 4-5). Of the *Alphaproteobacteria*, *Acidocella*-related strains were only isolated from acidic zones, whereas *Acidiphilium*-related strains were isolated from all sediment depths. Bacterial clone libraries generally supported and complemented these patterns. *Geobacter*-related clone sequences were only obtained from deep sediment zone, and *Geobacter*-specific quantitative PCR yielded 8 x 10^5 gene copy numbers. Isolates related to *Acidobacterium*, *Acidocella*, *Alicyclobacillus*, and unknown *Dyella*-like-genus showed a broad pH tolerance ranging from 2.5 to 5.0, and preferred schwertmannite to goethite for Fe(III) reduction. This study highlighted the variety of acidophilic microorganisms that are

responsible for iron cycling in acidic environments, extending recent laboratory based studies that showed this trait to be widespread among acidophiles.

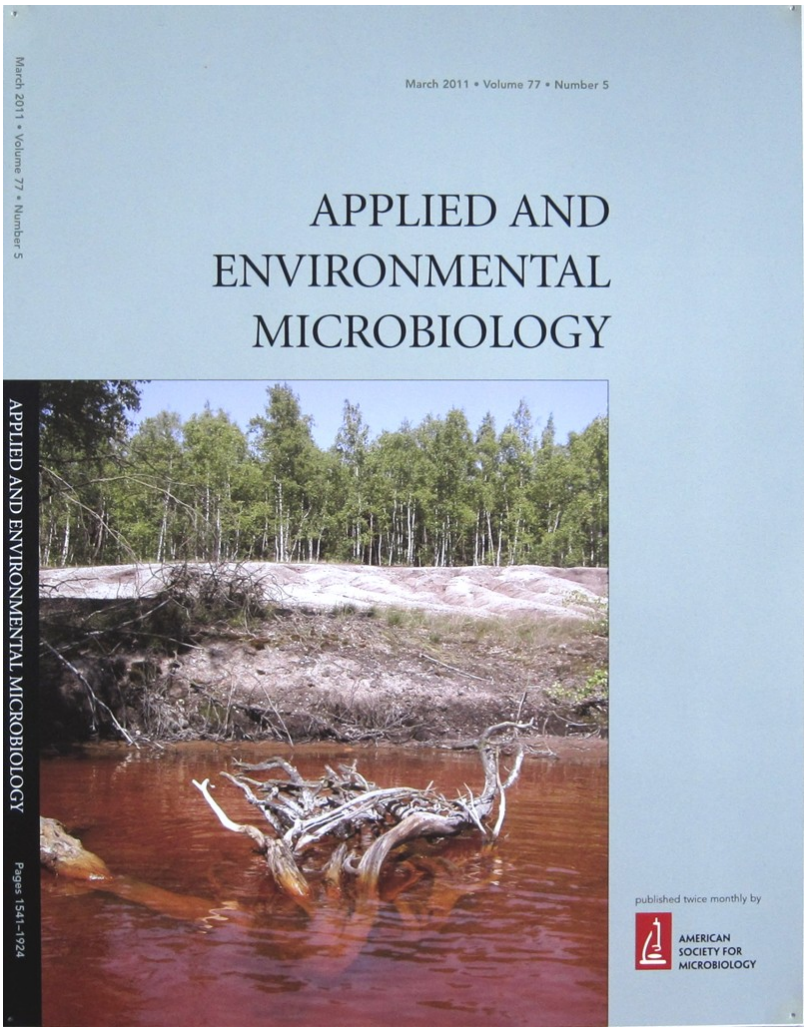

Cover photograph of Applied and Environmental Microbiology on March 2011. 77:(5) for the related article of Lu *et al*. (2010) 76: 8174-8183. (Copyright ©2011, American society for Microbiology, Photo by Marco Reiche)

APPLIED AND ENVIRONMENTAL MICROBIOLOGY, Dec. 2010, p. 8174–8183 Vol. 76, No. 24
0099-2240/10/$12.00 doi:10.1128/AEM.01931-10

Ecophysiology of Fe-Cycling Bacteria in Acidic Sediments[▽]†

Shipeng Lu,[1] Stefan Gischkat,[1] Marco Reiche,[1] Denise M. Akob,[1]
Kevin B. Hallberg,[2] and Kirsten Küsel[1]*

Institute of Ecology, Friedrich Schiller University Jena, Dornburger Strasse 159, D-07743 Jena, Germany,[1] and School of Biological Sciences, College of Natural Sciences, Bangor University, Bangor LL57 2UW, United Kingdom[2]

Received 13 August 2010/Accepted 13 October 2010

Using a combination of cultivation-dependent and -independent methods, this study aimed to elucidate the diversity of microorganisms involved in iron cycling and to resolve their *in situ* functional links in sediments of an acidic lignite mine lake. Using six different media with pH values ranging from 2.5 to 4.3, 117 isolates were obtained that grouped into 38 different strains, including 27 putative new species with respect to the closest characterized strains. Among the isolated strains, 22 strains were able to oxidize Fe(II), 34 were able to reduce Fe(III) in schwertmannite, the dominant iron oxide in this lake, and 21 could do both. All isolates falling into the *Gammaproteobacteria* (an unknown *Dyella*-like genus and *Acidithiobacillus*-related strains) were obtained from the top acidic sediment zones (pH 2.8). *Firmicutes* strains (related to *Bacillus* and *Alicyclobacillus*) were only isolated from deep, moderately acidic sediment zones (pH 4 to 5). Of the *Alphaproteobacteria*, *Acidocella*-related strains were only isolated from acidic zones, whereas *Acidiphilium*-related strains were isolated from all sediment depths. Bacterial clone libraries generally supported and complemented these patterns. *Geobacter*-related clone sequences were only obtained from deep sediment zones, and *Geobacter*-specific quantitative PCR yielded 8×10^5 gene copy numbers. Isolates related to the *Acidobacterium*, *Acidocella*, and *Alicyclobacillus* genera and to the unknown *Dyella*-like genus showed a broad pH tolerance, ranging from 2.5 to 5.0, and preferred schwertmannite to goethite for Fe(III) reduction. This study highlighted the variety of acidophilic microorganisms that are responsible for iron cycling in acidic environments, extending the results of recent laboratory-based studies that showed this trait to be widespread among acidophiles.

Biologically mediated iron (Fe) cycling is performed by a number of prokaryotes that are capable of either ferrous iron [Fe(II)] oxidation or/and of dissimilatory ferric iron [Fe(III)] reduction, including respiratory growth with Fe(III) as the sole electron acceptor (43, 55, 56, 68). While Fe(III) exists predominantly in the solid phase as oxyhydroxide minerals at circumneutral pH, Fe(III) tends to be more soluble under extremely acidic conditions. This, coupled with the high redox potential of the redox pair Fe^{3+}/Fe^{2+} (+770 mV) at pH 1 compared with that of equivalent couples at neutral pH [ranging from +100 mV to −300 mV depending on the form of Fe(III) mineral (68)] makes ferric iron an attractive alternative to molecular oxygen as an electron acceptor. Therefore, prokaryotes involved in the microbial reduction of Fe(III) under acidic and pH-neutral conditions appear to be dissimilar.

The potential for Fe(III) reduction seems to be widespread among acidophilic heterotrophs (15), including bacteria of the genera *Acidiphilium* (15, 38, 51) and *Acidocella* (15), *Acidicaldus organivorans* (44) and *Acidimicrobium ferrooxidans* (10), *Ferrimicrobium acidiphilum* (36), *Ferrithrix thermotolerans* (36), and *Acidobacterium* spp., including the type strain *Acidobacterium capsulatum* DSM 11244^T (7, 15). Some, such as *Ferrimicrobium acidiphilum* and *Ferrithrix thermotolerans*, even have the capacity to oxidize Fe(II) with oxygen as the electron acceptor, a trait shared with the two chemolithoautotrophs *Acidithiobacillus ferrooxidans* (47) and *Acidithiobacillus ferrivorans* (26). Other reported non-Fe(III)-reducing Fe(II) oxidizers are *Acidianus brierleyi* (66), *Alicyclobacillus ferrooxydans* (35), *Leptospirillum ferrooxidans* (30), *Leptospirillum ferriphilum* (13), *Sulfobacillus acidophilus* (58), *Sulfolobus metallicus* (33), *Thiomonas* spp. (39), and *Ferroplasma* spp. (21). Most Fe(III) reducers cultured to date have no or only a minor capacity to reduce Fe(III) over a pH range from 3 to 6. *Acidiphilium cryptum* (ATCC 33463) and *Acidobacterium capsulatum* can reduce small amounts of Fe(III) up to pH 5 (6, 7), and the acidotolerant *Serratia*-related Mam Tor isolate reduces chelated Fe(III) at similar rates from pH 3 to 6 (1). However, due to the lack of a common functional gene marker and the lack of studies in the moderately acidic pH range (pH 4 to 5), the diversity of prokaryotes which are able to reduce Fe(III) is probably underestimated.

A number of acidic locations have been studied in the last 10 years with respect to Fe cycling, ranging from extremely acidic mine drainage within the Richmond Mine system, Iron Mountain, CA (20), to less acidic mine tailings (25, 70), acidic rivers (23), acidic lakes (7, 49, 61), and moderately acidic subsurface sediments and peatlands (50, 60). While proteomic analyses have greatly extended our knowledge about the ecophysiology of microbes inhabiting an extreme site with low diversity (5, 17), laboratory isolates are still paramount for a detailed analysis of their unique biological traits. We have studied Fe cycling in sediments of lignite mine lakes that are characterized by high concentrations of Fe(II), sulfate, and protons due to the oxidation of pyrite in the surrounding mine tailings (49). Microbial Fe(II) oxidation in the water column yields poorly

* Corresponding author. Mailing address: Aquatic Geomicrobiology Group, Institute of Ecology, Friedrich Schiller University Jena, Dornburger Strasse 159, D-07743 Jena, Germany. Phone: 49-3641-949461. Fax: 49-3649-949402. E-mail: kirsten.kuesel@uni-jena.de.

† Supplemental material for this article may be found at http://aem.asm.org/.

▽ Published ahead of print on 22 October 2010.

TABLE 1. Geochemistry of the north and deep central sediment cores obtained from lignite mine Lake 77

Sediment zone	Depth (cm)	pH	Amt (mM) of:			
			Fe(II)		Fe(III)	
			Dissolved[a]	HCl extracted[b]	Dissolved	HCl extracted
North I	0–1	2.8	4.5	17.4	ND[c]	211.7
North II	1–4	2.9	7.3	13.1	ND	87.5
North III	4–10.5	3.7	15.1	11.9	ND	ND
North IV	10.5–20.5	5.3	12.5	30.6	ND	ND
Deep I	0~1	2.7	1.5	7.0	ND	81.0
Deep II	1~4	2.9	4.6	11.9	ND	129.7
Deep III	4~10.5	3.2	5.9	13.8	ND	10.9
Deep IV	10.5~20.5	4.1	4.2	16.3	ND	ND

[a] Fe measured in the supernatant after centrifugation.
[b] Fe measured after preextraction of sediment in 0.5 M HCl.
[c] ND, not detected.

crystalline Fe(III) oxides that precipitate to the sediment, where they can be utilized as electron acceptors (51). Within 20 cm of the sediment surface, the pH in the sediment increases from 2.8 to 6, and previous molecular-based research has revealed a pH gradient-induced heterogeneity of Fe(III)-reducing microorganisms (7). However, the key drivers of iron reduction could not be identified in those studies. Here, we used a combination of cultivation-dependent and -independent approaches to elucidate the diversity of microorganisms involved in Fe cycling in the same lignite mine lake. With this approach, we extend the previous work to get a concrete handle on those microbes responsible for the reductive half of the cycle. The study of individual isolates can reveal the ecophysiology of potential drivers of Fe(III) reduction at low pH.

MATERIALS AND METHODS

Field site description and sampling. The acidic lignite mine lake (Lake 77) is located in Lower Lusatia near Lauchhammer in east-central Germany, a historical region which was shaped by the lignite industry and extensive open-pit mining. It is a dimictic lake with an anoxic hypolimnion during summer stratification. During each sampling period, pH, dissolved oxygen, and temperature were measured over the depth at the deep central part of the lake with a U-10 multiparameter water quality meter (Horiba, Japan). Sediment cores were obtained on the north shore line in 3 m of water (North) and in the deep central basin in 7 m of water (Deep) using a gravity corer equipped with Plexiglas tubes (60 cm in length) (see Fig. S1 in the supplemental material). The Deep site has been studied intensively over the last 12 years (7, 51, 59). A total of 3 cores were obtained during each sampling period (July 2008, November 2008, and December 2008) from each site, transported to the laboratory at 4°C, sectioned under anoxic conditions according to visual differences in stratification, and characterized geochemically (Table 1). Northern cores were used for DNA extraction (July 2008) and for potential Fe(III) reduction rate measurements (November 2008). Cores obtained from both sites after the lake became mixed were used for oxygen profile measurements (November 2008) with a microelectrode (tip diameter, 100 μm; Unisense, Aarhus, Denmark) connected to a picoammeter (PA2000; Unisense, Aarhus, Denmark) and for isolation studies (December 2008). The North cores contained an orange, fluffy upper sediment zone (North I) (dry weight, 13.3%) that was enriched with reactive iron, mainly schwertmannite [$Fe_8O_8(OH)_x(SO_4)_y$] (64). The second sediment zone (North II) was yellowish brown (see Fig. S1 in the supplemental material). The third sediment zone (North III) had dark stripes, and the remaining part of the sediment cores (North IV) was brownish to black and had a higher density (dry weight, 28.4%), with goethite (α-FeOOH) as the dominant Fe solid phase (59). In general, Deep core sediments (Deep I to IV) had a yellowish-brown color with fewer dark stripes (see Fig. S1 in the supplemental material).

Sediment Fe(III) reduction measurement. To study potential Fe(III) reduction, 20 g (fresh weight) of homogenized sediment were mixed under a continuous flow of sterile nitrogen with 10 ml of an anoxic 0.7% NaCl solution and placed into a sterile 180-ml incubation flask (Mueller & Krempel, Buelach, Switzerland). Flasks were closed with rubber stoppers and screw caps and incubated in the dark at 15°C with an initial overpressure of ~100 mbar in three replicates. The formation of Fe(II) during 9 days of incubation was determined by measuring the amount of Fe(II) after acid extraction (7). Fe(III) reduction rates were calculated from the linear increase of Fe(II) formation. HCl-extractable Fe(III) was calculated from the increase in Fe(II) concentration after the addition of ascorbic acid.

DNA extraction and PCR amplification. Samples from North I and North IV of the July 2008 core were pelleted by centrifugation, and amounts of 0.25 to 0.3 g of sediment (wet weight) were used for DNA extraction with a PowerSoil DNA kit according to the manufacturer's instructions (Mo Bio Laboratories, Solana Beach, CA). Aliquots of purified DNA were PCR amplified (Primus 96 advanced; Peqlab, Germany) using either the bacterial small-subunit rRNA gene-specific forward primer 27F (53) or the archaeal forward primer ARC363F (63) together with the universal reverse primer 1492R (57) for clone library construction. In addition, phylogenetic-group-specific primers for *Anaeromyxobacter*, *Acidiphilium*, and *Geothrix* "bioleaching-associated bacteria"(7) and for *Shewanella* (71) were used. The primer set specific for acidophilic bioleaching-associated bacteria detects seven bacterial phylotypes (*Acidithiobacillus ferrooxidans*, *Acidithiobacillus thiooxidans*, *Acidithiobacillus caldus*, *Sulfobacillus thermosulfidooxidans*, *Leptospirillum ferrooxidans*, *Acidiphilium cryptum*, and *Acidiphilium organovorum*) which are involved in the bioleaching of mineral ores. Bacterial isolates were picked and resuspended in 100 μl of 5% (wt/vol) Chelex-100 (Bio-Rad, United States) solution in 0.5-ml tubes. The tubes were then boiled in a water bath for 10 min, followed by 2 min of centrifugation at maximum speed. For the few isolates which failed to produce any PCR amplicon, a lysis solution (0.05 M NaOH and 0.25% SDS) was used following the method given by Johnson et al. (43). One or 2 μl of the supernatant served as template for bacterial 16S rRNA gene PCR with the universal primers 27F and 1492R.

Quantitative PCR for detecting *Geobacter* isolates was performed using *Geobacteraceae*-specific 16S rRNA gene primers 561F (69) and Geo858R (5′-CTAGGTGTTGCGGGTATTGA-3′) and 10 ng of purified environmental DNA as the template in the reaction mixture SensiMix LowRef (Quantace, distributed by Bioline GmbH, Luckenwalde, Germany). Thermocycling was performed with the following temperature program: 10 min at 95°C and 50 cycles of 15 s at 95°C, 30 s at 61°C, 30 s at 72°C, and 10 s at 78°C. Fluorescence measurements were made at 61, 72, and 78°C for each cycle, followed by a dissociation curve analysis with 1 min at 95°C, 30 s at 55°C, and heating to 95°C at a rate of 0.01°C s^{-1}. Genomic DNA from a pure culture of *Geobacter sulfurreducens* (DSM 12127) was used as the standard. Reactions that yielded cycle threshold (C_T) values with less than a three-cycle difference from those of nontemplate controls were considered to be within the error of measurement.

16S rRNA gene library construction and statistical analysis. For bacterial clone libraries, purified PCR products were ligated into the pGEM-T vector (Promega, United States) and transformed into *Escherichia coli* cells according to the manufacturer's instructions. Amplified rRNA gene restriction analysis (ARDRA) with restriction enzymes HhaI and BsuRI (HaeIII) (Fermentas, Canada) was applied, and clones were subsequently grouped into operational taxonomic units (OTUs) according to their ARDRA banding patterns. Representative clones of the respective OTUs were sequenced at Macrogen, Inc. (South Korea). For archaeal libraries, purified PCR products were ligated into the pCR4-TOPO vector (Invitrogen, United States) and sent to the Genome Center at Washington University, St. Louis, MO, for downstream processing. All sequences were pooled, assembled, end trimmed, and revised using Geneious Pro software (Biomatters Ltd., New Zealand). The sequences were checked for chimeric properties using the Bellerophon chimera detection program (34) and Chimera Check from Ribosomal Database Project II (11). The sequences were then aligned using the greengenes Align tool (18) and dereplicated using FastGroupII (76) with the percentage sequence identity method with gaps of 97% similarity. The phylogenetic affiliations were assigned using the greengenes Compare tool (18). Rarefaction curves and percent coverage were calculated using Analytic Rarefaction 1.3 (http://www.uga.edu/strata/software/anRareReadme.html) (32). EstimateS (12) was used to calculate the abundance-based coverage estimator (ACE), incidence-based coverage estimator (ICE), and Chao1 values, as well as the Shannon and Simpson's diversity indices.

Isolation of acidophilic microorganisms. One-gram subsamples of sediment from North core zones I and IV and from Deep core zones I and IV were diluted with 4 ml of filter-sterilized lake water (pH ~ 3) and homogenized by shaking for 30 min at ~1,000 rpm (Vortex-Genie2 shaker; Scientific Industries, United States). Samples were serially diluted (10^0 to 10^{-2}) with filter-sterilized lake water, and 100 μl of each dilution was plated in triplicate on one of several

selective solid overlay media specific for different groups of autotrophic and heterotrophic acidophilic microorganisms (40). These were (i) ferrous iron overlay medium (Feo, final pH 2.5) with tryptone soya broth (TSB; Oxoid, United Kingdom), (ii) ferrous sulfate and potassium tetrathionate overlay medium with TSB (FeSo, final pH 2.5), (iii) inorganic ferrous iron overlay medium without TSB (iFeo, final pH 2.5), (iv) ferrous iron and sodium thiosulfate (0.01 M) overlay medium with TSB (FeTo, final pH 4.3), and yeast extract overlay medium at (v) pH 3 (YE3) or (vi) pH 4 (YE4). Cycloheximide (Carl Roth, Germany) was added into the top-layer medium at 50 μg ml^{-1} to inhibit fungal growth. All plates were incubated at room temperature (~20°C) in the dark and checked frequently. The picked colonies were transferred at least 5 times, and purity was controlled both by colony morphology assessment and microscopic examination (Axiovert 25; Carl Zeiss, Germany). Fe(II) oxidation capacities were determined by the appearance of an orange Fe rust color of the colonies due to the microbial oxidation of ferrous sulfate contained in the media. Heterotrophic bacteria obtained from yeast extract media were transferred to other ferrous sulfate-containing media to determine their Fe(II) oxidation capacities. Purified colonies were screened by ARDRA, and representative OTUs were chosen for sequencing. Isolates were grouped if the 16S rRNA gene sequences and colony morphologies were identical. The cultivated strains and type strains closest to these isolates were determined through the online BLAST database (45) and EzTaxon server (9), respectively. Strain designations were assigned as follows, by combining information about the medium, source, and isolate number separated by hyphens. The first part designates the type of medium, and the second part designates the origin of the sediment, e.g., D1 or D4 means the Deep site of the lake (D) and either the upper sediment zone I (1) or the deeper sediment zone IV (4). N1 or N4 means the North shore site of the lake (N) and either the upper sediment zone I (1) or the deeper sediment zone IV (4). The next number is the sequential number of the isolate, and CH designates the presence of cycloheximide if it was added.

Fe(III) reduction assays of isolates. All the isolates obtained were first inoculated into 5 ml of liquid medium (same media as described above but without agarose) with fructose as the electron donor and incubated at room temperature on a rotary shaker. The Fe(III)-reducing capacities of the grown isolates were determined under microoxic and anoxic conditions in the dark. Microoxic conditions were established in sterile 150-ml conical flasks filled with 100 ml of sterile liquid medium (15, 38), while anoxic conditions were established using 20 ml of medium flushed with nitrogen (N_2) gas in 30-ml serum bottles (Wheaton, United States) in an anaerobic chamber (100% N_2 gas phase). The bottles were sealed with rubber stoppers and aluminum caps. After the medium was autoclaved, filter-sterilized fructose (~10 mM final concentration) and 100 mg schwertmannite (equivalent to 10 mM) were added as an electron donor and acceptor, respectively. Reduction assays started after the addition of 1 or 2 ml of active cultures into the flasks and bottles at room temperature. Uninoculated flasks or bottles were used as controls. Selected isolates (YE3-D1-10-CH [a strain of an unknown *Dyella*-like genus], FeSo-D4-20-CH and YE4-D4-4i-CH [*Alicyclobacillus*-related strains], YE3-D1-20 [an *Acidobacterium*-related strain], and YE4-N1-5-CH [an *Acidocella*-related strain]) were studied in more detail for their Fe(III)-reducing capacities by using 5 mM fructose and (i) chelated Fe(III) citrate (50 mM) and Fe(III) pyrophosphate (40 mM) under strict anoxic conditions and (ii) either artificially synthesized schwertmannite or goethite (10 mM) (14, 64) under microanoxic conditions. Potential microbial contamination in synthesized schwertmannite, which could not be autoclaved, was checked by spreading 0.5 ml of the suspension onto different overlay plates as described above and, also, on nutrient-rich Luria-Bertani agar plates. No growth was observed. Samples (1 ml) were taken from the flasks or bottles at intervals and used for measuring pH (Semi-Micro pH meter; Mettler Toledo, Switzerland) and Fe(II) concentration.

Nucleotide sequence accession numbers. The 16S rRNA gene sequences determined in this study have been deposited in the EMBL database under accession numbers FN870189 to FN870350.

RESULTS

Biogeochemical characteristics of sediment cores. Sediments obtained from the North site contained higher concentrations of dissolved and HCl-extractable Fe(II) than those from the deep part of the lake (Table 1). Similarly, the sulfate concentrations were higher in North (19.7 to 27.8 mM) samples than in Deep sediments (8.1 to 11.9 mM), suggesting a higher input from the surrounding mine tailings. Nonetheless, the pH was highest in North IV, reaching 5.3 (Table 1). The pH of the Deep sediment cores did not increase beyond 4.1 with depth, which was in contrast to the results of earlier studies (7, 49, 59). After seasonal mixing of the lake water in autumn, the dissolved oxygen concentration of the water in the center (Deep) of the lake was stable at 88% saturation near the surface and 83% above the sediment. However, oxygen microprofiles measured in the North and Deep sediment cores declined sharply, to levels below the detection limit for O_2 (314.9 μmol $liter^{-1}$), from the water sediment interface to within 2 and 10 mm deep, respectively (see Fig. S1 in the supplemental material). Anoxic Fe(III) reduction rates approximated 1.37 and 2.08 μmol g^{-1} (dry weight) day^{-1} in North I and North II samples, respectively, but were not detectable in North III or IV samples. Deep core sediment Fe(III) reduction rates approximated 6.19 and 1.2 μmol g^{-1} (dry weight) day^{-1} when sediments from depths of 0 to 6 and 6 to 10.5 cm, respectively, were incubated.

16S rRNA gene-based analyses of North sediments. As had been done in previous work with Deep sediments (7), we tried to identify microorganisms potentially involved in Fe cycling in the North I and IV sediment zones by using primer sets for known phylogenetic groups of bacteria and general primer sets for *Bacteria* and *Archaea*. PCR products were obtained from North I for the acidophilic genus *Acidiphilium* and bioleaching-associated bacteria but not for Fe(III)-reducing, neutrophilic bacteria of the genera *Anaeromyxobacter*, *Geothrix*, *Geobacter*, and *Shewanella*. However, with the newly designed primer set for quantitative PCR, *Geobacter* genes could be amplified, and copy numbers approximated 8.34×10^5 g^{-1} (fresh weight sediment) in North IV but only 4.89×10^3 g^{-1} (fresh weight sediment) in North I.

Totals of 127 and 144 clones of bacterial 16S rRNA genes from North I (BacI) and North IV (BacIV) were screened, and ARDRA revealed 36 and 65 distinct phylotypes, respectively (Table 2). There were no identical phylotypes present in either library based on FastGroupII results. The rarefaction curves did not indicate saturation (data not shown), and coverage was 81.4% for the BacI and 61.7% for the BacIV library. The ACE, ICE, and Chao1 values and the Shannon and Simpson's diversity indices indicated a higher diversity in the BacIV than in the BacI library (Table 2). The most frequently detected lineage in the BacI library was the *Actinobacteria* (37% of all clones), with members of the *Alphaproteobacteria* and *Cyanobacteria* each comprising 15.0% and 14.2% of the total clones, followed by *Gammaproteobacteria* (11.8%), *Acidobacteria* (9.4%), and *Firmicutes* (7.1%) (Fig. 1). The most frequently detected lineages in the BacIV library were *Deltaproteobacteria* (27.8%), *Acidobacteria* (22.9%), *Firmicutes* (9.7%), and *Nitrospirae* (8.3%). More lineages were detected in zone IV than in zone I (Fig. 1).

A total of 53 and 40 archaeal clones from the North I (ArcI) and North IV (ArcIV) libraries were screened, yielding 8 and 25 distinct phylotypes, respectively, based on ARDRA (Table 2). Again, identical phylotypes were not detected in both libraries, and indices indicated higher diversity in the ArcIV library than in the ArcI library (Table 2). The percent coverage was 79.3% for the ArcI and 38.2% for the ArcIV library. Only *Crenarchaeota* were detected in the ArcI library (17.5%), whereas members of the *Euryarchaeota* comprised 100 and 82.5% of the clones in zones I and IV, respectively (Fig. 1).

TABLE 2. Statistical analysis of 16S rRNA gene clone libraries using ecological and molecular estimates of phylotype diversity

Sediment sample[a]	No. of clones	No. of phylotypes	% Coverage	ACE[b]	ICE[c]	Chao1 ± SD	Diversity index	
							Shannon	Simpson's (1/*D*)
BacI	127	36	81.4	42.5	36	43.7 ± 5.6	3.13	17.39
BacIV	144	65	61.7	119.1	65	126.3 ± 29.4	3.85	40.54
ArcI	53	8	79.3	9.5	8	12.5 ± 7.2	1.27	2.34
ArcIV	40	25	38.2	38.1	25	41.1 ± 11.0	3.08	33.91

[a] BacI and BacIV designate the bacterial 16S rRNA gene clone libraries obtained from the northern shore of the lake from either the upper sediment zone I or the deeper sediment zone IV. ArcI and ArcIV designate the archaeal 16S rRNA gene clone libraries obtained from the northern shore of the lake from either the upper sediment zone I or the deeper sediment zone IV.
[b] ACE, abundance-based coverage estimator.
[c] ICE, incidence-based coverage estimator.

The *Sulfolobaceae* family was the only family detected in the phylum *Crenarchaeota*, whereas the phylum *Euryarchaeota* consisted of various families each representing 1.9 to 86.8% of the total clones in the ArcI and 7.5 to 37.5% in the ArcIV libraries (Fig. 1B; also see Table S3 in the supplemental material).

Isolation of acidophilic or acidotolerant microorganisms and their Fe(II)-oxidizing capacities. Media were chosen with a pH range to cover the pH range of the sediment in order to isolate acidophilic or acidotolerant Fe(II) oxidizers, aerobic heterotrophs, and potential Fe(III) reducers. Colonies appeared from 5 to 14 days after inoculation with North and Deep zone I and IV sediment dilutions. Based on the colony morphologies and the types of media, more than 240 single colonies were picked and isolated. From these, 117 isolates were grouped according to ARDRA fragment patterns (16, 13, 22, 21, 18, and 27 patterns from Feo, FeSo, FeTo, iFeo, YE3, and YE4 selective medium, respectively). The 16S rRNA genes of 38 representatives were sequenced (2, 8, 7, 2, 7, and 12 from Feo, FeSo, FeTo, iFeo, YE3, and YE4 medium, respectively),

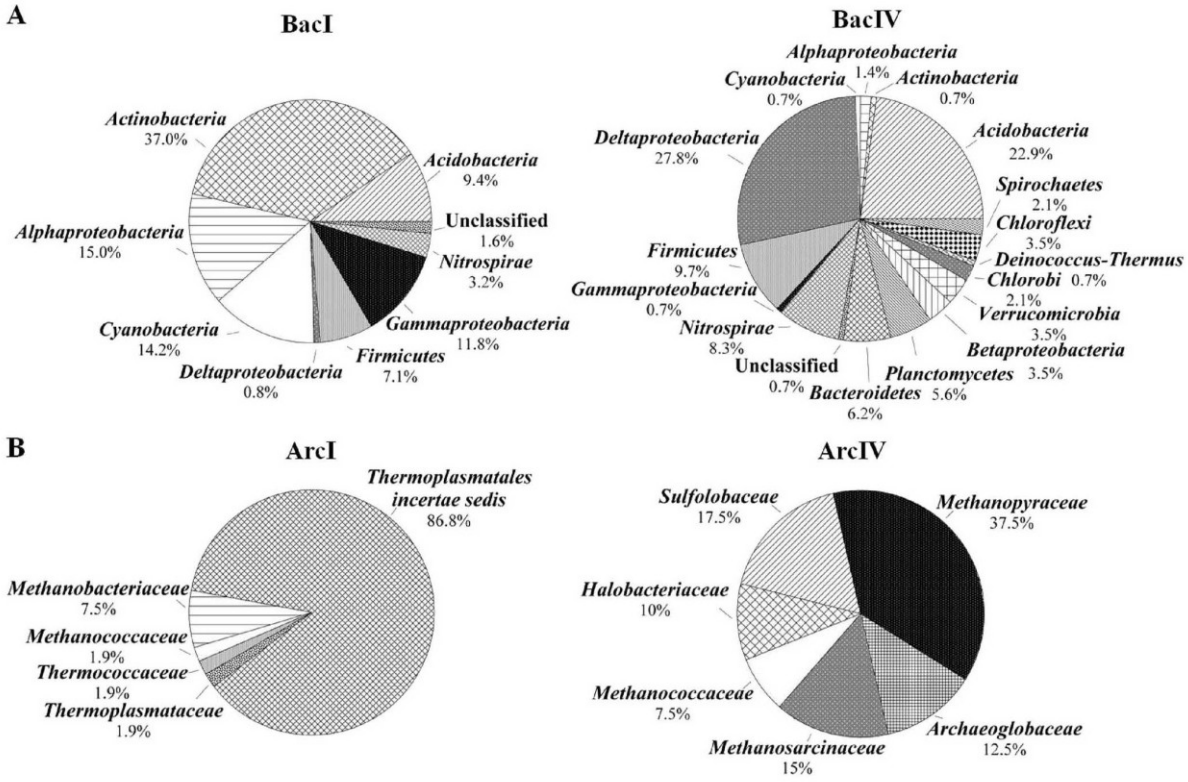

FIG. 1. Frequencies of bacterial (A) and archaeal (B) phylogenetic lineages detected in 16S rRNA gene clone libraries derived from sediment zones North I (BacI and ArcI) and North IV (BacIV and ArcIV) of a core obtained from the northern basin. Calculations were based on the total number of clones associated with phylotypes of sequenced representatives at the phylum or class level for *Proteobacteria* for *Bacteria* libraries and the family level for *Archaea* libraries.

TABLE 3. Bacterial isolates from acidic lignite mine lake sediments using 6 different agarose overlay plates, with taxonomic status, identity values based on analysis of 16S rRNA gene sequences, and the results of microoxic and anoxic Fe(III) reduction experiments and Fe(II) oxidation capacities observed on Fe(II)-containing agarose overlay plates

Representative strain[a]	No. of isolates[b]	Closest type strain (GenBank sequence accession no., % identity)	Fe-cycling capacity			
			Reported (reference[s])[c]	Oxidation[d]	Microoxic reduction[f]	Anoxic reduction[f]
YE3-D1-20	1	*Edaphobacter modestus* Jbg-1^T (DQ528760, 93.9)	UO, R (7, 25)	− (Feo)	+	+
YE4-D4-2-CH	2	*Streptomyces ferralitis* SFOp68^T (AY262826, 98.4)	UO, UR	NA[e]	+	+
FeSo-D1-6-CH	1	*Ferrimicrobium acidiphilum* T23^T (AF251436, 99.4)	O, R (36)	+	+	+
YE4-D4-16-CH	1	*Actinocorallia aurea* IFO 14752^T (AB006177, 94.2)	UO, UR	− (FeTo)	+	(−)
YE4-D4-1-CH	1	*Bacillus acidicola* 105-2^T (AF547209, 99.8)	UO, UR	NA	+	(−)
YE4-D4-4-CH	1	*Bacillus pocheonensis* Gsoil 420^T (AB245377, 99)	UO, UR	− (FeTo)	+	(+)
YE3-D4-3i-CH	2	*Alicyclobacillus contaminans* 3-A191^T (AB264026, 89.6)	O (37), UR	+ (iFeo)	+	+
iFeo-D4-31-CH	1	*Alicyclobacillus contaminans* 3-A191^T (AB264026, 90.6)	O, R (42)	+	−	+
YE3-D4-31i-CH	3	*Alicyclobacillus ferrooxydans* TC-34^T (EU137838, 98.6)	O (72), UR	+ (FeTo)	+	+
Feo-D4-16-CH	1	*Alicyclobacillus ferrooxydans* TC-34^T (EU137838, 91.4)	O, R (42)	+	+	+
FeSo-D4-20-CH	1	*Alicyclobacillus pomorum* 3A^T (AB089840, 91)	O (19), UR	+	+	(−)
FeSo-N4-1-CH	2	*Alicyclobacillus tolerans* K1^T (AF137502, 95.1)	O (72), UR	+	+	+
YE4-D4-4i-CH	2	*Alicyclobacillus tolerans* K1^T (AF137502, 94.9)	O (72), UR	+ (FeTo)	+	+
Feo-N4-15-CH	1	*Alicyclobacillus tolerans* K1^T (AF137502, 100)	O, R (46)	+	+	+
FeSo-N4-2-CH	1	*Sulfobacillus acidophilus* DSM 10332^T (AB089842, 94.2)	O (58, 72), UR	−	+	+
FeSo-N4-3-CH	1	*Sulfobacillus thermotolerans* Kr1^T (DQ124681, 99.1)	O, R (42)	+	+	+
FeSo-D1-15-CH	1	*Acidiphilium acidophilum* ATCC 27807^T (D86511, 99.8)	UO, R (38)	−	+	+
YE3-D4-63i-CH	1	*Acidiphilium acidophilum* ATCC 27807^T (D86511, 98.2)	UO, R (38)	NA	+	+
YE3-D1-35	1	*Acidiphilium cryptum* ATCC 33463^T (D30773, 100)	UO, R (6, 51)	NA	+	+
FeTo-D1-1-CH	1	*Acidisphaera rubrifaciens* HS-AP3^T (D86512, 99.7)	UO, NR (15)	−	−	(−)
YE4-N1-5-CH	2	*Acidocella facilis* ATCC 35904^T (D30774, 97)	UO, R (15)	− (FeTo)	+	+
FeTo-D4-17-CH	1	*Methylocella tundrae* T4^T (AJ555244, 99.9)	UO, UR	+	−	(−)
YE3-D4-2i-CH	1	*Methylocapsa acidiphila* DSM 13967^T (AJ278726, 98.6)	UO, UR	NA	(−)	(−)
YE4-D1-1-CH	1	*Thiomonas cuprina* NBRC 102094^T (AB331953, 98.8)	UO, UR	− (FeTo)	+	−
YE3-D1-10-CH	4	*Dyella yeojuensis* R2A16-10^T (DQ181549, 94.3)	O, R (15, 72)	+ (FeTo)	+	+
FeSo-D1-9-CH	1	*Acidithiobacillus ferrivorans* NO-37^T (AF376020, 99.4)	O, R (26)	+	+	(−)
FeSo-N1-1-CH	1	*Acidithiobacillus ferrooxidans* ATCC 23270^T (AF465604, 99.3)	O, R (26)	+	+	(−)
FeTo-N1-3-CH	1	*Acidithiobacillus ferrooxidans* ATCC 23270^T (AF465604, 99.5)	O, R (26)	−	+	(−)

[a] Strain designation was constructed as follows, by combining information about the medium, source, and isolate number separated by hyphens. The first part designates the medium type, the second part designates the origin of the sediment, e.g., D1 or D4 means deep site of the lake (D) and either upper sediment zone I (1) or deeper sediment zone IV (4). N1 or N4 means north shore site of the lake (N) and either upper sediment zone I (1) or deeper sediment zone IV (4). The next number is the sequential number of the isolate, and CH designates the presence of cycloheximide (CH) if it was added. The pHs of the media Feo, iFeo, FeSo, FeTo, YE3, and YE4 were 2.5, 2.5, 2.5, 4.3, 3.0, and 4.0, respectively. Strains which appear to be putative new species are presented in boldface.

[b] A number greater than one indicates that isolates were grouped based on identical 16S rRNA gene sequences and colony morphologies on the plates.

[c] Known Fe redox capacities of the closest cultivated strains based on the literature: O means Fe(II) oxidation; R means Fe(III) reduction; NO means no Fe(II) oxidation; NR means no Fe(III) reduction; UO means unknown for Fe(II) oxidation function; and UR means unknown for Fe(III) reduction.

[d] Colonies from yeast extract media were checked for Fe(II) oxidation capacities on iron-rich media. +, positive for Fe(II) oxidation; −, negative for Fe(II) oxidation. The medium code in brackets indicates the iron-rich medium on which the colonies were able to grow.

[e] NA, not applicable. Colonies from yeast extract media were tested for Fe(II) oxidation capacities on iron-rich media, but strains could not grow on the indicated medium.

[f] +, Fe(II) formation in the liquid medium; −, no Fe(III) formation compared to uninoculated controls with cells growing in the medium; (−), tested, but no cell growth or Fe(III) formation was observed; (+), Fe(II) formation detected but not confirmed.

yielding a total of 28 representative strains (Table 3). According to ARDRA patterns, the occurrence of some strains was restricted to the upper acidic sediment zone from the North and Deep cores, whereas others could be obtained from both sediment zones (see Table S2 in the supplemental material). At the genus level, 36% of the isolates were related to 16S rRNA genes detected in bacterial clone libraries obtained from North I and North IV (see Table S2 in the supplemental material).

One strain belonging to the *Acidobacteria* family *Acidobacteriaceae* was obtained from a YE3 plate (YE3-D1-20) (Table 3 and Fig. 2). Strains related to the phylum *Actinobacteria* were YE4-D4-2-CH (*Streptomycetaceae* related), FeSo-D1-6-CH (*Acidimicrobiaceae* related), and YE4-D4-16i-CH (*Thermomonosporaceae* related). Isolate FeSo-D1-6-CH produced rusty, orange-brown precipitates on the plate (see Table S1 in the supplemental material) and was identical to a heterotrophic, iron-oxidizing, extremely acidophilic *Actinobacterium* able to reduce Fe(III) (36). Seventeen *Firmicutes* strains were obtained from all six media and were affiliated with the families *Bacillaceae* and *Alicyclobacillaceae*. Strain YE4-D4-1-CH was most closely related to *Bacillus acidicola* 105-2^T, which grows at pH 3.5 to 7 (2). Thirteen of the 15 *Alicyclobacillaceae* strains were affiliated with the genus *Alicyclobacillus* and showed "fried-egg"-shaped rusty orange-brown colonies. Three appeared to be new species, based on <97% sequence similarity (see Table S1 in the supplemental material). Two other putative novel strains were affiliated with the genus *Sulfobacillus*. Isolate FeSo-N4-2-CH did not show an Fe(II)-oxidizing capacity, in contrast to *Sulfobacillus acidophilus* DSM 10332^T (94%) (58). In contrast, strain FeSo-N4-3-CH oxidized Fe(II) and was highly related (99.1%) to *Sulfobacillus thermotolerans* Kr1^T, a mixotrophic Fe(II) oxidizer with a pH range of 1.2 to 2.4 (8).

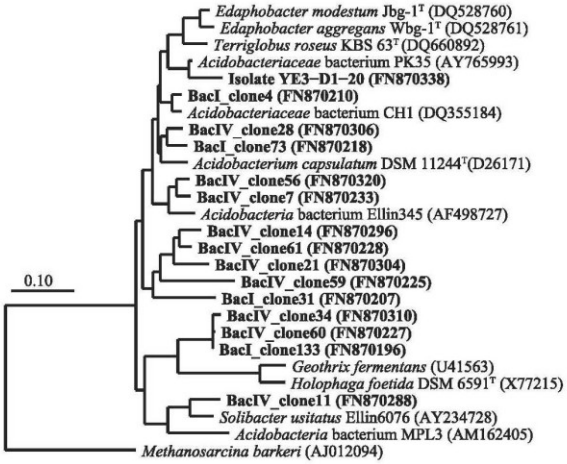

FIG. 2. Phylogenetic tree of *Acidobacteriaceae*-related sequences showing the close relationship of 16S rRNA gene clones obtained from sediment zones I and IV of a core obtained from the northern basin and of a strain isolated from sediment zone I of a core obtained from the deep central basin. GenBank sequence accession numbers are shown; sequences from this study are shown in boldface. The *Archaea Methanosarcina barkeri* (AJ012094) was used as an out-group. Scale bar shows 0.1 change per nucleotide position.

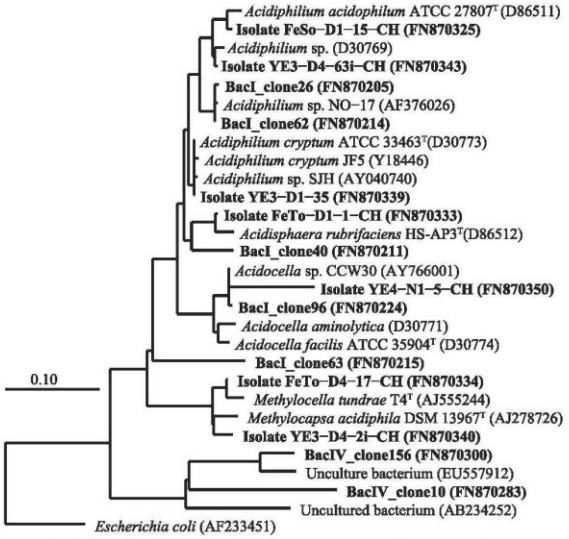

FIG. 3. Phylogenetic tree of *Alphaproteobacteria*-related sequences showing the close relationship of 16S rRNA gene clones obtained from sediment zones I and IV of a core obtained from the northern basin and of the strains isolated from sediment zones I and IV of cores obtained from the northern and deep central basin. GenBank sequence accession numbers are shown; sequences from this study are shown in boldface. The *Gammaproteobacteria Escherichia coli* (AF233451) was used as an out-group. Scale bar shows 0.1 change per nucleotide position.

Within the *Alphaproteobacteria*, representative strains FeSo-D1-15-CH, YE3-D4-63i-CH, YE3-D1-35, and YE4-N1-5-CH were related to the *Acetobacteraceae* family (Fig. 3 and Table 3). One strain was related to *Acidisphaera rubrifaciens* HS-AP3^T (31), an aerobe that can grow in a pH range of 3.5 to 6.0, and strain YE4-N1-5-CH was identical to *Acidocella* sp. CCW30 (AY766001) isolated from acidic, metal-rich mine waters (25). None of our *Acetobacteraceae*-related isolates oxidized Fe(II) (Table 3). Of two *Beijerinckiaceae* strains (FeTo-D4-17-CH and YE3-D4-2i-CH) related to methane-oxidizing acidophiles (16), only one (FeTo-D4-17-CH) could oxidize Fe(II).

The only *Betaproteobacteria* strain isolated (YE4-D1-1-CH) could not oxidize Fe(II). A total of 7 strains were isolated from the *Gammaproteobacteria*. Strain YE4-D1-10-CH (within the *Xanthomonadaceae*) was identical to strain WJ2 from acidic mine drainage waters (27) and produced orange precipitates. *Acidithiobacillaceae*-related strains FeSo-D1-9-CH and FeSo-N1-1-CH were related to known Fe(II)-oxidizing strains (26), but no oxides were produced by FeTo-N1-3-CH (see Table S1 in the supplemental material).

Fe(III)-reducing capacities of isolates and potential Fe cycling. Thirty-six of the 38 tested representatives showed the capacity to form Fe(II) under microoxic and/or anoxic conditions when incubated with schwertmannite, the dominant Fe(III) mineral of Lake 77 (Table 3). The exceptions were strain FeTo-D1-1-CH that is related to *Acidisphaera rubrifaciens* HS-AP3^T, which is unable to reduce Fe(III) (15), and strain YE3-D4-2i-CH. The highest levels of Fe(II) formation were observed for FeSo-N4-1-CH, FeSo-D1-15-CH, FeSo-D1-9-CH, Feo-N4-15-CH, FeSo-N4-3-CH, and FeSo-D1-6-CH (data not shown). Specific rates of reduction could not be determined because conditions might vary within a flask, from anoxic in the bottom of the flasks to oxic at the medium-air interface, leading to a partial reoxidation of Fe(II). In general, Fe(II) formation did not increase under strictly anoxic conditions. After another 4 weeks, we observed evidence of Fe(II) reoxidation, with some isolates forming a rusty orange solid layer (YE4-D4-4-CH, final medium pH 5.8) or a light yellowish soft layer (YE3-D4-3i-CH, final medium pH 3.3) on the top of the medium. Another isolate (FeSo-N4-1-CH, final medium pH 3.7) had a rusty orange crust attached to the inner flask surface at the medium-air interface. Raman spectroscopy revealed that the solid iron that reformed at the medium-air interface consisted of schwertmannite (YE3-D4-3i-CH and FeSo-N4-1-CH) or ferrihydrite (YE4-D4-4-CH) (Valerian Ciobota, personal communication).

The following five isolates were selected for further experiments (Table 4): YE3-D1-20 due to the high relative abundance of *Acidobacteria*-related sequences in clone libraries; two new *Alicyclobacillus* species with high Fe(III)-reducing capacities; YE4-N1-5-CH because little is known about Fe(III) reduction by *Acidocella*; and YE3-D1-10-CH. Most of these strains showed a broad pH range for growth, ranging from 1.5 to 6.0, and the pH optimum for most strains was 3.5 (Table 4). While all 5 of these isolates could reduce iron in schwertmannite, chelated forms of Fe(III), e.g., ferric citrate and ferric pyrophosphate, were not reduced during 14 days. However, after this lag phase, two isolates (FeSo-D4-20-CH and YE3-D1-10-CH) formed up to 7.5 mM Fe(II) (data not shown). Only very small amounts of synthetic goethite were reduced (Table 4).

TABLE 4. Growth pH range and Fe(II) formation assay results for five selected isolates

Genus, strain	Growth pH range (optimal growth pH)[a]	Schwertmannite[b]			Goethite[b]		
		pH on day:		Amt of Fe(II) (mM) on day 22	pH on day:		Amt of Fe(II) (mM) on day 22
		0	22		0	22	
Acidobacteria sp. YE3-D1-20	2.5–5.0 (3.5)	3.0 ± 0.0	4.0 ± 0.2	3.1 ± 0.3	3.2 ± 0.2	3.2 ± 0.1	0.6 ± 0.3
Alicyclobacillus spp. FeSo-D4-20-CH	1.5–6.0 (3.5)	3.0 ± 0.0	3.6 ± 0.6	2.4 ± 1.6	3.1 ± 0.2	2.9 ± 0.2	0.1 ± 0.1
YE4-D4-4i-CH	2.5–5.0 (3.5)	3.0 ± 0.1	3.9 ± 0.1	3.6 ± 0.0	3.0 ± 0.0	3.0 ± 0.1	0.9 ± 0.2
Acidocella sp. YE4-N1-5-CH	2.5–4 (2.5)	3.0 ± 0.0	3.6 ± 0.4	2.6 ± 0.8	3.2 ± 0.2	3.1 ± 0.2	0.7 ± 0.2
Unknown *Dyella*-like genus sp. YE3-D1-10-CH	2.0–5.0 (3.5)	3.0 ± 0.0	4.0 ± 0.1	3.6 ± 0.6	3.3 ± 0.1	3.3 ± 0.2	0.8 ± 0.1
Control		3.1 ± 0.0	2.8 ± 0.0	0.1 ± 0.1	3.1 ± 0.0	3.0 ± 0.0	0.1 ± 0.1

[a] Tested in the YE media under oxic conditions without the presence of Fe(III) minerals.
[b] Tested in the YE media under microoxic conditions.

DISCUSSION

The diversity of microorganisms involved in Fe cycling in acidic sediments was elucidated by cultivation-based and molecular methods. This approach extended previous knowledge by providing information on those microbes responsible for the reductive half of the cycle at low pHs. From 117 selected isolates, a total of 28 different 16S rRNA gene sequences were obtained. Despite identical 16S rRNA genes, some isolates showed different morphologies or differed in their Fe-cycling capabilities. Sequence analysis suggests that 18 isolates are putative new species when compared to fully characterized relatives. However, the number decreases to 5 new species if we make our comparison to isolates which have been obtained over the last several years but have not been fully characterized. For example, strains YE3-D4-3i-CH and iFeo-D4-31-CH shared only 90 and 91% identity, respectively, with the type strain *Alicyclobacillus contaminans* 3-A191^T (24) but more than 99 and 94%, respectively, with the closest cultivated strains SLC66 (iron-oxidizing acidophile, GenBank sequence accession number AY040739) (37) and Y0010 (GenBank sequence accession number AY140235) (42). Not surprisingly, many of these closest cultivated relatives were isolated from acidic hot springs, gold mine soils, porphyry copper tailings, or sulfide ores (19, 42, 72, 75). Thus, the use of "overlay" plates has greatly improved the isolation success of a diversity of autotrophic and heterotrophic acidophiles, which tend to grow poorly on normal solid media (40). The greater diversity of isolates beyond the well-known acidophiles *Acidithiobacillus ferrooxidans* and *Acidiphilium cryptum* isolated in other studies (70) might be due to the broad pH range of the different media used in this study. Nonetheless, 15 and 33 isolates in our study were related to those two species, respectively.

Several phylogenetic groups involved in Fe(II) oxidation were restricted to the top acidic sediment zones of Lake 77 as revealed by the combination of our methods (Fig. 4). All isolates of the genus *Acidithiobacillus* were obtained from the acidic top zones of the Deep and North basins of the lake, but *Acidithiobacillus* spp.-related sequences were not detected in the clone library. From the other *Gammaproteobacteria* family *Xanthomonadaceae*, 8 isolates and 15 clones were obtained only from the top sediment zones. These 15 clones were closely related to those obtained from the river Rio Tinto, Spain

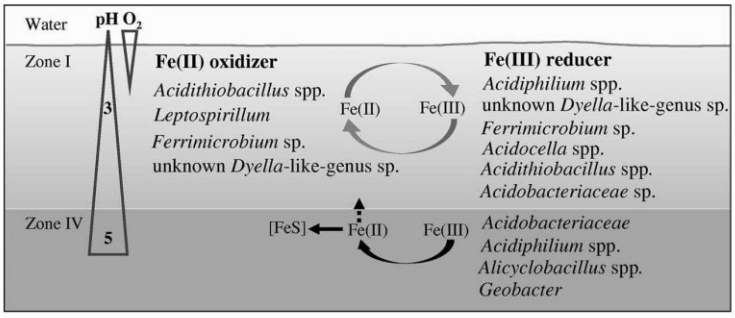

FIG. 4. Schematic of the key microbial players involved in Fe cycling in the acidic lignite mine Lake 77 ecosystem. Microbial players detected by isolation and 16S rRNA gene cloning included Fe(II) oxidizers and Fe(III) reducers. The oxygen content declined sharply to 0 at 2 to 10 mm below the water-sediment interface, and the pH increased from 3 in the water and the top sediment zone I to ca. 5 in zone IV.

(GenBank sequence accession number DQ303270) (22), from acid mine drainage (GenBank sequence accession numbers DQ480485 and AY096032) (15, 29), and also from the top sediment zone of a manipulated lignite mine lake (KacFeR1-3, GenBank sequence accession number EF544680) (61). Isolate YE3-D1-10-CH showed Fe(II)-oxidizing and Fe(III)-reducing capacities, a trait shared with the closely related strain WJ2 (27). Additional clones were related to the well-known Fe(II) oxidizer *Leptospirillum* from the *Nitrospiraceae* family.

Groups of Fe(III)-reducing bacteria varied in their distribution over sediment zones (Fig. 4). All of the 13 *Acidocella* isolates were obtained from the top acidic zones, matching the pH optimum of the more thoroughly investigated isolate YE4-N1-5-CH. This isolate could reduce schwertmannite similarly to the other four isolates tested (15) but did not oxidize Fe(II). Clones related to the known Fe(III)-reducing genus *Acidiphilium* (15, 51) were only detected in the BacI library (Fig. 3), but isolates of this genus, with high capacities to reduce schwertmannite under strictly anoxic conditions, could be obtained from all sediment depths and sites. Since at least one *Acidiphilium* isolate can reduce Fe(III) at a pH of up to 5 (6), bacteria of the genus *Acidiphilium* might be important drivers for Fe(III) respiration in acidic sediments.

Acidobacteria occurred at higher relative abundances in the deeper sediment zones, and the majority of clones were affiliated with the *Acidobacteria* subdivision 1, which contains known Fe(III) reducers. Despite the dominance of subdivision 1 *Acidobacteria* in various habitats, including uranium-contaminated subsurface sediments (4), mine tailings (74), the soil surrounding iron-manganese nodules (28), extremely acidic, metal-rich streams (65), and acidic lignite mine lakes (7, 48), their ecological roles remain poorly documented. *Acidobacterium capsulatum* DSM 11244^T and other related isolates (PK35, RIT23, KP3, and WJ7) are capable of dissimilatory Fe(III) reduction (7, 15, 27) under strict anoxic or microoxic conditions, similar to our isolate YE3-D1-20 that was closely related to strain PK35. The genome study of *Acidobacteria* strains, including an *A. capsulatum* strain, strain Ellin345 (subdivision 1), and strain Ellin6076 (subdivision 3), provides some evidence for a probable Fe(III) reduction pathway (73).

All of the 20 *Alicyclobacillus*-related isolates were obtained from deep, slightly acidic sediment zones despite their Fe(II)-oxidizing capacities. Characterization of these acidophilic iron- and sulfur-oxidizing *Firmicutes* shows that they are aerobes or facultative anaerobes with considerable metabolic versatility (46, 75). Thirteen of our tested isolates could oxidize Fe(II) and reduce schwertmannite, but the extent of Fe(II) formation was not enhanced under strictly anoxic conditions. Several *Alicyclobacillus* strains can utilize Fe(III), and one *Alicyclobacillus* isolate, GSM, is able to couple Fe(III) reduction with cell growth under anoxic conditions (75). Isolate FeSo-D4-20-CH, which probably represents a new species, could grow within a pH range of 1.5 to 6, suggesting a high adaptability to geochemical gradients. Surprisingly, none of the molecular techniques detected members of the *Alicyclobacillaceae* family, although these organisms were cultivated in abundance. This missing overlap might be due to the inherent biases of molecular techniques and/or to their low *in situ* abundance.

Geobacter-related sequences were obtained from the deep but not from the top acidic sediment zone, a result which was supported by *Geobacter*-specific quantitative PCR. Sixteen of 17 clones were closely related to *Geobacter* sp. G02 or *Geobacter chapellei* strain 172 (54), suggesting that some *Geobacteraceae* species may be more acid tolerant than previously thought. However, attempts to isolate Fe(III) reducers at pH 5 from zone IV under strictly anoxic conditions failed. Sulfate reducer sequences from the families *Desulfuromonadaceae*, *Desulfobulbaceae*, *Desulfobacteraceae*, and *Desulfovibrionaceae* were not closely related to strains known for Fe(III) reduction.

In contrast to previous work (7), archaeal sequences were obtained, which might be due to the different primer set used in this study. Unfortunately, no archaeal strain could be isolated. Both libraries were dominated by *Euryarchaeota*, including known methanogens. In addition, one clone was affiliated with the family *Archaeoglobaceae*, which contains strains capable of sulfur reduction (67), a process that appears to be restricted to the deeper, moderately acidic sediment zone of this lignite mine lake (59). *Picrophilaceae* and *Thermoplasmatales*-like phylotypes (but not *Ferroplasma* related) were detected which were related to sequences from an extremely acidic, metal-rich stream in Spain (65). This result is similar to those from other acid mine drainage sites where *Thermoplasmatales* represent a dominant group (3, 20, 22, 62) but contrasts with the results for other sites where *Ferroplasma* spp. appear to be responsible for pyrite leaching (20, 21).

Collectively, these results demonstrate that cultivation revealed a much broader diversity of microorganisms with the capacity to reduce Fe(III) under both acidic and moderately acidic conditions (Fig. 4). These findings broaden our previous understanding of the lignite mine Lake 77 ecosystem obtained from a molecular-based study (7). In this work, molecular methods showed that 13 of 101 distinctive phylotypes obtained in the bacterial clone libraries were closely related to our isolated strains. The presence of Fe(II) oxidizers appeared to be restricted to the top acidic sediment zone, where oxygen is present after lake water mixing (Fig. 4). Fe(III)-reducing bacteria included many genera, such as *Acidobacterium*, *Acidocella*, *Alicyclobacillus*, and an unknown *Dyella*-like genus, which are not commonly found in moderately acidic habitats. The isolates studied in more detail showed an average pH range for growth from 2.5 to 5 with a maximum range of 1.5 to 6, suggesting that they can inhabit a wide ecological niche. In addition to this broad pH tolerance, the isolates obtained reduced Fe(III) under ecosystem-relevant conditions. We found that the isolates preferred microoxic conditions to reduce Fe(III) and were unable to reduce chelated forms of Fe(III), which is in contrast to the results for the commonly studied neutrophilic Fe(III) reducers. Since other acidophilic Fe(III) reducers have been shown to reduce Fe(III) in the presence of oxygen (41) or even to corespire Fe(III) and oxygen (52), the presence of low oxygen concentrations will not inhibit the reduction of Fe(III) in acidic sediments. Thus, the order of redox processes might differ at the sediment-water interface of acidic ecosystems compared to the order of these processes in neutral-pH sediments, with pH acting as a major driving force in shaping biogeochemical redox processes.

ACKNOWLEDGMENTS

This work was supported by the Graduate School of Excellence Jena School for Microbial Communication (JSMC) and grant KU 1367/8-1

funded by the German Research Foundation (Deutsche Forschungsgemeinschaft [DFG]).

We thank Peter Bouwma for proofreading the manuscript and Susanne Grube for technical assistance.

REFERENCES

1. **Adams, L. K., C. Boothman, and J. R. Lloyd.** 2007. Identification and characterization of a novel acidotolerant Fe(III)-reducing bacterium from a 3000-year-old acidic rock drainage site. FEMS Microbiol. Lett. **268:**151–157.
2. **Albert, R. A., J. Archambault, R. Rossello-Mora, B. J. Tindall, and M. Matheny.** 2005. *Bacillus acidicola* sp. nov., a novel mesophilic, acidophilic species isolated from acidic sphagnum peat bogs in Wisconsin. Int. J. Syst. Evol. Microbiol. **55:**2125–2130.
3. **Almeida, W. I., R. P. Vieira, A. M. Cardoso, C. B. Silveira, R. G. Costa, A. M. Gonzalez, R. Paranhos, J. A. Medeiros, F. A. Freitas, R. M. Albano, and O. B. Martins.** 2009. Archaeal and bacterial communities of heavy metal contaminated acidic waters from zinc mine residues in Sepetiba Bay. Extremophiles **13:**263–271.
4. **Barns, S. M., E. C. Cain, L. Sommerville, and C. R. Kuske.** 2007. *Acidobacteria* phylum sequences in uranium-contaminated subsurface sediments greatly expand the known diversity within the phylum. Appl. Environ. Microbiol. **73:**3113–3116.
5. **Belnap, C. P., C. Pan, N. C. VerBerkmoes, M. E. Power, N. F. Samatova, R. L. Carver, R. L. Hettich, and J. F. Banfield.** 2010. Cultivation and quantitative proteomic analyses of acidophilic microbial communities. ISME J. **4:**520–530.
6. **Bilgin, A. A., J. Silverstein, and J. D. Jenkins.** 2004. Iron respiration by *Acidiphilium cryptum* at pH 5. FEMS Microbiol. Ecol. **49:**137–143.
7. **Blöthe, M., D. M. Akob, J. E. Kostka, K. Goschel, H. L. Drake, and K. Küsel.** 2008. pH gradient-induced heterogeneity of Fe(III)-reducing microorganisms in coal mining-associated lake sediments. Appl. Environ. Microbiol. **74:**1019–1029.
8. **Bogdanova, T. I., I. A. Tsaphna, T. F. Kondra'eva, V. I. Duda, N. E. Suzina, V. S. Melamud, T. P. Tourova, and G. I. Karavaiko.** 2006. *Sulfobacillus thermotolerans* sp. nov., a thermotolerant, chemolithotrophic bacterium. Int. J. Syst. Evol. Microbiol. **56:**1039–1042.
9. **Chun, J., J. H. Lee, Y. Jung, M. Kim, S. Kim, B. K. Kim, and Y. W. Lim.** 2007. EzTaxon: a web-based tool for the identification of prokaryotes based on 16S ribosomal RNA gene sequences. Int. J. Syst. Evol. Microbiol. **57:** 2259–2261.
10. **Clark, D. A., and P. R. Norris.** 1996. *Acidimicrobium ferrooxidans* gen. nov., sp. nov.: mixed-culture ferrous iron oxidation with *Sulfobacillus* species. Microbiology (Reading, England) **142:**785–790.
11. **Cole, J. R., B. Chai, T. L. Marsh, R. J. Farris, Q. Wang, S. A. Kulam, S. Chandra, D. M. McGarrell, T. M. Schmidt, G. M. Garrity, and J. M. Tiedje.** 2003. The Ribosomal Database Project (RDP-II): previewing a new autoaligner that allows regular updates and the new prokaryotic taxonomy. Nucleic Acids Res. **31:**442–443.
12. **Colwell, R. K., C. X. Mao, and J. Chang.** 2004. Interpolating, extrapolating, and comparing incidence-based species accumulation curves. Ecology **85:** 2717–2727.
13. **Coram, N. J., and D. E. Rawlings.** 2002. Molecular relationship between two groups of the genus *Leptospirillum* and the finding that *Leptosphillum ferriphilum* sp. nov. dominates South African commercial biooxidation tanks that operate at 40°C. Appl. Environ. Microbiol. **68:**838–845.
14. **Cornell, R. M., and U. Schwertmann.** 2003. The iron oxides: structure, properties, reactions, occurrences and uses, 2nd ed. Wiley-VCH Verlagsgesellschaft, Weinheim, Germany.
15. **Coupland, K., and D. B. Johnson.** 2008. Evidence that the potential for dissimilatory ferric iron reduction is widespread among acidophilic heterotrophic bacteria. FEMS Microbiol. Lett. **279:**30–35.
16. **Dedysh, S. N., Y. Y. Berestovskaya, L. V. Vasylieva, S. E. Belova, V. N. Khmelenina, N. E. Suzina, Y. A. Trotsenko, W. Liesack, and G. A. Zavarzin.** 2004. *Methylocella tundrae* sp. nov., a novel methanotrophic bacterium from acidic tundra peatlands. Int. J. Syst. Evol. Microbiol. **54:**151–156.
17. **Denef, V. J., R. S. Mueller, and J. F. Banfield.** 2010. AMD biofilms: using model communities to study microbial evolution and ecological complexity in nature. ISME J. **4:**599–610.
18. **DeSantis, T. Z., P. Hugenholtz, N. Larsen, M. Rojas, E. L. Brodie, K. Keller, T. Huber, D. Dalevi, P. Hu, and G. L. Andersen.** 2006. Greengenes, a chimera-checked 16S rRNA gene database and workbench compatible with ARB. Appl. Environ. Microbiol. **72:**5069–5072.
19. **Diaby, N., B. Dold, H. R. Pfeifer, C. Holliger, D. B. Johnson, and K. B. Hallberg.** 2007. Microbial communities in a porphyry copper tailings impoundment and their impact on the geochemical dynamics of the mine waste. Environ. Microbiol. **9:**298–307.
20. **Druschel, G. K., B. J. Baker, T. M. Gihring, and J. F. Banfield.** 2004. Acid mine drainage biogeochemistry at Iron Mountain, California. Geochem. Trans. **5:**13–32.
21. **Edwards, K. J., P. L. Bond, T. M. Gihring, and J. F. Banfield.** 2000. An archaeal iron-oxidizing extreme acidophile important in acid mine drainage. Science **287:**1796–1799.
22. **Garcia-Moyano, A., E. Gonzalez-Toril, A. Aguilera, and R. Amils.** 2007. Prokaryotic community composition and ecology of floating macroscopic filaments from an extreme acidic environment, Rio Tinto (SW, Spain). Syst. Appl. Microbiol. **30:**601–614.
23. **Gonzalez-Toril, E., E. Llobet-Brossa, E. O. Casamayor, R. Amann, and R. Amils.** 2003. Microbial ecology of an extreme acidic environment, the Tinto River. Appl. Environ. Microbiol. **69:**4853–4865.
24. **Goto, K., K. Mochida, Y. Kato, M. Asahara, R. Fujita, S. Y. An, H. Kasai, and A. Yokota.** 2007. Proposal of six species of moderately thermophilic, acidophilic, endospore-forming bacteria: *Alicyclobacillus contaminans* sp. nov., *Alicyclobacillus fastidiosus* sp. nov., *Alicyclobacillus kakegawensis* sp. nov., *Alicyclobacillus macrosporangiidus* sp. nov., *Alicyclobacillus sacchari* sp. nov and *Alicyclobacillus shlzuokensis* sp. nov. Int. J. Syst. Evol. Microbiol. **57:**1276–1285.
25. **Hallberg, K. B., K. Coupland, S. Kimura, and D. B. Johnson.** 2006. Macroscopic streamer growths in acidic, metal-rich mine waters in north Wales consist of novel and remarkably simple bacterial communities. Appl. Environ. Microbiol. **72:**2022–2030.
26. **Hallberg, K. B., E. Gonzalez-Toril, and D. B. Johnson.** 2010. *Acidithiobacillus ferrivorans*, sp. nov.; facultatively anaerobic, psychrotolerant iron-, and sulfur-oxidizing acidophiles isolated from metal mine-impacted environments. Extremophiles **14:**9–19.
27. **Hallberg, K. B., and D. B. Johnson.** 2003. Novel acidophiles isolated from moderately acidic mine drainage waters. Hydrometallurgy **71:**139–148.
28. **He, J. Z., L. M. Zhang, S. S. Jin, Y. G. Zhu, and F. Liu.** 2008. Bacterial communities inside and surrounding soil iron-manganese nodules. Geomicrobiol. J. **25:**14–24.
29. **He, Z. G., S. M. Xiao, X. H. Xie, H. Zhong, Y. H. Hu, Q. H. Li, F. L. Gao, G. Y. Li, J. S. Liu, and G. Z. Qiu.** 2007. Molecular diversity of microbial community in acid mine drainages of Yunfu sulfide mine. Extremophiles **11:**305–314.
30. **Hippe, H.** 2000. *Leptospirillum* gen. nov. (*ex* Markosyan 1972), nom. rev., including *Leptospirillum ferrooxidans* sp. nov. (*ex* Markosyan 1972), nom. rev., and *Leptospirillum thermoferrooxidans* sp. nov. (Golovacheva *et al*). Int. J. Syst. Evol. Microbiol. **50:**501–503.
31. **Hiraishi, A., Y. Matsuzawa, T. Kanbe, and N. Wakao.** 2000. *Acidisphaera rubrifaciens* gen. nov., sp. nov., an aerobic bacteriochlorophyll-containing bacterium isolated from acidic environments. Int. J. Syst. Evol. Microbiol. **50:**1539–1546.
32. **Holland, S. M.** 2003. Analytic Rarefaction 1.3 user's guide. University of Georgia, Athens, GA.
33. **Huber, G., and K. O. Stetter.** 1991. *Sulfolobus metallicus*, sp. nov., a novel strictly chemolithoautotrophic thermophilic archaeal species of metal-mobilizers. Syst. Appl. Microbiol. **14:**372–378.
34. **Huber, T., G. Faulkner, and P. Hugenholtz.** 2004. Bellerophon: a program to detect chimeric sequences in multiple sequence alignments. Bioinformatics **20:**2317–2319.
35. **Jiang, C. Y., Y. Liu, Y. Y. Liu, X. Y. You, X. Guo, and S. J. Liu.** 2008. *Alicyclobacillus ferrooxydans* sp. nov., a ferrous-oxidizing bacterium from solfataric soil. Int. J. Syst. Evol. Microbiol. **58:**2898–2903.
36. **Johnson, D. B., P. Bacelar-Nicolau, N. Okibe, A. Thomas, and K. B. Hallberg.** 2009. *Ferrimicrobium acidiphilum* gen. nov., sp. nov. and *Ferrithrix thermotolerans* gen. nov., sp. nov.: heterotrophic, iron-oxidizing, extremely acidophilic actinobacteria. Int. J. Syst. Evol. Microbiol. **59:**1082–1089.
37. **Johnson, D. B., P. Bacelar-Nicolau, N. Okibe, A. Yahya, and K. B. Hallberg.** 2001. Role of pure and mixed cultures of gram-positive eubacteria in mineral leaching, p. 461–470. *In* V. S. T. Ciminelli and O. J. Garcia (ed.), Biohydrometallurgy: fundamentals, technology and sustainable development, 1st ed., vol. 11A. Elsevier Science, Amsterdam, Netherlands.
38. **Johnson, D. B., and T. A. M. Bridge.** 2002. Reduction of ferric iron by acidophilic heterotrophic bacteria: evidence for constitutive and inducible enzyme systems in *Acidiphilium* spp. J. Appl. Microbiol. **92:**315–321.
39. **Johnson, D. B., and K. B. Hallberg.** 2005. Biogeochemistry of the compost bioreactor components of a composite acid mine drainage passive remediation system. Sci. Total Environ. **338:**81–93.
40. **Johnson, D. B., and K. B. Hallberg.** 2007. Techniques for detecting and identifying acidophilic mineral-oxidizing microorganisms, p. 237–261. *In* D. E. Rawlings and D. B. Johnson (ed.), Biomining. Springer-Verlag, Berlin, Germany.
41. **Johnson, D. B., and S. McGinness.** 1991. Ferric iron reduction by acidophilic heterotrophic bacteria. Appl. Environ. Microbiol. **57:**207–211.
42. **Johnson, D. B., N. Okibe, and F. F. Roberto.** 2003. Novel thermo-acidophilic bacteria isolated from geothermal sites in Yellowstone National Park: physiological and phylogenetic characteristics. Arch. Microbiol. **180:**60–68.
43. **Johnson, D. B., S. Rolfe, K. B. Hallberg, and E. Iversen.** 2001. Isolation and phylogenetic characterization of acidophilic microorganisms indigenous to acidic drainage waters at an abandoned Norwegian copper mine. Environ. Microbiol. **3:**630–637.
44. **Johnson, D. B., B. Stallwood, S. Kimura, and K. B. Hallberg.** 2006. Isolation and characterization of *Acidicaldus organivorus*, gen. nov., sp. nov.: a novel

sulfur-oxidizing, ferric iron-reducing thermo-acidophilic heterotrophic *Proteobacterium*. Arch. Microbiol. **185:**212–221.
45. **Johnson, M., I. Zaretskaya, Y. Raytselis, Y. Merezhuk, S. McGinnis, and T. L. Madden.** 2008. NCBI BLAST: a better web interface. Nucleic Acids Res. **36:**W5–W9.
46. **Karavaiko, G. I., T. I. Bogdanova, T. P. Tourova, T. F. Kondrat'eva, I. A. Tsaplina, M. A. Egorova, E. N. Krasil'nikova, and L. M. Zakharchuk.** 2005. Reclassification of "*Sulfobacillus thermosulfidooxidans* subsp thermotolerans" strain K1 as *Alicyclobacillus tolerans* sp. nov. and *Sulfobacillus disulfidooxidans* Dufresne *et al.* 1996. as *Alicyclobacillus disulfidooxidans* comb. nov., and emended description of the genus *Alicyclobacillus.* Int. J. Syst. Evol. Microbiol. **55:**941–947.
47. **Karavaiko, G. I., T. P. Turova, T. F. Kondrat'eva, A. M. Lysenko, T. V. Kolganova, S. N. Ageeva, L. N. Muntyan, and T. A. Pivovarova.** 2003. Phylogenetic heterogeneity of the species *Acidithiobacillus ferrooxidans*. Int. J. Syst. Evol. Microbiol. **53:**113–119.
48. **Kleinsteuber, S., F. D. Müller, A. Chatzinotas, K. Wendt-Potthoff, and H. Harms.** 2008. Diversity and *in situ* quantification of *Acidobacteria* subdivision 1 in an acidic mining lake. FEMS Microbiol. Ecol. **63:**107–117.
49. **Küsel, K.** 2003. Microbial cycling of iron and sulfur in acidic coal mining lake sediments. Water Air Soil Pollut. **3:**67–90.
50. **Küsel, K., M. Blöthe, D. Schulz, M. Reiche, and H. L. Drake.** 2008. Microbial reduction of iron and porewater biogeochemistry in acidic peatlands. Biogeosciences **5:**1537–1549.
51. **Küsel, K., T. Dorsch, G. Acker, and E. Stackebrandt.** 1999. Microbial reduction of Fe(III) in acidic sediments: isolation of *Acidiphilium cryptum* JF-5 capable of coupling the reduction of Fe(III) to the oxidation of glucose. Appl. Environ. Microbiol. **65:**3633–3640.
52. **Küsel, K., U. Roth, and H. L. Drake.** 2002. Microbial reduction of Fe(III) in the presence of oxygen under low pH conditions. Environ. Microbiol. **4:**414–421.
53. **Lane, D. J.** 1991. 16S/23S rRNA sequencing in *E. coli*, p. 115–175. *In* E. Stackebrandt and M. Goodfellow (ed.), Nucleic acid techniques in bacterial systematics. John Wiley & Sons, New York, NY.
54. **Lonergan, D. J., H. L. Jenter, J. D. Coates, E. J. P. Phillips, T. M. Schmidt, and D. R. Lovley.** 1996. Phylogenetic analysis of dissimilatory Fe(III)-reducing bacteria. J. Bacteriol. **178:**2402–2408.
55. **Lovley, D. R.** 2006. Dissimilatory Fe (III)- and Mn (IV)-reducing prokaryotes, p. 635–658. *In* M. Dworkin (ed.), The prokaryotes, 3rd ed., vol. 2. Springer, New York, NY.
56. **Lovley, D. R., D. E. Holmes, and K. P. Nevin.** 2004. Dissimilatory Fe(III) and Mn(IV) reduction, p. 219–286. *In* R. K. Poole, Advances in microbial physiology, vol. 49. Academic Press Ltd., London, United Kingdom.
57. **Loy, A., A. Lehner, N. Lee, J. Adamczyk, H. Meier, J. Ernst, K. H. Schleifer, and M. Wagner.** 2002. Oligonucleotide microarray for 16S rRNA gene-based detection of all recognized lineages of sulfate-reducing prokaryotes in the environment. Appl. Environ. Microbiol. **68:**5064–5081.
58. **Norris, P. R., D. A. Clark, J. P. Owen, and S. Waterhouse.** 1996. Characteristics of *Sulfobacillus acidophilus* sp. nov. and other moderately thermophilic mineral-sulphide-oxidizing bacteria. Microbiology (Reading, England) **142:**775–783.
59. **Peine, A., A. Tritschler, K. Küsel, and S. Peiffer.** 2000. Electron flow in an iron-rich acidic sediment—evidence for an acidity-driven iron cycle. Limnol. Oceanogr. **45:**1077–1087.
60. **Petrie, L., N. N. North, S. L. Dollhopf, D. L. Balkwill, and J. E. Kostka.** 2003. Enumeration and characterization of iron(III)-reducing microbial communities from acidic subsurface sediments contaminated with uranium(VI). Appl. Environ. Microbiol. **69:**7467–7479.
61. **Porsch, K., J. Meier, S. Kleinsteuber, and K. Wendt-Potthoff.** 2009. Importance of different physiological groups of iron reducing microorganisms in an acidic mining lake remediation experiment. Microb. Ecol. **57:**701–717.
62. **Qiu, G. Z., M. X. Wan, L. Qian, Z. Y. Huang, K. Liu, X. D. Liu, W. Y. Shi, and Y. Yang.** 2008. Archaeal diversity in acid mine drainage from Dabaoshan Mine, China. J. Basic Microbiol. **48:**401–409.
63. **Raskin, L., J. M. Stromley, B. E. Rittmann, and D. A. Stahl.** 1994. Group-specific 16S rRNA hybridization probes to describe natural communities of methanogens. Appl. Environ. Microbiol. **60:**1232–1240.
64. **Regenspurg, S., A. Brand, and S. Peiffer.** 2004. Formation and stability of schwertmannite in acidic mining lakes. Geochim. Cosmochim. Acta **68:**1185–1197.
65. **Rowe, O. F., J. Sanchez-Espana, K. B. Hallberg, and D. B. Johnson.** 2007. Microbial communities and geochemical dynamics in an extremely acidic, metal-rich stream at an abandoned sulfide mine (Huelva, Spain) underpinned by two functional primary production systems. Environ. Microbiol. **9:**1761–1771.
66. **Segerer, A., A. Neuner, J. K. Kristjansson, and K. O. Stetter.** 1986. *Acidianus infernus* gen. nov., sp. nov., and *Acidianus brierleyi* comb. nov.: facultatively aerobic, extremely acidophilic thermophilic sulfur-metabolizing archaebacteria. Int. J. Syst. Bacteriol. **36:**559–564.
67. **Speich, N., C. Dahl, P. Heisig, A. Klein, F. Lottspeich, K. O. Stetter, and H. G. Truper.** 1994. Adenylylsulphate reductase from the sulphate-reducing archaeon *Archaeoglobus fulgidus*: cloning and characterization of the genes and comparison of the enzyme with other iron-sulphur flavoproteins. Microbiology (Reading, England) **140:**1273–1284.
68. **Straub, K. L., M. Benz, and B. Schink.** 2001. Iron metabolism in anoxic environments at near neutral pH. FEMS Microbiol. Ecol. **34:**181–186.
69. **Stults, J. R., O. Snoeyenbos-West, B. Methe, D. R. Lovley, and D. P. Chandler.** 2001. Application of the 5′ fluorogenic exonuclease assay (TaqMan) for quantitative ribosomal DNA and rRNA analysis in sediments. Appl. Environ. Microbiol. **67:**2781–2789.
70. **Tan, G. L., W. S. Shu, K. B. Hallberg, F. Li, C. Y. Lan, and L. N. Huang.** 2007. Cultivation-dependent and cultivation-independent characterization of the microbial community in acid mine drainage associated with acidic Pb/Zn mine tailings at Lechang, Guangdong, China. FEMS Microbiol. Ecol. **59:**118–126.
71. **Todorova, S. G., and A. M. Costello.** 2006. Design of *Shewanella*-specific 16S rRNA primers and application to analysis of *Shewanella* in a minerotrophic wetland. Environ. Microbiol. **8:**426–432.
72. **Wakeman, K., H. Auvinen, and D. B. Johnson.** 2008. Microbiological and geochemical dynamics in simulated-heap leaching of a polymetallic sulfide ore. Biotechnol. Bioeng. **101:**739–750.
73. **Ward, N. L., J. F. Challacombe, P. H. Janssen, B. Henrissat, P. M. Coutinho, M. Wu, G. Xie, D. H. Haft, M. Sait, J. Badger, R. D. Barabote, B. Bradley, T. S. Brettin, L. M. Brinkac, D. Bruce, T. Creasy, S. C. Daugherty, T. M. Davidsen, R. T. Deboy, J. C. Detter, R. J. Dodson, A. S. Durkin, A. Ganapathy, M. Gwinn-Giglio, C. S. Han, H. Khouri, H. Kiss, S. P. Kothari, R. Madupu, K. E. Nelson, W. C. Nelson, I. Paulsen, K. Penn, Q. H. Ren, M. J. Rosovitz, J. D. Selengut, S. Shrivastava, S. A. Sullivan, R. Tapia, L. S. Thompson, K. L. Watkins, Q. Yang, C. H. Yu, N. Zafar, L. W. Zhou, and C. R. Kuske.** 2009. Three genomes from the phylum *Acidobacteria* provide insight into the lifestyles of these microorganisms in soils. Appl. Environ. Microbiol. **75:**2046–2056.
74. **Winch, S., H. J. Mills, J. E. Kostka, D. Fortin, and D. R. S. Lean.** 2009. Identification of sulfate-reducing bacteria in methylmercury-contaminated mine tailings by analysis of SSU rRNA genes. FEMS Microbiol. Ecol. **68:**94–107.
75. **Yahya, A., K. B. Hallberg, and D. B. Johnson.** 2008. Iron and carbon metabolism by a mineral-oxidizing *Alicyclobacillus*-like bacterium. Arch. Microbiol. **189:**305–312.
76. **Yu, Y. N., M. Breitbart, P. McNairnie, and F. Rohwer.** 2006. FastGroupII: a web-based bioinformatics platform for analyses of large 16S rDNA libraries. BMC Bioinform. **7:**9.

Supplementary information

Table S1: Phylogenetic information and colony morphology of representative isolates obtained from top and bottom sediment zones at the deep central basin (D1 and D4, respectively) and the north shore (N1 and N4, respectively).

Taxa (phylum)	Taxa (family)	Representative strains [a]	Accession No.	Number of isolates identified by ARDRA pattern	Number of isolates obtained from sediment zones identified by ARDRA patterns	Number of isolates based on media type identified by ARDRA patterns	Media pH	Colony morphology	Closest type strain (Ac. No.)	% Identity	Closest cultivated relative (Ac. No.)	% Identity
Acidobacteria	*Acidobacteriaceae*	YE3-D1-20	FN870338	1	D1 (1)	YE3 (1)	3	small, entire and pink pigmented	*Edaphobacter modestus* Jbg-1 (DQ528760)	93.9	*Acidobacteriaceae* bacterium PK35 (AY765993)	99.9
Actinobacteria	*Streptomycetaceae*	YE4-D4-2-CH	FN870347	5	D4 (5)	YE4 (5)	4	extensively branched substrate mycelium and aerial hyphae	*Streptomyces ferralitis* SFOp68 (AY262826)	98.4	*Streptomyces* mucoflavus (AB184555)	98.5
	Acidimicrobiaceae	FeSo-D1-6-CH	FN870326	1	D1 (1)	FeSo (1)	2.5	large, entire and 'fried eggs' shaped rusty orange-brown	*Ferrimicrobium acidiphilum* strain T23 (AF251436)	99.4	*Ferrimicrobium acidiphilum* strain T23[T] (AF251436)	99.4
	Thermomonosporaceae	YE4-D4-16i-CH	FN870346	1	D4 (1)	YE4 (1)	4	small, entire, white and smooth-surface	*Actinocorallia aurea* HO 14752 (AB006177)	94.2	*Bacterium* Ellin5129 (AY234546)	97.1
Firmicutes	*Bacillaceae*	YE4-D4-1-CH	FN870345	3	D4 (3)	YE4 (3)	4	small, entire and white	*Bacillus acidicola* 105-2 (AF547209)	99.8	*Bacillus acidicola* 105-2 (AF547209)	99.8
		YE4-D4-4-CH	FN870348	1	D4 (1)	YE4 (1)	4	small, circular and entire, smooth with a slight yellow tint	*Bacillus pocheonensis* Gsoil 420 (AB245377)	99	*Bacillus pocheonensis* Gsoil 420[T] (AB245377)	99
	Alicyclobacillaceae	YE3-D4-3i-CH	FN870341	3	D4 (3)	iFeo (1), YE4 (2)	2.5-4	'fried egg'-shaped rusty orange-brown (iFeo); small and light yellow (YE)	*Alicyclobacillus contaminans* 3-A191 (AB264026)	89.6	Gram-positive iron-oxidizing acidophile SLC66 (AY140739)	99
		iFeo-D4-31-CH	FN870342	1	D4 (1)	iFeo (1)	2.5	'fried egg'-shaped rusty orange-brown	*Alicyclobacillus contaminans* 3-A191 (AB264026)	90.6	Gram-positive iron-oxidizing acidophile Y0010 (AY140235)	94.4
		YE3-D4-31i-CH	FN870336	4	D4 (3), N4 (1)	FeTo (3), YE3 (1)	3-4.3	'fried egg'-shaped rusty orange-brown (FeTo); small and light yellow (YE)	*Alicyclobacillus ferrooxydans* TC-34 (EU137838)	98.6	*Alicyclobacillus* sp. Talvoil (EU282873)	99.2
		Feo-D4-16-CH	FN870323	1	D4 (1)	Feo (1)	2.5	'fried egg'-shaped rusty orange-brown	*Alicyclobacillus ferrooxydans* TC-34 (EU137838)	91.4	Gram-positive iron-oxidizing acidophile Y0010 (AY140235)	99.5
		FeSo-D4-20-CH	FN870328	1	D4 (1)	FeSo (1)	2.5	'fried egg'-shaped rusty orange-brown	*Alicyclobacillus pomorum* 3A5 (AB089840)	91	Gram-positive iron-oxidizing acidophile CH2 (DQ355185)	94.4
		FeSo-N4-1-CH	FN870330	5	N4 (1), D4 (4)	FeSo (2), YE4 (3)	2.5-4	'fried egg'-shaped rusty orange-brown (FeSo); small and light yellow (YE)	*Alicyclobacillus tolerans* strain K1 (AF137502)	95.1	*Alicyclobacillus* sp. CLD (EU282872)	99.9
		YE4-D4-4i-CH	FN870349	4	D4 (3), N4 (1)	FeTo (3), YE4 (1)	4-4.3	'fried egg'-shaped rusty orange-brown (FeTo); small and light yellow (YE)	*Alicyclobacillus tolerans* strain K1 (AF137502)	94.9	*Alicyclobacillus* sp. CLD (EU282872)	96.5
		Feo-N4-15-CH	FN870324	1	N4	Feo (1)	2.5	'fried egg' shaped rusty orange-brown	*Alicyclobacillus tolerans* strain K1 (AF137502)	100	*Alicyclobacillus tolerans* strain K1[T] (AF137502)	100
		FeSo-N4-2-CH	FN870331	3	N4 (2), D4(1)	FeSo (3)	2.5	entire and white	*Sulfobacillus acidophilus* DSM 10332 (AB089842)	94.2	*Sulfobacillus* sp. 4G (AY371272)	95.7
		FeSo-N4-3-CH	FN870332	1	N4 (1)	FeSo (1)	2.5	rusty orange-brown	*Sulfobacillus thermotolerans* Kr1 (DQ124681)	99.1	*Sulfobacillus* sp. Y0017 (AY140239)	99.4
Alphaproteobacteria	*Acetobacteraceae*	FeSo-D1-15-CH	FN870325	1	D1 (1)	FeSo (1)	2.5	small and white	*Acidiphilium acidophilum* ATCC 27807 (D86511)	99.8	*Acidiphilium acidophilum* ATCC 27807[T] (D86511)	99.8
		YE3-D4-63i-CH	FN870343	1	D4 (1)	YE3 (1)	3	small and white	*Acidiphilium acidophilum* ATCC 27807 (D86511)	98.2	*Acidiphilum* sp. CH3 (DQ355186)	99.8
		YE3-D1-35	FN870339	33	D1 (8), D4 (15), N1 (3), N4 (7)	Feo (10), iFeo (16), YE3 (5), YE4 (2)	2.5-4	small and pinkish white tint	*Acidiphilium cryptum* ATCC 33463 (D30773)	100	*Acidiphilium cryptum* ATCC 33463[T] (D30773)	100
		FeTo-D1-1-CH	FN870333	3	D1 (3)	FeTo (3)	4.3	light white with a clear decolorized zone around the colonies	*Acidisphaera rubrifaciens* HS-AP3 (D86512)	99.7	*Acidisphaera rubrifaciens* HS-AP3[T] (D86512)	99.7
		YE4-N1-5-CH	FN870350	13	N1 (6), D1 (7)	YE3 (5), YE4 (8)	3-4	small, entire and white	*Acidocella facilis* ATCC 35904 (D30774)	96.9	*Acidocella* sp. CCW30 (AY766001)	100
	Beijerinckiaceae	FeTo-D4-17-CH	FN870334	4	D4 (4)	FeTo (4)	4.3	rusty orange color	*Methylocella tundrae* T4 (AJ555244)	99.9	*Methylocella tundrae* T4[T] (AJ555244)	99.9
		YE3-D4-2i-CH	FN870340	1	D4 (1)	YE3 (1)	3	milky white with irregular fungi-look shape	*Methylocapsa acidiphila* DSM 13967 (AJ278726)	98.6	*Beijerinckiaceae* bacterium BW872 (FM252035)	99.2
	Burkholderiales (order)	YE4-D1-1-CH	FN870344	1	D1 (1)	YE4 (1)	4	tiny, white	*Thiomonas cuprina* NBRC 102094 (AB331953)	98.8	*Thiomonas* sp. N4-1H (AB219370)	99.9
Gammaproteobacteria	*Xanthomonadaceae*	YE3-D1-10-CH	FN870337	8	D1 (7), N1 (1)	FeTo (4), YE3 (2), YE4 (2)	3-4.3	iron rusty orange (FeTo); small, white with metallic luster (YE)	*Dyella yeojuensis* R2A16-10 (DQ181549)	94.3	Gammaproteobacterium W12 (AY096032)	99.9
	Acidithiobacillaceae	FeSo-D1-9-CH	FN870327	1	D1 (1)	FeSo (1)	2.5	'fried egg'-shaped rusty orange-brown	*Acidithiobacillus ferrivorans* strain NO-37 (AF376020)	99.4	*Acidithiobacillus ferrivorans* strain NO-37 (AF376020)	99.4
		FeSo-N1-1-CH	FN870329	10	N1 (6), D1 (4)	Feo (4), iFeo (3), FeSo (3)	2.5	'fried egg'-shaped rusty orange-brown	*Acidithiobacillus ferrooxidans* ATCC 23270 (AF465604)	99.3	*Acidithiobacillus ferrooxidans* strain DX-2 (DQ676506)	99.8
		FeTo-N1-3-CH	FN870335	5	N1 (5)	FeTo (5)	4.3	white powdered-milk-like, non-smooth-surface, overspreaded the plate surface	*Acidithiobacillus ferrooxidans* ATCC 23270 (AF465604)	99.5	*Acidithiobacillus ferrooxidans* strain DX-2 (DQ676506)	99.8

[a] Strain designation was made as follows by combining information about the media, source, and isolate number separated by hyphens. The first part designates the media type, the second part designates the origin of the sediment, e.g. D1 or D4 means deep site of the lake (D) and either upper sediment zone I (1) or deeper sediment zone IV (4). N1 and N4 means north shore site of the lake (N) and either upper sediment zone I (1) or deeper sediment zone IV (4). The next number is the sequential number of the isolate, and CH designates the presence of cycloheximide (CH) if it was added. .

Table S2: Summary of phylogenetic affiliation and distribution of 16S rRNA gene sequences from clone libraries BacI and BacIV of sediment cores obtained from top and bottom sediment zones at the northern shore line (N1 and N4, respectively) and from isolates obtained from top and bottom sediment zones at the deep central basin (D1 and D4, respectively) and the north shore.

Taxa (phylum)	Taxa (family)	No. of clones		No. of isolates	Number of isolates obtained from sediment zones identified by ARDRA pattern
		BacI	BacIV		
Acidobacteria	*Acidobacteriaceae*	12	33	1	1, D1 (1)
Actinobacteria	*Acidimicrobiaceae*	6	0	1	1, D1 (1)
	Microbacteriaceae	2	0	0	
	Micrococcaceae	22	0	0	
	Micromonosporaceae	1	0	0	
	Pseudonocardiaceae	6	0	0	
	Streptomycetaceae	7	1	2	5, D4 (5)
	Thermomonosporaceae	0	0	1	1, D4 (1)
	Unclassified	3	0	0	
Firmicutes	*Alicyclobacillaceae*	0	0	15	24, D4 (17), N4 (7)
	Bacillaceae	5	2	2	4, D4 (3), D4 (1)
	Ruminococcaceae	0	1	0	
	Thermoanaerobacteraceae	2	6	0	
	Unclassified	2	5	0	
Alphaproteobacteria	*Acetobacteraceae*	18	1	6	51, D1 (19), D4 (16), N1 (9), N4 (7)
	Beijerinckiaceae	0	0	2	5, D4 (5)
	Rhodospirillaceae	0	1	0	
	Unclassified	1	0	0	
Betaproteobacteria	*Burkholderiaceae*	0	1	0	
	Alcaligenaceae	0	3	0	
	Burkholderiales (order)	0	0	1	1, D1 (1)
	Rhodocyclaceae	0	1	0	
Deltaproteobacteria	*Polyangiaceae*	1	0	0	
	Desulfobacteraceae	0	5	0	
	Desulfobulbaceae	0	5	0	
	Desulfovibrionaceae	0	1	0	
	Desulfuromonadaceae	0	11	0	
	Geobacteraceae	0	17	0	
	Cystobacterineae	0	1	0	
Gammaproteobacteria	*Xanthomonadaceae*	15	0	4	8, D1 (7), N1 (1)
	Acidithiobacillaceae	0	0	3	16, D1 (5), N1 (11)
	Halomonadaceae	0	1	0	
Spirochaetes	*Spirochaetaceae*	0	3	0	
Chlorobi	*Chlorobiaceae*	0	3	0	
Chloroflexi	Unclassified	0	5	0	
Cyanobacteria	Unclassified	18	1	0	
Deinococcus-Thermus	*Thermaceae*	0	1	0	
Verrucomicrobia	*Xiphinematobacteriaceae*	0	5	0	
Nitrospira	*Nitrospiraceae*	4	12	0	
Planctomycete	*Planctomycetaceae*	0	7	0	
	Unclassified	0	1	0	
Bacteroidetes	*Crenotrichaceae*	0	1	0	
	Porphyromonadaceae	0	2	0	
	Rikenellaceae	0	4	0	
	Unclassified	0	2	0	
Unclassified	Unclassified	2	1	0	
sum		127	144	38	117

Table S3: Summary of phylogenetic affiliation and distribution of 16S rRNA gene sequences from archaeal clone libraries ArcI and ArcIV of sediment cores obtained from top and bottom sediment zones at the north shore line.

Library	Taxa (family)	Genus	No. of clones	Accession No.	Nearest clone in Genbank (Ac. No., % Identity)
ArcI	*Thermoplasmatales incertae sedis*	*Thermogymnomonas*	46	FN870277, FN870274, FN870279, FN870275	archaeon clone anta6 (DQ303248, 99)
	Methanobacteriaceae	*Methanothermobacter*	4	FN870276	archaeon clone ORCMO.17 (EF396245, 91.8)
	Picrophilaceae	*Picrophilus*	1	FN870278	archaeon clone antb9 (EF446193, 91.3)
	Methanococcaceae	*Methanococcus*	1	FN870280	archaeon clone ORCMO.17 (EF396245, 94)
	Thermococcaceae	*Pyrococcus*	1	FN870281	archaeon clone ORCMO.17 (EF396245, 88.5)
ArcIV	*Sulfolobaceae*	*Sulfolobus*	7	FN870251, FN870266, FN870267	archaeon clone MH1492_B9G (EU155993, 99.6)
	Methanopyraceae	*Methanopyrus*	15	FN870250, FN870252, FN870253, FN870254, FN870256, FN870258, FN870259, FN870265, FN870273	archaeon clone NR (AB243795, 97.1)
	Halobacteriaceae	*Natronomonas*	3	FN870263, FN870272	archaeon clone FenA-16S (AJ548935, 95.8)
		Halobacterium	1	FN870271	archaeon clone LCT43 (AM503916, 99.9)
	Methanococcaceae	*Methanococcus*	3	FN870249, FN870261	archaeon clone tlsA1-2 (DQ857287, 92.5)
	Methanosarcinaceae	*Methanosarcina*	6	FN870255, FN870257, FN870262, FN870264, FN870270	archaeon clone YBCAr26 (FM165682, 99.1)
	Archaeoglobaceae	*Archaeoglobus*	5	FN870260, FN870268, FN870269	archaeon clone MH1492_B9G (EU155993,99.3)

Figure S1. Representative sediment cores obtained from the deep central basin and from the north shore line. Cores were sectioned based on visual stratification. Oxygen microprofiles starting in the overlying water phase above the water-sediment interface (0 mm) down to 5 or 10 mm depths were measured with microelectrodes.

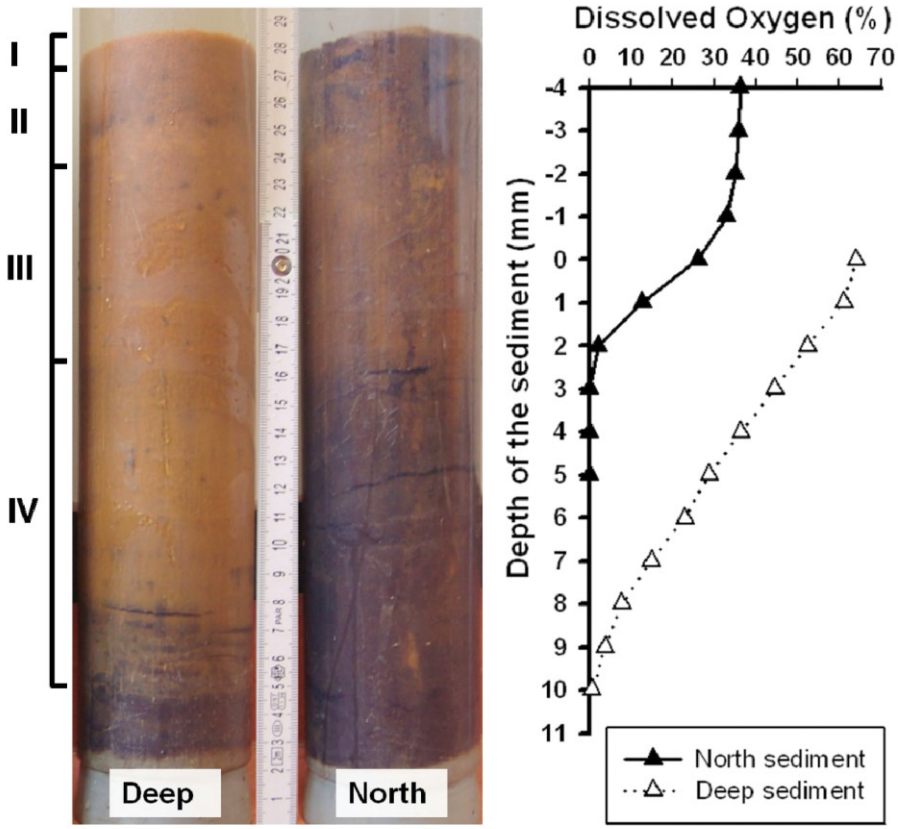

3 Pelagic boundary conditions affect the biological formation of iron-rich particles (iron snow) and their microbial communities

Marco Reiche, Shipeng Lu, Valerian Ciobotă, Thomas R. Neu, Sandor Nietzsche, Petra Rösch, Jürgen Popp, and Kirsten Küsel

Manuscript published in *Limnology and Oceanography* (Jul. 2011) Vol. 56, pp. 1386-1398

Abstract

We studied the formation of iron-rich particles at steeply opposing gradients of oxygen and Fe(II) within the redoxcline of an acidic lignite mine lake (pH 2.9). Particles formed had a diameter of up to 380 µm, showed high sedimentation velocity (~ 2 m h^{-1}), and were dominated by the iron mineral schwertmannite. Although the particles were highly colonized by microbial cells (~ 10^{10} cells [g dry weight]$^{-1}$), the organic carbon content was below 11%. Bathymetry and the inflow of less acidic, Fe(II)-rich groundwater into the northern basin of the lake results in two distinct mixing regimes in the same lake. The anoxic monimolimnion of the northern basin had higher pH, Fe(II), dissolved organic carbon, and CO_2 values compared with the more central basin. Particles formed in the northern basin differed in color, were smaller, had higher organic carbon contents, but were still dominated by schwertmannite. Microcosm incubations revealed the dominance of microbial Fe(II) oxidation. Comparison of bacterial clone libraries suggested that pH was a major driving force, shaping the microbial communities responsible for the oxidation of Fe(II) in both basins. Acidophilic *Ferrovum* spp. and *Chlorobia*-related bacteria were present in the central basin, whereas neutrophilic *Sideroxydans* spp. dominated the northern basin. Snow-like particles had a high sinking velocity and acted as a carrier for organic carbon, microorganisms, trace metals, and Fe(III) to the sediment. Because these particles are

fundamentally different from organic-rich ‘‘snows’’ from lakes, rivers, and oceans, we propose a new term, ‘‘iron snow.’’

Limnol. Oceanogr., 56(4), 2011, 1386–1398

doi:10.4319/lo.2011.56.4.1386

Pelagic boundary conditions affect the biological formation of iron-rich particles (iron snow) and their microbial communities

Marco Reiche,[a] Shipeng Lu,[a] Valerian Ciobotă,[b] Thomas R. Neu,[c] Sandor Nietzsche,[d] Petra Rösch,[b] Jürgen Popp,[b,e] and Kirsten Küsel[a,1,*]

[a] Institute of Ecology, Friedrich Schiller University Jena, Jena, Germany
[b] Institute of Physical Chemistry, Friedrich Schiller University Jena, Jena, Germany
[c] Department of River Ecology, Helmholtz Centre for Environmental Research – UFZ, Magdeburg, Germany
[d] Centre of Electron Microscopy, University Hospital Jena, Friedrich Schiller University Jena, Jena, Germany
[e] Institute of Photonic Technology, Jena, Germany

Abstract

We studied the formation of iron-rich particles at steeply opposing gradients of oxygen and Fe(II) within the redoxcline of an acidic lignite mine lake (pH 2.9). Particles formed had a diameter of up to 380 μm, showed high sedimentation velocity (~ 2 m h^{-1}), and were dominated by the iron mineral schwertmannite. Although the particles were highly colonized by microbial cells (~ 10^{10} cells [g dry weight]$^{-1}$), the organic carbon content was below 11%. Bathymetry and the inflow of less acidic, Fe(II)-rich groundwater into the northern basin of the lake results in two distinct mixing regimes in the same lake. The anoxic monimolimnion of the northern basin had higher pH, Fe(II), dissolved organic carbon, and CO_2 values compared with the more central basin. Particles formed in the northern basin differed in color, were smaller, had higher organic carbon contents, but were still dominated by schwertmannite. Microcosm incubations revealed the dominance of microbial Fe(II) oxidation. Comparison of bacterial clone libraries suggested that pH was a major driving force, shaping the microbial communities responsible for the oxidation of Fe(II) in both basins. Acidophilic *Ferrovum* spp. and Chlorobia-related bacteria were present in the central basin, whereas neutrophilic *Sideroxydans* spp. dominated the northern basin. Snow-like particles had a high sinking velocity and acted as a carrier for organic carbon, microorganisms, trace metals, and Fe(III) to the sediment. Because these particles are fundamentally different from organic-rich "snows" from lakes, rivers, and oceans, we propose a new term, "iron snow."

Oxic–anoxic interfaces are hotspots for the cycling of elements because they provide continuously favorable conditions for both biotic and abiotic redox reactions. In aquatic ecosystems, these interfaces may appear as pelagic boundaries by separating an upper oxic and a lower anoxic water body, yielding permanently or temporally stratified conditions. These boundaries, or redoxclines, may occur in the water column of marine (Jørgensen et al. 1991; Taylor et al. 2001; Pimenov and Neretin 2006) and of freshwater bodies (Boehrer and Schultze 2008; Casamayor et al. 2008). Within such redoxclines, opposing gradients of oxygen and more reduced components, i.e., Fe(II), S^{2-}, and CH_4, may establish. While the oxidation of S^{2-} (Jørgensen et al. 1991; Lüthy et al. 2000) and CH_4 (Rudd et al. 1974; Liu et al. 1996; Bédard and Knowles 1997) at redoxclines has been extensively investigated, less information is available about the oxidation of Fe(II). Some evidence for the cycling of iron at pelagic boundaries exists (Campbell and Torgersen 1980; Boehrer and Schultze 2006; Díez et al. 2007), and the formation of Fe(III)-minerals in acidic aquatic environments has been linked to a microbial oxidation of Fe(II) in the water column (Childs et al. 1998; Peine et al. 2000; Kawano and Tomita 2001). Similar processes might have occurred in the Late Paleoproterozoic, leading to the formation of Paleozoic ironstones within the redoxclines of ancient marine sediments (Bekker et al. 2010). Since Fe(II) persists under abiotic conditions at pH values below 3.5 despite the presence of oxygen (Singer and Stumm 1970), acidophilic aerobic Fe(II)-oxidizing bacteria (FeOB) likely do not compete with the chemical oxidation of Fe(II) as compared to circumneutral conditions. However, no experiments at pelagic redoxclines have been performed which demonstrate whether this occurs and identify which microorganisms are involved in Fe(II) oxidation.

Opposing gradients of oxygen and Fe(II) can be found at redoxclines in iron-rich lakes that have been established worldwide in pyrite-rich or post-mining landscapes (Blodau 2006; Boehrer and Schultze 2006; Díez et al. 2007). In Germany, > 500 pit lakes originating from lignite mining exist with pH values ranging from below 2.5 to above 7 (Nixdorf and Kapfer 1998; Nixdorf et al. 2001). Pit lakes are characterized by the release of protons, sulfate, and Fe(II) from the oxidative weathering of Fe(II) sulfides in weakly buffered and dump-affected catchments. The subsequent oxidation of Fe(II) in ground- or surface waters leads to dissolved Fe(III) species which then transform into polymeric Fe(III) colloids prior to their precipitation as poorly crystalline Fe(III) oxyhydroxides (Davison 1993; Cornell and Schwertmann 2003; Hansel et al. 2003). Consequently, pit lake sediments are dominated by large quantities of amorphous $Fe(OH)_3$, goethite, or Fe(III)

* Corresponding author: kirsten.kuesel@uni-jena.de

[1] Present address: Aquatic Geomicrobiology Group, Institute of Ecology, Friedrich Schiller University Jena, Jena, Germany

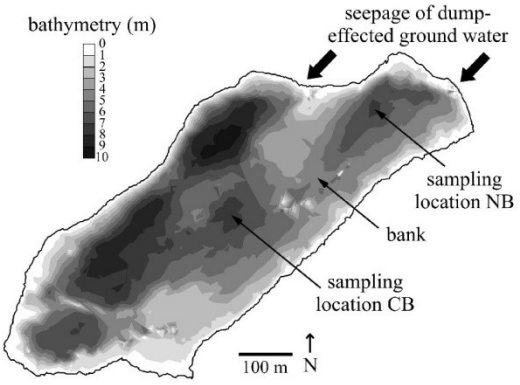

Fig. 1. Sampling sites and bathymetry of Lake 77 (modified after Fleckenstein et al. 2009). Groundwater flows from the north to the south and enters the lake from the dump area in the northern part. A bank rising to about 4 m from the surface separates the northeastern from the southern bottom water layers.

oxyhydroxysulfates, e.g., schwertmannite or jarosite, which are formed according to the pH and geochemistry (Bigham et al. 1992; Bigham and Murad 1997) present in the water column above (Peine et al. 2000; Regenspurg et al. 2004). Since Fe(III) oxyhydroxides can coprecipitate or adsorb organic carbon, heavy metals, and organisms (Eichler and Pfennig 1990; Martinez and McBride 1998; Eusterhues et al. 2008), they could play an important role in these pelagic processes.

In this study, we investigated the potential microbial formation of iron-rich particles at the pelagic redoxcline of an acidic lignite mine lake (Lake 77) in east-central Germany. Because the inflow of less acidic, Fe(II)- and sulfate-rich groundwater from the dump area in the northeast (Blodau et al. 2004) has potential implications for the pelagic boundary conditions, particles were sampled from both the central and northeastern basin of the lake and were characterized with mineralogical and molecular methods. We hypothesized that the oxidation of Fe(II) and the formation of iron-rich particles depends on the activity of FeOB.

Methods

Site description and sampling—The acidic lignite mine lake (Lake 77, pH ~ 3) is located in the Lusatian mining area in east-central Germany and was created after lignite mining had ceased in the area in 1960s. The lake has a surface area of ~ 0.24 km^2, a volume of ~ 1 km^3, and a maximum depth of about 9 m. The general pattern of water exchange is characterized by the Fe(II)- and sulfate-rich groundwater inflow from the dump area at the north end of the lake and the outflow of lake water to the aquifer in the south (Fig. 1). Exchange rates range from -1.7 L m^{-2} d^{-1} (outflow) to > 200 L m^{-2} d^{-1} (inflow) (Fleckenstein et al. 2009).

Sampling sites were located in the central basin of the lake (location CB, depth 7 m, 51°31′8.2″N, 13°41′34.7″E) and in the northeastern basin of the lake (location NB, depth 7 m, 51°31′13.3″N, 13°41′45.8″E) (Fig. 1). On each sampling date (April, July, August, September, and October 2009, and January and April 2010), pH, dissolved oxygen, conductivity, and temperature were measured over depth with a multiparameter water quality checker U-10 (Horiba, Japan). High-resolution water samples in steps of up to 5 cm were obtained using a water sampler (55-cm length) based on the Ruttner design. For gas analysis, 50-mL water samples were added to 150-mL glass flasks, sealed gas tight with rubber stoppers, and treated with 1 mL of 4 mol L^{-1} HCl. Sediment traps (three Plexiglas tubes sealed with a removable cup at the bottom, 5-cm diameter, 40-cm total length) were installed at a depth of 5.3 m at location CB from which particles were collected every 3 to 4 weeks from April to October 2009. At location NB, particles were enriched by centrifugation of water samples obtained from 5-m depth or collected with sediment traps (April 2010 only). All samples were transported at 4°C and processed within 24 h. Sediment cores were obtained in September 2009 using a gravity corer (5.9-cm inside diameter) and the upper 5 mm were used for microbial diversity analysis. The sediment at location CB was characterized by an upper brownish-orange zone of about 20 cm and a black zone below. In contrast, the brownish-orange zone was < 3 cm deep at location NB. Below this, thin orange and black bands appeared. In general, the sediments contained large amounts of schwertmannite and goethite. Detailed geochemical descriptions of the sediment at location CB have been given elsewhere (Peine et al. 2000; Regenspurg et al. 2004).

Characterization of particles—The sinking velocity of single particles in 10 replicates was estimated at 21°C in a 3-liter glass cylinder filled with lake water. Sedimentation rate was calculated per m^2 d^{-1} and was performed after drying (105°C for 24 h) of each subsample of the sediment trap material. Total cell abundance in the particles from location CB was enumerated by the 4,6-diamidino-2-phenylindole (DAPI) method (Porter and Feig 1980) after fixation (4% formaldehyde buffered with 1× phosphate buffered saline [PBS] at pH 7.4, washed three times with 1× PBS) and oxalate extraction (75 mmol L^{-1} oxalate, 15-min incubation, washed three times with 1× PBS) with a Zeiss Axiolab microscope at ×1000 magnification (Carl Zeiss). The particle density in the water column was quantified on white polycarbonate filters (0.2-μm pore size, 39-mm diameter; Whatman) after filtration of defined volumes of lake water from 0, 3, and 5 m of location CB and 6 m from location NB with a Zeiss Axiolab microscope (Carl Zeiss) at 20× magnification. Mineral phases were determined using Raman spectroscopy and were recorded with a high-resolution LabRam spectrometer (Jobin Yvon Horiba) using 532-nm radiations from a frequency-doubled neodymium:yttrium–aluminum–garnet laser. The laser beam of about 20 μW was focused on the samples by a Leica PLFluoar 100× (numerical aperture [NA] 0.75) microscope objective down to a spot diameter of approximately 0.7 μm. The spectral resolution was around 8 cm^{-1} and the acquisition time for each Raman spectrum varied between 60 and 300 s.

Confocal laser scanning microscopy (CLSM)—To analyze the distribution of microbial cells in the particles, we counterstained bacteria in a fixed (3.4% formaldehyde) subsample of the sediment trap material obtained from location CB in September 2009 with SYTOX Orange (Molecular Probes) nucleic acid stain at a dilution of 1 : 1000 with deionized water for 5 min. Samples were rinsed once with tap water and transferred into Cover Well imaging chambers with a 0.2-mm spacer (Invitrogen), and immediately examined by CLSM using a true confocal scanner (TCS SP5X, Leica), equipped with an upright microscope and 63× NA 1.2 water immersion lens. Samples were analyzed by CLSM using laser lines at 547 and 633 nm. Emission signals were detected from 540 to 555 nm (inorganic and mineral compounds; detected by reflection signals), 560 to 620 nm (nucleic acid signals of SYTOX Orange), and from 650 to 750 nm (chlorophylls; detected by autofluorescence). Optical sections were scanned in the xy direction up to a depth of 100 μm with a step size of 1 μm. Images were recorded at a resolution of 1024 × 1024 pixels, corresponding to a 246-μm edge length. For visualization, image stacks were presented as overlays as maximum intensity projections. Blind deconvolution was calculated with Huygens version 3.5 (Scientific Volume Imaging).

Scanning electron microscopy (SEM) with energy-dispersive X-ray spectroscopy (EDX)—A subsample of the sediment trap material from either location CB or microcosm incubations was directly dried on adhesive conductive carbon tabs at 60°C to determine the overall morphology of the particles. The cell morphotypes present in the particles were determined after fixation (2.5% glutaraldehyde in PBS at pH 7.4, followed by washing three times with PBS), oxalate extraction (75 mmol L^{-1} oxalate, 15-min incubation, washed three times with PBS), dehydration for 5 min each in ascending ethanol concentrations (10%, 20%, 30%, 50%, 70%, 80%, 90%, and 100%), and critical-point drying using liquid CO_2. Samples were sputter coated with platinum for high-resolution SEM or carbon coated by vacuum evaporation for EDX and finally examined under the SEM (LEO 1530 Gemini, Carl Zeiss) at magnifications of up to 20,000×. Elemental distribution was investigated using EDX (Quantax 200 with XFlash detector, Bruker) at a SEM (LEO 1450 VP, Carl Zeiss).

Determination of microbial Fe(II) oxidation in microcosms—At location CB, water was sampled from depths of either 3 m (oxic zone) or 6 m (anoxic zone) and at location NB, water was sampled from depths of 4.8 m (redoxcline) or 5.5 m (anoxic zone) in September and October 2009. Fifty milliliters of untreated lake water was transferred to sterile 150-mL incubation flasks (Mueller and Krempel) in triplicates. Headspace was air with an oxygen content of 21%. Samples poor in Fe(II) from 3 m were amended with sterile Fe(II)SO_4 solution to yield 3 and 12 mmol L^{-1} Fe(II). Microcosms were closed with rubber stoppers, screw-capped, and incubated in the dark at 15°C for 9 d. Potential chemical Fe(II) oxidation was determined in abiotic controls after sterile filtration (0.2 μm).

Analytical techniques—The oxidation of Fe(II) was determined by measuring the amount of Fe(II) after acid extraction. Aliquots (0.5 mL) were removed daily from the microcosms with sterile syringes, transferred to 9.5 mL of 0.5 mol L^{-1} HCl, and then incubated for 1 h at room temperature. Fe(II) concentrations were measured spectrophotometrically (DR3800, Hach Lange) by the phenanthroline method (Tamura et al. 1974). Rates of Fe(II) oxidation were calculated for the time period over which a linear decrease in the Fe(II) concentration was observed. After addition of ascorbic acid, HCl-extractable Fe(III) was calculated from the increase in Fe(II) concentration. Sulfate was measured turbidimetrically by the barium chloride–gelatin method (Tabatabai 1974). Water sample density was measured with a hydrometer at 6°C. Headspace CO_2 and CH_4 was measured with 5890 series II gas chromatographs equipped with a thermal conductivity detector or flame ionization detector (Hewlett-Packard) (Küsel and Drake 1995). The elemental composition of dried (60°C) and milled particles was directly analyzed with an elemental analyzer (vario Max or vario EL II, Elementar) or by inductively coupled plasma mass spectrometry (ICP-MS; XSeries II, Thermo Fisher Scientific) and inductively coupled plasma optical emission spectrometry (ICP-OES; Spectroflame, Spectro) after aqua regia decomposition. Heavy metal concentrations in lake water were analyzed with ICP-MS or ICP-OES without further treatment. Dissolved organic carbon (DOC) and dissolved nitrogen in water samples from both locations were measured with a total organic carbon analyzer (TOC-V CPN equipped with a total nitrogen module, Shimadzu).

Deoxyribonucleic acid (DNA) extraction and polymerase chain reaction (PCR) amplification of 16S ribosomal ribonucleic acid (rRNA) genes—Genomic DNA was directly extracted from particles captured in the sediment traps of location CB or obtained from the water column at location NB, and from the sediments at both locations using the PowerSoil, DNA Isolation Kit according to the manufacturer's instructions (MO BIO Laboratories). Samples from microcosms were concentrated by centrifugation (5 min at 10,000 × *g*) after scraping off the rust-colored crust or the extraction of rust-colored flakes before treatment. DNA extracts were PCR amplified with the bacteria domain-specific 16S rRNA gene primers 27F and 1492R-2 (Lane 1991) and purified using the NucleoSpin Extract II PCR purification kit (Macherey-Nagel). Thermocycling was performed with a T-Gradient cycler (Primus 96advanced, peqLab). Reactions were run for 30 cycles of amplification at an annealing temperature of 56°C.

Denaturing gradient gel electrophoresis (DGGE) fingerprinting—Bacterial community DNA extracted from the particles and sediments was fingerprinted using a nested-PCR–DGGE approach. Nested amplification of the bacteria domain-specific 16S rRNA products was executed with the universal bacterial primers GM5F-GC-clamp and 907R (Muyzer et al. 1995) with an annealing temperature of 55°C and 20 cycles of amplification. PCR products were separated on an 8% polyacrylamide gel with a 30% to 70%

denaturant gradient (Muyzer et al. 1993) in 1× tris-acetate-ethylene diamine tetraacetic acid buffer using the DGGE 1001 system (C.B.S. Scientific). DGGE gels were run for 15 h at 60°C and 100 V. To compare the bacterial community composition between sites, sampling dates, and sampling sources, Jaccard Similarity values were calculated (Schloss and Handelsman 2006). These values consider how many bands are shared between DGGE band patterns relative to the total number of bands. Similarity matrices were turned into dendrograms to visualize the clustering of bacterial communities based on their similarities in band composition, utilizing the Clustering Calculator programs of Brzustowski (2002) and Interactive Tree of Life (Letunic and Bork 2006).

Clone library construction and phylogenetic analyses—Bacteria domain-specific 16S rRNA PCR products obtained in September 2009 from the particles at both locations were ligated into pCR4-TOPO vector (Invitrogen Corporation), cloned according to the manufacturer's recommendations, and sequenced at Macrogen. Cloning and bidirectional sequencing was also done at The Genome Center at Washington University. Sequences were processed with Geneious software (Drummond et al. 2009), aligned against the 16S Greengenes rRNA gene database using NAST (DeSantis et al. 2006*a*), and analyzed with the ARB software package (Ludwig et al. 2004) in combination with the Greengenes database (DeSantis et al. 2006*b*). Sequences sharing > 97% similarity were grouped as the same phylotype using FastGroup II (Yu et al. 2006). The percentage of coverage between the clone libraries was calculated with the formula $(1 - [n/N]) \times 100$, where n is the number of unique phylotypes and N is the total number of phylotypes. Double-reciprocal analysis of rarefaction data was then used to estimate the maximum amount of expected phylotypes.

Nucleotide sequence accession numbers—The 16S rRNA gene sequences determined in this study have been deposited in the European Molecular Biology Laboratory database under accession numbers FR667757 to FR667847.

Results

Biogeochemical characteristic of the water column—A dimictic stratification scenario, with typical spring and fall mixes, occurred at CB. Early thermal stratification was established in April with a decrease from 15°C to 9°C between 3- and 5-m depths (data not shown), whereas the other measured parameters remained stable over depth. An anoxic hypolimnion occurred from July to September (Fig. 2A and data not shown) with higher Fe(II) and pH values as compared to April and no change in sulfate concentrations and conductivity. Density of both surface and bottom water was approximately 1.000 g mL^{-1}. The anoxic hypolimnion was separated from the overlaying oxic mixolimnion by a pronounced redoxcline of about 60-cm thickness within the thermocline starting at about 4.8 m. The stratification at CB disappeared due to changing temperature in October and parameters returned to spring values (Fig. 2C). In the winter, the water body was again thermally stratified, but under ice coverage (data not shown).

At NB, values for Fe(II), sulfate, pH, and conductivity increased sharply within the redoxcline and reached the highest values in the hyoplimnion, respectively (Fig. 2B,D). Fe(II) and oxygen coincided within the redoxcline by forming a distinct transition zone of about 30 cm (Fig. 2). The density of the bottom water was always higher (1.001 g mL^{-1}) than that of the surface water (1.000 g mL^{-1}). As stratification did not disappear at NB, the water column was continuously divided into an oxic mixolimnion and an anoxic monimolimnion by the sharp redoxcline centered at about 4.3 m (Fig. 2B,D). Even when the surface water was colder than the bottom water, complete vertical mixing was inhibited (Fig. 2D), suggesting a permanent separation of the bottom water bodies at CB and NB, which might be due to a bank (4 m deep) separating the central and the northern basins (Fig. 1).

Lake 77 can therefore be classified as meromictic with a distinct monimolimnion in the northern basin. In contrast to location CB, acid-releasable CO_2 increased from 0.4 mmol L^{-1} in the mixolimnion within the bottom water layer up to 11.3 mmol L^{-1} (Table 1). Concentrations for CH_4 were always below the detection limit (< 40 nmol L^{-1}) at both locations. Water from the bottom at NB was slightly opaque and characterized by a yellowish color. Water from the surface and water samples obtained from CB never showed visible coloration.

Dissolved Ni, Co, Cu, Zn, Pb, As, Cd, and U concentrations were below 4 μmol L^{-1} and appeared similar at CB and NB during stratification in September (data not shown). In contrast, concentrations for Al were lowest in the monimolimnion of location NB (9 μmol L^{-1}) as compared to the hypolimnion at CB (152 μmol L^{-1}) and the connected surface mixolimnion (264 μmol L^{-1}). Concentrations of DOC were high, ranging from about 0.4 mmol L^{-1} in the mixolimnion to about 2.3 mmol L^{-1} in the monimolimnion at NB (Table 1).

Characteristics of lake particles—Particles obtained from the oxic mixolimnion were up to 380 μm in size. Single particles in samples collected directly from the anoxic hypolimnion typically ranged from 60 to about 240 μm at CB, and from 20 to 120 μm in the anoxic monimolimnion at NB (Table 2). The sinking velocity of single particles from location CB was 1.5 to 2 m h^{-1} which equals 3.5 to 4.7 h for horizontal passage through the whole water column or < 1.8 h through the anoxic water layers at the bottom of Lake 77 under undisturbed conditions. Particle densities were lower in the mixolimnion than the hypolimnion at CB and the monimolimnion at NB in September (Table 2). The sedimentation rate of particles obtained with sediment traps from August to October was approximately 3.9 ± 1.1 g (dry wt) m^{-2} d^{-1} at CB, yielding an annual precipitation of about 1400 g (dry wt) m^{-2}. A single measurement in July 2010 at NB revealed 5.5 g (dry wt) m^{-2} d^{-1} and 2000 g (dry wt) m^{-2} over 1 yr.

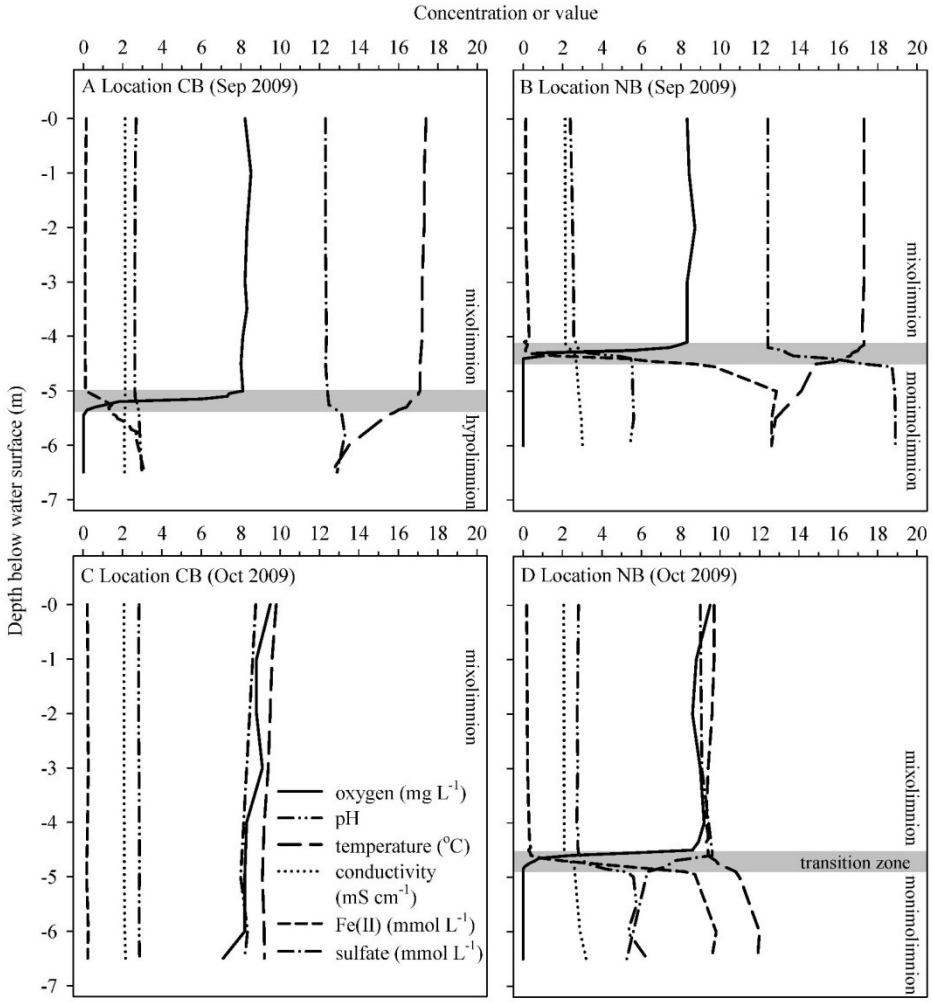

Fig. 2. Water profiles of biogeochemical parameters measured at two sampling locations within the acidic lignite mine Lake 77 in September (A and B) and October (C and D) 2009. CB (A and C) has a dimictive regime with an anoxic hypolimnion in summer and NB (B and D) has a continuous anoxic monimolimnion.

Particles obtained at location CB appeared as rust-colored floating flakes. Flakes were composed of aggregates of hedgehog-like spheres with diameters of 0.7 to 13 μm determined by SEM (Fig. 3A). The hedgehog-like morphology of the aggregates is characteristic for schwertmannite (ideal formula: $Fe_8O_8(OH)_6SO_4$), a poorly crystalline, yellowish-brown Fe(III) oxyhydroxysulfate mineral (Bigham et al. 1990, 1994; Regenspurg et al. 2004). Mass

Table 1. Water characteristics in different water layers of the acidic lignite mine Lake 77. Samples were obtained at two locations (central basin [CB] and northeastern basin [NB]), which differ in their stratification patterns.

Water layer	Location	Depth (m)	pH*	DOC† (mmol L^{-1})	CO_2† (mmol L^{-1})	Fe* (mmol L^{-1})	Al* (mmol L^{-1})
Mixolimnion	CB	3	2.6	0.4	0.4	1.8	0.26
Hypolimnion	CB	6	2.9	0.4	0.4	3.8	0.15
Monimolimnion	NB	5	5.6	2.3	11.3	11.7	0.01

* Samples obtained in September 2009.
† Samples obtained in January 2010.

Table 2. Iron-rich particle (iron snow) characteristics in different water layers of the acidic lignite mine Lake 77. Samples were obtained during lake stratification during the summer at two locations (central basin [CB] and northeastern basin [NB]), which differ in their stratification patterns.

Water layer	Location	Depth (m)	Particles (L^{-1})	Particle size range (μm)	Sinking velocity (m h^{-1})	Sedimentation rate (g [dry wt] m^{-2} d^{-1})
Mixolimnion	CB	3	$\sim 10^6$	60–380	n.d.	n.d.
Hypolimnion	CB	6	$\sim 10^8$	60–240	1.5–2	3.9
Monimolimnion	NB	5	$\sim 10^9$	20–120	n.d.	5.5

n.d., not determined.

ratios of elements detected using SEM-EDX and direct scanning using Raman spectroscopy revealed schwertmannite as the dominant mineral (Fig. 4 and data not shown). Minor amounts of the Fe(III) minerals goethite, ferrihydrite, and jarosite, as well as quartz, coal, and gypsum, were also identified by Raman spectroscopy (Fig. 4). Raman spectra did not reveal Fe(II) minerals like pyrite, marcasite, siderite, vivianite, or magnetite. The precipitated particles in the central basin contained 6.9 mmol Fe (g dry wt)$^{-1}$, which is 39% of the dry weight mass, followed by S (5.0%), C (3.1%), Al (1.8%), Ca (0.4%), and nitrogen (0.2%) (Table 3). The proportions of Ni, Co, Cu, Zn, Pb, As, Cd, and U were all below 0.07% (data not shown).

At NB, particles were more yellowish-orange than those at CB. Spherical structures were about 1 μm in diameter and less structured. Raman spectra revealed high amounts of schwertmannite, gypsum, and other unidentified sulfate-containing minerals. Minor amounts of non-coal carbon and ferrihydrite were also detected. Again, no Fe(II) minerals appeared. These particles contained 35% Fe (equal to 6.3 mmol Fe [g dry wt]$^{-1}$), followed by C (10.9%), S (3.8%), nitrogen (0.3%), Al (0.2%), and Ca (0.2%) (Table 3). Proportions of Ni, Co, Cu, Zn, Pb, As, Cd, and U were all below 0.04% (data not shown).

Biotic vs. abiotic Fe(II) oxidation—Oxic microcosms incubated with Fe(II)-poor surface water (initial pH 2.9) obtained from the mixolimnion at CB showed a decrease in Fe(II) concentrations over time after addition of Fe(II). Potential Fe(II) oxidation rates were approximately 0.2 or 0.6 mmol L^{-1} Fe(II) d^{-1} when 3 or 12 mmol L^{-1} Fe(II) were added, respectively (Fig. 5A and data not shown). HCl-extractable Fe(III) concentrations increased similarly with rates of 0.2 and 0.5 mmol L^{-1} Fe(III) d^{-1} (data not shown). No chemical Fe(II) oxidation occurred. Oxic microcosms incubated with Fe(II)-rich water (3.1 mmol L^{-1} Fe(II), initial pH 3.1) obtained from the anoxic hypolimnion at CB yielded an initial potential Fe(II) oxidation rate of 0.7 mmol L^{-1} Fe(II) d^{-1} (Fig. 5B). Fe(II) was totally oxidized within 5 d of incubation and the rate of Fe(III) formation was 0.4 mmol L^{-1} Fe(III) d^{-1} (data not shown). Again, no chemical Fe(II) oxidation occurred.

Initial potential Fe(II) oxidation in Fe(II)-rich water samples (4.3 mmol L^{-1} Fe(II), initial pH 3.2) obtained from the redoxcline at NB yielded potential oxidation rates of 0.3 mmol L^{-1} Fe(II) d^{-1} (Fig. 5B), and Fe(II) concentrations in sterile filtrated or poisoned samples did not change over time.

Iron particles formed in microcosms—Fe(II) oxidation led to an iron crust attached to the inner glass surface of the microcosms in water samples obtained from CB, whereas iron flakes sedimented in microcosms with water from NB. However, Raman spectroscopy revealed no difference in composition between locations, showing schwertmannite as the dominant Fe(III) oxide. The morphology of the minerals in NB samples was dominated by hedgehog-like spheres as compared to the crumb- and clod-like structures

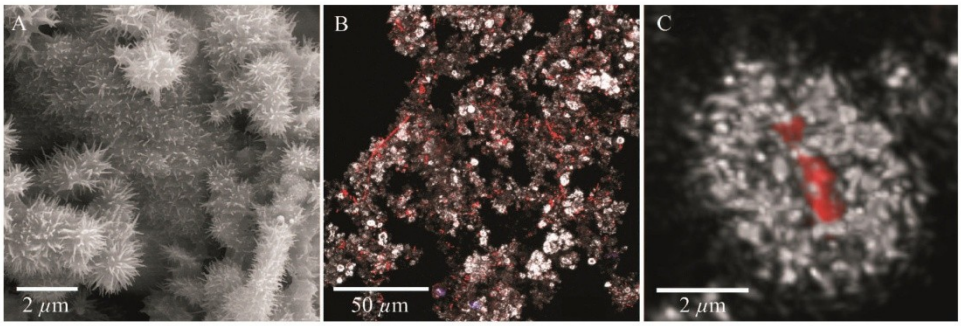

Fig. 3. Micrographs of iron-rich particles (iron snow) captured in sediment traps at CB of the acidic lignite mine Lake 77 in September 2009. (A) Scanning electron micrograph showing hedgehog-like spheres characteristic for schwertmannite, a poorly crystalline, yellowish-brown Fe(III) oxyhydroxysulfate mineral. (B) Confocal laser scanning microscopy (CLSM) of an aggregate colonized by bacteria of different morphology. (C) Close-up of a single bacterium inside reflective material after deconvolution. CLSM color allocation: reflection signal = white, nucleic acid stain = red, phototrophic signals = blue.

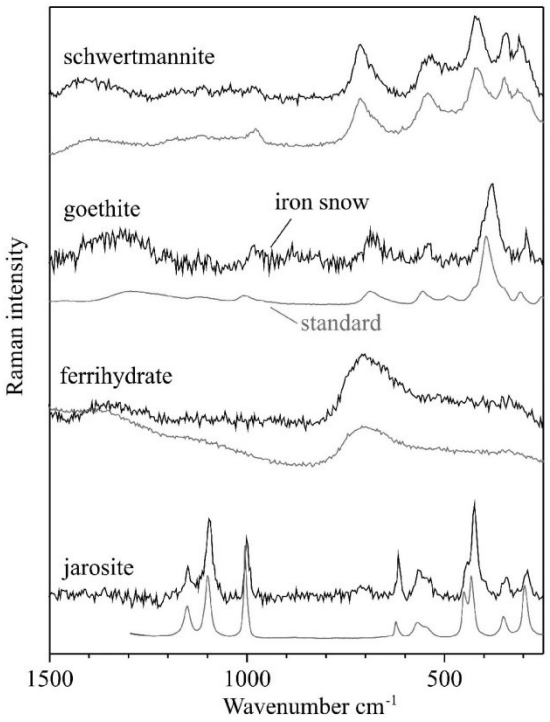

Fig. 4. Raman spectra of the iron particles (iron snow) obtained at CB (black lines) and spectra of authentic standards (gray lines). The main mineral detected was schwertmannite. The particles contained also small amounts of goethite, ferrihydrite, and jarosite.

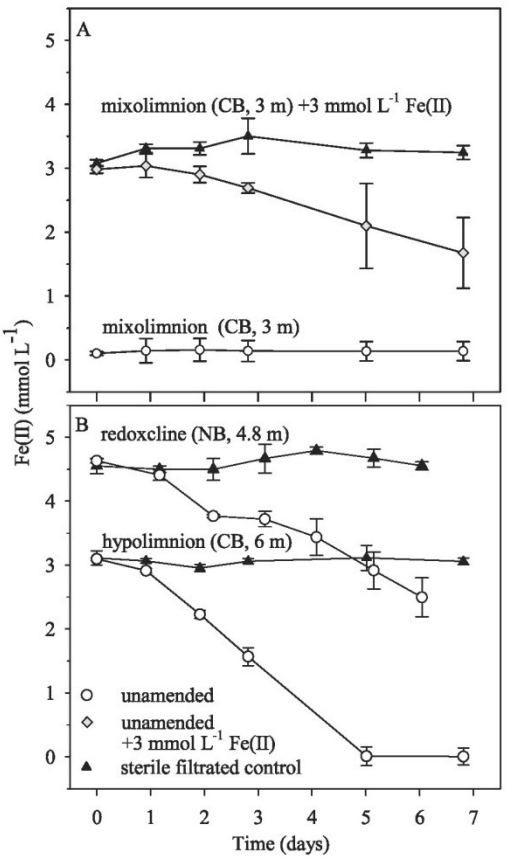

Fig. 5. Fe(II) oxidation in oxic microcosm flasks over time in water samples obtained from different water zones at the central (CB: A and B) and northern basin (NB: B) of the acidic lignite mine Lake 77 in September 2009.

in CB samples. Recently, Lu et al. (2010) also demonstrated that acidophilic and acid-tolerant Fe(II)-oxidizing bacteria isolated from this lake form schwertmannite.

Biotic composition of lake particles—Stained microbial cells and unstained phototrophs were detected in precipitated particles obtained at location CB using CLSM (Fig. 3B). Microbial cells were homogeneously distributed and cells were often present within the reflective schwertmannite spheres (Fig. 3C). Total DAPI counts yielded up to 10^{10} cells (g dry wt)$^{-1}$. Cell morphology was generally dominated by filamentous (up to 200-μm length), cocci (up to 2.3-μm diameter), rods (up to 5-μm length), and club rods (up to 2.5-μm length). Phototrophic signals were rare at a maximum of two algal cells per particle. Two unicellular diatom species with a length of about 22 μm were morphologically similar to *Eunotia* spp. as identified by SEM after oxalate extraction. One of these diatoms and several rod-shaped bacteria, covered or decorated by needle- and coral-like iron minerals, were present in close association with the schwertmannite spheres as detected by SEM. *Eunotia* spp. are widely distributed in both acidic aquatic environments and lignite mining–associated lakes (Nixdorf et al. 2001).

16S rRNA gene-based community analysis—PCR products obtained from particles sampled at CB and NB at

Table 3. Elemental composition of iron-rich particles (iron snow) in the acidic lignite mine Lake 77 obtained from sediment traps at the temporally stratified central location (CB) in September 2009 and obtained from water samples at the permanently stratified northern location (NB) in April 2010.

Water layer	Location	Depth (m)	C (%)	N (%)	Fe (mmol g [dry wt]$^{-1}$)	S (mmol g [dry wt]$^{-1}$)	Al (mmol g [dry wt]$^{-1}$)	Ca (μmol g [dry wt]$^{-1}$)	Mg (μmol g [dry wt]$^{-1}$)	Mn (μmol g [dry wt]$^{-1}$)
Hypolimnion	CB	6	3.1	0.2	6.9	1.6	0.7	105	30	1
Monimolimnion	NB	5	10.9	0.3	6.3	1.2	0.1	61	15	1

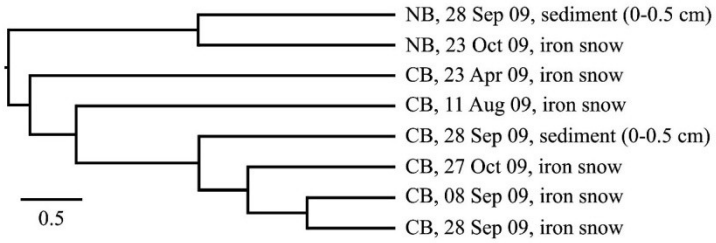

Fig. 6. Similarities of DGGE patterns of bacterial 16S rRNA genes in iron-rich particles (iron snow) and the sediment surface obtained from the northern (NB) and central basin (CB) of Lake 77 based on Jaccard Similarity values.

different times of the year and their respective sediment surfaces produced different DGGE patterns (data not shown). A maximum of 38 different bands was differentiated in each pattern. Clustering of bacterial communities based on their similarities in band composition demonstrated that particles at location CB differed in April and August but appeared to be more similar at the beginning and end of September, and of October (Fig. 6). Consequently, clone library construction was done with the CB particles from the end of September, as it was likely most representative for the period of late stratification. DGGE patterns from particles and sediment surfaces shared great similarity within NB and CB. Patterns were most dissimilar between NB and CB (Fig. 6), suggesting that the different pelagic conditions at each location were responsible for shaping the microbial communities of the particles.

Screening of the clone libraries obtained in September 2009 from CB and NB revealed the presence of 52 and 46 phylotypes out of 90 and 74 clones in the particles, respectively. Both clone libraries shared about 5.5% similarity and had 62% and 66% saturation with respect to the expected number of phylotypes in locations CB and NB, respectively. Many of the clones obtained at CB belonged to four classes (Fig. 7), and were related to acidophilic FeOB, e.g., nine clones were related to *Ferrovum myxofaciens* (Betaproteobacteria, sequence similarity up to 96%), five clones to *Acidimicrobium ferrooxidans* (Actinobacteria, sequence similarity up to 89%), and two clones to *Chlorobium ferrooxidans* (Chlorobia, sequence similarity up to 98%). Some clones were also related to neutrophilic Fe(III)-reducing bacteria like *Geobacter chapellei* (Deltaproteobacteria, sequence similarity up to 97%) and *Geobacter psychrophilus* (sequence similarity up to 99%).

In contrast, particles from NB were dominated only by Betaproteobacteria (Fig. 7), within which 44% of the sequences were related to the neutrophilic FeOB *Sideroxydans lithotrophicus* (sequence similarity up to 98%). One *Sideroxydans* strain is known to oxidize Fe(II) between pH 4.0 and 6.0 (Lüdecke et al. 2010). Several Fe(III) reducers were also detected with sequences related to *Albidiferax ferrireducens*, *Pelobacter propionicus*, *Geobacter chapellei*, and *Geobacter psychrophilus* strain P35.

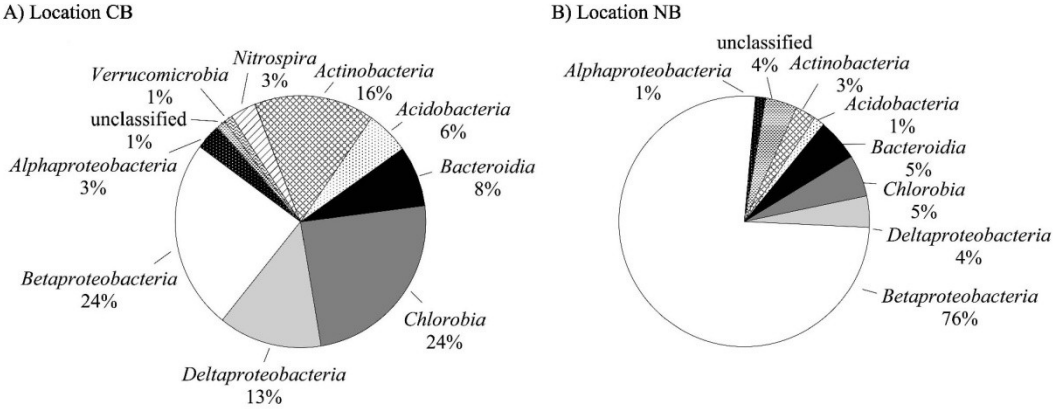

Fig. 7. Frequencies of bacterial phylogenetic lineages detected in 16S rRNA gene-based clone libraries derived from iron-rich precipitated particles (iron snow) below the redoxcline in September 2009 at two sampling locations of acidic lignite mine Lake 77, which differ in stratification patterns and water chemistry. (A) CB has a dimictive regime with an anoxic hypolimnion in summer and (B) NB has a continuous anoxic monimolimnion. Calculations were based on the total number of clones associated with phylotypes of sequenced representatives.

Discussion

The two sampling locations investigated within this iron-rich, acidic lignite mine lake were similar in total water depth but differed in stratification patterns and pelagic boundary conditions. These differences might be caused both by the bank which rises to about 4-m depth and separates the bottom water layers of the northeastern basin from the rest of the lake (Fig. 1) and by local differences in groundwater inflow. At NB, seepage from the northeastern dump area enters the lake. This inflow of less acidic, Fe(II)- and sulfate-rich groundwater (pH 3.8, 3.5 mmol L^{-1} and 10 mmol L^{-1} each; J. Beer pers. comm. 2010) to the separated northern basin may lead to an advective accumulation of dissolved substances, resulting in a density stratification and monimolimnion. In contrast, CB showed a seasonal thermal stratification with a typical mixolimnion and hypolimnion during summer. The hypolimnion was likely less affected by outflow from the dump area and chemical gradients appeared to be more diffusion limited. Dissolved Fe(II) might then only be supplied by the ongoing Fe(III) reduction in the anoxic sediment (Küsel et al. 1999; Blöthe et al. 2008).

High amounts of snow-like particles occurred in the anoxic bottom water layers at both locations. Pelagic particles formed in freshwater or marine environments are generally called "lake snow," "river snow," or "marine snow" depending on their respective environment (Grossart and Simon 1993; Neu 2000). These "snows" are important for the turnover and sinking flux of organic and inorganic matter (Simon et al. 2002) and usually contain a large organic fraction dominated by transparent exopolymers, copepod carcasses, phytoplankton, bacteria, protozoa, and fungi (Simon et al. 2002; Rother and Kohler 2005; Tang et al. 2006). Aggregates in oceans and lakes are usually larger than 500 μm (Alldredge and Silver 1988; Grossart and Simon 1993), whereas the median size in rivers is generally < 60 μm (Berger et al. 1996; Rother and Kohler 2005). Due to their slow sinking velocities and long residence times within the water column, these snow-like particles become hotspots for microbial respiration and growth efficiency (Ploug et al. 1999; Grossart and Ploug 2000; Luef et al. 2007). Particles formed in Lake 77 were generally smaller than 380 μm in diameter and were dominated by an Fe(III)-rich fraction of $> 35\%$ rather than organic matter. These Fe(III)-dominated, microscopic particles and aggregates sedimented as visible rust-colored snow, yielding an estimated Fe(III) sedimentation rate of about 1.5 and 1.9 g Fe m^{-2} d^{-1} at CB and NB, respectively. Their higher sinking velocity compared to classical lake snow may not allow all of the potentially complex aspects of aggregate formation, microbial colonization, and decomposition to occur. Therefore, we propose a new term, "iron snow," for these types of aggregates.

That the size, color, composition, and mineral morphology of iron snow differed at both locations apparently was caused by the different pelagic boundary conditions and microbial communities present during formation. Particle characteristics may have shown even greater variety were samples analyzed that had been taken with higher temporal and spatial variation. Raman spectroscopy and SEM-EDX revealed schwertmannite as the dominant iron mineral in all samples. Schwertmannite typically forms in acidic, sulfate-rich waters (Bigham et al. 1990; Schwertmann et al. 1995; Childs et al. 1998) but can form at pH values up to 6.3 (Murad and Rojik 2005). Due to its high specific surface area of a range of 75 to 200 m^2 g^{-1} (Bigham et al. 1994; Regenspurg et al. 2004), iron snow provides reactive Fe(III) as electron acceptor for anaerobic microbial respiration not only after, but also during, sedimentation. Indeed, iron snow clone libraries harbored numerous clones related to Fe(III)-reducing bacteria like *Geobacter* spp. (Deltaproteobacteria), although *Geobacter* species are not known to inhabit such acidic environments (Lovley et al. 2004). The similarity of the DGGE patterns obtained from the iron snow and sediment surface at both locations suggest further that the iron snow may serve as carrier for general microbial transport to the sediment. It appeared to also have a carrier function for Al, Ca, Mn, Mg, and heavy metals which likely either coprecipitated during iron snow formation or adsorbed to its surface similarly to what is known for other Fe(III)-precipitates (Spark et al. 1995; Martinez and McBride 1998).

Aquatic particles generally contribute to the sedimentary organic carbon pool (de Vicente et al. 2009). The carbon (C) content of iron snow was 3.1% and 10.9% at CB and NB, respectively, and was mainly attributed to microbes and associated organic matter. The equivalent C sinking loss of iron snow estimated from its C content and sedimentation rate is approximately 121 and 600 mg C m^{-2} d^{-1} at CB and NB, respectively. However, this rough estimate is one to two orders of magnitude lower than C sedimentation rates observed in pH-neutral lakes (Grossart and Simon 1998; Moreira-Turcq et al. 2004), where less extreme geochemical conditions result in a higher planktonic primary production (Gyure et al. 1987; Nixdorf et al. 2003; Kamjunke et al. 2005).

The amount of particles was highest in the anoxic bottom water layer, indicating that they are formed within or next to the redoxcline. Steep gradients of oxygen and Fe(II) formed a transition zone 30 to 60 cm deep within the redoxcline during stratification with suitable conditions for aerobic Fe(II) oxidation. The lack of nitrate in the water column should exclude nitrate-dependent Fe(II) oxidation in the anoxic water depths below the redoxcline. Morphology and mineral composition of the rust-colored aggregates formed during oxic microcosm incubations was similar to iron snow sampled from the lake. Because chemical oxidation was never observed, microorganisms appeared to mediate both Fe(II) oxidation and iron snow formation as was assumed in previous studies (Bigham et al. 1990; Childs et al. 1998; Kawano and Tomita 2001). Bacterial cell surfaces may trigger the precipitation of mineral phases as indicated by the CLSM data (Fig. 3C). The capacity for aerobic Fe(II) oxidation was not restricted to water samples obtained from the oxic–anoxic transition zone, but could be initiated both in Fe(II)-poor surface water and in anoxic bottom water (Fig. 5). The zone of aerobic microbial Fe(II) oxidation is likely to span several centimeters within the redoxcline similar to the Fe(II) oxidation zone observed in

an acidic, iron-rich fen (Lüdecke et al. 2010). After mixis in fall, this zone will be temporarily enlarged to the whole water body in the central basin. The oxic–anoxic interface will then move to the sediment surface, similar to what is observed in more pH-neutral environments, where the zone of microbial Fe(II) oxidation is restricted to a few millimeters or less (Mendelssohn et al. 1995; Roden et al. 2004; Druschel et al. 2008).

DGGE analyses revealed the presence of different microbial communities colonizing the iron snow at CB during the beginning and late stratification. However, the differences between sampling locations was more pronounced. Additionally, the libraries from these locations shared only 5.5% similarity, which might be due to the pH discrepancy. *Sideroxydans*-related clones were highly abundant in the NB clone library but did not appear in the CB clone library. These clones have been isolated from a number of pH-neutral to moderately acidic soils and sediments (Emerson and Moyer 1997; Weiss et al. 2007; Lüdecke et al. 2010). Species of this genus are microaerophiles that use Fe(II) as energy for chemolithotrophic growth with CO_2 as the sole carbon source (Emerson and Moyer 1997). Clones closely related to *Ferrovum myxofaciens* were the most prominent species in the CB clone library. These acidophilic, obligate autotrophs use Fe(II) solely as an energy source (Rowe and Johnson 2008). Within the Actinobacteria, several of our clones were related to the acidophilic, Fe(II)-oxidizing organism *Acidimicrobium ferrooxidans*. Members of this species have been isolated or identified molecularly from warm, acidic, iron-, sulphur-, or mineral-sulfide-rich environments (Clum et al. 2009). The average Secchi depth of about 3 m (data not shown) should provide favorable conditions for phototrophic FeOB as well within and below the redoxcline. At CB, several clones clustered within the phylum Chlorobia, which contains phototrophic sulfur bacteria. A member of this phylum, the green sulfur bacterium *Chlorobium ferrooxidans* strain KoFox, oxidizes Fe(II) under pH-neutral conditions (Heising et al. 1999), even in the presence of low light saturation (Hegler et al. 2008). The NB clone library did not contain clones related to phototrophic bacteria, apparently due to the high particle density and the opaque-yellowish color of the water below the redoxcline which would restrict the light available for phototrophic bacteria near the bottom.

Our data highlight the importance of pelagic boundary conditions on the microbial oxidation of Fe(II) and the formation of iron-rich particles, here introduced as "iron snow," in an iron-rich, acidic lake. The redoxcline favored the activity of aerobic FeOB by providing strong vertical gradients of oxygen and Fe(II) within a centimeter range and the formation of schwertmannite appeared to result from a biological process independent of the pH and the microbial communities involved. Therefore, Fe(II) oxidation in this lake can be attributed primarily to microbial activity. The formation of iron snow links the redoxcline strongly with the sediment, providing a mechanism for rapid removal of not only iron, but also of microbial cells, organic carbon, and trace metals from the water column down to the sediment. This microbially mediated formation of iron snow might occur not only in lignite mine lakes but also in other lakes with redoxclines of opposing oxygen and Fe(II) gradients.

Acknowledgments

We thank I. Hilke, T. Walter, H. Köpf, J. Beer, and C. Neumann for technical assistance and support, and U. Kuhlicke and S. Linde for sample preparation, confocal laser scanning microscopy, and scanning electron microscope imaging. We thank D. Akob and M. Herrmann for helpful discussions and P. Bouwma for critical reading. This work was supported by the German Research Foundation (Deutsche Forschungsgemeinschaft [DFG]) grant KU 1367/8-1 and by the Jena School for Microbial Communication (JSMC).

References

Alldredge, A. L., and M. W. Silver. 1988. Characteristics, dynamics and significance of marine snow. Prog. Oceanogr. **20:** 41–82, doi:10.1016/0079-6611(88)90053-5

Bédard, C., and R. Knowles. 1997. Some properties of methane oxidation in a thermally stratified lake. Can. J. Fish. Aquat. Sci. **54:** 1639–1645, doi:10.1139/f97-300

Bekker, A., J. F. Slack, N. Planavsky, B. Krapez, A. Hofmann, K. O. Konhauser, and O. J. Rouxel. 2010. Iron formation: The sedimentary product of a complex interplay among mantle, tectonic, oceanic, and biospheric processes. Econ. Geol. **105:** 467–508, doi:10.2113/gsecongeo.105.3.467

Berger, B., B. Hoch, G. Kavka, and G. J. Herndl. 1996. Bacterial colonization of suspended solids in the River Danube. Aquat. Microb. Ecol. **10:** 37–44, doi:10.3354/ame010037

Bigham, J. M., L. Carlson, and E. Murad. 1994. Schwertmannite, a new iron oxyhydroxysulphate from Pyhasalmi, Finland, and other localities. Mineral. Mag. **58:** 641–648, doi:10.1180/minmag.1994.058.393.14

———, and E. Murad. 1997. Mineralogy of ochre deposits formed by the oxidation of iron sulfide minerals, p. 193–225. *In* K. Auerswald, H. Stanjek, and J. M. Bigham [eds.], Soils and environment: Soil processes from mineral to landscape scale. Advances in GeoEcology. Catena-Verlag.

———, U. Schwertmann, and L. Carlson. 1992. Mineralogy of precipitates formed by the biogeo-chemical oxidation of Fe(II) in mine drainage, p. 219–232. *In* H. G. W. Skinner and R. W. Fitzpatrick [eds.], Biomineralization processes of iron and manganese— modern and ancient environments. Catena Supplement, Catena-Verlag.

———, ———, ———, and E. Murad. 1990. A poorly crystallized oxyhdroxysulfate of iron formed by bacterial oxidation of Fe(II) in acidic-mine waters. Geochim. Cosmochim. Acta **54:** 2743–2758, doi:10.1016/0016-7037(90)90009-A

Blodau, C. 2006. A review of acidity generation and consumption in acidic coal mine lakes and their watersheds. Sci. Total Environ. **369:** 307–332, doi:10.1016/j.scitotenv.2006.05.004

———, N. Basiliko, and T. R. Moore. 2004. Carbon turnover in peatland mesocosms exposed to different water table levels. Biogeochemistry **67:** 331–351, doi:10.1023/B:BIOG.0000015788.30164.e2

Blöthe, M., D. M. Akob, J. E. Kostka, K. Goschel, H. L. Drake, and K. Küsel. 2008. pH gradient-induced heterogeneity of Fe(III)-reducing microorganisms in coal mining-associated lake sediments. Appl. Environ. Microbiol. **74:** 1019–1029, doi:10.1128/AEM.01194-07

Boehrer, B., and M. Schultze. 2006. On the relevance of meromixis in mine pit lakes, p. 200–213. *In* R. I. Barnhisel [ed.], 7th international conference on acid rock drainage (ICARD). American Society of Mining and Reclamation.

———, AND ———. 2008. Stratification of lakes. Rev. Geophys **46:** 1–27, doi:10.1029/2006RG000210

BRZUSTOWSKI, J. 2002. Clustering Calculator [Internet]. [Accessed 2009 October 16]. Available from http://www.biology.ualberta.ca/jbrzusto/cluster.php

CAMPBELL, P., AND T. TORGERSEN. 1980. Maintenance of iron meromixis by iron redeposition in a rapidly flushed monimolimnion. Can. J. Fish. Aquat. Sci. **37:** 1303–1313, doi:10.1139/f80-166

CASAMAYOR, E. O., J. GARCIA-CANTIZANO, AND C. PEDROS-ALIO. 2008. Carbon dioxide fixation in the dark by photosynthetic bacteria in sulfide-rich stratified lakes with oxic–anoxic interfaces. Limnol. Oceanogr. **53:** 1193–1203, doi:10.4319/lo.2008.53.4.1193

CHILDS, C. W., K. INOUE, AND C. MIZOTA. 1998. Natural and anthropogenic schwertmannites from Towada-Hachimantai National Park, Honshu, Japan. Chem. Geol. **144:** 81–86, doi:10.1016/S0009-2541(97)00121-6

CLUM, A., M. NOLAN, E. LANG, T. GLAVINA DEL RIO, H. TICE, A. COPELAND, J.-F. CHENG, S. LUCAS, F. CHEN, D. BRUCE, L. GOODWIN, S. PITLUCK, N. IVANOVA, K. MAVROMATIS, N. MIKHAILOVA, A. PATI, A. CHEN, K. PALANIAPPAN, M. GOEKER, S. SPRING, M. LAND, L. HAUSER, Y.-J. CHANG, C. C. JEFFRIES, P. CHAIN, J. BRISTOW, J. A. EISEN, V. MARKOWITZ, P. HUGENHOLTZ, N. C. KYRPIDES, H.-P. KLENK, AND A. LAPIDUS. 2009. Complete genome sequence of *Acidimicrobium ferrooxidans* type strain (ICP^T). Stand. Genomic Sci. **1:** 38–45, doi:10.4056/sigs.1463

CORNELL, R. M., AND U. SCHWERTMANN. 2003. The iron oxides: Structure, properties, reactions, occurrences and uses, 2nd ed. Wiley-VCH Verlagsgesellschaft.

DAVISON, W. 1993. Iron and manganese in lakes. Earth-Sci. Rev. **34:** 119–163, doi:10.1016/0012-8252(93)90029-7

DESANTIS, T. Z., P. HUGENHOLTZ, K. KELLER, E. L. BRODIE, N. LARSEN, Y. M. PICENO, R. PHAN, AND G. L. ANDERSEN. 2006*a*. NAST: A multiple sequence alignment server for comparative analysis of 16S rRNA genes. Nucleic Acids Res. **34:** 394–399, doi:10.1093/nar/gkl244

———, ———, N. LARSEN, M. ROJAS, E. L. BRODIE, K. KELLER, T. HUBER, D. DALEVI, P. HU, AND G. L. ANDERSEN. 2006*b*. Greengenes, a chimera-checked 16S rRNA gene database and workbench compatible with ARB. Appl. Environ. Microbiol. **72:** 5069–5072, doi:10.1128/AEM.03006-05

DE VICENTE, I., E. ORTEGA-RETUERTA, O. ROMERA, R. MORALES-BAQUERO, AND I. RECHE. 2009. Contribution of transparent exopolymer particles to carbon sinking flux in an oligotrophic reservoir. Biogeochemistry **96:** 13–23, doi:10.1007/s10533-009-9342-8

DÍEZ, S., G. O. NOONAN, J. K. MACFARLANE, AND P. M. GSCHWEND. 2007. Ferrous iron oxidation rates in the pycnocline of a permanently stratified lake. Chemosphere **66:** 1561–1570, doi:10.1016/j.chemosphere.2006.08.017

DRUMMOND, A. J., B. ASHTON, M. CHEUNG, J. HELED, M. KEARSE, R. MOIR, S. STONES-HAVAS, T. THIERER, AND A. WILSON. 2009. Geneious v4.8 [Internet]. Auckland (New Zealand): Biomatters, Ltd., [accessed 2009 September 12]. Available from http://www.geneious.com/

DRUSCHEL, G. K., D. EMERSON, R. SUTKA, P. SUCHECKI, AND G. W. LUTHER. 2008. Low-oxygen and chemical kinetic constraints on the geochemical niche of neutrophilic iron(II) oxidizing microorganisms. Geochim. Cosmochim. Acta **72:** 3358–3370, doi:10.1016/j.gca.2008.04.035

EICHLER, B., AND N. PFENNIG. 1990. Seasonal development of anoxygenic phototrophic bacteria in a holomictic drumlin lake (Schleinsee, F.R.G.). Arch. Hydrobiol. **119:** 369–392.

EMERSON, D., AND C. MOYER. 1997. Isolation and characterization of novel iron-oxidizing bacteria that grow at circumneutral pH. Appl. Environ. Microbiol. **63:** 4784–4792.

EUSTERHUES, K., F. E. WAGNER, W. HAUSLER, M. HANZLIK, H. KNICKER, K. U. TOTSCHE, I. KOGEL-KNABNER, AND U. SCHWERTMANN. 2008. Characterization of ferrihydrite-soil organic matter coprecipitates by X-ray diffraction and Mossbauer spectroscopy. Environ. Sci. Technol. **42:** 7891–7897, doi:10.1021/es800881w

FLECKENSTEIN, J. H., C. NEUMANN, N. VOLZE, AND J. BEER. 2009. Spatio-temporal patterns of lake-groundwater exchange in an acid mine lake. Grundwasser **14:** 207–217, doi:10.1007/s00767-009-0113-1

GROSSART, H. P., AND H. PLOUG. 2000. Bacterial production and growth efficiencies: Direct measurements on riverine aggregates. Limnol. Oceanogr. **45:** 436–445, doi:10.4319/lo.2000.45.2.0436

———, AND M. SIMON. 1993. Limnetic macroscopic organic aggregates (lake snow)— occurrence, characteristics, and microbial dynamics. Limnol. Oceanogr. **38:** 532–546, doi:10.4319/lo.1993.38.3.0532

———, AND ———. 1998. Significance of limnetic organic aggregates (lake snow) for the sinking flux of particulate organic matter in a large lake. Aquat. Microb. Ecol. **15:** 115–125, doi:10.3354/ame015115

GYURE, R. A., A. KONOPKA, A. BROOKS, AND W. DOEMEL. 1987. Algal and bacterial activities in acidic (pH 3) strip mine lakes. Appl. Environ. Microbiol. **53:** 2069–2076.

HANSEL, C. M., S. G. BENNER, J. NEISS, A. DOHNALKOVA, R. K. KUKKADAPU, AND S. FENDORF. 2003. Secondary mineralization pathways induced by dissimilatory iron reduction of ferrihydrite under advective flow. Geochim. Cosmochim. Acta **67:** 2977–2992, doi:10.1016/S0016-7037(03)00276-X

HEGLER, F., N. R. POSTH, J. JIANG, AND A. KAPPLER. 2008. Physiology of phototrophic iron(II)-oxidizing bacteria: Implications for modern and ancient environments. FEMS Microbiol. Ecol **66:** 250–260, doi:10.1111/j.1574-6941.2008.00592.x

HEISING, S., L. RICHTER, W. LUDWIG, AND B. SCHINK. 1999. *Chlorobium ferrooxidans* sp. nov., a phototrophic green sulfur bacterium that oxidizes ferrous iron in coculture with a "*Geospirillum*" sp. strain. Arch. Microbiol. **172:** 116–124, doi:10.1007/s002030050748

JØRGENSEN, B. B., H. FOSSING, C. O. WIRSEN, AND H. W. JANNASCH. 1991. Sulfide oxidation in the anoxic Black-Sea chemocline. Deep-Sea Res. **38:** S1083–S1103.

KAMJUNKE, N., J. TITTEL, H. KRUMBECK, C. BEULKER, AND J. POERSCHMANN. 2005. High heterotrophic bacterial production in acidic, iron-rich mining lakes. Microb. Ecol. **49:** 425–433, doi:10.1007/s00248-004-0270-9

KAWANO, M., AND K. TOMITA. 2001. Geochemical modeling of bacterially induced mineralization of schwertmannite and jarosite in sulfuric acid spring water. Am. Miner. **86:** 1156–1165.

KÜSEL, K., T. DORSCH, G. ACKER, AND E. STACKEBRANDT. 1999. Microbial reduction of Fe(III) in acidic sediments: Isolation of *Acidiphilium cryptum* JF-5 capable of coupling the reduction of Fe(III) to the oxidation of glucose. Appl. Environ. Microbiol. **65:** 3633–3640.

———, AND H. L. DRAKE. 1995. Effects of environmental parameters on the formation and turnover of acetate by forest soils. Appl. Environ. Microbiol. **61:** 3667–3675.

LANE, D. J. 1991. 16S/23S rRNA sequencing, p. 115–175. *In* E. Stackebrandt and M. Goodfellow [eds.], Nucleic acid techniques in bacterial systematics. Wiley.

Letunic, I., and P. Bork. 2006. Interactive Tree Of Life (iTOL): an online tool for phylogenetic tree display and annotation. Bioinformatics **23:** 127–128, doi:10.1093/bioinformatics/btl529

Liu, R. M., A. Hofmann, F. O. Gulacar, P. Y. Favarger, and J. Dominik. 1996. Methane concentration profiles in a lake with a permanently anoxic hypolimnion (Lake Lugano, Switzerland–Italy). Chem. Geol. **133:** 201–209, doi:10.1016/S0009-2541(96)00090-3

Lovley, D. R., D. E. Holmes, and K. P. Nevin. 2004. Dissimilatory Fe(III) and Mn(IV) reduction. Adv. Microb. Physiol. **49:** 219–286, doi:10.1016/S0065-2911(04)49005-5

Lu, S., S. Gischkat, M. Reiche, D. M. Akob, K. B. Hallberg, and K. Küsel. 2010. Ecophysiology of Fe-cycling bacteria in acidic sediments. Appl. Environ. Microbiol. **76:** 8174–8183, doi:10.1128/AEM.01931-10

Lüdecke, C., M. Reiche, K. Eusterhues, and K. Küsel. 2010. Microorganisms involved in iron cycling at the oxic–anoxic interface in an acidic fen. Environ. Microbiol. **12:** 2814–2825.

Ludwig, W., O. Strunk, R. Westram, L. Richter, H. Meier, Yadhukumar, A. Buchner, T. Lai, S. Steppi, G. Jobb, W. Forster, I. Brettske, S. Gerber, A. W. Ginhart, O. Gross, S. Grumann, S. Hermann, R. Jost, A. Konig, T. Liss, R. Lussmann, M. May, B. Nonhoff, B. Reichel, R. Strehlow, A. Stamatakis, N. Stuckmann, A. Vilbig, M. Lenke, T. Ludwig, A. Bode, and K. H. Schleifer. 2004. ARB: A software environment for sequence data. Nucleic Acids Res. **32:** 1363–1371, doi:10.1093/nar/gkh293

Luef, B., F. Aspetsberger, T. Hein, F. Huber, and P. Peduzzi. 2007. Impact of hydrology on free-living and particle-associated microorganisms in a river floodplain system (Danube, Austria). Freshw. Biol. **52:** 1043–1057, doi:10.1111/j.1365-2427.2007.01752.x

Lüthy, L., M. Fritz, and R. Bachofen. 2000. In situ determination of sulfide turnover rates in a meromictic alpine lake. Appl. Environ. Microbiol. **66:** 712–717, doi:10.1128/AEM.66.2.712-717.2000

Martinez, C. E., and M. B. McBride. 1998. Solubility of Cd^{2+}, Cu^{2+}, Pb^{2+}, and Zn^{2+} in aged coprecipitates with amorphous iron hydroxides. Environ. Sci. Technol. **32:** 743–748, doi:10.1021/es970262+

Mendelssohn, I. A., B. A. Kleiss, and J. S. Wakeley. 1995. Factors controlling the formation of oxidized root channels—a review. Wetlands **15:** 37–46, doi:10.1007/BF03160678

Moreira-Turcq, P., J. M. Jouanneau, B. Turcq, P. Seyler, O. Weber, and J. L. Guyot. 2004. Carbon sedimentation at Lago Grande de Curuai, a floodplain lake in the low Amazon region: Insights into sedimentation rates. Paleogeogr. Paleoclimatol. Paleoecol. **214:** 27–40.

Murad, E., and P. Rojik. 2005. Iron mineralogy of mine-drainage precipitates as environmental indicators: Review of current concepts and a case study from the Sokolov Basin, Czech Republic. Clay Miner. **40:** 427–440, doi:10.1180/0009855054040181

Muyzer, G., E. C. Dewaal, and A. G. Uitterlinden. 1993. Profiling of complex microbial-populations by denaturing gradient gel-electrophoresis analysis of polymerase chain reaction-amplified genes-coding for 16S ribosomal-RNA. Appl. Environ. Microbiol. **59:** 695–700.

———, A. Teske, C. O. Wirsen, and H. W. Jannasch. 1995. Phylogenetic-relationships of *Thiomicrospira* species and their identification in deep-sea hydrothermal vent samples by denaturing gradient gel-electrophoresis of 16S rDNA fragments. Arch. Microbiol. **164:** 165–172, doi:10.1007/BF02529967

Neu, T. R. 2000. In situ cell and glycoconjugate distribution in river snow studied by confocal laser scanning microscopy. Aquat. Microb. Ecol. **21:** 85–95, doi:10.3354/ame021085

Nixdorf, B., A. Fyson, and H. Krumbeck. 2001. Review: Plant life in extremely acidic waters. Environ. Exp. Botany **46:** 203–211, doi:10.1016/S0098-8472(01)00104-6

———, and M. Kapfer. 1998. Stimulation of phototrophic pelagic and benthic metabolism close to sediments in acidic mining lakes. Water Air Soil Pollut. **108:** 317–330, doi:10.1023/A:1005165615804

———, H. Krumbeck, J. Jander, and C. Beulker. 2003. Comparison of bacterial and phytoplankton productivity in extremely acidic mining lakes and eutrophic hard water lakes. Acta Oecol. Int. J. Ecol. **24:** S281–S288.

Peine, A., A. Tritschler, K. Küsel, and S. Peiffer. 2000. Electron flow in an iron-rich acidic sediment—evidence for an acidity-driven iron cycle. Limnol. Oceanogr. **45:** 1077–1087, doi:10.4319/lo.2000.45.5.1077

Pimenov, N. V., and L. N. Neretin. 2006. Composition and activities of microbial communities involved in carbon, sulfur, nitrogen and manganese cycling in the oxic/anoxic interface of the Black Sea, p. 501–521. *In* L. N. Neretin [ed.], Past and present water column anoxia. NATO science series, IV. Earth and environmental sciences. Springer.

Ploug, H., H. P. Grossart, F. Azam, and B. B. Jorgensen. 1999. Photosynthesis, respiration, and carbon turnover in sinking marine snow from surface waters of Southern California Bight: Implications for the carbon cycle in the ocean. Mar. Ecol. Prog. Ser. **179:** 1–11, doi:10.3354/meps179001

Porter, K. G., and Y. S. Feig. 1980. The use of Dapi for identifying and counting aquatic microflora. Limnol. Oceanogr. **25:** 943–948, doi:10.4319/lo.1980.25.5.0943

Regenspurg, S., A. Brand, and S. Peiffer. 2004. Formation and stability of schwertmannite in acidic mining lakes. Geochim. Cosmochim. Acta **68:** 1185–1197, doi:10.1016/j.gca.2003.07.015

Roden, E. E., D. Sobolev, B. Glazer, and G. W. Luther. 2004. Potential for microscale bacterial Fe redox cycling at the aerobic–anaerobic interface. Geomicrobiol. J. **21:** 379–391, doi:10.1080/01490450490485872

Rother, A., and J. Kohler. 2005. Formation, transport and retention of aggregates in a river–lake system (Spree, Germany). Int. Rev. Hydrobiol. **90:** 241–253, doi:10.1002/iroh.200410777

Rowe, O. F., and D. B. Johnson. 2008. Comparison of ferric iron generation by different species of acidophilic bacteria immobilized in packed-bed reactors. Syst. Appl. Microbiol. **31:** 68–77, doi:10.1016/j.syapm.2007.09.001

Rudd, J. W. M., R. D. Hamilton, and N. E. Campbell. 1974. Measurement of microbial oxidation of methane in lake water. Limnol. Oceanogr. **19:** 519–524, doi:10.4319/lo.1974.19.3.0519

Schloss, P. D., and J. Handelsman. 2006. Introducing SONS, a tool for operational taxonomic unit-based comparisons of microbial community memberships and structures. Appl. Environ. Microbiol. **72:** 6773–6779, doi:10.1128/AEM.00474-06

Schwertmann, U., J. M. Bigham, and E. Murad. 1995. The first occurrence of schwertmannite in a natural stream environment. Eur. J. Mineral. **7:** 547–552.

Simon, M., H. P. Grossart, B. Schweitzer, and H. Ploug. 2002. Microbial ecology of organic aggregates in aquatic ecosystems. Aquat. Microb. Ecol. **28:** 175–211, doi:10.3354/ame028175

SINGER, P. C., AND W. STUMM. 1970. Acidic mine drainage: The rate-determining step. Science **167:** 1121–1123, doi:10.1126/science.167.3921.1121

SPARK, K. M., B. B. JOHNSON, AND J. D. WELLS. 1995. Characterizing heavy-metal adsorption on oxides and oxyhydroxides. Eur. J. Soil Sci. **46:** 621–631, doi:10.1111/j.1365-2389.1995.tb01358.x

TABATABAI, M. A. 1974. Rapid method for determination of sulfate in water samples. Environ. Lett. **7:** 237–243, doi:10.1080/00139307409437403

TAMURA, H., K. GOTO, T. YOTSUYAN, AND M. NAGAYAMA. 1974. Spectrophotometric determination of Iron(II) with 1,10-phenanthroline in presence of large amounts of Iron(III). Talanta **21:** 314–318, doi:10.1016/0039-9140(74)80012-3

TANG, K. W., K. M. L. HUTALLE, AND H. P. GROSSART. 2006. Microbial abundance, composition and enzymatic activity during decomposition of copepod carcasses. Aquat. Microb. Ecol. **45:** 219–227, doi:10.3354/ame045219

TAYLOR, G. T., M. IABICHELLA, T. Y. HO, M. I. SCRANTON, R. C. THUNELL, F. MULLER-KARGER, AND R. VARELA. 2001. Chemoautotrophy in the redox transition zone of the Cariaco Basin: A significant midwater source of organic carbon production. Limnol. Oceanogr. **46:** 148–163, doi:10.4319/lo.2001.46.1.0148

WEISS, J. V., J. A. RENTZ, T. PLAIA, S. C. NEUBAUER, M. MERRILL-FLOYD, T. LILBURN, C. BRADBURNE, J. P. MEGONIGAL, AND D. EMERSON. 2007. Characterization of neutrophilic Fe(II)-oxidizing bacteria isolated from the rhizosphere of wetland plants and description of *Ferritrophicum radicicola* gen. nov. sp. nov., and *Sideroxydans paludicola* sp. nov. Geomicrobiol. J. **24:** 559–570, doi:10.1080/01490450701670152

YU, Y. N., M. BREITBART, P. MCNAIRNIE, AND F. ROHWER. 2006. FastGroupII: A web-based bioinformatics platform for analyses of large 16S rDNA libraries. BMC Bioinformatics **7:** 1–9, doi:10.1186/1471-2105-7-57

Associate editor: Markus H. Huettel

Received: 19 September 2010
Accepted: 28 February 2011
Amended: 15 April 2011

4 Elucidating microbial communities and their metabolic functions in iron-rich aggregates (iron snow) of an acidic lake

Shipeng Lu[1], Karuna Chourey[2], Marco Reiche[1], Sandor Nietzsche[3], Manesh B. Shah[2], Robert L. Hettich[2] and Kirsten Küsel[1,]

[1] Institute of Ecology, Friedrich Schiller University Jena, Jena, Germany

[2] Chemical Sciences Division, Oak Ridge National Laboratory, Oak Ridge, TN, USA

[3] Center of Electron Microscopy, University Hospital Jena, Friedrich Schiller University Jena, Jena, Germany

Manuscript submitted to *ISME Journal* (ISMEJ-12-00473OA)

Abstract

Metaproteomics combined with total nucleic acid-based methods aided in deciphering the roles of microorganisms in the formation and transformation of iron-rich macroscopic aggregates (iron snow) formed in the redoxcline of an acidic lignite mine lake. Iron snow had high total bacterial 16S rRNA gene copies, with 2 x 10^9 copies g (dry wt)$^{-1}$ in the acidic (pH 3.5) central lake basin and 4 x 10^{10} copies g (dry wt)$^{-1}$ in the less acidic (pH 5.5) northern lake basin. Active microbial communities in the central basin were dominated by *Alphaproteobacteria* (36.6%) and *Actinobacteria* (21.4%), and by *Betaproteobacteria* (36.2%) in the northern basin. Microbial Fe-cycling appeared to be the dominant metabolism in the schwertmannite-rich iron snow, because cloning and qPCR assigned up to 61% of active bacteria as Fe-cycling bacteria (FeB). Metaproteomics revealed 70 unique proteins from central basin iron snow and 283 unique proteins from 43 genera from northern basin. Protein

identification provided a glimpse into *in situ* processes, such as primary production, motility, metabolism of acidophilic FeB, and survival strategies of neutrophilic FeB. Expression of carboxysome shell proteins and RubisCO indicated active CO_2 fixation by Fe(II) oxidizers. Flagellar proteins from heterotrophs indicated their activity to reach and attach surfaces. Gas vesicle proteins related to CO_2-fixing *Chlorobium* suggested that microbes could influence iron snow sinking. We suggest that iron snow formed by autotrophs in the redoxcline acts as a microbial parachute, since it is colonized by motile heterotrophs during sinking which start to dissolve schwertmannite.

Introduction

Acid mine drainage (AMD) and acidic lignite mine lakes are characterized by low pH, high Fe(II) and sulfate concentrations, and high Fe(III) solubility (Hoffert, 1947; Lundgren and Silver, 1980). These harsh conditions are prime habitats for extremophilic microorganisms with various metabolic activities (Belnap *et al.*, 2010; Johnson and Hallberg, 2009; Rowe *et al.*, 2007). Highly concentrated Fe(II) can function as electron donor for Fe-oxidizing microorganisms (FeOM) under both oxic and anoxic conditions. Resulting Fe(III) is an attractive terminal electron acceptor for Fe-reducing microorganisms (FeRM) due to the high redox potential of the Fe^{3+}/Fe^{2+} redox pair at low pH (+770 mV at pH 1) close to the one of O_2/H_2O (Kappler and Straub, 2005). Many acidophilic FeRM prefer microoxic conditions to reduce Fe(III) (Johnson and McGinness, 1991; Lu *et al.*, 2010) and some can co-respire oxygen and Fe(III) (Küsel *et al.*, 2002). A considerable fraction of acidophiles have the capacity to reduce and oxidize Fe (Johnson, 2009; Lu *et al.*, 2010).

In surface waters Fe(II) oxidation leads to dissolved Fe(III), which then precipitates according to surrounding geochemistry as poorly crystalline Fe(III) oxyhydroxides or oxyhydroxysulfates, e.g., goethite, schwertmannite, or jarosite (Bigham and Murad, 1997; Cornell and Schwertmann, 2003). Opposing gradients of oxygen and Fe(II) in streams, lakes, and marine habitats are critical for the formation of these minerals (Boyd and Ellwood, 2010; Brown *et al.*, 2011; Reiche *et al.*, 2011), which can be the nucleus for pelagic aggregate formation either by adsorption or co-precipitation of organic matter (OM) (Eusterhues *et al.*, 2008) and rapid microbial colonization. These aggregates are called "iron snow" to emphasize their high Fe(III) fraction and other unique features different from more organic-rich snow-like aggregates known from marine and freshwater environments (Reiche *et al.*, 2011). All pelagic aggregates become hotspots for microbial processes and are important for the turnover and sinking flux of organic and inorganic matter to the sediment (Grossart and Ploug, 2000; Simon *et al.*, 2002). Reactive iron species are important for stabilizing OM in ocean and freshwater sediments pointing to a tight coupling between the biogeochemical cycles of carbon and iron (Eglinton, 2012). However, we have only a limited understanding of iron redox reactions and complex OM transformations occurring in these pelagic aggregates before they reach the sediment.

To obtain deeper insights into the microbial ecology of iron snow, we combined metaproteomic analyses with quantification of active FeB using cDNA-based qPCR and 16S rRNA clone libraries. We sampled iron snow in and below the redoxcline of an acidic lignite lake with basins differing in pH to broaden our knowledge of bacterial functional roles in lake biogeochemistry.

Materials and Methods

Lake characteristics and sampling

The acidic Lake 77 located in the Lusatian mining area in east-central Germany, has two basins with distinct mixing regimes (Fleckenstein *et al.*, 2009; Reiche *et al.*, 2011). The northern basin is meromictic and has a pH of 5.9 and higher Fe(II) and sulfate concentrations due to inflow of less acidic, contaminated groundwater. The central basin (pH 3) has dimictic mixing in autumn and spring. Sampling sites were the same as in the study of Reiche *et al.* (2011) and abbreviated as follows: central basin redoxcline (CR), central basin anoxic bottom water (CB), northern basin redoxcline (NR), and northern basin anoxic bottom water (NB).

Sediment traps were installed in and below the redoxcline to collect iron snow (Reiche *et al.*, 2011). From July 2010 to October 2011, lake water geochemistry was monitored according to the method of Reiche *et al.* (2011). Dissolved CO_2 and CH_4 were measured in discrete depths in May 2011, as described in the Supplementary Information.

Geochemical characterization of iron snow

Iron snow was dried (60°C) and ground for elemental analysis. Total carbon, nitrogen and sulphur were measured by an elemental analyzer vario El cube (Elementar, Germany) using thermal oxidation at 1150°C. Metals, metalloids, ions, and anions were measured by inductively coupled plasma optical emission spectrometry (ICP-OES; Spectroflame, Spectro) or inductively coupled plasma mass spectrometry (ICP-MS; XSeries II, Thermo Fisher Scientific).

Material contrast scanning electron microscopy (SEM) and energy-dispersive X-ray spectroscopy (EDX)

A droplet of each four wet iron snow samples was air dried on an electrically conductive and adhesive Leit-Tab (Plano GmbH, Germany) and coated with carbon (thickness approx. 15 nm) by vacuum vaporization. Samples were then investigated for EDX, conventional SEM and material contrast SEM using LEO-1450 (Carl Zeiss NTS GmbH, Germany).

Total nucleic acids extraction and 16S rRNA clone library construction

Total nucleic acids were extracted from 2-3 ml wet iron snow samples from July 2010 using the RNA PowerSoil Total RNA Isolation Kit (MO BIO Laboratories, USA), followed by RNA and DNA separation step using the DNA Elution Accessory Kit (MO BIO Laboratories, USA). Residual DNA was removed from RNA extracts with TURBO DNA-free kit (Ambion, USA). One to five µg of RNA extract was used for reverse transcription to complementary DNA (cDNA) using ArrayScript Reverse Transcriptase kit (Ambion, USA). 10 to 50 ng of cDNA was then used for standard PCR using HotStarTaq Master Mix Kit (Qiagen, Germany) followed by 16S rRNA clone library construction and analysis (Lu *et al.*, 2010). Additional DNA extracts were obtained for qPCR by extracting 1.5 ml wet aliquots of iron snow samples with the PowerSoil DNA Isolation Kit (MO BIO Laboratories, USA).

Quantitative PCR (qPCR)

qPCR for known FeB groups, *Acidimicrobium*, *Ferrovum*, *Albidiferax* (formerly affiliated as *Rhodoferax*), *Geobacter,* and *Acidiphilium*, were performed using 16S rRNA gene-specific primers and the respective thermocycling conditions described in

Supplementary Table S1. As *Acidiphilium cryptum* strain JF-5 was isolated from Lake 77 (Küsel *et al.*, 1999), an additional assay was designed to target its cytochrome c Type I gene (ApcA, YP_001235217) using Primer3Plus (Untergasser *et al.*, 2007), resulting in primers AphmCytoc-254F (5'-ACA AGT TCC TGG CCA ATC C-3') and AphmCytoc-358R (5'-TCT GCA GAT AGG CGA CCA C-3'). An aliquot of 10-50 ng of RNA-derived cDNA and DNA extracts were used as templates for amplification with the Maxima SYBR Green qPCR Mastermix kit (Fermentas, Canada). Thermocyclings were performed with Mx3000P real-time PCR system (Stratagene, USA). Plasmids containing environmental clone sequences were used as standards (Supplementary Table S1).

Metaproteomics analysis

Total proteins were extracted from 11-22 g of thawed iron snow (~ 0.15 to 0.4 g dry weight) using a direct soil protein extraction method (SDS-TCA), as described in Chourey *ea al.* (2010). Proteins were digested, and peptides were purified and quantified as described earlier (Chourey *et al.*, 2010; Thompson *et al.*, 2007). All nanoLC-MS/MS (Liquid chromatography–mass spectrometry) measurements were made using a hybrid LTQ/Orbitrap Velos mass spectrometer (ThermoFisher Scientific, Germany) interfaced with an Ultimate 3000 HPLC system (Dionex, USA) and operated in data dependent mode, regimented by Thermo Xcalibur software V2.1.0. Instrument setup and parameters were similar to as described earlier (Brown *et al.*, 2006; Thompson *et al.*, 2007) and in Supplementary Information.

In the absence of an iron snow metagenome, an artificial database was created from targeted sequenced microbial genomes from the Integrated Microbial Genomes server (Markowitz *et al.*, 2009) December 2010 version. The database included 114

full bacteria genomes, 9 bacterial plasmids, 38 full archaeal genomes, and 14 archaeal plasmids (Supplementary Table S2). Genomes and plasmids were selected based on the presence of genera detected in Lake 77 clone libraries and isolates (Lu *et al.*, 2010; Reiche *et al.*, 2011), in addition to genome sequences of known acidophiles or microbes with Fe-cycling capacities (Cárdenas *et al.*, 2010; Markowitz *et al.*, 2009). All datasets and the database can be accessed at http://compbio.ornl.gov/Iron_Snow/microbial_communities. Bioinformatics and analysis was performed as previously described (Chourey *et al.*, 2010; Chourey *et al.*, 2009; Thompson *et al.*, 2007).

Nucleotide sequence accession numbers

The 16S rRNA sequences determined in this study have been deposited in the European Molecular Biology Laboratory database under accession numbers HE603991 to HE604098.

Results

Lake biogeochemistry and iron snow characterization

Similar to previous years, lake water in summer was characterized by a redoxcline with steep opposing gradients of oxygen and Fe(II). Oxygen declined within 3.8 to 4.5 depth, whereas Fe(II) increased from 1 mM to ~ 3 mM in the anoxic hypolimnion in the central basin (Supplementary Figure S1). Dissolved CO_2 was only detected below 4.2 m depth reaching a maximum of 2.5 mM at 5.5 m. Small amounts of CH_4 were detected above the redoxcline (0.83 to 2.61 µM), whereas up to 3 µM occurred below. In the northern basin, oxygen was already depleted in 4.2 m depth and concentrations of Fe(II) increased up to 12 mM and sulfate up to 20 mM in the separated

hypolimnion that was pH 5.9. Dissolved CO_2 and CH_4 reached up to 5.7 mM, and 5.20 µM, respectively below the redoxcline.

When iron snow was sampled within and below the redoxcline in both basins, sedimentation rates were ~ 1.8 times higher in the northern compared to the central basin (Table 1). The chemical composition of iron snow showed higher differences between basins than between depths. TOC, P, and N contents were significantly elevated in the northern basin. Total Fe was similar in the two redoxcline samples, CR and NR, but Fe was lowest in northern bottom water (NB). In contrast, S contents were highest in NB samples. Cd, Co, Cu, Ni, Pb, and U concentrations were all below 0.12 µM g(dry wt)$^{-1}$ (Table 1). The unique hedgehog-like morphology indicative for schwertmannite was observed in all four iron snow samples by SEM (Figure 1B, 1D, 1F, 1H). The presence of schwertmannite as dominant mineral was supported by the mass ratios of Fe, S, and O detected using EDX (Supplementary Table S3). However, hedgehog-like spheres were smaller with shorter needles in the northern compared to central basin samples and planar structures were also observed in northern samples (Figure 1H). Back scattered electrons micrographs (Figure 1A, 1C, 1E and 1G) showed high iron contents in spheres with sharp and narrow pin-structures about 30.3 nm in diameter (Figure 1G, white arrow).

cDNA-based 16S rRNA community analysis of iron snow

The 16S rRNA amplicons were obtained from cDNA from CB and NR iron snow samples. Reverse transcription of CR and NB RNA extracts were unsuccessful in two attempts. A total of 131 and 142 clones were screened from CB-cDNA and NR-cDNA 16S rRNA clone libraries, equaling 88.6% coverage for CB-cDNA library and 77.2% for NR-cDNA, respectively (Supplementary Table S4). The diversity indices

Table 1 Characterization of lake water and iron snow of Lake 77 obtained in July 2010 from sediment traps exposed at the redoxcline and in the anoxic bottom water of the central and northern basin: central redoxcline (CR) and central bottom (CB); and northern basin: northern redoxcline (NR) and northern bottom (NB).

Water and iron snow characteristics	*CR*	*CB*	*NR*	*NB*
Sampling depth (m)	4	7	4	6
pH	3.3	4.0	3.4	5.9
Sedimentation rate (g(dry wt.) m^{-2} d^{-1})	2.6	2.9	4.7	5.5
Fe (µM g(dry wt)$^{-1}$) [a,c]	6 380.13 ± 29.12	7 114.48 ± 17.74	6 230.45 ± 12.10	5 344.82 ± 14.00
C (µM g(dry wt)$^{-1}$)	1 654.27 ± 0.5%	2 138.07 ± 0.5%	4 930.62 ± 0.5%	4 556.03 ± 0.5%
S (µM g(dry wt)$^{-1}$)	1 866.85 ± 5%	1 791.15 ± 5%	1 479.18 ± 5%	2 006.15 ± 5%
Al (µM g(dry wt)$^{-1}$) [a,c]	1 212.52 ± 3.78	691.15 ± 3.67	794.26 ± 3.33	1 191.41 ± 5.07
Ca (µM g(dry wt)$^{-1}$) [a,c]	325.13 ± 0.15	194.68 ± 0.35	354.85 ± 2.25	469.13 ± 1.48
N (µM g(dry wt)$^{-1}$)	114.84 ± 5%	156.82 ± 5%	236.01 ± 5%	236.23 ± 5%
Mg (µM g(dry wt)$^{-1}$) [a,c]	53.99 ± 0.33	51.69 ± 0.33	83.05 ± 0.08	157.53 ± 1.60
P (µM g(dry wt)$^{-1}$) [a,c]	< 3.87[b]	< 3.87[b]	5.97 ± 0.35	7.68 ± 0.39
Mn (µM g(dry wt)$^{-1}$) [a,d]	2.75 ± 0.04	2.60 ± 0.02	3.91 ± 0.02	8.05 ± 0.07
Zn (µM g(dry wt)$^{-1}$) [a,c]	0.76 ± 0.02	0.78 ± 0.00	1.07 ± 0.01	1.30 ± 0.00
As (µM g(dry wt)$^{-1}$) [a,d]	0.04 ± 0.00	0.06 ± 0.00	0.14 ± 0.00	0.11 ± 0.01

[a] Standard deviations were shown for average of three replicate measurements of the solution, but not three replicate digestions.

[b] Concentrations below the detection limit are indicated as "<".

[c] Measured by ICP-OES.

[d] Measured by ICP-MS.

indicated a higher diversity in the NR-cDNA than in the CB-cDNA library with more lineages detected in NR than in CB (Figure 2).

The most frequently detected lineage in the CB-cDNA library was the

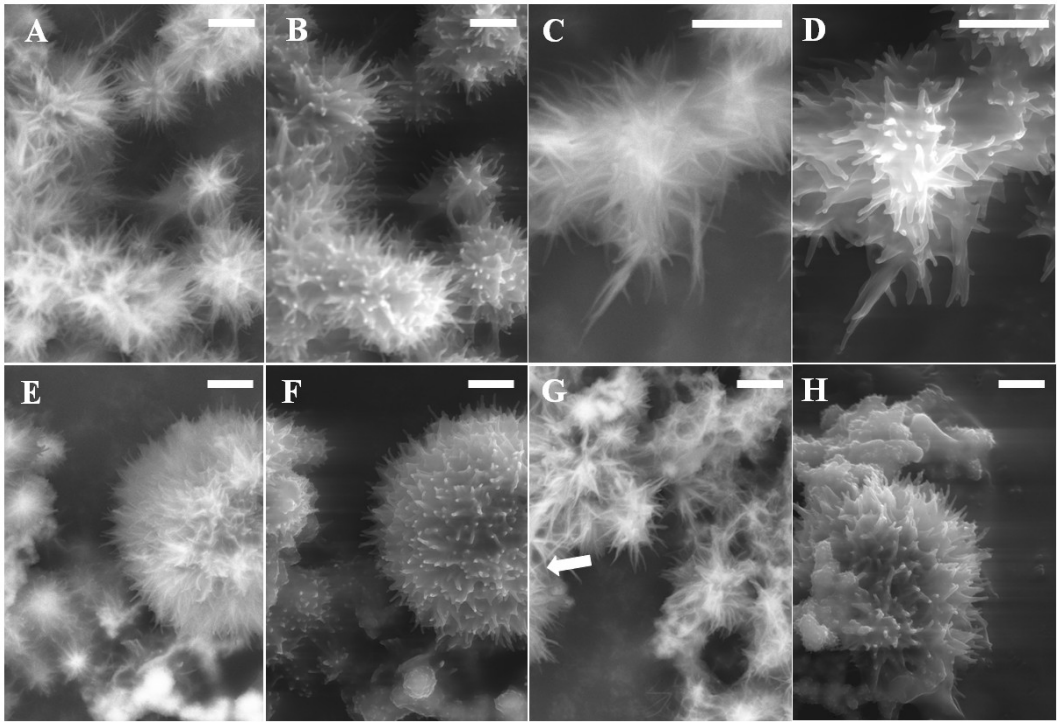

Figure 1. SEM micrographs of iron snow from the acidic lignite mine Lake 77 obtained from sediment traps at the seasonally stratified central basin: central redoxcline (A, B) and central bottom water layer (C, D), and northern basin: northern redoxcline (E, F) and northern bottom water layer (G, H). The unique hedgehog-like morphology of four iron snow samples was revealed by SEM (B, D, F, and H) and back scattered electrons micrographs (A, C, E and G) proved high iron content in schwertmannite and revealed the sharp pin-structures measuring about 30.3 nm in diameter (white arrow in G). All scale bars indicate 1 μm.

Proteobacteria (Figure 2 and Supplementary Table S5), with *Alpha*-, *Gamma*-, *Beta*- and *Deltaproteobacteria* comprising 36.6%, 19.1%, 6.1%, and 0.8%, respectively. *Actinobacteria* and *Acidobacteria* were detected at frequency of 21.4% and 10.7%. While in NR-cDNA library *Betaproteobacteria* was the dominant group (36.2%), followed by *Alpha*- (9.9%), *Delta*- (7.1%) and *Gammaproteobacteria* (0.7%). The

Actinobacteria and *Firmicutes* were also obtained at frequency of 9.2% and 7.8%, respectively.

Clone sequences with > 97% similarity to a cultured FeB representative made up 25.3% and 38.2% of the clones obtained from central and northern basin,

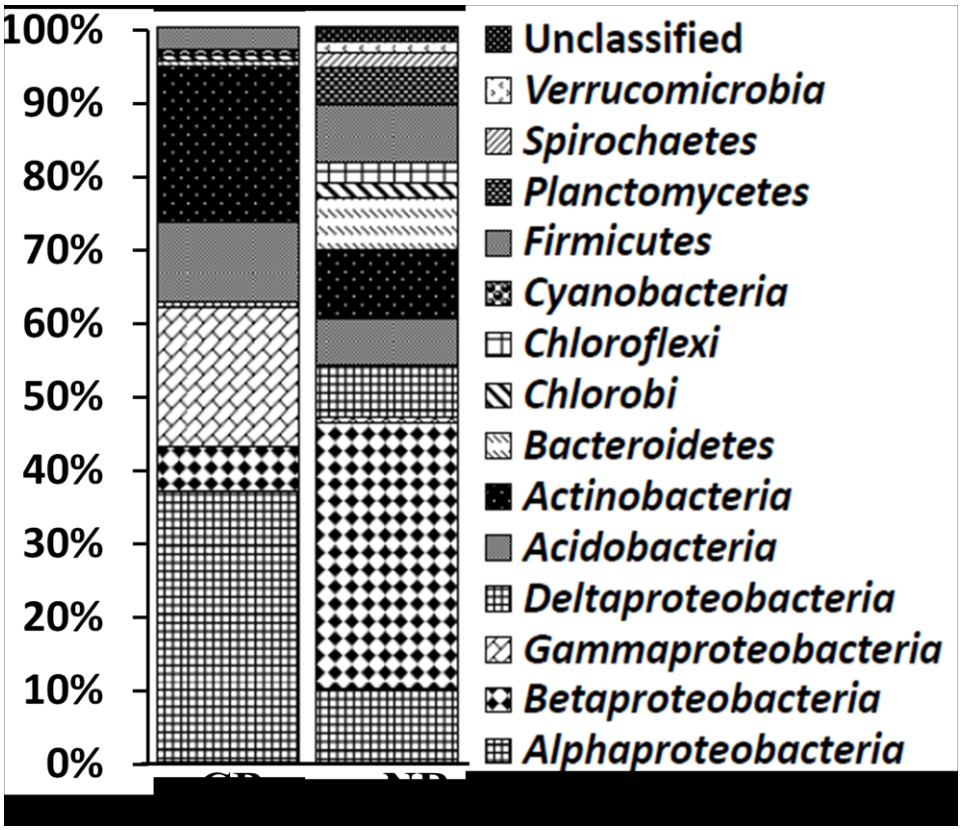

Figure 2. Comparison of active bacteria phylogenetic lineages detected in cDNA-based 16S rRNA clone libraries derived from iron snow sampled from central basin bottom water column (CB) and northern basin redoxcline (NR). Calculations were based on the total number of clones associated with phylotypes of sequenced representatives at the phylum or class lever for *Proteobacteria*.

respectively (Table 2). *Acidimicrobium* and *Ferrovum* were retrieved only in the CB-cDNA library, comprising of 13.0% and 3.1 of total clones. Whereas *Chlorobium*-like FeOM-related clones were also observed in NR-cDNA. *Albidiferax* was the most abundant FeRM-related group found in the NR-cDNA library only, comprising approximately one third of all clones. Surprisingly, clones related to the acidophilic

FeRM *Acidiphilium* and to the neutrophilic FeRM *Geobacter* were retrieved from both sites.

Table 2 Frequencies of Fe-cycling bacteria detected using cDNA-based 16S rRNA clone libraries and qPCR analysis of iron snow samples from central basin bottom water column (CB) and northern basin redoxcline (NR). Sequences in cDNA libraries, which were >97% similar to known Fe-cycling bacteria were used for calculation.

Fe-cycling capacity	*16S rRNA clone libraries*		*qPCR*	
	CB (%)	*NR (%)*	*CB (%)*	*NR (%)*
Iron oxidizers				
Acidimicrobium	13.0	n.d.[a]	19.7	5.0
Chlorobium	n.d.	2.1	ND[b]	ND
Ferrovum	3.1	n.d.	19.2	3.3
Iron reducers				
Acidiphilium	5.3	2.1	10.1	3.0
Albidiferax[c]	n.d.	32.6	3.3	33.5
Geobacter	0.8	1.4	0.6	15.8
Acidobacteria spp.	3.1	n.d.	ND	ND
Total	25.3	38.2	52.9	60.6

[a] n.d., not detected

[b] ND, not determined.

[c] *Albidiferax* was formerly affiliated as *Rhodoferax*.

Quantitative PCR of total bacteria and of FeB

Using genomic DNA as templates, total bacterial 16S rRNA gene copies reached up to 3.97 x 10^{10} g (dry wt)$^{-1}$ in NB iron snow, but copy numbers were ~ 80 times lower in CR iron snow (Table 3). Differences between CR and CB or NR and NB were not significant. The 16S rRNA copy numbers from CB-cDNA were 1.37 x 10^{12} g(dry wt)$^{-1}$ and 9.31 x 10^{11} g(dry wt)$^{-1}$ in NR-cDNA samples. The *Acidimicrobium*-related

group showed the highest copy numbers in the CB-DNA samples comprising > 25% of the total 16S rRNA gene copies, while in the NB-DNA library they were < 4.5%. The *Ferrovum* group dominated the CB-DNA (34.7%) community. In contrast, *Albidiferax* was detected in low frequency in CR- and CB-DNA samples, but comprised 15.0% of total bacterial gene copy numbers in the NB-DNA samples and 33.5% of active bacteria in NR-cDNA. Similarly, *Geobacter* were found in low frequency (< 0.3%) in the CR- and CB-DNA samples or in CB-cDNA (< 0.6%) (Table 2) but were > 15.8% of active bacteria in the NB-cDNA. The *Acidiphilium* was abundant in CB-DNA (20.5%) and CB-cDNA (10.1%), but not in CR-DNA (0.4%) or in the northern basin (8.7% in NR-DNA, 6.2% in NB-DNA and 3.0% in NR-cDNA). The results of detecting the ApcA gene of *A. cryptum* JF-5 showed that this organism was ubiquitous in all samples, reaching > 40% of total *Acidiphilium* in CR-DNA sample (Table 3).

Metaproteomics

Due to the absence of an actual metagenome for iron snow from Lake 77, an artificial database was constructed using genome sequenced acidophiles and archaea for database matching. To investigate any similarity in acidophilic population of Lake 77 and Richmond mine at Iron Mountain which is dominated by *Leptospirillum* species, the raw mass spectral datasets were also searched against the Iron Mountain AMD database (Ram *et al.*, 2005; Tyson *et al.*, 2004). However we detected no protein matches to Iron Mountain AMD database, suggesting totally dissimilar microbial communities in both these ecosystems.

Although 70 proteins were detected from central basin iron snow (25 proteins from only CR and 27 from only CB samples) (Table 4 and Supplementary Table S6),

Table 3 Quantitative PCR analyses of cDNA and DNA extracts from iron snow of central basin: central redoxcline (CR) and central bottom (CB); and northern basin: northern redoxcline (NR) and northern bottom (NB). Total bacterial 16S rRNA genes and Fe-cycling related bacterial phylogenetic groups were detected. Fe(III) reduction related cytochrome *c* class I (ApcA) gene copies of *Acidiphilium cryptum* JF-5 were also determined. DNA samples were obtained from co-elution of RNA extracts.

Sample	*Total Bacteria*	*Acidimicrobium*	*Ferrovum*	*Albidiferax*	*Geobacter*	*Acidiphilium*	*ApcA*
CR-DNA	4.99E+08[a]	1.08E+08	1.29E+07	3.03E+04	4.82E+05	1.77E+06	7.38E+05
CB-DNA	1.59E+09	3.96E+08	5.52E+08	1.88E+07	4.51E+06	3.26E+08	1.81E+06
NR-DNA	3.73E+10	2.80E+09	2.19E+09	5.65E+09	5.04E+09	3.26E+09	7.36E+07
NB-DNA	3.97E+10	1.76E+09	2.31E+09	5.97E+09	3.47E+09	2.47E+09	4.50E+07
CB-cDNA	1.37E+12	2.70E+11	2.63E+11	4.55E+10	8.58E+09	1.39E+11	1.71E+06
NR-cDNA	9.31E+11	4.69E+10	3.08E+10	3.12E+11	1.47E+11	2.79E+10	7.48E+06

[a]All values in units of gene copies g(dry wt)$^{-1}$.

their detection at low levels (two peptides in most cases) raised caution about attributing too much value to their actual identifications. However observation of proteins from *Acidiphilium, Chlorobium and Geobacter* was in accord with results acquired from 16S cDNA analysis of the same iron snow samples. Several gas vesicle-related proteins were detected in *Chlorobium* and OmpA/MotB domain protein and the periplasmic protein cytochrome c class I from *Acidiphilium*. Other proteins were annotated as ATP synthase, stress-response proteins and chaperonin GroEL proteins.

Unlike the low protein abundance from the central basin iron snow samples, the protein measurements were much more definitive from the northern basin. A total of 283 different proteins from 43 microbial genera were retrieved from iron snow collected in the northern basin, including 140 proteins in NR and 66 proteins in NB (Table 4 and Supplementary Table S7). The molecular weight of the proteins detected ranged from 7.2 to 156.3 Kda. Proteins could be allotted to thirty-four genera and the most represented groups were *Chlorobium* (19.1%, 54 proteins), *Acidiphilium* and *Burkholderia* (8.1%, 23 proteins each), *Acidovorax* (7.8%, 22 proteins), *Albidiferax* (6%, 17 proteins). Other FeB, *Geobacter*, *Acidithiobacillus*, *Pelobacter*, *Leptothrix,* and *Acidimicrobium*, were also detected. Proteins were identified from various functional categories, such as heat shock-hsp60 or chaperonin GroEL proteins, ATP synthases, translation elongation factor proteins, gram-negative type outer membrane porins, ribosomal proteins, RNA polymerases and gas vesicle-related proteins. In addition, flagellin and OmpA/MotB domain proteins were detected; mainly from *Acidovorax*, *Acidiphilium*, *Albidiferax,* and *Diaphorobacter*. Proteins representing carboxysome shell/microcompartment proteins were found in NR possibly derived from *Acidithiobacillus* species (protein accession numbers YP_002426105,

YP_002426106, ZP_05293097 to ZP_05293099, YP_002219821 and YP_002219822), *Thiobacillus* (YP_316402 to YP_316404) and *Acidimicrobium* (YP_003108766 to YP_003108768) (Supplementary Table S7). The periplasmic protein cytochrome c class I was also retrieved in NR samples and another cytochrome c oxidase (YP_002361568) from *Methylocella* was detected in CB samples. Bacteriochlorophyll C binding proteins from *Chlorobium* were found in high abundance (ZP_01386130 and YP_002019351).

Table 4 Proteomics analyses of total protein extracts from iron snow of central basin: central redoxcline (CR) and central bottom (CB); and northern basin: northern redoxcline (NR) and northern bottom (NB).

Microbial species	*Central Basin*				*Northern Basin*			
	CR only	*CB only*	*CR and CB both*	*Total*	*NR only*	*NB only*	*NR and NB both*	*Total*
Acetobacter	2	0	0	2	0	1	1	2
Acidimicrobium	0	0	0	0	3	0	0	3
Acidiphilium	7	1	4	12	10	6	7	23
Acidithiobacillus	0	0	0	0	9	1	0	10
Acidothermus	1	0	0	1	0	0	0	0
Acidovorax	2	1	0	3	8	11	3	22
Anoxybacillus	0	1	0	1	0	0	0	0
Arthrobacter	0	0	0	0	1	1	0	2
Azoarcus	0	0	1	1	1	4	4	9
Azospirillum	1	0	1	2	1	0	1	2
Bacillus	0	0	0	0	1	0	0	1
Beijerinckia	0	0	0	0	2	0	0	2
Bordetella	0	0	0	0	1	1	0	2
Burkholderia	1	2	0	3	17	4	2	23
C.A. phosphatis	0	0	0	0	1	0	0	1
Carboxydothermus	0	0	1	1	0	0	1	1
Chromohalobacter	1	0	0	1	0	0	0	0
Chlorobaculum	0	0	0	0	5	4	1	10
Chlorobium	1	7	0	8	16	11	27	54
Comamonas	1	0	0	1	3	0	1	4
Dechloromonas	0	0	0	0	1	1	0	2
Delftia	1	0	0	1	2	0	3	5

Desulfatibacillum	0	0	0	0	1	1	0	2
Desulfotalea	0	0	0	0	0	1	0	1
Desulfovibrio	0	2	1	3	2	0	4	6
Desulfuromonas	0	0	1	1	1	0	2	3
Diaphorobacter	1	0	0	1	1	2	1	4
Ferroplasma[a]	0	1	0	1	0	0	0	0
Flavobacteriaceae	1	0	0	1	0	0	1	1
Gallionella	0	0	0	0	0	0	1	1
Geobacter	0	3	5	8	10	1	4	15
Haloterrigena[a]	0	0	0	0	1	0	0	1
Hydrogenobaculum	0	1	0	1	0	0	0	0
Leptothrix	0	0	0	0	2	1	0	3
Magnetospirillum	2	0	1	3	0	0	3	3
Methanococcus[a]	0	1	0	1	0	0	0	0
Methylibium	0	0	0	0	0	2	1	3
Methylocella	1	0	0	1	1	2	0	3
Moorella	0	0	1	1	1	0	1	2
Pelobacter	0	0	2	2	1	0	2	3
Prosthecochloris	0	0	0	0	2	2	0	4
Ralstonia	0	1	0	1	13	2	0	15
Albidiferax	0	0	0	0	9	5	3	17
Rhodospirillum	2	1	0	3	5	0	1	6
Syntrophobacter	0	0	0	0	1	0	0	1
Syntrophus	0	0	0	0	1	0	0	1
Sulfolobus[a]	0	4	0	4	0	0	0	0
Thiobacillus	0	0	0	0	5	0	1	6
Thiomonas	0	1	0	1	0	2	0	2
Variovorax	0	0	0	0	1	0	1	2
Total	25	27	18	70	140	66	77	283

[a]*Archaea*, others bacteria.

Discussion

Biogeochemistry of iron snow

Redoxclines present in the central and northern basins of Lake 77 favored the activity of aerobic FeOM by providing strong vertical gradients of oxygen and Fe(II) within a centimeter range (Reiche *et al.*, 2011). Fe(II) oxidation also appears to be dominated by microbial activity in the northern basin despite a pH allowing chemical oxidation, but low temperatures and the steep oxygen decline appear to favor microbial

oxidation. The two-fold higher sedimentation rates observed in the northern basin were likely caused by the four-fold higher Fe(II) concentration in the northern compared with the central hypolimnion due to its Fe(II)-rich groundwater inflow (Fleckenstein *et al.*, 2009). At all sites, iron-rich precipitates were dominated by schwertmannite with shorter needles of hedgehog-like spheres in the samples collected in the northern basin. The higher TOC content of iron snow collected in the northern compared to the central basin might reflect the higher numbers of microorganisms colonizing these aggregates. In addition, higher amounts of organic carbon might have adsorbed to these reactive iron species or might have co-precipitated in this DOC-richer basin during mineral formation, a process known from terrestrial studies (Lützow *et al.*, 2006). The tight association between iron minerals and organic matter appears to be responsible for the long-term sequestration of carbon, especially in marine sediments (Lalonde *et al.*, 2012).

Previous studies demonstrated that the microbial community patterns in iron snow collected from anoxic bottom water of both basins share great similarities with the corresponding sediment surface (Reiche *et al.*, 2011). A broad range of microorganisms were detected and/or isolated from these sediments, e.g., *Acidiphilium*, *Ferrovum*, *Ferrimicrobium*, *Acidimicrobium*, *Alicyclobacillus*, *Acidocella*, *Acidisphaera*, *Acidithiobacillus*, *Thiobacillus*, *Leptospirillum* and *Dyella*-, *Geobacter*-, and *Sulfolobus*-like species (Küsel *et al.*, 1999; Lu *et al.*, 2010; Porsch *et al.*, 2009; Wenderoth and Abraham, 2005). Many of them are capable of both oxidizing and reducing iron (Johnson, 2009; Lu *et al.*, 2010). Quantitative PCR results suggested that at least 52.9% and 60.6% of total active bacterial gene copies could be assigned to FeB groups for the active CB and NR communities, respectively. Similarly, 25.3% and 38.2% of sequences detected in the 16S rRNA clone libraries

were > 97% related to cultured FeB representatives (Table 2) suggesting that microbial iron cycling is the dominant metabolism in iron snow. Both methods yielded similar quantitative results showing for instance that *Acidimicrobium* and *Ferrovum* were the main FeOM in CB but not in NR, while *Albidiferax* were the main FeRM in NR. The general consistency of these results confirmed the reliability of conventional nucleic acid-based techniques for determining dominant phylogenetic groups.

Metabolic functions of iron snow bacteria

Proteins retrieved from iron snow were identified using an artificial database containing all publically available genomic sequences of acidophiles or Fe-cycling microbes from various environments (Cárdenas *et al.*, 2010; Markowitz *et al.*, 2009). Unfortunately, proteins potentially retrieved from abundant microbial groups, such as *Ferrovum*, could not be identified due to the lack of genome-sequenced relatives. Thus, our post-metaproteomic data analysis is incomplete, which will be improved if metagenomic information of iron snow samples is available, thereby allowing a re-matching of the two meta-omics datasets in the future. Nonetheless, part of the mystery of *in situ* activity and metabolism of the diverse microorganisms inhabiting these aggregates was unveiled.

Many flagellin domain proteins from FeB, such as *Acidovorax*, *Acidiphilium*, and *Albidiferax,* were detected in different iron snow samples suggesting that flagellar motility is helpful to reach surfaces and to switch from a pelagic to an attached lifestyle. These complex organelles play also an important role in adhesion to substrates and biofilm formation (Soutourina and Bertin, 2003). Some microorganisms expressed high amounts of shock- or protein refolding-related

chaperones such as DnaK or GroEL similar to the presence of such proteins in other acidic environments (Bertin *et al.*, 2011; Bruneel *et al.*, 2011; Ram *et al.*, 2005) and in *Ferroplasma acidarmanus* cultured aerobically (Dopson *et al.*, 2005), suggesting that low pH conditions might be a key challenge for cell survival due to its potential damage to DNA and proteins. ATP synthases using the energy stored in the transmembrane pH were also found in high abundance from many microorganisms in all samples. It is suggested that for acidophilic FeOM, like *Leptospirillum* group II, the ATP synthase complex is involved in the electron transport chain (Ram *et al.*, 2005).

Primary production as important metabolic strategy for Fe(II) oxidizers

A number of autotrophic acidophiles use the Calvin-Benson-Bassham cycle to obtain their cellular carbon (Johnson and Hallberg, 2009). Its key enzyme is ribulose bisphosphate carboxylase/oxygenase (RuBisCO) that was detected in *Acidithiobacillus thiooxidans* (Suzuki and Werkman, 1958), *At. ferrooxidans* (Gale and Beck, 1967; Valdés *et al.*, 2008a) and *Acidimicrobium ferrooxidans* (Johnson and Hallberg, 2009). While RuBisCO can be present in the cytoplasm, it is often found packaged in microcompartments called carboxysomes (Cannon *et al.*, 2003; Shively *et al.*, 1998). Clusters of carboxysome genes in acidithiobacilli and *Tb. denitrificans* are closely associated to RuBisCO-related genes, mostly in identical operons (Cannon *et al.*, 2003; Esparza *et al.*, 2010; Yeates *et al.*, 2008). While RuBisCO- or carboxysome-related genes are putatively identified in *Acidithiobacillus, Acidimicrobium* and *Thiobacillus* species mostly based on genomic analysis (Esparza *et al.*, 2010; Johnson and Hallberg, 2009; Valdés *et al.*, 2008b; Yeates *et al.*, 2008), the expression of carboxysome shell proteins related to *Acidimicrobium*,

Acidithiobacillus, and *Thiobacillus* species in northern basin iron snow indicated their active metabolic function of CO_2 fixation. Additionally, we observed, using MicrobesOnline (Dehal *et al.*, 2009), that genes coding for *Am. ferrooxidans* microcompartment proteins (Afer_0124 to Afer_0126) were located downstream of the two RuBisCO subunit genes (Afer_0119 and Afer_0120) in the same transcriptional direction. This suggests that they may be concurrently expressed as intact carboxysomes for CO_2 fixation. Thus, *Acidimicrobium*, *Acidithiobacillus,* and *Thiobacillus* are likely acting as primary producers coupled with Fe(II) oxidation.

The green sulfur bacteria *Chlorobium*-like group was recognized by 16S rRNA cloning and a number of different proteins were assigned to this group, including bacteriochlorophyll (BChl) *c* binding proteins of FeOM *Cb. ferrooxidans* (Heising *et al.*, 1999) and *Cb. clathratiforme*. BChl serves as light-harvesting and energy-transforming chromophore in photosynthetic microorganisms (Lokstein and Grimm, 2007). Gas vesicle proteins were found in both central and northern basin samples from *Chlorobium*-like groups. Gas vesicles of aquatic bacteria are small, hollow protein structures that provide buoyancy allowing positioning at a favorable depth for growth (Walsby and Hayes, 1989). Therefore, CO_2-fixing *Chlorobium*-related microbes (Heising *et al.*, 1999) attached to or captured within the iron snow tried, apparently, to stay in the redoxcline where there is enough light for photosynthesis and sufficient Fe(II) for Fe(II) oxidation. Gas vesicles inside the cells might also reduce sinking velocity of the iron snow, which helps to maintain temporally an ecological niche in the redoxcline.

Acidophilic Fe(III) reducers

Acidophilic FeRM belonging to the *Acidiphilium* group was detected in all iron snow samples suggesting their ubiquitous distribution, but their highest fraction was detected in CB. *Acidiphilium*-related proteins were one of the most frequently identified groups, including 12 proteins from central basin and 23 from northern basin, among which 11 proteins were found in both sites including stress-related chaperones. This high frequency was not surprising since the artificial database included the genome of strain JF-5 that was isolated from this lake (Küsel *et al.*, 1999). Five proteins might be involved in the electron transfer chain of *Acidiphilium*: OmpA/MotB domain protein (YP_001233320, YP_001233321, YP_001233507), TonB-dependent receptor (YP_001220344), and ApcA (YP_001235217). Genes encoding two OmpA/MotB domain proteins (Acry_0173 for YP_001233320 and Acry_0174 for YP_001233321) were located downstream of a gene for a 17.2 kD NADH-ubiquinone oxidoreductase subunit (Acry_0170) which implied its simultaneous transcription. Recently, one TonB-dependent receptor homologue from *Shewanella oneidensis* (SO2907) was shown to be involved in the dissimilatory reduction of chelated Fe(III) species but not of solid iron oxides (Qian *et al.*, 2011b). However, more experimental evidence is required to explain the roles of OmpA/MotB domain and TonB-dependent receptor proteins in acidophiles which have the advantage of also accessing soluble Fe(III) at pH below 3. ApcA is essential electron transfer proteins composed of respiratory chains for reducing electron acceptors like Fe(III) or hexavalent chromium in the neutrophilic *S. oneidensis* and *Geobacter sulfurreducens* (Qian *et al.*, 2011a; Richter *et al.*, 2012; Shi *et al.*, 2011). However, very little is known about such enzymology in acidophilic FeRM, although purified and reduced ApcA from *A. cryptum* JF-5 can reduce chromate at low pH (Magnuson

et al., 2010). ApcA coding genes were quantified in all DNA and cDNA iron snow samples and ApcA were observed in both basins indicating a high expression level of this protein. The results of our polyphasic approach suggests that *Acidiphilium* is active in the iron snow formed in both basins and it might be involved in the reductive dissolution of schwertmannite under oxic to suboxic conditions in the redoxcline and under anoxic conditions during sedimentation of iron snow.

The dominance of neutrophilic Fe(III) reducers in the northern basin

Albidiferax ferrireducens is a metabolically versatile microorganism that likely plays an important role in subsurface carbon and metal cycles (Finneran *et al.*, 2003; Risso *et al.*, 2009). According to its pH optimum of 7.0 (Finneran *et al.*, 2003), it was not surprising to find much higher abundances of the *Albidiferax* genus in the northern compared to the central basin. Although some of these members are capable of autotrophic growth, *A. ferrireducens* has only incomplete pathways associated with CO_2 fixation in its genome (Risso *et al.*, 2009). We detected mostly chaperonin GroEL and nucleic acid/protein synthesis related proteins in iron snow samples. Interestingly, retrieved flagellin-like proteins (Rfer_0630 and Rfer_0631) indicated motility which was coherent with previous findings (Finneran *et al.*, 2003; Risso *et al.*, 2009). Malate dehydrogenase (Rfer_1803), a carbon metabolism protein involved in the citric acid cycle, was also detected. The *Geobacter*-like group was one of the second most abundant bacterial groups in the northern basin. Despite the low number of proteins retrieved from the central basin, proteins from the *Geobacter*-like group were identified which referred mostly to ATP synthase and the translation elongation factor Tu, suggesting activity of this genus under pH 3 conditions. Other proteins related to ATP synthase, shock related and various chaperones were retrieved,

however, since no protein potentially involved in an electron transfer chain was found, it remains unclear if these organisms actively participate in the reduction of Fe(III).

Microbes parachuting on iron snow through redox gradients

The high iron snow sedimentation rates observed in Lake 77 links the redoxcline strongly to the sediment by providing a rapid removal mechanism of not only iron and organic carbon, but also living microorganisms from the water column to the sediment. Here we propose three developmental stages of iron snow which are influenced by microorganisms (Figure 3).

First, in the redoxcline, where Fe(II) meets oxygen, mainly acidophilic autotrophic FeOM, such as *Ferrovum, Acidimicrobium Acidithiobacillus*, and *Thiobacillus* and a small population of neutrophilic *Sideroxydans* sp., are likely to be responsible for the initial step of Fe(II) oxidation. "*Ferrovum myxofaciens*" known for its copious quantities of excreted exopolysaccharides (Hallberg, 2010) might serve as nucleation site for the precipitation of schwertmannite as dominant Fe-mineral. The lack of encrustation of most acidophilic FeOM will be advantageous since the cells are still able to contact ferrous iron and to proceed with oxidation (Hedrich *et al.*, 2011). Nonetheless, some microorganisms will be wrapped in the centre of schwertmannite minerals (Reiche *et al.*, 2011). Gas vesicle containing phototrophic *Chlorobium* may also serve as primary producers for the next trophic level, but chemolithoautotrophy is likely advantageous in this lake where light penetration is limited by high amounts of iron aggregates in the water column.

In the second stage, the iron minerals will be colonized by heterotrophs feeding on autotrophically fixed carbon or on organic matter adsorbed to or co-

precipitated during schwertmannite formation. Favored by their flagellar motility, heterotrophic bacteria, like *Acidovorax*, *Acidiphilium,* and *Albidiferax,* are likely the first colonizers of iron minerals. The pincushion-like structure of schwertmannite provides a very high specific surface area highly suited to also adsorb organic matter excreted from other inhabitants making the iron snow an attractive ecological niche on its way through the redoxcline down to the sediment.

Sedimentation is the third stage where iron minerals start to be reductively dissolved by abundant heterotrophic FeRM, e.g., *Albidiferax, Geobacter,* and *Acidiphilium*. Depending on the pH, some Fe(II) will stay adsorbed to the shrinking

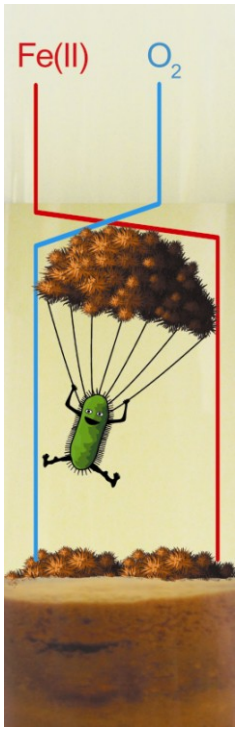

Figure 3. Schematic of iron snow development in the redoxcline of a lignite mine lake acting as a microbial parachute.

iron aggregates. Due to the shallow nature of these lakes the majority of iron snow will reach the sediment within one day at least in the central basin. In the northern bottom water, the higher salinity might slightly reduce iron snow sedimentation velocity. In these sediments the reduction of schwertmannite is the dominating

electron-accepting process for the oxidation of organic matter (Peine *et al.*, 2000). The reduced Fe(II) will accumulate in the hypolimnion until the iron cycle is closed by autumn turnover in the central basin, where bottom water mixes with oxygenated surface water. In contrast, closing of the iron cycle in the northern basin is dependent on diffusion through the redoxcline.

Acknowledgements

This work was supported by the Graduate School of Excellence Jena School for Microbial Communication (JSMC) funded by the German Research Foundation (DFG) and proteomic work at ORNL in part by the Department of Energy, Biological and Environmental Research Carbon-cycle program. We thank Marco Jung, Maren Sickinger, Denise Akob, Juanjuan Wang, Anna Rusznyák, and Martina Hermann for technical assistances, discussion and manuscript proofreading and Peter Bouwma for the parachute cartoon.

References

Belnap CP, Pan C, VerBerkmoes NC, Power ME, Samatova NF, Carver RL *et al*. (2010). Cultivation and quantitative proteomic analyses of acidophilic microbial communities. *ISME J* **4:** 520-530.

Bertin PN, Heinrich-Salmeron A, Pelletier E, Goulhen-Chollet F, Arsene-Ploetze F, Gallien S *et al*. (2011). Metabolic diversity among main microorganisms inside an arsenic-rich ecosystem revealed by meta- and proteo-genomics. *ISME J* **5:** 1735-47.

Bigham JM, Murad E. (1997). *Mineralogy of ochre deposits formed by the oxidation of iron sulfide minerals*. In: Auerswald K, Stanjek H and Bigham JM (eds). *Soils and Environment: Soil Processes from Mineral to Landscape Scale*. Advances in GeoEcology, Catena-Verlag, Reiskirchen, Germany. pp 193-225.

Boyd P, Ellwood M. (2010). The biogeochemical cycle of iron in the ocean. *Nat Geosci* **3:** 675-682.

Brown JF, Jones DS, Mills DB, Macalady JL, Burgos WD. (2011). Application of a depositional facies model to an acid mine drainage site. *Appl Environ Microbiol* **77:** 545-554.

Brown SD, Thompson MR, VerBerkmoes NC, Chourey K, Shah M, Zhou JZ *et al*. (2006). Molecular dynamics of the *Shewanella oneidensis* response to chromate stress. *Mol Cell Proteomics* **5:** 1054-1071.

Bruneel O, Volant A, Gallien S, Chaumande B, Casiot C, Carapito C *et al*. (2011). Characterization of the active bacterial community involved in natural attenuation processes in arsenic-rich creek sediments. *Microb Ecol* **61:** 793-810.

Cannon GC, Baker SH, Soyer F, Johnson DR, Bradburne CE, Mehlman JL *et al*. (2003). Organization of carboxysome genes in the thiobacilli. *Curr Microbiol* **46:** 115-119.

Cárdenas JP, Valdes J, Quatrini R, Duarte F, Holmes DS. (2010). Lessons from the genomes of extremely acidophilic bacteria and archaea with special emphasis on bioleaching microorganisms. *Appl Microbiol Biotechnol* **88:** 605-620.

Chourey K, Jansson J, VerBerkmoes N, Shah M, Chavarria KL, Tom LM *et al*. (2010). Direct cellular lysis/protein extraction protocol for soil metaproteomics. *J Proteome Res* **9:** 6615-6622.

Chourey K, Thompson MR, Shah M, Zhang B, VerBerkmoes NC, Thompson DK *et al*. (2009). Comparative temporal proteomics of a response regulator (SO2426)-deficient strain and wild-type *Shewanella oneidensis* MR-1 during chromate transformation. *J Proteome Res* **8:** 59-71.

Cornell RM, Schwertmann U. (2003). *The iron oxides: Structure, properties, reactions, occurrences and uses*, 2nd edn. Wiley-VCH Verlagsgesellschaft: Weinheim, Germany.

Dehal PS, Joachimiak MP, Price MN, Bates JT, Baumohl JK, Chivian D *et al*. (2009). MicrobesOnline: an integrated portal for comparative and functional genomics. *Nucleic Acids Res* **38:** D396-D400.

Dopson M, Baker-Austin C, Bond PL. (2005). Analysis of differential protein expression during growth states of *Ferroplasma* strains and insights into electron transport for iron oxidation. *Microbiology-Sgm* **151:** 4127-4137.

Eglinton TI. (2012). Geochemistry: A rusty carbon sink. *Nature* **483:** 165-166.

Esparza M, Cardenas JP, Bowien B, Jedlicki E, Holmes DS. (2010). Genes and pathways for CO_2 fixation in the obligate, chemolithoautotrophic acidophile, *Acidithiobacillus ferrooxidans*, carbon fixation in *A. ferrooxidans*. *BMC Microbiol* **10:** 15.

Eusterhues K, Wagner FE, Hausler W, Hanzlik M, Knicker H, Totsche KU *et al*. (2008). Characterization of ferrihydrite-soil organic matter coprecipitates by X-ray diffraction and mossbauer spectroscopy. *Environ Sci Technol* **42:** 7891-7897.

Finneran KT, Johnsen CV, Lovley DR. (2003). *Rhodoferax ferrireducens* sp. nov., a psychrotolerant, facultatively anaerobic bacterium that oxidizes acetate with the reduction of Fe(III). *Int J Syst Evol Microbiol* **53:** 669-673.

Fleckenstein JH, Neumann C, Volze N, Beer J. (2009). Spatio-temporal patterns of lake-groundwater exchange in an acid mine lake. *Grundwasser* **14:** 207-217.

Gale NL, Beck JV. (1967). Evidence for the Calvin cycle and hexose monophosphate pathway in *Thiobacillus ferrooxidans*. *J Bacteriol* **94:** 1052-1059.

Grossart HP, Ploug H. (2000). Bacterial production and growth efficiencies: direct measurements on riverine aggregates. *Limnol Oceanogr* **45:** 436-445.

Hallberg KB. (2010). New perspectives in acid mine drainage microbiology. *Hydrometallurgy* **104:** 448-453.

Hedrich S, Lunsdorf H, Keeberg R, Heide G, Seifert J, Schlomann M. (2011). Schwertmannite Formation Adjacent to Bacterial Cells in a Mine Water Treatment Plant and in Pure Cultures of *Ferrovum myxofaciens*. *Environ Sci Technol* **45:** 7685-7692.

Heising S, Richter L, Ludwig W, Schink B. (1999). *Chlorobium ferrooxidans* sp. nov., a phototrophic green sulfur bacterium that oxidizes ferrous iron in coculture with a "*Geospirillum*" sp. strain. *Arch Microbiol* **172:** 116-124.

Hoffert JR. (1947). Acid mine drainage. *Ind Eng Chem* **39:** 642-646.

Johnson DB. (2009). *Extremophiles (overview): acid environments*. In: Schaechter M (ed). *The desk encyclopedia of microbiology*, 2nd edn. Academic Press: Oxford. pp 463-482.

Johnson DB, Hallberg KB. (2009). Carbon, iron and sulfur metabolism in acidophilic micro-organisms. *Adv Microb Physiol* **54:** 201-255.

Johnson DB, McGinness S. (1991). Ferric iron reduction by acidophilic heterotrophic bacteria. *Appl Environ Microbiol* **57:** 207-211.

Kappler A, Straub KL. (2005). *Geomicrobiological cycling of iron*. *Molecular Geomicrobiology*. Mineralogical Society of America: Chantilly. pp 85-108.

Küsel K, Dorsch T, Acker G, Stackebrandt E. (1999). Microbial reduction of Fe(III) in acidic sediments: Isolation of *Acidiphilium cryptum* JF-5 capable of coupling the reduction of Fe(III) to the oxidation of glucose. *Appl Environ Microbiol* **65:** 3633-3640.

Küsel K, Roth U, Drake HL. (2002). Microbial reduction of Fe(III) in the presence of oxygen under low pH conditions. *Environ Microbiol* **4:** 414-421.

Lalonde K, Mucci A, Ouellet A, Gelinas Y. (2012). Preservation of organic matter in sediments promoted by iron. *Nature* **483:** 198-200.

Lokstein H, Grimm B. (2007). *Chlorophyll-binding Proteins*. *Encyclopedia of Life Sciences*. eLS.

Lu S, Gischkat S, Reiche M, Akob DM, Hallberg KB, Küsel K. (2010). Ecophysiology of Fe-cycling bacteria in acidic sediments. *Appl Environ Microbiol* **76:** 8174-8183.

Lundgren D, Silver M. (1980). Ore leaching by bacteria. *Annu Rev Microbiol* **34:** 263-283.

Lützow Mv, Kögel-Knabner I, Ekschmitt K, Matzner E, Guggenberger G, Marschner B *et al*. (2006). Stabilization of organic matter in temperate soils: mechanisms and their relevance under different soil conditions- a review. *Eur J Soil Sci* **57:** 426-445.

Magnuson TS, Swenson MW, Paszczynski AJ, Deobald LA, Kerk D, Cummings DE. (2010). Proteogenomic and functional analysis of chromate reduction in *Acidiphilium cryptum* JF-5, an Fe(III)-respiring acidophile. *Biometals* **23:** 1129-1138.

Markowitz VM, Chen IMA, Palaniappan K, Chu K, Szeto E, Grechkin Y *et al*. (2009). The integrated microbial genomes system: an expanding comparative analysis resource. *Nucleic Acids Res* **38:** D382-D390.

Peine A, Tritschler A, Küsel K, Peiffer S. (2000). Electron flow in an iron-rich acidic sediment - evidence for an acidity-driven iron cycle. *Limnol Oceanogr* **45:** 1077-1087.

Porsch K, Meier J, Kleinsteuber S, Wendt-Potthoff K. (2009). Importance of different physiological groups of iron reducing microorganisms in an acidic mining lake remediation experiment. *Microb Ecol* **57:** 701-717.

Qian X, Mester T, Morgado L, Arakawa T, Sharma ML, Inoue K *et al*. (2011a). Biochemical characterization of purified OmcS, a *c*-type cytochrome required for insoluble Fe(III) reduction in *Geobacter sulfurreducens*. *Biochimica Et Biophysica Acta-Bioenergetics* **1807:** 404-412.

Qian Y, Shi L, Tien M. (2011b). SO2907, a putative TonB-dependent receptor, is involved in dissimilatory iron reduction by *Shewanella oneidensis* strain MR-1. *J Biol Chem* **286:** 33973-33980.

Ram RJ, VerBerkmoes NC, Thelen MP, Tyson GW, Baker BJ, Blake RC *et al*. (2005). Community proteomics of a natural microbial biofilm. *Science* **308:** 1915-1920.

Reiche M, Lu S, Ciobota V, Neu TR, Nietzsche S, Rösch P *et al*. (2011). Pelagic boundary conditions affect the biological formation of iron-rich particles (iron snow) and their microbial communities. *Limnol Oceanogr* **56:** 1386-1398.

Richter K, Schicklberger M, Gescher J. (2012). Dissimilatory reduction of extracellular electron acceptors in anaerobic respiration. *Appl Environ Microbiol* **78:** 913-921.

Risso C, Sun J, Zhuang K, Mahadevan R, DeBoy R, Ismail W *et al*. (2009). Genome-scale comparison and constraint-based metabolic reconstruction of the facultative anaerobic Fe (III)-reducer *Rhodoferax ferrireducens*. *BMC Genomics* **10:** 447.

Rowe OF, Sanchez-Espana J, Hallberg KB, Johnson DB. (2007). Microbial communities and geochemical dynamics in an extremely acidic, metal-rich stream at an abandoned sulfide mine (Huelva, Spain) underpinned by two functional primary production systems. *Environ Microbiol* **9:** 1761-1771.

Shi L, Belchik SM, Wang Z, Kennedy DW, Dohnalkova AC, Marshall MJ *et al*. (2011). Identification and characterization of $UndA_{(HRCR-6)}$, an outer membrane endecaheme *c*-Type cytochrome of *Shewanella* sp. strain HRCR-6. *Appl Environ Microbiol* **77:** 5521-5523.

Shively JM, van Keulen G, Meijer WG. (1998). Something from almost nothing: carbon dioxide fixation in chemoautotrophs. *Annu Rev Microbiol* **52:** 191-230.

Simon M, Grossart HP, Schweitzer B, Ploug H. (2002). Microbial ecology of organic aggregates in aquatic ecosystems. *Aquat Microb Ecol* **28:** 175-211.

Soutourina OA, Bertin PN. (2003). Regulation cascade of flagellar expression in Gram-negative bacteria. *FEMS Microbiol Rev* **27:** 505-523.

Suzuki I, Werkman C. (1958). Chemoautotrophic carbon dioxide fixation by extracts of *Thiobacillus thiooxidans*. I. Formation of oxalacetic acid. *Arch Biochem Biophys* **76:** 103-111.

Thompson MR, VerBerkmoes NC, Chourey K, Shah M, Thompson DK, Hettich RL. (2007). Dosage-dependent proteome response of *Shewanella oneidensis* MR-1 to acute chromate challenge. *J Proteome Res* **6:** 1745-1757.

Tyson GW, Chapman J, Hugenholtz P, Allen EE, Ram RJ, Richardson PM *et al*. (2004). Community structure and metabolism through reconstruction of microbial genomes from the environment. *Nature* **428:** 37-43.

Untergasser A, Nijveen H, Rao X, Bisseling T, Geurts R, Leunissen JAM. (2007). Primer3Plus, an enhanced web interface to Primer3. *Nucleic Acids Res* **35:** W71-W74.

Valdés J, Pedroso I, Quatrini R, Dodson RJ, Tettelin H, Blake R, II *et al*. (2008a). *Acidithiobacillus ferrooxidans* metabolism: from genome sequence to industrial applications. *BMC Genomics* **9:** 597.

Valdés J, Pedroso I, Quatrini R, Holmes DS. (2008b). Comparative genome analysis of *Acidithiobacillus ferrooxidans*, *A. thiooxidans* and *A. caldus*: insights into their metabolism and ecophysiology. *Hydrometallurgy* **94:** 180-184.

Walsby AE, Hayes PK. (1989). Gas vesicle proteins. *Biochem J* **264:** 313-322.

Wenderoth DF, Abraham WR. (2005). Microbial indicator groups in acidic mining lakes. *Environ Microbiol* **7:** 133-139.

Yeates TO, Kerfeld CA, Heinhorst S, Cannon GC, Shively JM. (2008). Protein-based organelles in bacteria: carboxysomes and related microcompartments. *Nat Rev Microbiol* **6:** 681-691.

Supplementary Materials and Methods

Geochemical analysis of lake water

Dissolved carbon dioxide was measured over the whole depth of the water column and methane was measured in water samples from depth of 3.6 m to 5.5 m in central basin and 3.8 m to 5.5 m in northern basin in May 2011. For these two analyses, 10 ml water samples were filled in 30 ml serum bottles, sealed tightly with rubber stoppers. Samples were treated with 0.1 ml of 2 M HCl and incubated for at least 30 min. The inner volume of serum bottle was calculated by mass differences between empty and water-filled (assumed density of 1 g/cm^3) bottle with rubber stopper and aluminium cap on. Five bottles were selected randomly and the mean value was used for later calculation. CO_2 and CH_4 in pre-treated samples were then measured in triplicates, with a gas chromatograph (HP 5890 series II, Hewlett-Packard Co., USA) with respective column and machine setting (Küsel and Drake, 1995).

Metaproteomics analysis

Protein extraction and sample preparation: The direct soil protein extraction method (SDS-TCA) was employed for total protein extraction (Chourey *et al.*, 2010) from iron snow samples. In brief, 11-22 g of thawed iron snow samples (equal to 0.15 to 0.4 g dry weight) were transferred to glass bottles and dispersed in alkaline-SDS buffer (1:2 sample to buffer ratio). Following vigorous vortexing for 2-3 min, the slurry was placed in boiling water bath for 15 min for effective cellular lyses and inactivation of the proteases. Partially cooled sediment was pelleted by centrifugation, the supernatant was transferred to a new tube and chilled 100% tricholoroacetic acid (TCA) was added to a final concentration of 25% and kept at -20 ℃ overnight.

Samples were centrifuged at 14000 rpm for 20 min to obtain a tight protein pellet which was washed three times with 1 ml chilled acetone, air dried and solubilized in 6 M Guanidine buffer at 60 ℃ as described earlier (Chourey *et al.*, 2010). Proteins were digested, peptides desalted and solvent exchanged as described earlier (Thompson *et al.*, 2007). Protein estimation was performed using the RC/DC protein estimation kit (Bio-Rad, USA) as per the manufacturer's protocol. BSA was used as standard for the assay. All chemicals were obtained from Sigma Chemical Co. (St. Louis, MO) unless mentioned otherwise. Modified sequencing grade trypsin (Promega, Madison, WI) was used for proteolysis. Formic acid (99%) was purchased from EM Science (Darmstadt, Germany, HPLC-grade water, acetonitrile and acetone were obtained from Burdick & Jackson (Muskegon, MI).

NanoLC-MS/MS analysis: All LC-MS/MS measurements were made using hybrid LTQ XL/Orbitrap Velos mass spectrometer (ThermoFisher Scientific, Germany) interfaced with an Ultimate 3000 HPLC system (Dionex, USA) and operated in data dependent mode, regimented by Thermo Xcalibur software V2.1.0. Peptides were loaded onto a 5 cm SCX (Luna, Phenomenex, CA) in-house packed column and subjected to an offline wash with solvent A (5% acetonitrile, 95% HPLC-grade water, 0.1% formic acid) for 15 minutes to remove any lingering interferences followed by a gradient to 100% solvent B (70% acetonitrile, 30% HPLC-grade water, 0.1% formic acid) over 30 minutes. Following wash, the sample column was placed in step with C18 packed Picotip emitter (New Objective, USA) coupled to a Proxeon nanospray source (Odense, Denmark) placed facing the mass spectrometer. Peptides were analyzed via 24-hr MudPIT 2D-LC-MS/MS (11 salt-pulses of ammonium acetate) followed by a 100 minute gradient to 50% solvent B) in an operating in data-

dependent mode. Full MS1 scans with 10 MS/MS per full scan were obtained using an Orbitrap mass analyzer set to 60K resolution. Rest of the instrument setup was similar to as described earlier (Brown *et al.*, 2006; Thompson *et al.*, 2007). Two replicate measurements were obtained for each sample.

Proteome bioinformatics and data analysis: In absence of an actual metagenomic sequence of iron snow from Lake 77, an artificial database was generated by including sequenced microbial genomes from Integrated Microbial Genomes server (Markowitz *et al.*, 2009) December 2010 version, including 114 bacteria full genomes, 9 bacterial plasmid sequences, 38 archaeal full genomes and 14 archaeal plasmid sequences (Supplementary Table S3). The microbial genomes were selected based on the presence of genera reported from lake sediment, water and iron snow clone libraries and isolates (Lu *et al.*, 2010; Reiche *et al.*, 2011) in addition to published genome sequences of known acidophiles or microbes with Fe-cycling capacities (Cárdenas *et al.*, 2010; Markowitz *et al.*, 2009). Sequences for common contaminant such as trypsin, keratin, etc. were concatenated towards end of the assembled database. Peptide fragmentation spectra obtained for each sample was searched for database matches via SEQUEST v.27 (Eng *et al.*, 1994). All the datasets and the database can be accessed at https://compbio.ornl.gov/mspipeline/Kuesel/. Output files were filtered using DTASelect (Tabb *et al.*, 2002) set to following filtering criteria for the SEQUEST searches: tryptic peptides only, delCN value of at least 0.08, and X correlation values of 1.8 (+1), 2.5 (+2), 3.5 (+3). Detection of at least two peptides per protein sequence was set as prerequisite for protein identification. The datasets were further evaluated using the Poisson regression model as described by Chourey *et al*. (Chourey *et al.*, 2009) wherein spectral counts of a

protein is normalized to make it comparable across different datasets and p values generated were further adjusted using the Benjamini-Hochberg correction to obtain the q value (Chourey *et al.*, 2009). A q value of 0.05 (corresponding to 1% False Discovery Rate) was used to call out significant, differentially expressed proteins.

Supplementary Figure S1. Profiles of water geochemistry measured at the central basin and northern basin within the acidic lignite mine lake 77 in May 2011. The central basin has a dimictic regime with an anoxic hypolimnion in summer and the northern basin has a continuous anoxic monimolimnion. A typical redoxcline was detected from water depth of 3.5 m to 4.8 m in central basin while the redoxcline started from around 3.6 m deep and extended to around 4.7 m in northern basin. The pH, conductivity, oxygen content and temperature were measured *in situ*, and the others were measured in water samples in laboratory.

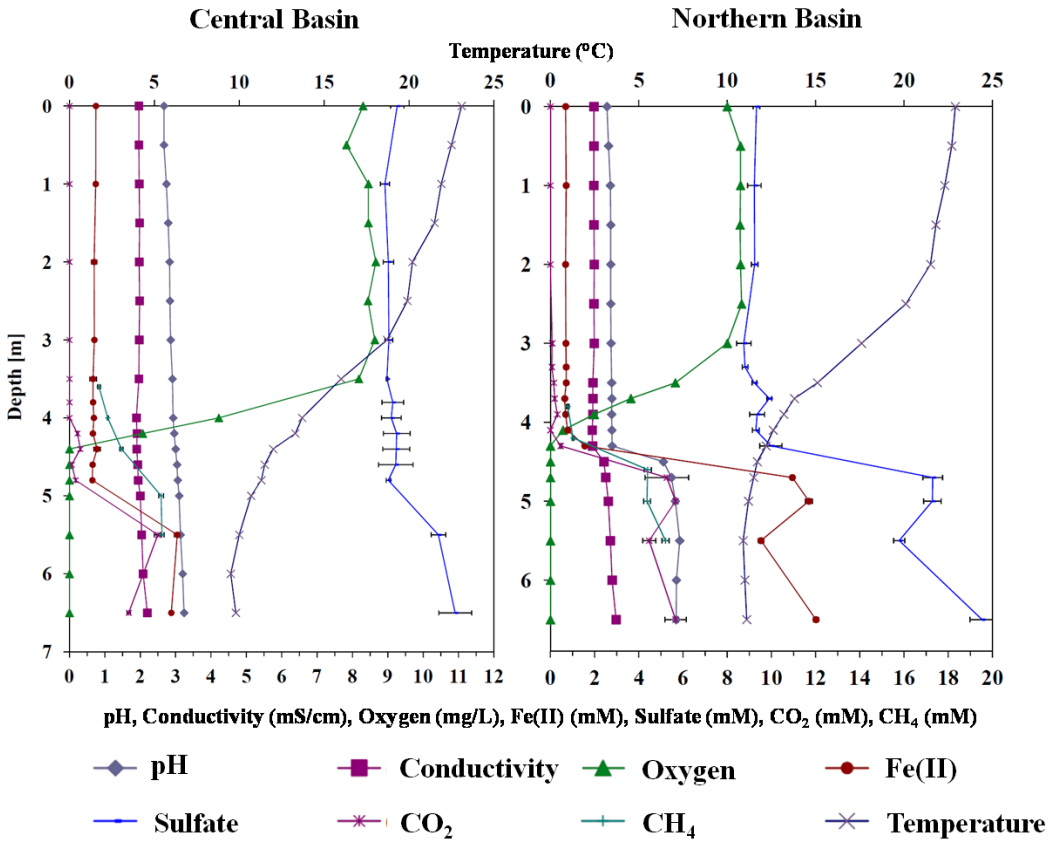

Supplementary Table S1 Primers used for qPCR detecting Fe-cycling bacteria groups in iron snow samples.

Target	*Primer*	*Sequence (5'-3')*	*Amplicon length (bp)*	*Annealing temperature (°C)*	*AFC[a] temperature (°C)*	*Reference*	*Standard clone (acc. no.)*
Bacteria	Uni-338F-RC	ACT CCT ACG GGA GGC AGC	571	57	78	(Lane, 1991)	HE604015
	Uni-907R	CCG TCA ATT CMT TTG AGT TT				(Lane, 1991)	
Acidimicrobium	Amf995	CTC TGC GGC TTT TCC CTC CAT G	110	53	79	(Cleaver *et al.*, 2007)	HE604007
	Uni-907R-RC	AAA CTC AAA KGA ATT GAC GG				(Lane, 1991)	
Ferrovum	Ferrovum643F	ACA GAC TCT AGC TTG CCA GT	323	61	78	(Heinzel *et al.*, 2009)	HE604015
	Uni-338F-RC	ACT CCT ACG GGA GGC AGC				(Lane, 1991)	
Albidiferax[b]	RdoR-RC	GAC CTG CAT TTG TGA CTG YA	312	57	78	(Zhou, 2008), modified	HE604080
	Uni-907R	CCG TCA ATT CMT TTG AGT TT				(Lane, 1991)	
Geobacter	Geo561F	GCG TGT AGG CGG TTT BTT AA	297	56	78	(Stults *et al.*, 2001), modified	JN885810[d]
	Geo858R	TCA ATA CCC GCA ACA CCT AG				(Lu *et al.*, 2010)	
Acidiphilium	ACD840	CGA CAC TGA AGT GCT AAG C	505	61	78	(Bond and Banfield, 2001)	HE604018
	Uni-338F-RC	ACT CCT ACG GGA GGC AGC				(Lane, 1991)	
ApcA[c]	AphmCytoc-254F	ACA AGT TCC TGG CCA ATC C	104	58	83	This study	YP_001235217
	AphmCytoc-358R	TCT GCA GAT AGG CGA CCA C				This study	

[a] AFC: Amplification fluorescence collection

[b] Previously known as *Rhodoferax ferrireducens* (Ramana and Sasikala, 2009)

[c] *Acidiphilium* JF-5 cytochrome *c* class I gene

[d] Reference for clone, Fabish *et al.* (unpublished)

Supplementary Table S3. Energy-dispersive X-ray spectroscopy analysis of iron snow in the Lake 77 obtained from sediment traps at central basin: central redoxcline (CR) and central bottom (CB); and northern basin: northern redoxcline (NR) and northern bottom (NB) on July 2010.

Elements	*CB (Mass %)*	*CR (Mass %)*	*NR (Mass %)*	*NB (Mass %)*	*Schwertmannite ideal formula*
Fe	63.4±1.8	59.7±1.6	53.8±1.4	61.3±1.7	58
O	31.6±3.4	34.9±3.6	41.9±4.3	34.7±3.6	37
S	5.1±0.2	5.4±0.2	4.2±0.2	4.0±0.2	4

Supplementary Table S4. Statistical analysis of cDNA-based 16S rRNA gene clone libraries using ecological and molecular estimates of phylotype diversity.

Sample[a]	*No. of clones*	*No. of phylotypes*	*Coverage (%)*	*ACE*[b]	*Chao1 ± SD*	*Diversity index*	
						Shannon	*Simpson's (1/D)*
CB	131	43	88.6	85.9	95.1±30.6	3.17	16.86
NR	142	66	77.2	138.8	146.7±34.9	3.59	17.23

[a] CB and NR stand for the iron snow bacterial cDNA-based 16S rRNA gene clone libraries obtained from the central basin bottom or the northern basin redoxcline of Lake 77.

[b] ACE stands for abundance-based coverage estimator.

Related information of **Supplementary Table S2, S6** and **S7** (22 pages in submitted documents) can be found at **http://compbio.ornl.gov/Iron_Snow/microbial_communities**.

Related information of **Supplementary Table S5** (5 pages in submitted documents) can be found at **http://www.ncbi.nlm.nih.gov/nuccore/** with accession numbers from HE603991 to HE604098.

Supplementary References

Bond PL, Banfield JF. (2001). Design and performance of rRNA targeted oligonucleotide probes for in situ detection and phylogenetic identification of microorganisms inhabiting acid mine drainage environments. *Microb Ecol* **41:** 149-161.

Cleaver AA, Burton NP, Norris PR. (2007). A novel *Acidimicrobium* species in continuous cultures of moderately thermophilic, mineral-sulfide-oxidizing acidophiles. *Appl Environ Microbiol* **73:** 4294-4299.

Eng JK, McCormack AL, Yates JR. (1994). An approach to correlate tandem mass spectral data of peptides with amino acid sequences in a protein database. *J Am Soc Mass Spectrom* **5:** 976-989.

Heinzel E, Janneck E, Glombitza F, Schlomann M, Seifert J. (2009). Population dynamics of iron-oxidizing communities in pilot plants for the treatment of acid mine waters. *Environ Sci Technol* **43:** 6138-6144.

Küsel K, Drake HL. (1995). Effects of environmental parameters on the formation and turnover of acetate by forest soils. *Appl Environ Microbiol* **61:** 3667-3675.

Lane DJ. (1991). *16S/23S rRNA Sequencing in E. coli.* In: Stackebrandt E and Goodfellow M (eds). *Nucleic acid techniques in bacterial systematics*. John Wiley & Sons: New York, NY. pp 115-175.

Ramana CV, Sasikala C. (2009). *Albidoferax*, a new genus of *Comamonadaceae* and reclassification of *Rhodoferax ferrireducens* (Finneran et al., 2003) as Albidoferax ferrireducens comb. nov. *J Gen Appl Microbiol* **55:** 301-304.

Stults JR, Snoeyenbos-West O, Methe B, Lovley DR, Chandler DP. (2001). Application of the 5' fluorogenic exonuclease assay (TaqMan) for quantitative ribosomal DNA and rRNA analysis in sediments. *Appl Environ Microbiol* **67:** 2781-2789.

Tabb DL, McDonald WH, Yates JR. (2002). DTASelect and contrast: Tools for assembling and comparing protein identifications from shotgun proteomics. *J Proteome Res* **1:** 21-26.

Zhou J. (2008). *The development of molecular tools for the evaluation of the bioremediation of chlorinated solvents*. PhD thesis. Proquest, Umi Dissertation Publishing: Utah, United States.

5 Quantification of the inorganic phase of iron snow aggregates provides valuable information concerning aggregate formation

Valerian Ciobotă[a], Shipeng Lu[b], Nicolae Tarcea[a], Petra Rösch[a], Kirsten Küsel[b] and Jürgen Popp[a,c]

[a] Institute of Physical Chemistry and Abbe School of Photonics, Friedrich Schiller University, Jena, Germany

[b] Institute of Ecology, Friedrich Schiller University, Jena, Germany

[c] Institute of Photonic Technology, Jena, Germany

Manuscript submitted to *Journal of Environmental Monitoring*

Abstract

A quantitative investigation of the inorganic phase of pelagic, iron-rich aggregates (iron snow) formed by microorganisms was performed by means of Raman spectroscopy. Iron snow samples were collected from two basins of an acidic lignite mine lake (central and northern basin) and from two different water depths (redoxcline and deeper anoxic water layer). Although the water chemistry differed at all four sites with respect to oxygen, pH, and Fe(II) concentrations, the Raman analyses showed that the main mineral formed was schwertmannite with concentrations of more than 91% in all iron snow samples. Highest concentrations of schwertmannite were detected in samples of the central basin. Goethite and calcite were identified additionally in the deep anoxic sample from the northern basin which showed the highest pH value (pH 5.9). Hematite was detected in the northern redoxcline, while ferrihydrite was detected in trace amount in the central deeper anoxic water layer with a pH of 3.5. In addition, small amounts of graphite, quartz, rutile and anatase were also present in some of the aggregates. To determine potential differences in the microbial

communities of the iron snow samples we used a DNA-based fingerprinting method called denaturing gradient gel electrophoresis (DGGE). Microbial communities differed between two basins, but showed similarities between redoxcline and deeper water layers of iron snow samples from the same basin. Surprisingly, these microbiological differences did not lead to strikingly qualitative dissimilarities in the mineral composition, although the initial step in mineral formation, the oxidation of Fe(II) to Fe(III), is a pure microbial process at low pH. Thus, a quantitative method was necessary to elucidate differences in the consecutive mineralization process which is apparently more controlled by water geochemical conditions.

Environmental impact

In this contribution we investigate the mineral phases of pelagic aggregates from two basins an acidic iron-rich mine lake that differ in pH. The relations between the mineral phases, microbial communities and water chemistry from two different sites and depths are analyzed, and the factors which influence the formation of the pelagic aggregates are determined. The outcome suggests that although the initiation of the mineral formation is a microbial process, the mineral phases are mainly dictated by the abiotic conditions of the aquatic environment. Therefore, the implications of these findings should be considered before any attempt of bioremediation performed on similar polluted ecosystems.

Introduction

Raman spectroscopy uses the inelastic scattered radiation by the investigated samples to gain information about their vibrational and rotational energy levels. The energy levels of the molecules are highly specific; therefore it is possible using Raman spectroscopy to distinguish between molecules with very similar chemical composition or between substances with the same chemical compositions but different crystal structures. In contrast to other methods (XRD or magnetic techniques), Raman spectroscopy can be successfully applied for

the identification of minerals with crystals in the nanometer range [1, 2]. In the mineralogy field, Raman spectroscopic approaches were used for the identification of various soil components[3-5], the characterization of different rocks [6-9], the discrimination between closely related minerals [10-14] or the identification of minerals used as dyes in paintings [15-17], for example. In addition, Raman imaging techniques were applied to distribution studies of various minerals [18], or for quantification of the amount of various minerals in different samples [4, 19].

Iron-containing minerals were widely investigated by means of Raman spectroscopy. Various authors showed that using this spectroscopic technique discrimination between polymorphic iron oxides, hydroxides or similar iron sulfides, for example, was achievable[1,2,20,21]. Iron-rich precipitates were extensively studied for their pollution potential in acid mine drainage [22, 23]. However, the mineral composition of pelagic aggregates formed in aquatic ecosystems has been rarely studied. The particulate matter formed in lakes and oceans consists of both organic and inorganic materials derived from a variety of sources like authigenic production by biota, colonization by microorganisms, precipitation of inorganic minerals, fluvial and aeolian inputs, suspension of sedimentary material, , etc. [24]. Most pelagic aggregates, named lake snow or marine snow depending on the environment where they appear, are dominated by dead organic matter and living biomass consisting of bacteria, protozoa, and fungi [25]. A number of studies were devoted to the organic phase of different pelagic particles formed in various aquatic environments [26, 32, 33]. In aquatic ecosystems characterized by many terrestrial-aquatic coupling processes, the mineral fraction is very important for many biological and chemical processes taking place in the water [26, 27]. However, the quantification of the inorganic phase has not been investigated in detail.

Recently, the term iron snow was defined for specific pelagic aggregates which are formed in lakes with opposing oxygen and Fe(II) gradients to highlight their predominant iron fraction [28]. Under low pH conditions, the oxidation of Fe(II) to Fe(III), which is the first

step in the iron mineral formation, is dominated by autotrophic bacteria. In contrast to lake snow, which reaches an aggregate size of more than 500 μM, iron snow aggregates are smaller and precipitate faster due to their higher amount of iron-containing minerals. Thus, microbial colonization of iron snow aggregates has to occur rapid due their limited residence time in the water [28]. The high surface area of the iron minerals present in the iron snow will alleviate adsorption of dissolved organic compounds serving as potential electron donor for the activity of heterotrophic microorganisms colonizing the aggregates.. Similarly, anaerobic iron-reducing microorganisms would profit, because a high surface area allows better access to iron as alternative electron acceptor when the aggregates reach the anoxic water layer [30]. Since the amount and type of iron-containing minerals will drastically influence the activity of iron-reducing bacteria [31], not only a descriptive but also quantitative information regarding the inorganic phase of the aggregates is required to achieve a better understanding of the biological iron-cycling processes.

To our knowledge, the only analysis of the mineral phase of the pelagic particulate matter was performed on the inorganic colloids from a slightly alkaline ultra-oligotrophic lake [34, 35]. The authors used a combination of three techniques (energy dispersive X-ray spectroscopy, selected area electron diffraction and transmission electron microscopy) to gain semi-quantitative information about the mineral phase of the pelagic aggregates. Different types of aluminosilicates were detected and characterized, however problems appear in the identification of different oxides and hydroxides [35]. In addition, a limited number of measurements were performed and the size of the particles was not considered. Since Raman spectroscopy is a powerful technique capable to distinguish between various oxides and hydroxides [1], we propose Raman imaging as an approach for the quantification of various minerals which form the particulate matter of an aquatic environment. Beside the advantage that a single method (implicit a single device) is used for the quantification of the minerals which form the pelagic aggregates, no sample preparation is required for the investigation of

the minerals. Raman measurements can be performed even under anoxic conditions if the sample is introduced in a glass cell containing an inert gas, and measured thorough the glass window. Thus the transformations which could take place when metastable components come in contact with air can be avoided. Furthermore, the Raman mapping results are not influenced by the size of the particles. By selecting the distance between two adjacent measurement points equal to the laser spot and the thickness of the sample layer equal to the penetration depth of the laser, all particles located in the scanned area are measured during the Raman mapping. The big particles are measured at different points, and the number of measurements is proportional to the surface area of the particle. However, a relatively long running time is required using this spectroscopic approach for a single Raman mapping scan.

In this report, a semi-quantitative study has been established and carried out to quantify the inorganic phase of pelagic aggregates formed in an acidic lignite mine lake using Raman spectroscopy. In addition, the microbial communities of the aggregates were compared using a DNA-based fingerprinting method called denaturing gradient gel electrophoresis (DGGE) to evaluate if potential differences in the mineral composition are reflected by differences of the microbial communities potentially involved in iron cycling.

Materials and methods

Site description and sampling

The acidic lignite mine lake (Lake 77) is located in the Lusatian mine area in east central Germany. A bank on the bottom of the lake rising to about 4 m depth separates the bottom water of the northern basin from the rest of the lake (Figure 1). The central basin shows a dimictic stratification scenario with typical spring and fall mixes, while the stratification remains stable in the northern basin with an oxic surface water layer and a deeper anoxic water layer separated by a sharp redoxcline. The inflow of less acidic, Fe(II)- and sulfate-rich groundwater reaches the northern basin [28]. Sediment traps (3 plexiglas tubes with

removable cups at the bottom of each tube, 5 cm diameter, 40 cm total length) were installed for two weeks at both central and northern basins for collecting iron snow formed within redoxcline and in deeper (bottom) anoxic water layer, respectively. The sample name CR stands for

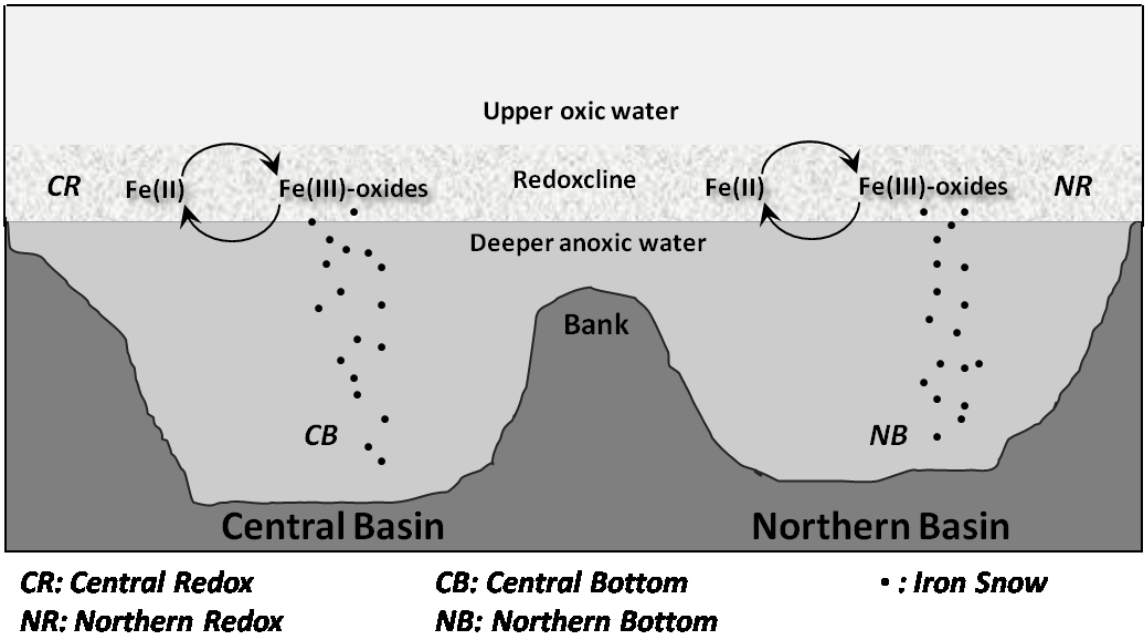

Figure 1: Schematically representation of acidic lignite mine Lake 77 with stratification scenario during summer season when the iron snow samples were collected.

central basin redoxcline, CB for central basin bottom; NR for northern basin redoxcline and NB for northern basin bottom. Fresh samples were collected on July 2010 and transferred to the laboratory in an ice box before using for Raman microscopy investigation and molecular microbial community analysis.

Lake water chemistry

Dissolved oxygen, pH, conductivity and temperature were measured over depth with the multi-parameter water quality checker U-10 (Horiba, Japan). Water samples were collected with a water sampler based on Ruttner design and transported at 4 °C and processed within

24 h. Fe(II) and Fe(III) contents of water sample were measured after acidification with 1 M HCl [36]. Sulfate concentration was measured using the barium-chloride method [37].

Sample preparation for Raman investigations

A very thin layer of each iron snow was spread on the fused silica glass slide and dried at room temperature. Raman measurements were carried out on the dried samples.

Raman setup

The Raman measurements of iron snow were performed with a commercial micro-Raman setup (HR LabRam inverse system, Jobin Yvon Horiba). A frequency doubled Nd:YAG laser at a wavelength of 532 nm was used to excite the Raman scattering. To avoid changes in the mineral structure or composition due to heat generated by the laser, a power of 20 μW was chosen for Raman imaging measurements. The laser beam was focused on the sample by means of a Zeiss LD EC Epiplan-Neofluar 100x/0.75 microscope objective down to a spot diameter of approximately 1 μm. The dispersive spectrometer had an entrance slit of 100 μm, a focal length of 800 mm and was equipped with a grating of 300 lines/mm. The Raman scattered light was detected by a Peltier cooled CCD detector. Each Raman spectrum was collected with 40 s total integration time. For the Raman mapping experiments, an automatically tunable x-y stage (Merzhäuser) was used. The distance between two adjacent points in the x and y direction was 1 μm. On average, 25 scans for each location were performed, which correspond to a total number of circa 16500 spectra.

Data analysis of the Raman outcome

The spectra were first background corrected to minimize the effect of the fluorescence background. The presence or absence of a mineral in the sample was decided based on the intensity of the characteristic Raman band or the intensity ratio of two bands (in case of

ferrihydrite). The threshold value of the Raman marker band used for the detection of the mineral was manually set for each scan. If the intensity of a Raman band was higher or lower than the selected threshold value, then the mineral was considered present or absent in the probe, respectively. The decision to manually select the threshold values for all the Raman bands used for the identification of the minerals was taken due to the high variance of the fluorescence background observed in various samples. The amount (in percentage) of a mineral present at a location was calculated as the ratio between the number of spectra which presented the Raman marker band of the mineral divided by the total number of spectra recorded on the samples from the analyzed site.

Deoxyribonucleic acid (DNA) extraction and denaturing gradient gel electrophoresis (DGGE) fingerprinting analysis

Total genomic DNA was directly extracted from fresh iron snow samples captured in the sediment traps using the PowerSoil DNA Isolation Kit (MO BIO laboratories, USA) according to the manufacturer's instructions. Bacterial community was fingerprinted using a nested-polymerase chain reaction (PCR)-DGGE approach. First, nested amplification of the bacterial 16S ribosomal ribonucleic acid (rRNA) products was executed with the universal bacterial primer EUB-341F-GC with GC-clamp (5'-CGC CCG CCG CGC CCC GCG CCC GTC CCG CCG CCC CCG CCC GCC TAC GGG AGG CAG CAG-3') and reverse primer 907R (5'-CCGTCAATTCMTTTRAGTTT-3') with an annealing temperature of 65 °C for 20 cycles of amplification, followed by 10 cycles with annealing temperature of 55 °C. The *Taq* enzyme for PCR was from Jena Bioscience (Jena Bioscience, Germany) and other reagents were from Sigma (Sigma-Aldrich, Germany). The PCR Thermocycling was performed with a T-Gradient cycler (Primus 96advanced, peqLab). PCR products were separated on a polyacrylamide gel with denature reagent concentration ranging from 20% to 70% at the

consistent temperature of 60 °C for 15 hours. The polyacrylamide gel was stained with SYBR Gold before documentation.

Results and discussion

Water geochemistry

The microbial oxidation of Fe(II) to Fe(III) is the initial step in iron oxide formation at low pH, however it is still unclear to which extent the subsequent mineralization is controlled by microorganisms. Mineral formation and mineral stability is also influenced by geochemical conditions of the surrounding water phase [22, 38]. Thus, we studied the water chemistry to obtain a better understanding of the biogeochemical processes. The oxic overlaying water layer showed similar characteristics in both basins with pH values of about 3, similar sulfate and Fe(III) concentrations of about 8 mM and 2 mM, respectively, but lacking Fe(II). In the redoxcline of the central and northern basin, oxygen concentrations declined to 2.9 and 1.7 mg/L whereas Fe(II) concentrations increased to 1.1 and 1.7 mM, respectively (Table 1). Highest pH value, sulfate and Fe(II) concentrations were observed in the bottom water of the northern basin (Table 1) which is affected by the inflow of less acidic iron-rich groundwater[28]. Due to the considerable variations in pH between deeper water layers in central basin and northern basins different mineral phases of iron oxyhydroxides were expected to be formed. Fe(III) sedimentation rates approximate 1.5 and 1.9 g Fe m^{-2} d^{-1} at central and northern basin [28]. Transformation reactions are not likely to occur due to the low residence time of the particles in the lake. Schwertmannite is also the dominant mineral of the upper sediment collected in the central basin [53].

Qualitative analysis of the mineral phase

Preliminary measurements of the iron snow samples performed under anoxic conditions (the samples were measured in a glass cell in the absence of oxygen) and oxic conditions (the

sample was dried of the substrate and measured in atmospheric conditions) showed no difference in the mineral phases of the samples. In addition, no changes in the color of the iron snow was noticed during the drying process, therefore transformation of metastable iron sulfides (black minerals) to schwertmannite (yellow mineral) can be excluded. Because the spectra measured in atmospheric conditions had higher signal noise ratio than the spectra measured through a glass window, we decided for the further investigations to perform Raman measurements only under oxic conditions. Therefore, all the data presented in this contribution were measured under atmospheric conditions.

Table 1: Geochemical parameters were measured in water samples obtained from the redoxcline and the deeper, anoxic bottom water layer of the central and the northern basin of lignite mine Lake 77, from where the iron snow samples were obtained. CR strands for central redoxcline, while CB for central bottom, NR for northern redoxcline, NB for northern bottom.

	Depth [m]	**pH**	**Oxygen content** [mg/L]	**Sulfate** [mM]	**Fe(II)** [mM]	**Fe(III)**[a] [mM]	**Conductivity** [mS/cm]	**Temperature** [°C]
CR	3.9	3.3	2.9	8.3	1.1	2.3	2.0	16.0
CB	6.0	3.5	0	10.3	6.9	0.3	2.1	10.0
NR	3.8	3.3	1.7	8.2	1.7	1.9	2.0	15.5
NB	6.0	5.9	0	15.4	20.0	0.0	3.0	11.3

[a] Fe(III) concentrations were measured from the water phases without iron snow particles included.

[b] All data were obtained from the day the sediment traps were placed into the lake.

In a previous study we showed that these lake snow aggregates contain high amounts of inorganic materials [28]. The mineral phase of the investigated pelagic aggregates was dominated by the iron-containing minerals. Figure 2 showed the Raman spectra of various minerals detected in the investigated iron snow samples and the corresponding Raman marker bands which were used for the identification of the minerals in the Raman imaging experiments (the grey boxes). By far, the most abundant mineral detected in the samples was

schwertmannite, an Fe(III) oxyhydroxysulfate (Figure 2(a), Table 2). Schwertmannite is a mineral which is usually formed in acidic fresh waters rich in dissolved iron and sulfate [39]. The interaction between Fe(III) and $(SO_4)^{2-}$ in schwertmannite is via hydrogen bonds. In an acidic liquid solution, the Fe cations form a complex with the sulfates trough hydrogen

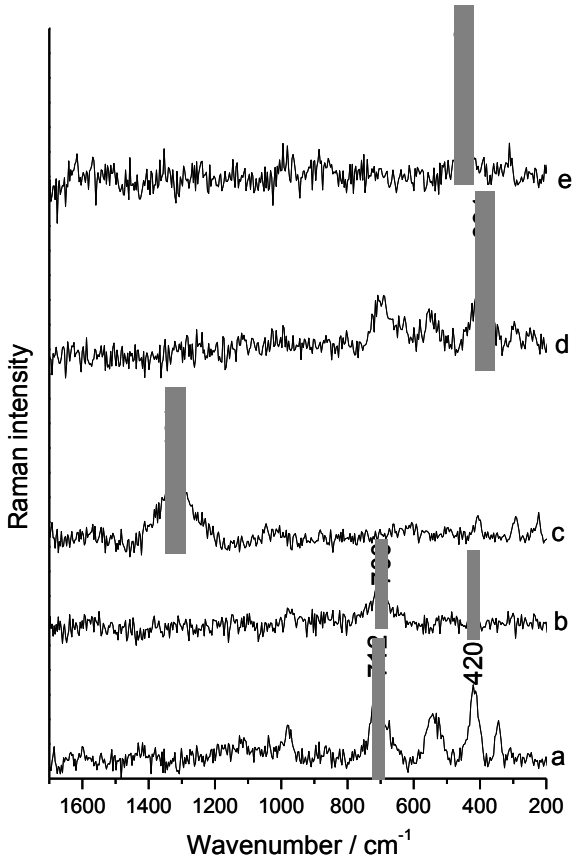

Figure 2: Raman spectra of a- schwertmannite, b- ferrihydrite, c- hematite, d- goethite, and e- quartz. The grey boxes show the regions of the Raman marker bands used for the quantification of various minerals in the sample.

bonds. These similarities of the interaction between Fe(III) and $(SO_4)^{2-}$ is likely the reason why schwertmannite is a common mineral of the acid mine drainage precipitates [40]. Therefore, the dominance of schwertmannite in the iron snow from an acidic lignite mine lake with a pH around 3 was not surprising. Schwertmannite is a stable mineral at a pH in the range of 3 to 5, however in anoxic conditions at higher pH values and in the presence of Fe(II) cations, the stability of the schwertmannite decrease drastically [41]. Interestingly, high

amounts of schwertmannite were detected also in the samples from the anoxic monimolimnion of the north site, although there the pH value of the water was around 6. The Raman spectrum of schwertmannite consists of five relatively intense bands, among them the most prominent band at 712 cm^{-1} served as marker band for the analysis of the distribution of schwertmannite mineral in the samples. In the region around 700 cm^{-1} not only schwertmannite gives a Raman signal but also ferrihydrite ($Fe_2O_3 \cdot 0.5H_2O$) (Figure 2(b)). The Raman band of ferrihydrite at circa 700 cm^{-1} is very broad and has a low intensity compared to the 712 cm^{-1} band of schwertmannite, although it is the strongest Raman band of ferrihydrite. The Raman spectrum of schwertmannite presents also a strong Raman signal at circa 420 cm^{-1}, while ferrihydrite has no Raman band in that region. Therefore, the ratio of the intensities of the bands at 712 cm^{-1} and 420 cm^{-1} is higher for ferrihydrite than for schwertmannite. On the basis of the intensity ratio of the above mentioned bands, we were able to identify and distinguish ferrihydrite and schwertmannite in the Raman maps.

Table 2: The abundance of various minerals detected in iron snow samples at survey sites given by Raman spectroscopy.

	Schwertmannite	Goethite	Ferrihydrite	Hematite	Graphite	Quartz	Calcite	Rutile/Anatase
CR	96%	n.d.[a]	n.d.	n.d.	4%	n.d.	n.d.	n.d.
CB	96%	n.d.	<1%	n.d.	3%	<1%	n.d.	n.d.
NR	92%	n.d.	n.d.	3%	3%	<1%	n.d.	<1%
NB	91%	1%	n.d.	n.d.	4%	1%	1%	1%

[a] n.d., not detected.

Another Fe(III)-mineral identified in the samples from the transition zone of the north site was hematite (α-Fe_2O_3) (Figure 2(c)). The Raman spectrum of hematite can be distinguished easily from the spectra of other minerals by the strong Raman signal at approximate 1314 cm^{-1}, which was thus used as a marker band for the presence of hematite in the samples. Figure 2(d) shows the Raman spectrum of goethite, an iron oxyhydroxide (α-FeOOH). The

characteristic Raman band of this mineral used in this study is located at 391 cm^{-1}. The goethite mineral was detected only in the anoxic samples from the north site where the pH of the water is around 6. The formation of goethite at this site can be connected to the mineral transformation from schwertmannite at higher pH [39].

Not only iron-containing minerals were detected by means of Raman spectroscopy in the iron snow samples. Quartz (SiO_2) was detected in three locations (Table 2). The typical Raman band for this mineral is located at 464 cm^{-1}. Titanium dioxide (rutile and anatase), calcite and graphite were also detected. The presence of graphite in relatively high amounts in all the samples was expected since the samples were obtained from a lignite mine lake.

Interestingly, no iron mineral in the 2^+ oxidation state was detected in the samples, although the Raman technique has been successfully used in the past for the identification of various Fe(II)-minerals like siderite, magnetite, pyrite, or vivianite in earlier studies [1, 19, 42]. Hypothetically speaking, if iron sulfides (pyrrhotite, mackinawite or greigite, for example) were part of the iron snow, elemental sulfur and iron oxyhydroxide (goethite, ferrihydrite and/or lepidocrocite) should be present in the samples after the air drying process, as end products of the aerobic oxidation [43-45]. No elemental sulfur was detected in iron snow, hence the presence of ferrous sulfides in the pelagic aggregates is highly unlikely. Therefore it could be concluded that Fe(II) ions might be found in water as soluble iron and/or forming complexes with the organic matter.

In our previous measurements, small amount of jarosite was detected in the iron snow from central basin[28]. However, no jarosite was found in this study. This could be due to the sampling variation or different sampling time, or the jarosite was formed only under some known specific conditions from schwertmannite [46], and/or might be present in the iron snow in very small amounts, below Raman detection limit.

The pelagic aggregates are of great importance for the transformation and cycling of the elements in the aquatic ecosystem[26]. Being rich in inorganic and organic nutrients, the

aggregates are important sites for adsorption and desorption of soluble compounds and for biological processes which take place in the water [25]. To understand the dynamic processes which take place in this aquatic environment, a quantitative analysis of the aggregates is required.

Quantitative analysis of the inorganic phase

To quantify the amounts of minerals presented in the iron snow, Raman imaging was used. Figure 3 displays the analysis of the Raman map of a sample collected from the anoxic layer of the northern basin. Figure 3(A) shows the brightfield image of an iron snow sample where the box mark the region which was scanned by means of Raman spectroscopy. Three minerals were detected in this investigated sampling field: schwertmannite, graphite and quartz. The distribution of schwertmannite is presented in Figure 3(B), where the light grey pixels represent the spots where the mineral is present while the black pixels show the regions where schwertmannite is absent. Similarly, the distribution of graphite and quartz are presented in Figure 3(C) and Figure 3(D), respectively. The false color images presented in Figure 3 clearly shows that the main mineral in the investigated sample is schwertmannite while graphite and quartz are presented only in minor amounts. Since the sample was spread on the fused silica slide in a thin and uniform layer, the amount of various minerals within the sample was directly proportional to the surface region of the sample where the respective minerals were detected. The surface region of a mineral in a Raman map is proportional with the number of measured spots (pixels) where that mineral is identified. Therefore, by counting the number of spots where each mineral was detected, quantitative information could be obtained regarding to the minerals present in the sample. Subsequently, an overview over the quantities of different minerals present in the collected samples was able to be gained, by performing multiple scans on the iron snow samples.

We considered our approach semi-quantitative because the variation in Raman scattering efficiency of different minerals was not taken into account. However, it was expected that the overall quantification results were only minimally affected by this approach.

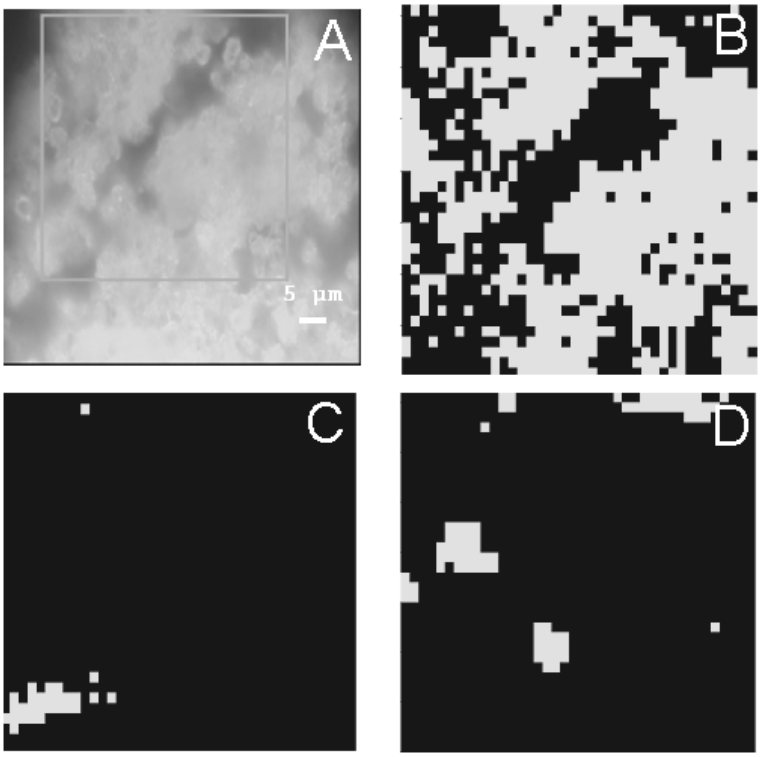

Figure 3: A - The brightfield image of a sample from northern basin bottom layer. The rectangle shows the region where Raman maps were performed. The spatial distribution of schwertmannite (B), graphite (C) and quartz (D) in the sample is illustrated by the false color images. The light grey pixels present the positions where the investigated mineral was detected, while black pixels show the regions where the mineral was not found. The pixel length represents the distance between two adjacent measurement points and is equal to 1 µm.

A summary of the minerals detected in the iron snow are shown in Table 2. Fe(III)-minerals dominate the inorganic phase of the aggregates. In all four iron snow samples, the main components of the pelagic aggregates were schwertmannite and graphite. As the iron snow originates from a lignite coal mine, the presence of graphite in all the samples was expected. Ferrihydrite was detected only in sample CB and in extreme low concentration (<1%). Goethite was found only in the sample NB (1%), where the bulk water pH was 5.9.

Previous studies have shown that the transformation rate of schwertmannite to goethite increase markedly at circumneutral pH values in the presence of soluble Fe(II) and absence of oxygen [41]. The transformation rate is highly enhanced by the sorption of Fe(II) on the surface of schwertmannite. Therefore, the low amount of goethite detected in the NB sample could be explained by a low number of sorption sites on the surface of schwertmannite. This imply that either other cations and organic matter blocked the dissolution sites of the schwertmannite in the iron snow samples or that the cations and organic matter prevent the polymerization of thermodynamically stable, crystalline ferric minerals [47]. Actually, the large majority of the Raman spectra collected from NB exhibit two small broad bands assigned to the C-C stretching vibrations of the aromatic compounds [48]. Apparently organic matter covered a large surface of the schwertmannite and in this way hindered the sorption of Fe(II) on the iron snow. The outcome is in concordance with the results reported by Collins and coworkers, who showed that silicate and natural organic matter retard the Fe(II)-catalyzed minerals transformation [49].

Hematite was identified only in the NR sample (3%). The presence of hematite in those samples is surprisingly since at a pH of 3 and a temperature of circa 10 °C, goethite and not hematite should be the most stable form of Fe(III)-containing minerals [38]. In addition, a small amount of titanium dioxide was also detected in the northern basin.

The quantification results offered us a nice picture over the iron minerals from iron snow. Similar mineral compositions were observed between iron snow samples from the same basin, whereas obvious differences were also noticed between basins, mentioning the content of schwertmannite and other iron containing minerals. The higher mineral diversity from the northern basin was probably caused by the seepage water inflow from the northeastern mine tailing dump area. As to the organic part, the microbial communities were also investigated. For this purpose we used DGGE.

Bacterial communities

The microbial community composition is always affected by the geochemical conditions of its habitat, especially by the oxygen content and the pH. Microbial Fe(II) oxidation can be mediated in a broad pH range (0 to 8) and can occur under oxic, microoxic and anoxic

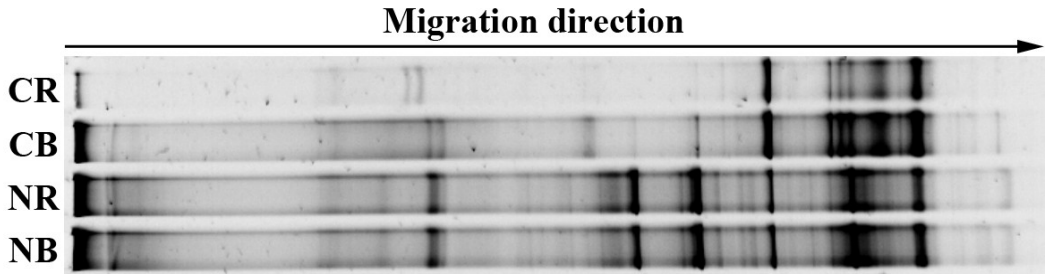

Figure 4: Denaturing gradient gel electrophoresis (DGGE) patterns showing diverse bacterial communities of iron snow samples from central redoxcline (CR); central bottom (CB); northern redoxcline (NR); northern bottom (NB) of acidic lignite mine Lake 77.

conditions. Since chemical Fe (II) oxidation is completely inhibited at pH values below 4.2[50], acidophilic or at least acid tolerant iron oxidizing bacteria are responsible for the initial step in iron oxyhydroxides mineral formation [51, 52]. PCR products obtained from iron snow particles sampled form the central basin (CR and CB) produced similar DGGE patterns indicating similar microbial communities, although some differences were observed at the upper part of the gel-lane (Figure 4). Fingerprints of iron snow particle samples of the northern basin (NR and NB) were identical to each other, suggesting high similarities between these two samples. Thus, the stronger pH and Fe(II) concentration gradients observed in the redoxcline of the northern basin did not affect apparently the iron snow microbial community composition, which suggested the majority microorganisms being metabolically active over the broad pH. In contrast, communities of iron snow particles sampled in the central and in the northern basin were dissimilar based on differences of the signal-intensive bands on a respective DGGE gel lane which should be indicative of abundant microorganisms in each sample. The distinctive microbial communities detected in northern

and central iron snow samples could have affected iron oxyhydroxides formation, the subsequent mineral colonization by several groups of microorganisms preferring a solid surface, and the microbial reduction of Fe(III) back to Fe(II) which can occur under anoxic conditions.

Mineral-microbe interaction

The microorganisms are the main force which drives the formation of iron minerals under acidic conditions [50]. The majority of the iron minerals of the iron snow had high surface area and poor crystallinity. These properties make them attractive for microbial and abiotic processes[29, 53]. Schwertmannite has been observed in numerous acidic mine drainage systems all over the world. The high stability of schwertmannite at pH values higher than 5, in the presence of Fe(II) might be due to the presence of natural organic matter (e.g. humic substances, exopolysaccharide excretion by biofilm bacteria) in this aquatic environment.

Hematite was detected only in the redoxcline of the northern basin but not in the deeper anoxic water. This absence of hematite in the anoxic water layer could be due to enhanced activity of Fe(III)-reducing bacteria, the reduction taking place before reaching the bottom of the lake, since hematite was shown to be bio-reducible at circum-neutral pH [54].

Ferrihydrite is widespread in many natural environments and it is used by a number of Fe(III)-reducing bacteria as electron acceptor or it is produced by other Fe(II)-oxidizing microorganisms at circum-neutral pH conditions [29]. Previous studies have shown that ferrihydrite appears mostly at a pH above 5 [22]. The detection of ferrrihydrite in more acidic iron snow samples suggest that and it can be also formed by acidophilic or at least acid tolerant microorganisms.

The aggregation of organic matter, inorganic matter, and microorganisms to form sinking snow particles plays a major part in aquatic ecosystems [55]. The high hydrolytic enzyme activities of bacteria convert the aggregate organic matter into non-sinking dissolved organic

matter (DOM), forming plumes in the ocean. However, formation of DOM plumes might not occur with iron snow due to its higher inorganic fraction leading to a higher sinking velocity[28]. Nonetheless, the intensely colonized aggregates create hot spots of microbial life having substantial roles in the cycling of iron in the acidic lignite mine lake. With the means of Raman spectroscopy which is able to reveal slight quantitative differences in the inorganic phase, we were able to obtain a deeper understanding on sophisticated microbe-mineral interactions in this aquatic habitat.

Conclusions

Raman spectroscopy was applied successfully for the quantification of the mineral phase of pelagic aggregates formed in an acidic iron- and sulfate-rich aquatic environment. Discrimination between minerals composed by nanocrystals (e.g., schwertmannite and ferrihydrite) or between closely related minerals (e.g., goethite and hematite) was doable using Raman spectroscopy. Schwertmannite was the main mineral in all aggregates regardless of the pH in the niche environment and differences in the bacterial communities inhabiting this aggregate. Although substantial differences in the microbial communities of the investigated sites were detected, only small variations of the mineral phase of the iron snow were revealed by Raman imaging. The outcome suggests that the formation of the mineral phase of the iron snow was mainly dictated by the geochemical conditions of the aquatic environment, despite the fact that microbial communities were actively involved in the initiation of iron mineral formation.

Acknowledgements

We highly acknowledge the financial supports from the Deutsche Forschungsgemeinschaft (Graduate School 1257 “Alteration and element mobility at the microbe-mineral interface”) as well as from the TMBWK (MikroPlex) PE113-1. Shipeng Lu was supported by the

Graduate School of Excellence Jena School for Microbial Communication (JSMC) funded by the German Research Foundation (Deutsche Forschungsgemeinschaft [DFG]). The authors thank Marco Reiche, Marco Jung and Martina Hermann for technical assistances.

References

1. M. Hanesch, Raman spectroscopy of iron oxides and (oxy)hydroxides at low laser power and possible applications in environmental magnetic studies, *Geophys. J. Int.*, 2009, **177**, 941-948.
2. J. Monnier, L. Bellot-Gurlet, D. Baron, D. Neff, I. Guillot and P. Dillmann, A methodology for Raman structural quantification imaging and its application to iron indoor atmospheric corrosion products, *J. Raman Spectrosc.*, 2011, **42**, 773-781.
3. R. L. Frost, T. Kloprogge, M. L. Weier, W. N. Martens, Z. Ding and H. G. H. Edwards, Raman spectroscopy of selected arsenates-implications for soil remediation, *Spectrochim. Acta A*, 2003, **59**, 2241-2246.
4. Z. C. Ling, A. Wang and B. L. Jolliff, Mineralogy and geochemistry of four lunar soils by laser-Raman study, *Icarus*, 2011, **211**, 101-113.
5. Z. Tomić, P. Makreski and B. Gajić, Identification and spectra–structure determination of soil minerals: Raman study supported by IR spectroscopy and X-ray powder diffraction, *J. Raman Spectrosc.*, 2010, **41**, 582-586.
6. J. Fritz, A. Greshake and D. Stoffler, Micro-Raman spectroscopy of plagioclase and maskelynite in Martian meteorites: evidence of progressive shock metamorphism, *Antarct. Meteorite Res.*, 2005, **18**, 96-116.
7. V. Ciobotă, W. Salama, N. Tarcea, P. Rösch, M. E. Aref, R. Gaupp and J. Popp, Identification of minerals and organic materials in Middle Eocene ironstones from the Bahariya Depression in the Western Desert of Egypt by means of micro-Raman spectroscopy, *J. Raman Spectrosc.*, 2012, **43**, 405-410.

8. T. Frosch, N. Tarcea, M. Schmitt, H. Thiele, F. Langenhorst and J. Popp, UV Raman imaging a promising tool for astrobiology: comparative Raman studies with different excitation wavelengths on SNC Martian Meteorites, *Anal. Chem.*, 2007, **79**, 1101-1108.
9. F. Rull, J. Martinez-Frias, A. Sansano, J. Medina and H. G. M. Edwards, Comparative micro-Raman study of the Nakhla and Vaca Muerta meteorites, *J. Raman Spectrosc.*, 2004, **35**, 497-503.
10. P. Vargas Jentzsch, R. M. Bolanz, V. Ciobotă, B. Kampe, P. Rösch, J. Majzlan and J. Popp, Raman spectroscopic study of calcium mixed salts of atmospheric importance, *Vib. Spectrosc.*, 2012, **61**, 206-213.
11. P. Vargas Jentzsch, V. Ciobotă, B. Kampe, P. Rösch and J. Popp, Origin of salt mixtures and mixed salts in atmospheric particulate matter, *J. Raman Spectrosc.*, 2012, **43**, 514-519.
12. P. Vargas Jentzsch, B. Kampe, P. Rösch and J. Popp, Raman spectroscopic study of crystallization from solutions containing $MgSO_4$ and Na_2SO_4: Raman spectra of double salts, *J. Phys. Chem. A*, 2011, **115**, 5540-5546.
13. S. Cîntă Pînzaru and B. P. Onac, Raman study of natural berlinite from a geological phosphate deposit, *Vib. Spectrosc.*, 2009, **49**, 97-100.
14. W. Schumacher, M. Kühnert, P. Rösch and J. Popp, Identification and classification of organic and inorganic components of particulate matter via Raman spectroscopy and chemometric approaches, *J. Raman Spectrosc.*, 2011, **42**, 383-392.
15. L. D. Kock and D. De Waal, Raman analysis of ancient pigments on a tile from the Citadel of Algiers, *Spectrochim. Acta A*, 2008, **71**, 1348-1354.
16. L. C. Prinsloo, W. Barnard, I. Meiklejohn and K. Hall, The first Raman spectroscopic study of San rock art in the Ukhahlamba Drakensberg Park, South Africa, *J. Raman Spectrosc.*, 2008, **39**, 646-654.

17. P. Vandenabeele, K. Lambert, S. Matthys, W. Schudel, A. Bergmans and L. Moens, In situ analysis of mediaeval wall paintings: a challenge for mobile Raman spectroscopy, *Anal. Bioanal. Chem.*, 2005, **383**, 707-712.
18. C. E. Amri, M.-C. Maurel, G. Sagon and M.-H. Baron, The micro-distribution of carbonaceous matter in the Murchison meteorite as investigated by Raman imaging, *Spectrochim. Acta A*, 2005, **61**, 2049-2056.
19. T. Dörfer, W. Schumacher, N. Tarcea, M. Schmitt and J. Popp, Quantitative mineral analysis using Raman spectroscopy and chemometric techniques, *J. Raman Spectrosc.*, 2010, **41**, 684-689.
20. S. N. White, Laser Raman spectroscopy as a technique for identification of seafloor hydrothermal and cold seep minerals, *Chem. Geol.*, 2009, **259**, 240-252.
21. D. Neff, L. Bellot-Gurlet, P. Dillmann, S. Reguer and L. Legrand, Raman imaging of ancient rust scales on archaeological iron artefacts for long-term atmospheric corrosion mechanisms study, *J. Raman Spectrosc.*, 2006, **37**, 1228-1237.
22. E. Murad and P. Rojik, Iron mineralogy of mine-drainage precipitates as environmental indicators: review of current concepts and a case study from the Sokolov Basin, Czech Republic, *Clay Miner.*, 2005, **40**, 427-440.
23. T. M. Valente and C. Leal Gomes, Occurrence, properties and pollution potential of environmental minerals in acid mine drainage, *Sci. Total Environ.*, 2009, **407**, 1135-1152.
24. S. W. Fowler and G. A. Knauer, Role of large particles in the transport of elements and organic compounds through the oceanic water column, *Prog. Oceanogr.*, 1986, **16**, 147-194.
25. H.-P. Grossart, T. Berman, M. Simon and K. Pohlmann, Occurrence and microbial dynamics of macroscopic organic aggregates (lake snow) in Lake Kinneret, Israel, in fall, *Aquat. Microb. Ecol.*, 1998, **14**, 59-67.

26. H.-P. Grossart and M. Simon, Limnetic macroscopic organic aggregates (lake snow): Occurrence, characteristics, and microbial dynamics in Lake Constance, *Limnol. Oceanogr.*, 1993, **38**, 532-546.

27. B. D. Honeyman, L. S. Balistrieri and J. W. Murray, Oceanic trace metal scavenging: the importance of particle concentration, *Deep Sea Res.*, 1988, **35**, 227-246.

28. M. Reiche, S. Lu, V. Ciobotă, T. R. Neu, S. Nietzsche, P. Rösch, J. Popp and K. Küsel, Pelagic boundary conditions affect the biological formation of iron-rich particles (iron snow) and their microbial communities, *Limnol. Oceanogr.*, 2011, **56**, 1386-1398.

29. A. Kappler and K. L. Straub, Geomicrobiological cycling of iron, *Rev. Mineral. Geochem.*, 2005, **59**, 85-108.

30. E. E. Roden, Fe(III) Oxide reactivity toward biological versus chemical reduction, *Environ. Sci. Technol.*, 2003, **37**, 1319-1324.

31. J. M. Zachara, J. K. Fredrickson, S. W. Li, D. W. Kennedy, S. C. Smith and P. L. Gassman, Bacterial reduction of crystalline Fe^{3+} oxides in single phase suspensions and subsurface materials, *Am. Mineral.*, 1998, **83**, 1426–1443.

32. T. R. Neu, In situ cell and glycoconjugate distribution in river snow studied by confocal laser scanning microscopy, *Aquat. Microb. Ecol.*, 2000, **21**, 85-95.

33. B. Schweitzer, I. Huber, R. Amann, W. Ludwig and M. Simon, α- and β-Proteobacteria control the consumption and release of amino acids on lake snow aggregates, *Appl. Environ. Microb.*, 2001, **67**, 632-645.

34. T. Schäfer, V. Chanudet, F. Claret and M. Filella, Spectromicroscopy mapping of colloidal/particulate organic matter in Lake Brienz, Switzerland, *Environ. Sci. Technol.*, 2007, **41**, 7864-7869.

35. V. Chanudet and M. Filella, A non-perturbing scheme for the mineralogical characterization and quantification of inorganic colloids in natural waters, *Environ. Sci. Technol.*, 2006, **40**, 5045-5051.

36. M. Blöthe, D. M. Akob, J. E. Kostka, K. Goschel, H. L. Drake and K. Küsel, pH gradient-induced heterogeneity of Fe(III)-reducing microorganisms in coal mining-associated lake sediments, *Appl. Environ. Microbiol.*, 2008, **74**, 1019-1029.
37. M. Tabatabai, A rapid method for determination of sulfate in water samples, *Environ. Lett.*, 1974, **7**, 237-243.
38. R. G. Robins, Hydrothermal precipitation in solutions of thorium nitrate, ferric nitrate and aluminium nitrate, *J. Inorg. Nucl. Chem.*, 1967, **29**, 431-435.
39. U. Schwertmann and R. M. Cornell, *The Iron Oxides: Structure, Properties, Reactions, Occurrences and Uses*, 2nd edn., Wiley-VCH Weinheim, 2003.
40. J. Majzlan and S. C. B. Myneni, Speciation of iron and sulfate in acid waters: aqueous clusters to mineral precipitates, *Environ. Sci. Technol.*, 2004, **39**, 188-194.
41. E. D. Burton, R. T. Bush, L. A. Sullivan and D. R. G. Mitchell, Schwertmannite transformation to goethite via the Fe(II) pathway: reaction rates and implications for iron-sulfide formation, *Geochim. Cosmochim. Ac.*, 2008, **72**, 4551-4564.
42. K. A. Rodgers, H. W. Kobe and C. W. Childs, Characterization of vivianite from Catavi, Llallagua Bolivia, *Miner. Petrol.*, 1993, **47**, 193-208.
43. N. Belzile, Y.-W. Chen, M.-F. Cai and Y. Li, A review on pyrrhotite oxidation, *J. Geochem. Explor.*, 2004, **84**, 65-76.
44. J. A. Bourdoiseau, M. Jeannin, R. Sabot, C. Rémazeilles and P. Refait, Characterisation of mackinawite by Raman spectroscopy: Effects of crystallisation, drying and oxidation, *Corros. Sci.*, 2008, **50**, 3247-3255.
45. J.-A. Bourdoiseau, M. Jeannin, C. Rémazeilles, R. Sabot and P. Refait, The transformation of mackinawite into greigite studied by Raman spectroscopy, *J. Raman Spectrosc.*, 2011, **42**, 496-504.
46. S. Regenspurg, A. Brand and S. Peiffer, Formation and stability of schwertmannite in acidic mining lakes, *Geochim. Cosmochim. Ac.*, 2004, **68**, 1185-1197.

47. A. M. Jones, R. N. Collins, J. Rose and T. D. Waite, The effect of silica and natural organic matter on the Fe(II)-catalysed transformation and reactivity of Fe(III) minerals, *Geochim. Cosmochim. Ac.*, 2009, **73**, 4409-4422.

48. B. Wopenka and J. D. Pasteris, Strucfural characterizxtion of kerogens to granulite-facies graphite: Applicability of Raman microprobe spectroscopy, *Am. Mineral.*, 1993, **78**, 533-557.

49. R. N. Collins, A. M. Jones and T. D. Waite, Schwertmannite stability in acidified coastal environments, *Geochim. Cosmochim. Ac.*, 2010, **74**, 482-496.

50. G. Meruane and T. Vargas, Bacterial oxidation of ferrous iron by *Acidithiobacillus ferrooxidans* in the pH range 2.5 - 7.0, *Hydrometallurgy*, 2003, **71**, 149-158.

51. D. Emerson, E. J. Fleming and J. M. McBeth, Iron-oxidizing bacteria: an environmental and genomic perspective, *Annu. Rev. Microbiol.*, 2010, **64**, 561-583.

52. S. Hedrich, M. Schlömann and D. B. Johnson, The iron-oxidizing *Proteobacteria*, *Microbiol.*, 2011, **157**, 1551-1564.

53. A. Peine, A. Tritschler, K. Küsel and S. Peiffer, Electron flow in an iron-rich acidic sediment- evidence for an acidity-driven iron cycle, *Limnol. Oceanogr.*, 2000, **45**, 1077-1087.

54. S. Bose, M. F. Hochella Jr, Y. A. Gorby, D. W. Kennedy, D. E. McCready, A. S. Madden and B. H. Lower, Bioreduction of hematite nanoparticles by the dissimilatory iron reducing bacterium *Shewanella oneidensis* MR-1, *Geochim. Cosmochim. Ac.*, 2009, **73**, 962-976.

55. F. Azam and F. Malfatti, Microbial structuring of marine ecosystems, *Nat. Rev. Micro.*, 2007, **5**, 782-791.

6 General discussion

1. Biogeochemistry of Lake 77 and Iron Snow

In Lake 77, a bank rising to about 4 m depth on the bottom between the central and northern water bodies permanently separated the bottom water layers of the northern basin from the rest of the lake. The central basin showed dimictic water regime with a typical mixolimnion and hypolimnion during the summer, while the northern basin was meromictic with stratification remaining over years. This was attributed to the less acidic, Fe(II)- and sulfate-rich groundwater inflow entering the lake from the north mine dump area into the northern basin, leading to an advective accumulation of dissolved substances thus resulting in a density stratification and monimolimnion. During the stratification period of the lake, the water column was divided into an oxic mixolimnion and an anoxic water body by the sharp redoxcline centered at about 4 m water depth, where Fe(II) and oxygen coincided by forming a distinct transition zone of about 30 cm thick. The water pH of anoxic monimolimnion could reach as high as 5.9 in northern basin while it remained around 3 throughout the whole water body in central basin. This two-basin-with-two-stratification-pattern characteristic of Lake 77 was unique comparing to other acidic mine lakes, which have either dimictic (Blodau *et al.*, 1998; Peine, 1998) or meromictic water regimes (Boehrer and Schultze, 2006; Karakas *et al.*, 2003). The Fe(III)-rich aggregates (iron snow) occured in the redoxcline of Lake 77. The iron snow was different from other 'snow' type pelagic particles in comparison of particle size, Fe and organic carbon content and sedimentation rate (Grossart and Simon, 1993; Neu, 2000; Silver *et al.*, 1978). They were generally smaller than 380 μm in diameter and were dominated by a higher Fe(III) fraction (> 35%) and a lower organic carbon content (<11%) (See chapter 3), whereas normal lake snow usually has diameter ranging from 3 to 20 mm and a high fraction of 20-40% of organic carbon (Grossart and Simon, 1993). Interestingly, there were differences between iron snow samples collected from the central and northern

basins. The iron snow obtained from the central basin appeared as rust-colored floating flakes while those from northern basin were more yellowish-orange (Figure 6.1). Despite the color difference, semi-quantitative Raman spectroscopy analyses showed that the main Fe(III)

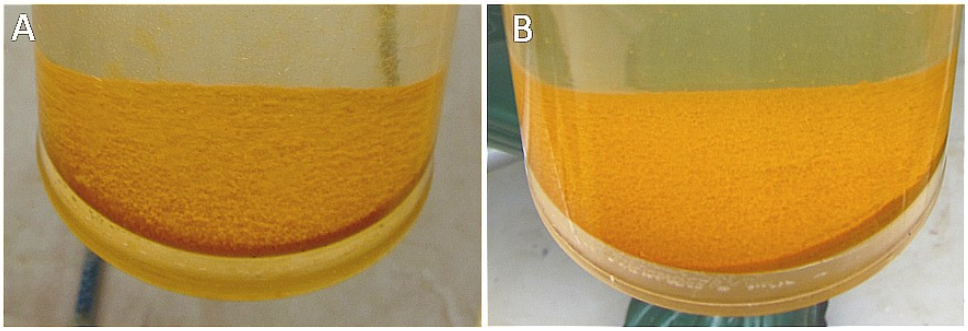

Figure 6.1. Iron snow obtained from central basin (A) and northern basin (B) of Lake 77.

mineral formed was schwertmannite with concentrations of more than 91% in all iron snow samples (See chapter 5). The highest concentrations of schwertmannite were detected in samples from the central basin. Additionally, goethite and hematite were identified in the northern basin iron snow which showed the highest pH value (pH 5.9). To our knowledge, this was the first quantitative analysis on the mineral phase of the pelagic particulate matter using Raman imaging.

In natural aquatic environments, pelagic aggregates are important for the turnover and sinking flux of organic and inorganic matter to the sediment and become hotspots for microbial processes (Boyd and Ellwood, 2010; Grossart and Ploug, 2000; Simon *et al.*, 2002). Reactive iron species are thought to be important for stabilizing organic matter in ocean sediments underlining the tight coupling between the biogeochemical cycles of carbon and iron (Eglinton, 2012). Opposing gradients of oxygen and Fe(II) in streams, lakes, and marine habitats are critical for the formation of iron minerals (Boyd and Ellwood, 2010; Brown *et al.*, 2011), which can be the nucleus for pelagic aggregate formation (Eusterhues *et al.*, 2008). The iron snow was one kind of these aggregates with unique features. Research on iron snow had provided us a novel limnetic model of a tight coupling between the

biogeochemical cycles of carbon and iron other than the one proposed for marine sediment (Boyd and Ellwood, 2010), in which bacteria dissolve particulate iron and at the same time release iron-binding ligands that complex with iron and therefore help to keep it in solution. Sinking particles, on the other hand, also scavenge iron from solution. The balance between these supply and removal processes determines the concentration of dissolved iron in the ocean. In iron snow, carbon dioxide was fixed as organic carbon coupled with Fe(III) formation by microorganisms. The particles that form subsequently settled down to the bottom part of the lake as fresh input material of lake sediment at a high estimated sinking velocity, together with decomposition by Fe(III) mineral reduction coupled with organic carbon consumption.

2. The Microbiology of iron Snow Biogenesis

The iron snow particles were highly colonized by microbial cells, which was determined both by DAPI total cell counting (~10^{10} cells per g dry weight) and quantitative PCR (~5×10^{8} to 4×10^{10} cells per g dry weight). Up to 81% of these inhabiting bacteria were related to Fe-cycling bacteria and up to 61% were found to be metabolically active by using the qPCR technique (See chapter 4). Microcosm incubations proved that iron snow can be generated by Fe(II)-oxidizing microorganisms and schwertmannite was the product of this biological oxidation process (See chapter 3). Molecular methods including 16S rRNA gene library construction, quantitative PCR and metaproteomics analyses had further revealed the microbial communities inhabiting the iron snow and a number of important Fe(II) oxidizers and Fe(III) reducers were identified. Community differences were found between iron snow from the central basin and the northern basin, which indicated that pH might be the main force influencing the microbial communities.

The metaproteomics method is used to analyze samples from Iron Mountain AMD (Lo *et al.*, 2007; Ram *et al.*, 2005) and the former mine near Carnoulès, France (Bertin *et al.*,

2011). Complete suites of proteins of specific complex environmental samples can be identified and linked with metagenomic information to organisms and community structures, especially to those with low biodiversity. The *Leptospirillum*, *Acidothiobacillus*, and *Thiobacillus* species are highlighted with the *in situ* metabolism functions annotated. In our research, with an artificial database containing all the publically available genomic sequences of acidophiles or Fe-cycling microbes from various environments (Cárdenas *et al.*, 2010; Markowitz *et al.*, 2009), metaproteomic analyses were applied successfully to iron snow samples. However, due to the lack of representative genome-sequenced relatives, proteins from microbial groups such as *Ferrovum* could not be annotated, though it was abundant in iron snow and seemed to be metabolically active. This will be accomplished in the near future by obtaining the metagenomic information of iron snow and re-matching the two meta-omics datasets. Fascinating outcomes are expected.

2.1 Chemoautotrophic Fe(II) Oxidizers

Chemoautotrophy is of crucial importance in AMD-impacted environments, since it is often the major form of primary production. Most autotrophic acidophiles obtain all of their carbon from the fixation of carbon dioxide via the Calvin-Benson-Bassham cycle (Johnson and Hallberg, 2009). This requires the enzyme ribulose 1,5-biphosphate carboxylase (RuBisCO), which is often concentrated into polyhedral organelles (carboxysomes) in order to maximize the efficiency of CO_2 uptake (Cannon *et al.*, 2003; Shively *et al.*, 1998). The energy associated with ferrous iron oxidation is relatively small. An Fe-oxidising acidophile has to oxidize 18.5 mol Fe^{2+} to assimilate 1 mol of carbon, assuming that ~ 500kJ of energy are required to fix this much carbon at 100% efficiency (Silverman and Lundgren, 1959). Efficiency values of 3-30% have been recorded, and it is therefore evident that Fe(II)-oxidising microorganisms must oxidize large amounts of iron in order to fix sufficient carbon

for growth. However, this is balanced by the fact that there is often an abundance of ferrous iron in many acid environments.

Acidimicrobium ferrooxidans belongs to the phylum *Actinobacteria* and was present in high cell numbers in iron snow (Figure 6.2 and chapter 4). Members of this species are acidophilic, Fe(II)-oxidizing organisms and have been isolated or identified molecularly from warm, acidic, iron-, sulphur-, or mineral-sulfide-rich environments (Clark and Norris, 1996; Clum *et al.*, 2009; Rowe *et al.*, 2007). Little is known about CO_2 fixation of *Am. ferrooxidans*, however, the expression of carboxysome shell proteins of *Am. ferrooxidans*

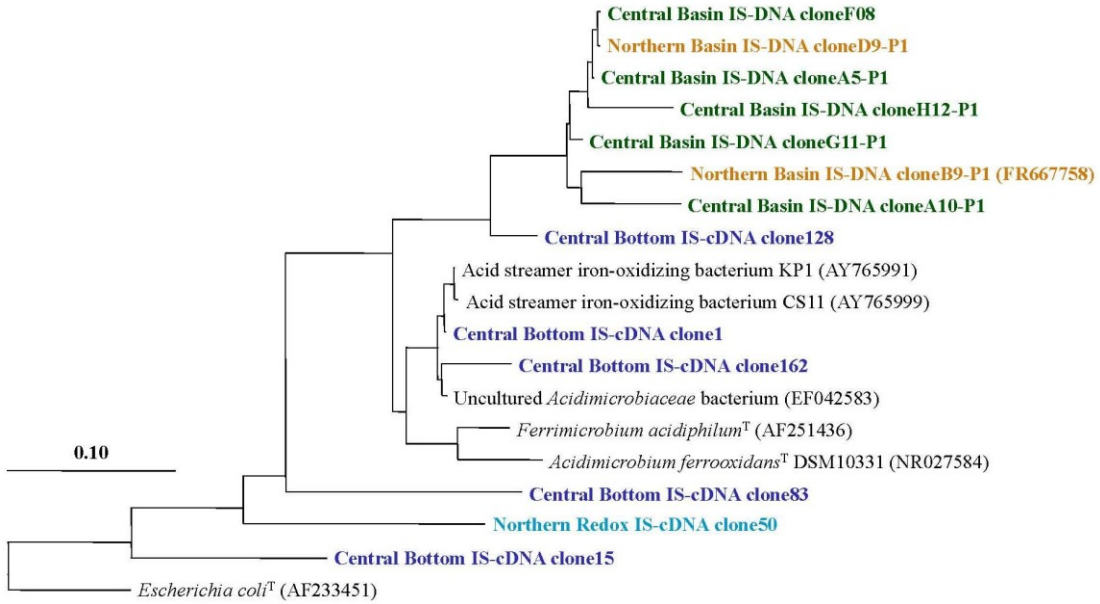

Figure 6.2. Phylogenetic tree of *Actinobacteria* 16S rRNA gene sequences obtained from iron snow samples of the central and northern basins. Sequences obtained from DNA of chapter 3 of this thesis are in green and orange and those obtained from cDNA samples of chapter 4 are in blue and turquoise. The *Gammaproteobacterium Escherichia coli* (AF233451) is used as an out-group. Scale bar indicates 0.1 change per nucleotide position and the type strains are marked with a superscript letter T.

indicate its active *in situ* metabolic function of CO_2 fixation. As one of the dominant groups in Lake 77 with CO_2 fixation capacity, *Am. ferrooxidans* seemed to be one of the main contributors to the lake primary production. Further studies of its metabolic pathways will help to improve our understanding about its ecological role in acidic environments.

Similar to *Am. ferrooxidans*, another acidophilic, obligate autotrophic bacterium *Ferrovum myxofaciens* was also one of the most prominent species in the iron snow (Figure 6.3) and it uses Fe(II) solely as an energy source (Rowe and Johnson, 2008). The *Ferrovum*-

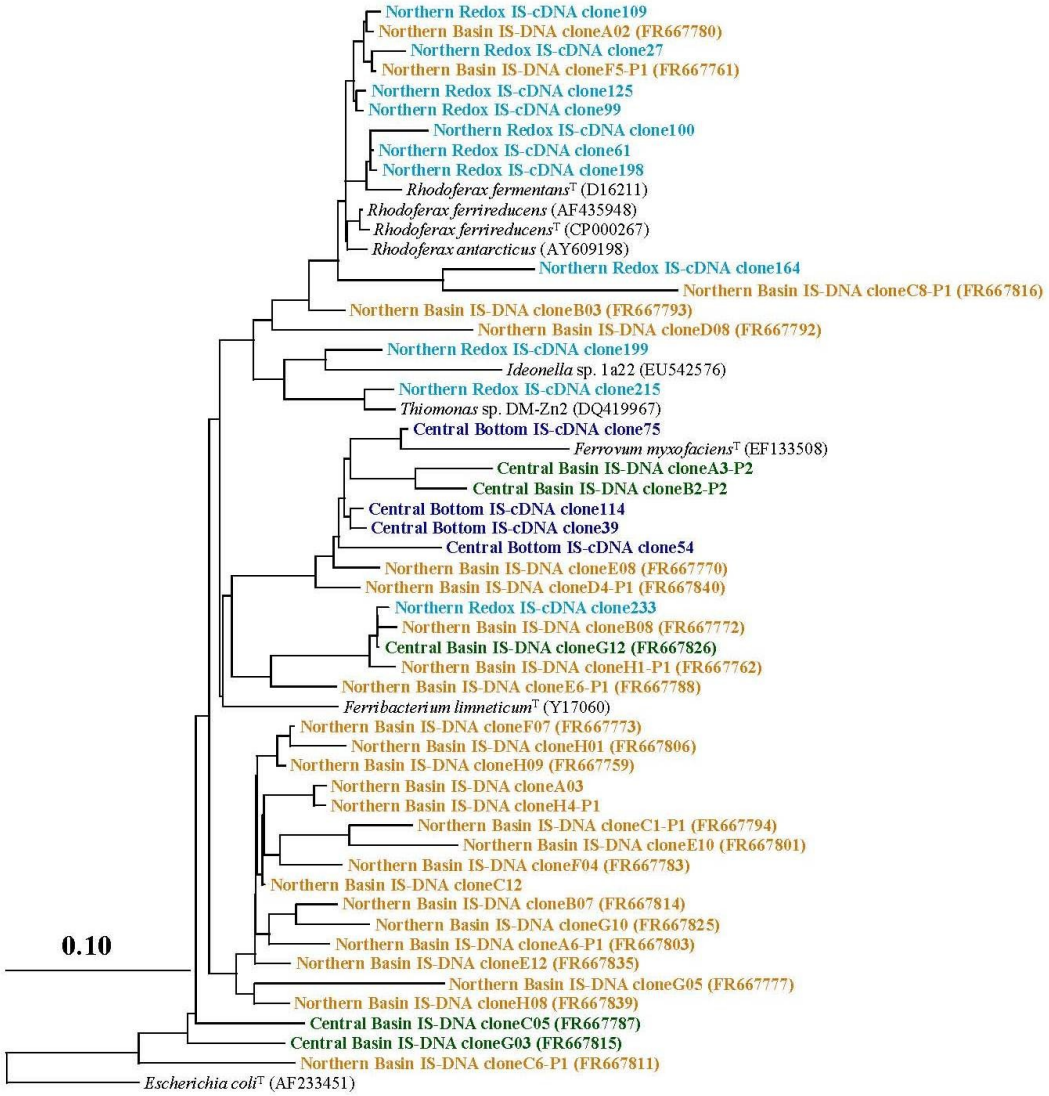

Figure 6.3. Phylogenetic tree of selective *Betaproteobacteria* 16S rRNA gene sequences obtained from iron snow samples of the central and northern basins. Sequences obtained from DNA of chapter 3 of this thesis are in green and orange and those obtained from cDNA samples of chapter 4 are in blue and turquoise. The *Gammaproteobacterium Escherichia coli* (AF233451) is used as an out-group. Scale bar indicates 0.1 change per nucleotide position and the type strains are marked with a superscript letter T.

related bacteria have also been found to dominate another AMD site (Brown *et al.*, 2011) and pilot plants for the treatment of acid mine waters (Heinzel *et al.*, 2009). *Fv. myxofaciens,* known for its copious quantities of excreted exopolysaccharides (Hallberg, 2010), might

serve as a nucleation site for the precipitation of schwertmannite as the dominant Fe-mineral. However, cells of *Ferrovum* are not found to be encrusted by the biogenic Fe-minerals; the lack of encrustation will be advantageous since the cells are still able to contact Fe(II) and proceed with oxidation (Hedrich *et al.*, 2011). Due to the lack of genomic information of *Ferrovum*-related species, no protein was able to be identified in this study using the metaproteomics approach which required an intact genome as a database for peptide mapping. Nevertheless, according to its population abundance in iron snow sample, we believed that the peptide signals from *Ferrovum*-related proteins were certainly detected and recorded by the advanced mass spectrometer. Once the *Ferrovum* genome is published or the metagenomic information of the iron snow is available, we will be able to re-map the mass spectrum and elucidate the role of *Ferrovum*.

The green sulfur bacterium *Chlorobium ferrooxidans* and related clones had been detected in low frequency in all iron snow samples from various sampling times and locations. A number of proteins from *Cb. ferrooxidans* and other *Chlorobium* strains had also been identified, including light-harvesting and energy-transforming chromophore bacteriochlorophyll (BChl) *c* binding proteins. The neutrophilic *Cb. ferrooxidans* strain KoFox is able to oxidize Fe(II) (Heising *et al.*, 1999), even in the presence of low light saturation (Hegler *et al.*, 2008). We suspected that the acid-tolerant relatives of *Cb. ferrooxidans* may exist in the mine lake and function as active primary producers.

The *Sideroxydans*-related clones were highly abundant DNA-based clone library of the northern basin iron snow but not the central basin. Closely related clones of this group have been recognized from a number of pH-neutral to moderately acidic soils and sediments (Emerson and Moyer, 1997; Lüdecke *et al.*, 2010; Weiss *et al.*, 2007). Isolated species of this genus are microaerophiles that use Fe(II) as energy for chemolithotrophic growth with CO_2 as the sole carbon source (Emerson and Moyer, 1997). However, in the following RNA-based research, clones from this group could not be found and only one protein (chaperonin GroEL,

YP_003522816) was identified using metaproteomic approaches. Collectively, we concluded that this group of Fe(II)-oxidizing bacteria were the active key player forming iron snow in Lake 77, despite its existence.

Autotrophic Fe(II) oxidizers *Acidithiobacillus* (Figure 6.4) and *Thiobacillus* were less abundant in iron snow. Occasionally, a few related clones were detected. However, their carboxysome shell proteins were found in the northern basin iron snow samples, which highlight these two groups as minor primary producers in Lake 77. Genomic analysis showed

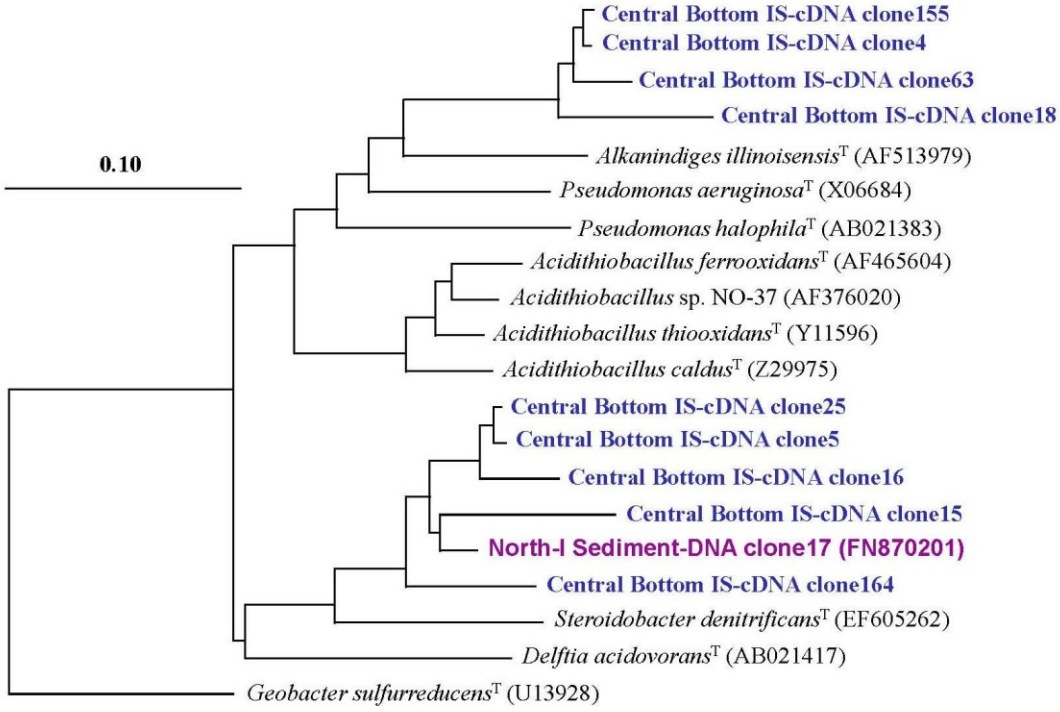

Figure 6.4. Phylogenetic tree of selective *Gammaproteobacteria* 16S rRNA gene sequences obtained from iron snow samples of the central and northern basins. Sequences obtained from cDNA samples of chapter 4 are in blue and turquoise and the sequences retrieved from sediment samples of chapter 2 are in purple. The *Deltaproteobacterium Geobacter sulfurreducens* (U13928) is used as an out-group. Scale bar indicates 0.1 change per nucleotide position and the type strains are marked with a superscript letter T.

that clusters of carboxysome genes in *Acidithiobacillus* spp. and *Tb. denitrificans* were closely associated to RuBisCO-related genes, mostly in identical operons (Cannon *et al.*, 2003; Esparza *et al.*, 2010; Gale and Beck, 1967; Suzuki and Werkman, 1958; Valdés *et al.*, 2008; Yeates *et al.*, 2008), which indicated active *in situ* CO_2 fixation. The carboxysome

shell proteins and RuBisCO related proteins have also been detected in arsenic-rich AMD sediments *Thiomonas* sp. and *Acidithiobacillus* sp. (Bertin *et al.*, 2011).

2.2 Dissimilatory Fe(III) Reducers

There were a number of Fe(III) reducer-related groups found in the iron snow samples. The acidophilic Fe(III) reducer *Acidiphilium*-related group (*Alphaproteobacteria*) (Figure 6.5) were detected in abundance of each iron snow sample from both the central and northern

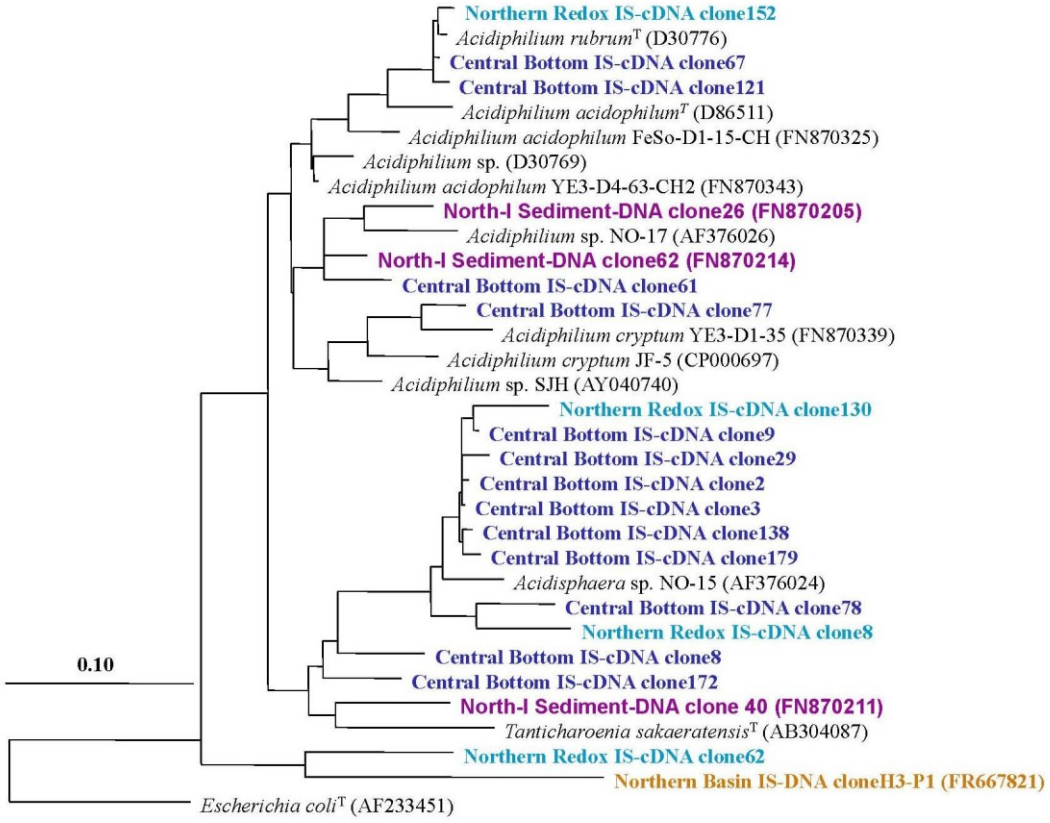

Figure 6.5. Phylogenetic tree of selective *Alphaproteobacteria* 16S rRNA gene sequences obtained from iron snow samples of the central and northern basins. Sequences obtained from DNA of chapter 3 of this thesis are in orange and those obtained from cDNA samples of chapter 4 are in blue and turquoise. The sequences retrieved from sediment samples of chapter 2 are in purple. The *Gammaproteobacterium Escherichia coli* (AF233451) is used as an out-group. Scale bar indicates 0.1 change per nucleotide position and the type strains are marked with a superscript letter T.

basins. Most of the members of *Acidiphilium* are obligate heterotrophs with the single exception of *A. acidophilum*. They are acidophilic (can grow in pH <2) and are capable of

ferric iron reduction (Coupland and Johnson, 2008; Johnson and McGinness, 1991; Küsel *et al.*, 1999). *Acidiphilium* strains were very active in reducing schwertmannite compared to any other reducing bacteria from Lake 77 (data not shown). The analysis of 16S rRNA gene sequences suggests that there are two separate sub-groups within the genus containing *A. cryptum* (the first described species) (Harrison, 1981): *A. organovorum*, *A. multivorum* and isolate SJH in the first sub-group, and *A. rubrum*, *A. angustum* and *A. acidophilium* in the second sub-group (Figure 6.5). In iron snow, *Acidiphilium*-related clones were detected from both groups. However, clones of RNA-derived libraries belonged to the second sub-group. Very little is known about the enzymology of this acidophilic Fe(III) reducer. Metaproteomics analysis highlighted several proteins which might be involved in the electron transfer chain of *Acidiphilium*: OmpA/MotB domain protein, TonB-dependent receptor and cytochrome *c* class I (ApcA) as discussed in chapter 4 of this thesis. Among these proteins, ApcA had the highest probability to be involved in the acidic Fe(III) reduction, partially because purified and reduced ApcA from *A. cryptum* JF-5 can reduce chromate at low pH (Magnuson *et al.*, 2010). A comparative genome analysis of ApcA and related genes from various published *Acidiphilium* genomes, together with lab-based molecular experiments, will be helpful to understand the mechanism of acidic dissimilatory Fe(III) reduction. One thing is for sure that this mechanism is quite different from those under pH-neutral conditions where ApcAs are essential electron transfer proteins composed of respiratory chains for reducing electron acceptors like Fe(III) or hexavalent chromium in the neutrophilic *Shewanella oneidensis* and *Geobacter sulfurreducens* (Qian *et al.*, 2011; Richter *et al.*, 2012; Shi *et al.*, 2011).

The neutrophilic Fe(III) reducer *Rhodoferax*-like group composed of up to 15% of total bacterial gene copy number in the northern basin samples using qPCR (Figure 6.3) but in very low frequency in the central basin. *Albidiferax ferrireducens* (former *Rhodoferax ferrireducens*) is a metabolically versatile microorganism that likely plays an important role

in subsurface carbon and metal cycles (Finneran *et al.*, 2003; Risso *et al.*, 2009) and has only incomplete pathways associated with CO_2 fixation in its genome (Risso *et al.*, 2009), which is different from other autotrophic *Rhodoferax* species. The *Rhodoferax*-like group we detected was on a different branch than other known *Rhodoferax* (*Albidiferax*) on the phylogenetic tree and it might represent a novel acidophilic or acid-tolerant sub-group. Proteins detected in chapter 4 had no relationship with known CO_2 fixation pathways or electron transfer chains. Whether this sub-group contained a complete CO_2 fixation pathway and/or was able to reduce Fe(III) remained unclear. However, our research had brought attention to this phylogenetic group of bacteria that functions at acidic conditions.

Similar to the *Rhodoferax*-like group, Fe(III)-reducing *Geobacter*-like group was less abundant in the central basin but was one of the next most abundant and frequently detected groups in the northern basin (Figure 6.6). Proteins identified referred mostly to ATP synthase, the translation elongation factor Tu, shock-related and various other chaperones, but none that were known to be associated with the electron transfer chain of *Geobacter* species. It remained unclear if these organisms actively participate in the reduction of Fe(III).

Ferroplasma was one of the few *Archaea* species detected from the iron snow. The finding of NADH-ubiquinone oxidoreductase, one of the key enzymes in the electron transport chain during Fe oxidation and reduction of *Ferroplasma* (Dopson *et al.*, 2005), suggested that *Ferroplasma* sp. participated in Fe-cycling in the iron snow, which had broadened our knowledge of microbial Fe-cycling in Lake 77.

Clear differences of microbial communities between sampling locations could be discerned: In the northern basin where the pH in the deepest water was higher, neutrophilic-related Fe-cycling microorganisms such as *Geobacter*, *Albidiferax* (*Rhodoferax*) and *Sideroxydans* were typically abundant, while in the central basin acidophiles as *Ferrovum*, *Acidimicrobium* and *Acidiphilium* were more dominant. This indicated that pH might be a major driving force shaping the microbial communities. Thus, despite their similar Fe(III)

mineral composition, iron snow from central and northern basin might be of different biogetic origins from various Fe(II) oxidizers thriving in the transition zone of Lake 77.

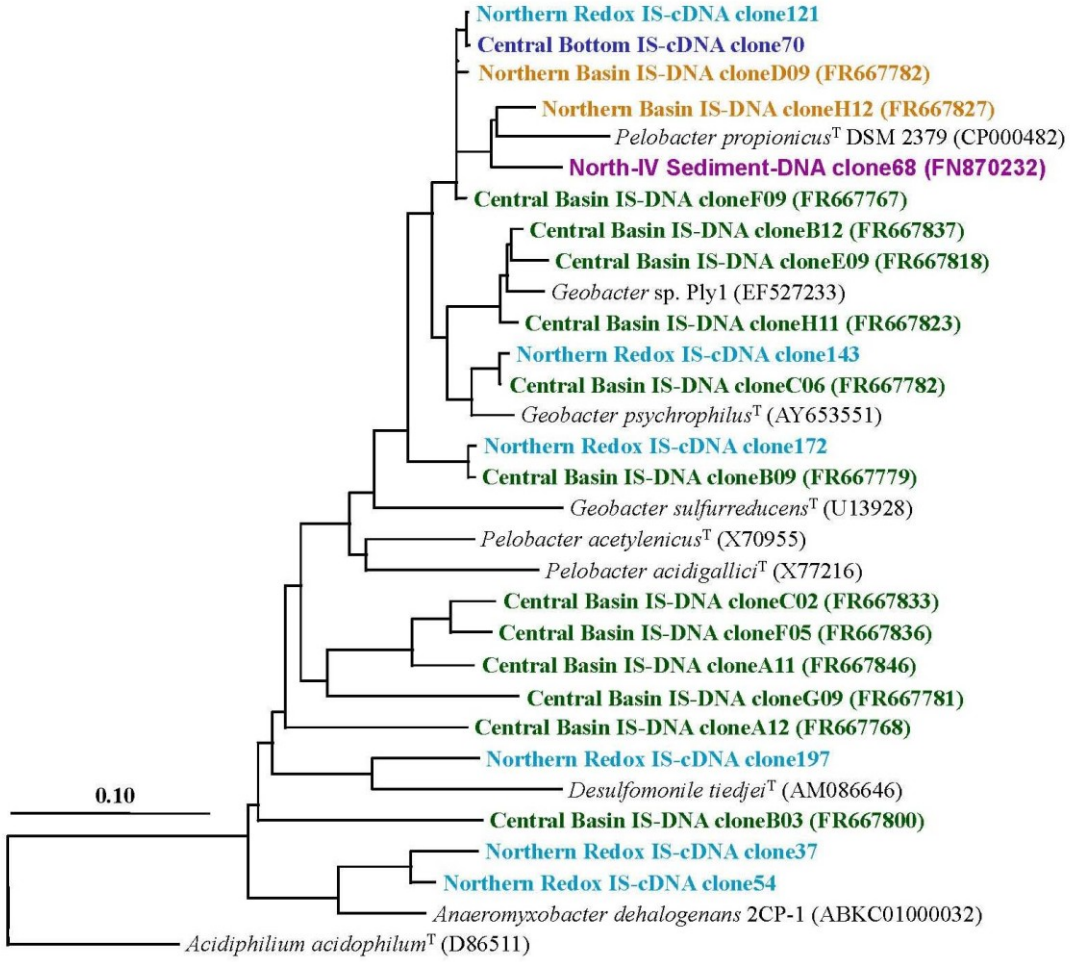

Figure 6.6. Phylogenetic tree of selective *Deltaproteobacteria* 16S rRNA gene sequences obtained from iron snow samples of the central and northern basins. Sequences obtained from DNA of chapter 3 of this thesis are in green and orange and those obtained from cDNA samples of chapter 4 are in blue and turquoise. The sequences retrieved from sediment samples of chapter 2 are in purple. The *Alphaproteobacterium Acidiphilium acidophilum* (D86511) is used as an out-group. Scale bar indicates 0.1 change per nucleotide position and the type strains are marked with a superscript letter T.

2.3 Developmental Stages of Iron Snow

The high iron snow sedimentation rates observed in Lake 77 linked the redoxcline strongly to the sediment by providing a rapid removal mechanism of not only iron and organic carbon, but also living microorganisms from the water column to the sediment. Nucleic acid-based 16S rRNA clone libraries and qPCR results showed that iron snow was dominated mainly by

active Fe-cycling microorganisms, thus functioned as hotspots for the cycling of iron. Moreover, proteins related to motility, gas vesicles, CO_2-fixing *et al.* had revealed other complex metabolic activities within these complex pelagic aggregates. Based on the research within this thesis, a comprehensive model of iron snow development was suggested (Figure 6.7) as in chapter 4. In brief:

First, in the redoxcline where Fe(II) met oxygen, mainly acidophilic autotrophic

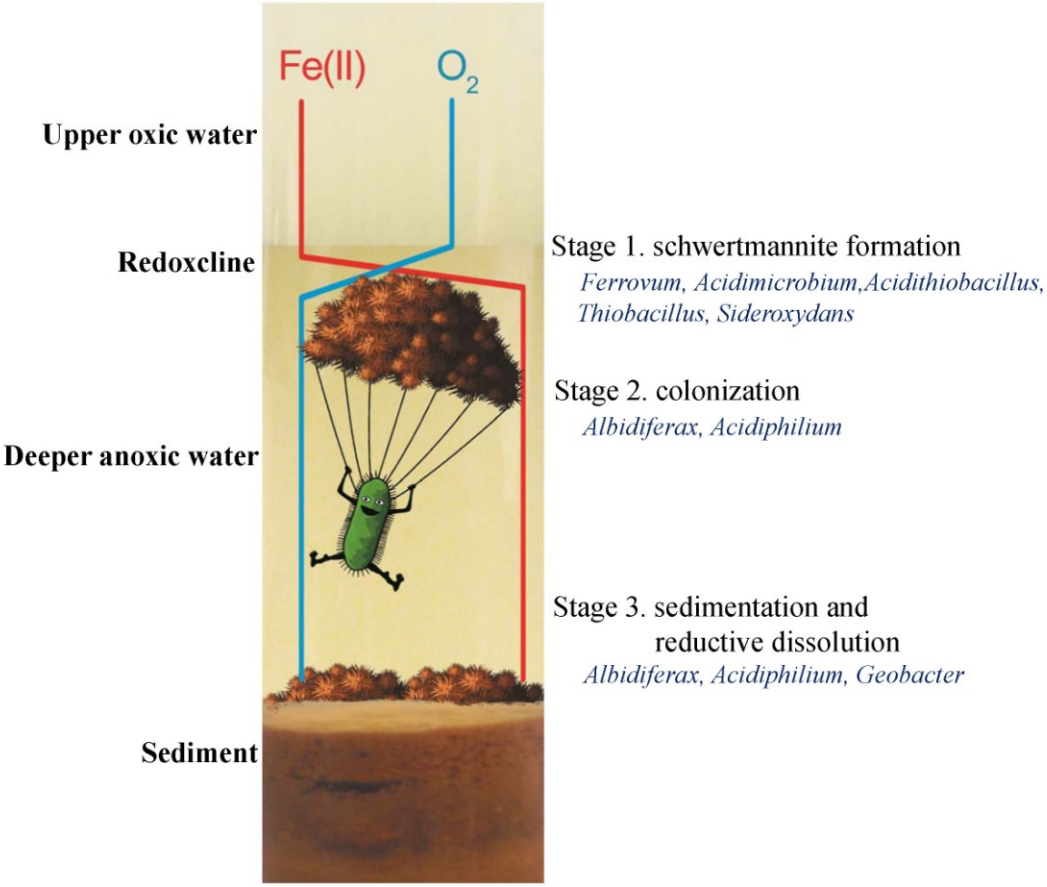

Figure 6.7. Schematic of iron snow development stages and the main active Fe-cycling microorganisms.

Fe(II) oxidizing microorganisms such as *Ferrovum, Acidimicrobium Acidithiobacillus*, and *Thiobacillus* were likely to be responsible for the initial step of Fe(II) oxidation, together with a small population of neutrophilic *Sideroxydans*. Chemolithoautotrophy was likely advantageous in this lake where light penetration was limited by high amounts of iron aggregates in the water column. This was supported by the detection of CO_2-fixation related microcompartment proteins from *Acidimicrobium*, *Acidithiobacillus* and *Thiobacillus*.

As the minerals grew bigger, in the second stage, some of the bacteria might be incorporated into the Fe(III)-oxide aggregates. Subsequently more microbes approached and inhabited the iron snow as the iron snow may provide autotrophically fixed carbon for those heterotrophs, such as *Acidiphilium*. Flagellar-containing heterotrophs were likely the first colonizers of iron minerals. Due to its high specific surface area, iron snow could easily provide reactive Fe(III) as an electron acceptor for anaerobic microbial respiration during and after sedimentation in the deeper anoxic water layers (third stage), as well as acted as a transport vector to bring iron, organic carbon and living microorganisms from the water column to the lake sediment. Iron minerals would then start to be reductively dissolved by the abundant Fe(III) reducers, e.g., *Acidiphilium*, *Albidiferax* and *Geobacter*, coupled with the oxidation of organic matter.

3. From Iron Snow to Sediment

Freshly formed iron snow, including not only iron minerals and organic carbon but also living microorganisms from the water column, settled down at high sedimentation velocity from the redoxcline to the lake bottom as top sediment material. Over time it was buried as deeper sediment material. The formation of the Fe(III) minerals and dominant microbial communities would all change accordingly (Blöthe *et al.*, 2008; Peine, 1998). The deeper layers of the sediment were also affected by the inflow of the underground water coming from the mine dump area at the north end of the lake.

Similar DGGE patterns were obtained from iron snow and sediment surface at the same locations, suggesting closely-related microbial communities (See chapter 3 and 5). However, the differences between the central and northern basins were more pronounced.

Research on microbial communities of the central basin sediment reveals that the majority of the clones from the top and bottom sediments belong to the *Acidobacteria* phylum (Blöthe *et al.*, 2008). Since moderately acidophilic *Acidobacteria* species have the

ability to oxidize Fe(II) and since *Acidobacterium capsulatum* reduced Fe(III)-oxides at pH ranging from 2 to 5, this group appears to be involved in the cycling of iron. Additionally, various species of *Acidiphilium*, *Acidisphaera*, *Acidithiobacillus*, *Geobacteraceae* and *Thiomonas* are also detected and assumed to be involved in Fe-cycling (Blöthe *et al.*, 2008).

The studies on sediments from the northern shore of Lake 77 (See chapter 2) revealed a more pronounced scenario. In the top acidic layer, Fe(II) oxidizers, such as *Leptospirillum*, *Ferrimicrobium* and *Dyella*-like-genus, and Fe(III) reducers, such as *Acidiphilium* (Figure 6.5), *Acidocella* and *Acidobacteriaceae* were detected. While in the bottom layer where the pH was above 5, *Acidobacteriaceae* and *Geobacteraceae* (Figure 6.6) were the dominant groups. The bacteria clone libraries generally supported and complemented isolation patterns. However, the fact that *Alicyclobacillus* and *Acidithiobacillus* could be isolated in large numbers from lake sediments but not be detected using molecular methods confirmed what we had learned from iron snow story that these two groups might not be the major players in the whole Lake 77 ecosystem. Many of the isolates obtained from the sediments were able to oxidize Fe(II) or/and reduce synthetic schwertmannite (See chapter 2) and preferred microoxic conditions for Fe(III) reduction. These Fe-cycling bacteria were affiliated with the *Dyella*-like genus, *Acidithiobacillus*, *Bacillus*, *Alicyclobacillus*, *Acidocella* and *Acidiphilium* and some of them showed a broad pH tolerance, ranging from 2.5 to 5.0, and preferred schwertmannite to goethite for Fe(III) reduction. Chelated forms of Fe(III), e.g., ferric citrate and ferric pyrophosphate, were not reduced during 14 days. Using the O-CAS assay (Pérez-Miranda *et al.*, 2007), two of the isolated *Alicyclobacillus* strains (growth pH from 2 to 6) were reacted as “positive” against the reagent which indicated siderophore-producing capacities. The *Alicyclobacillus acidocaldarius* Strain DSM 446 was detected containing pathways of biosynthesis of various siderophores based on its genome sequence (http://www.biocyc.org/AACI521098/NEW-IMAGE?object=Siderophores-Biosynthesis). However, our isolates were novel compared the type strain with about 94% 16S rRNA gene

similarity and were both acidic Fe(II) oxidizing bacteria. It will be interesting to detect their siderophore-related genes and to study how these iron-chelating compounds function in a soluble Fe(II)-rich environment.

4. Conclusions and Verification of Hypotheses

The water body of the acidic lignite mine Lake 77 was separated by a bank on the bottom of the lake, forming two basins differing in stratification patterns and pelagic boundary conditions. The central basin exhibited a dimictic water regime while the northern basin was meromictic with stratification remaining over many years. The water pH of an anoxic monimolimnion could reach as high as 5.9 in the northern basin while it remained around 3 throughout the whole water body in the central basin. In the redoxcline, acidophilic autotrophic Fe(II) oxidizing microorganisms initialized the first step of iron snow formation and served also as primary producers, followed by other heterotrophic microbes including Fe(III) reducers which started to colonize the iron snow during the sedimentation process. Fe-cycling microorganisms were abundant in the iron snow and sediment communities with several phylogenetic groups highlighted as main active oxidizers: *Ferrovum*, *Acidimicrobium*, *Acidithiobacillus, Thiobacillus*, and reducers: *Acidiphilium*, *Albidiferax (Rhodoferax)* and *Geobacter*. Comparisons of results obtained from iron snow and sediments from the central and northern basins suggested that pH is a major driving force to shape the microbial communities responsible for Fe-cycling in both basins.

The results of microbial community analyses and bacterial isolates from lake sediments in chapter 2 supported hypothesis I and the bio-geo-ecological relevancy of acidic Fe-cycling bacteria was discussed in detail. The iron snow was studied in chapters 2, 4 and 5 using a polyphasic approach for its geochemical characteristics, mineral composition and also their microbial communities and complex metabolic functions. The results addressed hypotheses II to IV.

References

Baker BJ, Banfield JF. (2003). Microbial communities in acid mine drainage. *FEMS Microbiol Ecol* **44:** 139-152.

Belnap CP, Pan C, VerBerkmoes NC, Power ME, Samatova NF, Carver RL *et al*. (2010). Cultivation and quantitative proteomic analyses of acidophilic microbial communities. *ISME J* **4:** 520-530.

Bertin PN, Heinrich-Salmeron A, Pelletier E, Goulhen-Chollet F, Arsene-Ploetze F, Gallien S *et al*. (2011). Metabolic diversity among main microorganisms inside an arsenic-rich ecosystem revealed by meta- and proteo-genomics. *ISME J* **5:** 1735-47.

Bigham JM, Carlson L, Murad E. (1994). Schwertmannite, a new iron oxyhydroxysulphate from Pyhasalmi, Finland, and other localities. *Mineral Mag* **58:** 641-648.

Blodau C. (2005). Groundwater inflow controls acidity fluxes in an iron rich and acidic lake. *Acta Hydrochim Hydrobiol* **33:** 104-117.

Blodau C. (2006). A review of acidity generation and consumption in acidic coal mine lakes and their watersheds. *Sci Total Environ* **369:** 307-332.

Blodau C, Hoffmann S, Peine A, Peiffer S. (1998). Iron and sulfate reduction in the sediments of acidic mine lake 116 (Brandenburg, Germany): Rates and geochemical evaluation. *Water Air Soil Pollut* **108:** 249-270.

Blöthe M, Akob DM, Kostka JE, Goschel K, Drake HL, Küsel K. (2008). pH gradient-induced heterogeneity of Fe(III)-reducing microorganisms in coal mining-associated lake sediments. *Appl Environ Microbiol* **74:** 1019-1029.

Blowes DW, Ptacek CJ, Jambor JL, Weisener CG. (2003). *The geochemistry of acid mine drainage*. In: Heinrich DH and Turekian KK (eds). *Treatise on Geochemistry*. Pergamon: Oxford. pp 149-204.

Boehrer B, Schultze M. (2006). *7th International conference on acid rock drainage (ICARD)*. Barnhisel RI (ed.). The American Society of Mining and Reclamation (ASMR): St. Louis MO, pp 200-213.

Boyd P, Ellwood M. (2010). The biogeochemical cycle of iron in the ocean. *Nat Geosci* **3:** 675-682.

Brown JF, Jones DS, Mills DB, Macalady JL, Burgos WD. (2011). Application of a depositional facies model to an acid mine drainage site. *Appl Environ Microbiol* **77:** 545-554.

Cannon GC, Baker SH, Soyer F, Johnson DR, Bradburne CE, Mehlman JL *et al*. (2003). Organization of carboxysome genes in the thiobacilli. *Curr Microbiol* **46:** 115-119.

Cárdenas JP, Valdes J, Quatrini R, Duarte F, Holmes DS. (2010). Lessons from the genomes of extremely acidophilic bacteria and archaea with special emphasis on bioleaching microorganisms. *Appl Microbiol Biotechnol* **88:** 605-620.

Clark DA, Norris PR. (1996). *Acidimicrobium ferrooxidans* gen nov, sp nov: Mixed-culture ferrous iron oxidation with *Sulfobacillus* species. *Microbiology* **142:** 785-790.

Clum A, Nolan M, Lang E, Del Rio TG, Tice H, Copeland A *et al*. (2009). Complete genome sequence of *Acidimicrobium ferrooxidans* type strain (ICP^{T}). *Standards in Genomic Sciences* **1:** 38-45.

Colmer AR, Hinkle M. (1947). The role of microorganisms in acid mine drainage: a preliminary report. *Science* **106:** 253-256.

Cornell RM, Schwertmann U. (2003). *The iron oxides: Structure, properties, reactions, occurrences and uses*, 2nd edn. Wiley-VCH Verlagsgesellschaft: Weinheim, Germany.

Coupland K, Johnson DB. (2008). Evidence that the potential for dissimilatory ferric iron reduction is widespread among acidophilic heterotrophic bacteria. *FEMS Microbiol Lett* **279:** 30-35.

Davis RA, Welty AT, Borrego J, Morales JA, Pendon JG, Ryan JG. (2000). Rio Tinto estuary (Spain): 5000 years of pollution. *Environ Geol* **39:** 1107-1116.

Davison W. (1993). Iron and manganese in lakes. *Earth-Sci Rev* **34:** 119-163.

Dopson M, Baker-Austin C, Bond PL. (2005). Analysis of differential protein expression during growth states of *Ferroplasma* strains and insights into electron transport for iron oxidation. *Microbiology-Sgm* **151:** 4127-4137.

Druschel GK, Baker BJ, Gihring TM, Banfield JF. (2004). Acid mine drainage biogeochemistry at Iron Mountain, California. *Geochem Trans* **5:** 13-32.

Eglinton TI. (2012). Geochemistry: A rusty carbon sink. *Nature* **483:** 165-166.

Emerson D, Moyer C. (1997). Isolation and characterization of novel iron-oxidizing bacteria that grow at circumneutral pH. *Appl Environ Microbiol* **63:** 4784-4792.

Esparza M, Cardenas JP, Bowien B, Jedlicki E, Holmes DS. (2010). Genes and pathways for CO_2 fixation in the obligate, chemolithoautotrophic acidophile, *Acidithiobacillus ferrooxidans*, carbon fixation in *A. ferrooxidans*. *BMC Microbiol* **10:** 15.

Eusterhues K, Wagner FE, Hausler W, Hanzlik M, Knicker H, Totsche KU *et al*. (2008). Characterization of ferrihydrite-soil organic matter coprecipitates by X-ray diffraction and mossbauer spectroscopy. *Environ Sci Technol* **42:** 7891-7897.

Finneran KT, Johnsen CV, Lovley DR. (2003). *Rhodoferax ferrireducens* sp. nov., a psychrotolerant, facultatively anaerobic bacterium that oxidizes acetate with the reduction of Fe(III). *Int J Syst Evol Microbiol* **53:** 669-673.

Friese K, Wendt-Potthoff K, Zachmann D, Fauville A, Mayer B, Veizer J. (1998). Biogeochemistry of iron and sulfur in sediments of an acidic mining lake in Lusatia, Germany. *Water Air Soil Pollut* **108:** 231-247.

Gale NL, Beck JV. (1967). Evidence for the Calvin cycle and hexose monophosphate pathway in *Thiobacillus ferrooxidans*. *J Bacteriol* **94:** 1052-1059.

Geller W, Klapper H, Schultze M. (1998). *Natural and anthropogenic sulforic acidification of lakes*. In: Geller W, Klapper H and Salomons W (eds). *Acid mining lakes: Acide mine drainage, Limnology and Reclamation*. Springer: Berlin, Germany. pp 3-14.

Gerhardt A, Janssens de Bisthoven L, Soares A. (2004). Macroinvertebrate response to acid mine drainage: community metrics and on-line behavioural toxicity bioassay. *Environ Pollut* **130:** 263-274.

Grossart HP, Ploug H. (2000). Bacterial production and growth efficiencies: direct measurements on riverine aggregates. *Limnol Oceanogr* **45:** 436-445.

Grossart HP, Simon M. (1993). Limnetic macroscopic organic aggregates (lake snow) - Occurrence, characteristics, and microbial dynamics in Lake Constanse. *Limnol Oceanogr* **38:** 532-546.

Hallberg KB. (2010). New perspectives in acid mine drainage microbiology. *Hydrometallurgy* **104:** 448-453.

Harrison AP. (1981). *Acidiphilium cryptum* gen. nov., nov., heterotrophic bacterium from acidic mineral environments. *International Journal of Systematic Bacteriology* **31:** 327-332.

Hedrich S, Lunsdorf H, Keeberg R, Heide G, Seifert J, Schlomann M. (2011). Schwertmannite Formation Adjacent to Bacterial Cells in a Mine Water Treatment Plant and in Pure Cultures of *Ferrovum myxofaciens*. *Environ Sci Technol* **45:** 7685-7692.

Hegler F, Posth NR, Jiang J, Kappler A. (2008). Physiology of phototrophic iron(II)-oxidizing bacteria: implications for modern and ancient environments. *FEMS Microbiol Ecol* **66:** 250-260.

Heinzel E, Janneck E, Glombitza F, Schlomann M, Seifert J. (2009). Population dynamics of iron-oxidizing communities in pilot plants for the treatment of acid mine waters. *Environ Sci Technol* **43:** 6138-6144.

Heising S, Richter L, Ludwig W, Schink B. (1999). *Chlorobium ferrooxidans* sp. nov., a phototrophic green sulfur bacterium that oxidizes ferrous iron in coculture with a "*Geospirillum*" sp. strain. *Arch Microbiol* **172:** 116-124.

Hill B, Willingham W, Parrish L, McFarland B. (2000). Periphyton community responses to elevated metal concentrations in a Rocky Mountain stream. *Hydrobiologia* **428:** 161-169.

Hoffert JR. (1947). Acid mine drainage. *Ind Eng Chem* **39:** 642-646.

Johnson DB. (1995). Acidophilic microbial communities: candidates for bioremediation of acidic mine effluents. *Int Biodeterior Biodegrad* **35:** 41-58.

Johnson DB. (2009). *Extremophiles (overview): acid environments*. In: Schaechter M (ed). *The desk encyclopedia of microbiology*, 2nd edn. Academic Press: Oxford. pp 463-482.

Johnson DB, Hallberg KB. (2009). Carbon, iron and sulfur metabolism in acidophilic micro-organisms. *Adv Microb Physiol* **54:** 201-255.

Johnson DB, McGinness S. (1991). Ferric iron reduction by acidophilic heterotrophic bacteria. *Appl Environ Microbiol* **57:** 207-211.

Jönsson J, Jönsson L, Lövgren L. (2006). Precipitation of secondary Fe (III) minerals from acid mine drainage. *Appl Geochem* **21:** 437-445.

Kappler A, Straub KL. (2005). Geomicrobiological cycling of iron. *Rev Mineral Geochem* **59:** 85-108.

Karakas G, Brookland I, Boehrer B. (2003). Physical characteristics of acidic mining Lake 111. *Aquat Sci* **65:** 297-307.

Klapper H, Schultze M. (1995). Geogenically acidified mining lakes- living conditions and possibilities of restoration. *Int Rev Hydrobiol* **80:** 639-653.

Küsel K. (2003). Microbial cycling of iron and sulfur in acidic coal mining lake sediments. *Water Air Soil Pollut: Focus* **3:** 67-90.

Küsel K, Dorsch T. (2000). Effect of supplemental electron donors on the microbial reduction of Fe(III), sulfate, and CO_2 in coal mining-impacted freshwater lake sediments. *Microb Ecol* **40:** 238-249.

Küsel K, Dorsch T, Acker G, Stackebrandt E. (1999). Microbial reduction of Fe(III) in acidic sediments: Isolation of *Acidiphilium cryptum* JF-5 capable of coupling the reduction of Fe(III) to the oxidation of glucose. *Appl Environ Microbiol* **65:** 3633-3640.

Küsel K, Roth U, Drake HL. (2002). Microbial reduction of Fe(III) in the presence of oxygen under low pH conditions. *Environ Microbiol* **4:** 414-421.

Lo I, Denef VJ, VerBerkmoes NC, Shah MB, Goltsman D, DiBartolo G *et al*. (2007). Strain-resolved community proteomics reveals recombining genomes of acidophilic bacteria. *Nature* **446:** 537-541.

Lovley DR. (2006). *Dissimilatory Fe (III)-and Mn (IV)-reducing prokaryotes*. In: Dworkin M (ed). *The Prokaryotes*, 3rd edn. Springer: New York, NY. pp 635-658.

Lüdecke C, Reiche M, Eusterhues K, Küsel K. (2010). Microorganisms involved in iron cycling at the oxic-anoxic interface in an acidic fen. *Environ Microbiol*.

Lundgren D, Silver M. (1980). Ore leaching by bacteria. *Annu Rev Microbiol* **34:** 263-283.

Magnuson TS, Swenson MW, Paszczynski AJ, Deobald LA, Kerk D, Cummings DE. (2010). Proteogenomic and functional analysis of chromate reduction in *Acidiphilium cryptum* JF-5, an Fe(III)-respiring acidophile. *Biometals* **23:** 1129-1138.

Markowitz VM, Chen IMA, Palaniappan K, Chu K, Szeto E, Grechkin Y *et al*. (2009). The integrated microbial genomes system: an expanding comparative analysis resource. *Nucleic Acids Res* **38:** D382-D390.

Meruane G, Vargas T. (2003). Bacterial oxidation of ferrous iron by *Acidithiobacillus ferrooxidans* in the pH range 2.5-7.0. *Hydrometallurgy* **71:** 149-158.

Moses CO, Kirk Nordstrom D, Herman JS, Mills AL. (1987). Aqueous pyrite oxidation by dissolved oxygen and by ferric iron. *Geochim Cosmochim Acta* **51:** 1561-1571.

Murad E, Rojik P. (2005). Iron mineralogy of mine-drainage precipitates as environmental indicators: Review of current concepts and a case study from the Sokolov Basin, Czech Republic. *Clay Minerals* **40:** 427-440.

Neu TR. (2000). In situ cell and glycoconjugate distribution in river snow studied by confocal laser scanning microscopy. *Aquat Microb Ecol* **21:** 85-95.

Nixdorf B, Fyson A, Krumbeck H. (2001a). Review: Plant life in extremely acidic waters. *Environ Exp Bot* **46:** 203-211.

Nixdorf B, Hemm M, Schlundt A, Kapfer M, Krumbeck H. (2001b). *Tagebauseen in Deutschland - ein Überblick*. UBA Texte: Berlin.

Nixdorf B, Kapfer M. (1998). Stimulation of phototrophic pelagic and benthic metabolism close to sediments in acidic mining lakes. *Water Air Soil Pollut* **108:** 317-330.

Nordstrom DK. (1982). *Aqueous pyrite oxidation and the consequent formation of secondary iron minerals*. In: Hossaer LR, Kittrick JA and Famin DF (eds). *Acid sulfate weathering*. Soil Science Society of American: Madison, WI. pp 37-56.

Peine A. (1998). *Saure Restseen des Braunkohletagebaus- Charakterisierung und Quantifizierung biogeochemischer Prozesse und Abschätzung ihrer Bedeutung für die seeinterne Neutralisierung*, Ph.D. Thesis. University of Bayreuth.Bayreuth, Germany.

Peine A, Tritschler A, Küsel K, Peiffer S. (2000). Electron flow in an iron-rich acidic sediment - evidence for an acidity-driven iron cycle. *Limnol Oceanogr* **45:** 1077-1087.

Pérez-Miranda S, Cabirol N, George-Téllez R, Zamudio-Rivera LS, Fernández FJ. (2007). O-CAS, a fast and universal method for siderophore detection. *J Microbiol Methods* **70:** 127-131.

Porsch K, Meier J, Kleinsteuber S, Wendt-Potthoff K. (2009). Importance of different physiological groups of iron reducing microorganisms in an acidic mining lake remediation experiment. *Microb Ecol* **57:** 701-717.

Pronk JT, Johnson DB. (1992). Oxidation and reduction of iron by acidophilic bacteria. *Geomicrobiol J* **10:** 153-171.

Qian X, Mester T, Morgado L, Arakawa T, Sharma ML, Inoue K *et al*. (2011). Biochemical characterization of purified OmcS, a *c*-type cytochrome required for insoluble Fe(III) reduction in *Geobacter sulfurreducens*. *Biochimica Et Biophysica Acta-Bioenergetics* **1807:** 404-412.

Ram RJ, VerBerkmoes NC, Thelen MP, Tyson GW, Baker BJ, Blake RC *et al*. (2005). Community proteomics of a natural microbial biofilm. *Science* **308:** 1915-1920.

Richter K, Schicklberger M, Gescher J. (2012). Dissimilatory reduction of extracellular electron acceptors in anaerobic respiration. *Appl Environ Microbiol* **78:** 913-921.

Risso C, Sun J, Zhuang K, Mahadevan R, DeBoy R, Ismail W *et al*. (2009). Genome-scale comparison and constraint-based metabolic reconstruction of the facultative anaerobic Fe (III)-reducer *Rhodoferax ferrireducens*. *BMC Genomics* **10:** 447.

Rowe OF, Johnson DB. (2008). Comparison of ferric iron generation by different species of acidophilic bacteria immobilized in packed-bed reactors. *Syst Appl Microbiol* **31:** 68-77.

Rowe OF, Sanchez-Espana J, Hallberg KB, Johnson DB. (2007). Microbial communities and geochemical dynamics in an extremely acidic, metal-rich stream at an abandoned sulfide mine (Huelva, Spain) underpinned by two functional primary production systems. *Environ Microbiol* **9:** 1761-1771.

Schippers A, Jozsa P, Sand W. (1996). Sulfur chemistry in bacterial leaching of pyrite. *Appl Environ Microbiol* **62:** 3424-3431.

Schultze M, Geller W. (1996). *The acid lakes of lignite mining districts of the former German Democratic Republic*. In: Reuther R (ed). *Geochemical Approachs to Environmental Engineering of Metals*. Springer: Berlin. pp 89-105.

Shi L, Belchik SM, Wang Z, Kennedy DW, Dohnalkova AC, Marshall MJ *et al*. (2011). Identification and characterization of $UndA_{(HRCR-6)}$, an outer membrane endecaheme *c*-

Type cytochrome of *Shewanella* sp. strain HRCR-6. *Appl Environ Microbiol* **77:** 5521-5523.

Shively JM, van Keulen G, Meijer WG. (1998). Something from almost nothing: carbon dioxide fixation in chemoautotrophs. *Annu Rev Microbiol* **52:** 191-230.

Silver MW, Shanks AL, Trent JD. (1978). Marine snow - Microplankton habitat and source of small-scale patchiness in pelagic populations. *Science* **201:** 371-373.

Silverman MP, Lundgren DG. (1959). Studies on the chemoautotrophic iron bacterium *Ferrobacillus ferrooxidans* II. Manometric studies. *J Bacteriol* **78:** 326.

Simon M, Grossart HP, Schweitzer B, Ploug H. (2002). Microbial ecology of organic aggregates in aquatic ecosystems. *Aquat Microb Ecol* **28:** 175-211.

Singer PC, Stumm W. (1970). Acidic mine drainage: The rate-determining step. *Science* **167:** 1121-1123.

Singh B, Harris P, Wilson M. (1997). Geochemistry of acid mine waters and the role of micro-organisms in such environments. *Adv Geoecol* **30:** 159-192.

Suzuki I, Werkman C. (1958). Chemoautotrophic carbon dioxide fixation by extracts of *Thiobacillus thiooxidans*. I. Formation of oxalacetic acid. *Arch Biochem Biophys* **76:** 103-111.

Temple KL, Colmer AR. (1951). The autotrophic oxidation of iron by a new bacterium, *Thiobacillus ferrooxidans*. *J Bacteriol* **62:** 605-611.

Valdés J, Pedroso I, Quatrini R, Dodson RJ, Tettelin H, Blake R, II *et al*. (2008). *Acidithiobacillus ferrooxidans* metabolism: from genome sequence to industrial applications. *BMC Genomics* **9:** 597.

Weber KA, Achenbach LA, Coates JD. (2006). Microorganisms pumping iron: anaerobic microbial iron oxidation and reduction. *Nat Rev Microbiol* **4:** 752-764.

Weber L. (2000). *Modellierung von Porenwasserprofilen in sauren Bergbaurestseen unter Berücksichtigung der advektiven Strömung im Sediment*, Ph.D. Thesis. Universität Heidelberg. Heidelberg, Germany.

Weiss JV, Rentz JA, Plaia T, Neubauer SC, Merrill-Floyd M, Lilburn T *et al*. (2007). Characterization of neutrophilic Fe(II)-oxidizing bacteria isolated from the rhizosphere of wetland plants and description of *Ferritrophicum radicicola* gen. nov. sp. nov., and *Sideroxydans paludicola* sp. nov. *Geomicrobiol J* **24:** 559-570.

Wenderoth DF, Abraham WR. (2005). Microbial indicator groups in acidic mining lakes. *Environ Microbiol* **7:** 133-139.

Wendt-Potthoff K, Bozau E, Frömmichen R, Meier J, Koschorreck M. (2010). Microbial iron reduction during passive *in situ* remediation of an acidic mine pit lake mesocosm. *Limnologica* **40:** 175-181.

Yeates TO, Kerfeld CA, Heinhorst S, Cannon GC, Shively JM. (2008). Protein-based organelles in bacteria: carboxysomes and related microcompartments. *Nat Rev Microbiol* **6:** 681-691.

Younger P. (2002). Mine water pollution from Kernow to KwaZulu-Natal: Geochemical remedial options and their selection in practice. *GeoSci South-West Engl* **10:** 255-266.

Statement of authorship

I hereby affirm that I have composed this doctoral thesis by myself and only with the assistance and literature cited in the text. Those who provided assistance for the experiments, data analysis and writing of the manuscript are listed as coauthors in respective chapter.

I confirm that I have read and fully understood the 'Course of Examination for Doctoral Candidates' (Promotionsordnung) by the School of Biology and Pharmacy at the Friedrich Schiller University Jena. I did not obtain any assistance from a consultant for doctorate thesis, and no third parties have received any direct or indirect substantial benefit in accordance with this dissertation. This work has not been previously submitted for scientific survey to the Friedrich Schiller University Jena or to any other university.

Jena, Aug. 2012

_____

Shipeng Lu

Acknowledgements

It is a great pleasure to thank all of the people who helped me during this period for my PhD degree.

First, I greatly appreciate Prof. Dr. Kirsten Küsel for her encouraging supervision of this thesis. With her enthusiasm, her inspiration, and her patience, she had guided me towards the beautiful acidic mine lake and trained me as a scientist.

I acknowledge Dr. Kevin Hallberg (University of Wales, Bangor, UK), Dr. Karuna Chourey and Dr. Robert L. Hettich (Oak Ridge National Laboratory, USA) for the training and helps during my research stays at their groups. I also wish to thank Prof. Dr. Joel Kostka (Georgia Institute of Technology, USA) and Prof. Dr. Gabriele Diekert (University Jena) for their interests and review of this thesis.

Thanks also go to the former iron cycling research team members: Marco Reiche, Stefan Gischkat, Heiko Köpf and Marco Jung. I won't forget the fabulous time we had spent on Lake 77. Other lab members in Limnology/Aquatic Microbiology Group are also very helpful: Denise Akob, Martina Hermann, Anna Rusznyák, Juanjuan Wang, Wolfgang Fischer, Jana Sitte, Susanne Grube, Maren Sickinger, Qing Bo Hu and Peter Bouwma.

I should also thank all the other excellent colleagues, for their contribution and collaboration to this thesis: Thomas R. Neu, Sandor Nietzsche and Valerian Ciobotă.

This work was supported by the Graduate School of Excellence Jena School for Microbial Communication (JSMC) funded by the German Research Foundation (DFG).

Thank all the friends in China, Korea and Germany. And finally I want to say thank you very much to my parents, my wife Min Jeong Park and my sister. Thank you for being with me all the time. I am greatly indebted to all of you.

Published articles and pending manuscripts

All thesis chapters have been published or submitted for publication in international peer-reviewed journals. My contributions to each manuscript preparation are documented below.

- Shipeng Lu, Stefan Gischkat, Marco Reiche, Denise M. Akob, Kevin B. Hallberg and Kirsten Küsel (2010) *Ecophysiology of Fe-cycling bacteria in acidic sediments*. **Applied and Environmental Microbiology** 76: 8174-8183.

  I did the geochemistry analyses, 16S rRNA gene library construction and data analyses, and the isolation of the bacteria. S. Gischkat helped me for the Fe(III) reduction test assay of all the isolates and the growth pH range assay of selective isolates. M. Reiche helped for the sampling and general lab techniques. K. H. Hallberg taught me the overlay solid media technique. I prepared the first draft of the manuscript and worked on the following versions. K. Küsel guided the planning and execution of the experiments as well as performed the manuscript accomplishment.

- Marco Reiche, Shipeng Lu, Valerian Ciobotă, Thomas R. Neu, Sandor Nietzsche, Petra Rösch, Jürgen Popp, and Kirsten Küsel (2011*) Pelagic boundary conditions affect the biological formation of iron-rich particles (iron snow) and their microbial communities.* **Limnology and Oceanography** 56: 1386-1398

  I did the sampling of the iron snow and lake geochemical parameters measurements together with M. Reiche. I constructed 16S rRNA gene libraries and made the data analyses. V. Ciobotă made the Raman spectroscopy analysis; T. R. Neu for fluorescence microscopy and S. Nietzsche for scanning electron microscopy. Other experiments were done by M. Reiche. I joined all the discussions of this project and contributed for the manuscript preparation. K. Küsel guided the planning and execution of the experiments as well as performed the manuscript accomplishment.

- Shipeng Lu, Karuna Chourey, Marco Reiche, Sandor Nietzsche, Manesh B. Shah, Robert L. Hettich and Kirsten Küsel (2012) *Elucidating microbial communities and their metabolic functions in iron-rich aggregates (iron snow) of an acidic lake*. Manuscript submitted to **ISME Journal** (ISMEJ-12-00473OA).

I did the all geochemistry analyses, 16S rRNA gene library construction and data analyses, and quantitative PCR analysis with minor helps from other lab member as stated in the acknowledgement part of this manuscript. K. Chourey, M. B. Shah and R. L. Hettich helped me for the metaproteomics analyses during my visit to their lab. S. Nietzsche for scanning electron microscopy. I prepared the first draft of the manuscript and worked on the following versions. K. Küsel guided the planning and execution of the experiments as well as performed the manuscript accomplishment.

- Valerian Ciobotă, Shipeng Lu, Nicolae Tarcea, Petra Rösch, Kirsten Küsel and Jürgen Popp (2012) *Quantification of the inorganic phase of iron snow aggregates provides valuable information concerning aggregate formation*. Manuscript submitted to **Journal of Environmental Monitoring.**

I did all the biogeochemistry measurement of the acidic lake and the iron snow, and prepared the dried samples for Raman spectroscopy analysis. The whole molecular biological experiments were done by me. V. Ciobotă made the quantitative Raman spectroscopy analysis and prepared the first draft of the manuscript. I worked on the first and following versions of the manuscript together with V. Ciobotă.

Confirmation of the individual contribution to the manuscript preparation:

Jena, Aug. 2012

_____

Kirsten Küsel

Curriculum Vitae

Shipeng Lu

Friedrich Schiller University Jena
Institute of Ecology
Limnology/Aquatic Geomicrobiology Group
Dornburger Strasse 159
07743 Jena
Germany
Tel.: +49 (0) 3641 949464
Fax: +49 (0) 3641 949402
Email: shipeng.lu@uni-jena.de

Personal Information

Date of Birth: 26th, Aug, 1980
Place of Birth: Nanjing, Jiangsu, P. R. China
Citizenship: P. R. China

Education, Employment and Research Stay

Nov.2010-Jan.2011	Three months research stay: Organic and Biological Mass Spectrometry Group, Oak Ridge National Laboratory, TN, USA. By Dr. Robert L. Hettich (Dr Hettich's group is one of the leading groups on metaproteomics research of various environment samples.)
Nov.2008	Two weeks research stay: The Bangor Acidophile Research Team (BART), University of Wales, UK. By Prof. Dr. D. B. Johnson and Dr. K. Hallberg, (BART is one of the leading groups on acidophilic microorganism research.)
Jul.2008-Aug.2012	PhD student, Research Group of Limnology, Institute of Ecology, Friedrich Schiller University Jena, Jena, Germany. Research topic: Microbial iron cycling in pelagic aggregates (iron snow) and sediments of an acidic mine lake. (Supervisor: Prof. Dr. Kirsten Küsel)
Mar.2007- Mar.2008	Researcher in Environmental Microbial Biotechnology Lab, GNU, Korea.
Feb.2005- Mar.2007	Master of Science, Environmental Microbial Biotechnology Lab, Division of Environmental Biotechnology, Gyeongsang National University, South Korea. M.S. Thesis Title: Microbial community analysis of activated sludge performing enhanced biological phosphorus removal in a sequencing batch reactor (Supervisor: Prof. Dr. Che Ok Jeon)
Jul. 2003- Jan. 2005	Employee of Soochow University, P. R. China.
Sep.1999- Jul.2003	Bachelor of Science, School of Life Science, Soochow University, P. R. China

B. S. Thesis Title: Effect of nano-TiO_2 on increasing vigor of naturally aged seeds and improving growth of spinach (Supervisor: Prof. Dr. Fashui Hong)

Sep.1996- Jul.1999 The High School affiliated to Nanjing Normal University.

Awards

2008-2011 Stipend from Jena School of Microbial Communication (JSMC, funded by DFG)
2005-2007 Scholarship for National Core Research Centre Students, Korea
2005-2007 Brain Korea 21 Students' Scholarship of Gyeongsang National University
2002 Second-class Student Scholarship of Soochow University (Honor for top 10%)
2001 First-class Student Scholarship of Soochow University (Honor for top 3% students)
2001 Zhu Jingwen Scholarship of Soochow University (Honor for top 3% students)

Academic Achievements

Publications

1. **Shipeng Lu**, Karuna Chourey, Marco Reiche, Sandor Nietzsche, Manesh B. Shah, Robert L. Hettich, and Kirsten Küsel. (2012). Elucidating microbial communities and their metabolic functions in iron-rich aggregates (iron snow) of an acidic lake. (Submitted to *ISME J.*)

2. Valerian Ciobotă, **Shipeng Lu**, Nicolae Tarcea, Petra Rösch, Kirsten Küsel, and Jürgen Popp. (2012). Quantification of the inorganic phase of iron snow aggregates provides valuable information concerning aggregate formation. (Submitted to *J. Environ. Monit.*)

3. Marco Reiche, **Shipeng Lu**, Valerian Ciobotă, Thomas R. Neu, Sandor Nietzsche, Petra Rösch, Jürgen Popp, and Kirsten Küsel. (2011). Pelagic boundary conditions affect the biological formation of iron-rich particles (iron snow) and their microbial communities. *Limnol. Oceanogr.* 56:1386-1398

4. **Shipeng Lu**, Stefan Gischkat, Marco Reiche, Denise M. Akob, Kevin B. Hallberg, and Kirsten Küsel. (2010). Identification and Ecophysiology of Fe-cycling bacteria in acidic sediments. *Appl. Environ. Microbiol.* 76:8174–8183

5. **Shipeng Lu**, Jung Ro Lee, Seung Hyun Ryu, Bok Sil Chung, Woo-Seok Choe and Che Ok Jeon. (2007).*Runella defluvii* sp. nov., isolated from a domestic wastewater treatment plant. *Int. J. Syst. Evol. Microbiol.* 57:2600-2603

6. **Shipeng Lu**, Seung Hyun Ryu, Bok Sil Chung, Young Ryun Chung, Woojun Park, and Che Ok Jeon. (2007).*Simplicispira limi* sp. nov., isolated from activated sludge. *Int. J. Syst. Evol. Microbiol.* 57:31-34

7. Minjeong Park, **Shipeng Lu**, Seung Hyun Ryu, Bok Sil Chung, Woojun Park, Chang-Jin Kim and Che Ok Jeon. (2006). *Flavobacterium croceum* sp. nov., isolated from activated sludge. *Int. J. Syst. Evol. Microbiol.* 56:2443–2447

8. **Shipeng Lu**, Minjeong Park, Hyeon-Su Ro, Dae Sung Lee, Woojun Park and Che Ok Jeon. (2006). Analysis of microbial communities using culture-dependent and culture-independent approaches in an anaerobic/aerobic SBR reactor. *J. Microbiol.* 44:155-161

9. Lei Zheng, Hong Fashui, **Lu Shipeng**, Liu Chao. (2005) Effect of nano-TiO_2 on strength of naturally aged seeds and growth of spinach. *Biol. Trace Elem. Res.* 104:83-92

Conference Proceedings

1. Shipeng Lu and Kirsten Küsel (2012) Parachuting on iron snow through redox gradients. *JSMC retreat 2012*, Bad Sulza/Germany. (Talk)

2. Shipeng Lu, Karuna Chourey, Marco Reiche, Valerian Ciobotă, Sandor Nietzsche, Robert L. Hettich, Kirsten Küsel (2011) Elucidating the functions of the active microbial community of Iron Snow in an acidic lake. *Goldschmidt 2011*, Prague/Czech Republic. (Abstract, 1360)

3. Karuna Chourey, Shipeng Lu, Abbie Green, S. Sun, S. Connon, Victoria Orphan, Kirsten Küsel, Robert L. Hettich (2011) Evaluation of a universal metaproteomics approach to explore microbial consortia in environmental samples. *ASM2011*, New Orleans/USA (Abstract).

4. Shipeng Lu, Stefan Gischkat, Marco Reiche and Kirsten Küsel (2010) Taking the iron snow shuttle to the microbial iron cycle in acidic lake sediments. *DGL2010*, Bayreuth/Germany. (Talk)

5. Shipeng Lu, Stefan Gischkat, Marco Reiche and Kirsten Küsel (2010) Taking the iron snow shuttle to the microbial iron cycle in acidic lake sediments. *MiCom2010*, Jena/Germany (Talk, P19).

6. Shipeng Lu, Marco Reiche and Kirsten Küsel (2009): Taking the iron snow shuttle to the microbial iron cycle in acidic lake sediments. *Goldschmidt* 2010, Knoxville, US. (Talk and abstract, A636).

7. Shipeng Lu, Marco Reiche and Kirsten Küsel (2009): Taking the lake snow shuttle to enter the microbial iron cycle in acidic sediments. *JSMC/ILRS symposium*, Jena, Germany. (Talk and abstract)

8. Shipeng Lu, Marco Reiche and Kirsten Küsel (2009) Diversity of Fe(III)-reducing prokaryotes in acidic coal mining lake sediments. *Goldschmidt* 2009, Davos, Switzerland. (Poster and abstract, A796).

9. Shipeng Lu, Marco Reiche and Kirsten Küsel (2009) Can we detect secondary metabolites from isolates involved in Fe-cycling? *Beutenberg Campus /JSMC Workshop (2009): Method and Concept Transfer on*, Jena, Germany. (Poster)

10. Shipeng Lu, Marco Reiche and Kirsten Küsel (2008) Towards a better understanding of the Mechanisms of microbial Fe(III) reduction in acidic habitats. *JSMC Symposium 2008*, Jena, Germany. (Poster and talk).

11. Thu Huong Thi Vu, Minjeong Park, Shipeng Lu, Che Ok Jeon (2007) Diversity of PHA synthase (phaC) genes from activated sludge in sequencing batch reactor. *2007 International Meeting of the Microbiological Society of Korea,* PyeongChang, Korea. (Poster and abstract, B066)

12. Thu Hien Thi Nguyen, Thu Huong Thi Vu, Shipeng Lu, Che Ok Jeon (2006) Effects of pH on microbial communities on activated sludge performing enhanced biological phosphorus removal in a sequencing batch reactor. *2006 International Meeting of the Federation of Korea Microbiological Societies,* Seoul, Korea. (Poster and abstract, B020)

13. Shipeng Lu, Thu-Huong Thi Vu, Thu-Hien Thi Nguyen and Che Ok Jeon (2006) Identification of two *Rhodocyclus*-related polyphosphate-accumulating organisms in a sequencing batch reactor. *2006 International Symposium and Annual Meeting of the KSABC, Applied biological and environmental chemistry,* Gyeongju, Korea. (Poster and abstract, PE-04)

14. Shipeng Lu, Minjeong Park and Che Ok Jeon (2006) Analysis of microbial communities responsible for enhanced biological phosphorus removal in a SBR reactor using stable isotope

probing approach. *11th International Symposium on Microbial Ecology-ISME-11, The Hidden Powers-Microbial Communities in Action.* Vienna, Austria. (Poster and abstract)

15. Shipeng Lu, Minjeong Park and Che Ok Jeon (2005) Analysis of microbial communities responsible for enhanced biological phosphorus removal in an anaerobic/aerobic SBR reactor using stable isotope probing approaches. *Proceedings of Current Biotechnology and Bioengineering (X VII), The Korean Society for Biotechnology and Bioengineering,* Jinju, Korea. (Poster and abstract)

16. Minjeong Park, Shipeng Lu, Eugene L. Madsen and Che Ok Jeon (2005) Protection of *Polaromonas naphthalenivorans* CJ2 from naphthalene toxicity by extracellular polysaccharide capsules. *2005 International Meeting of the Federation of Korean Microbiological Societies*. Seoul, Korea. (Poster and abstract, BO34)

17. Shipeng Lu, Minjeong Park and Che Ok Jeon (2005) Comparative Analysis of microbial communities in an anaerobic/aerobic SBR reactor by using cultivation-based techniques and 16S rRNA gene clone libraries, *2005 Annual Meeting & International Symposium, The Korean Society for Microbiology and Biotechnology*. Seoul, Korea. (Poster and abstract, G3)

18. Minjeong Park, Shipeng Lu, Eugene L. Madsen and Che Ok Jeon (2005) The naphthalene catabolic genes of *Polaromonas naphthalenivorans* CJ2 are split into two clusters that are regulated by their respective promoters and regulators, *2005 Annual Meeting & International Symposium, The Korean Society for Microbiology and Biotechnology.* Seoul, Korea. (Poster and abstract, G1)

Jena, Aug. 2012

_____

Shipeng Lu